UiT The Arctic University of Norway

Faculty of Biosciences, Fisheries and Economics

Department of Arctic and Marine Biology

Land-Ocean Interactions in a Changing Arctic:

Effects of terrestrial inputs on coastal food-web carbon source and contamination in Isfjorden, Svalbard

Maeve McGovern

A dissertation for the degree of Philosophy Doctor

March, 2022

Table of Contents

Acknowledgements

First and foremost, I'd like to thank my main supervisor Amanda Poste for giving me the opportunity to join the TerrACE project. I am very grateful for your time and energy, and your infectious passion for ecology and land-ocean interactions. I'd also like to thank my co-supervisors: Anita Evenset, Katrine Borgå and Janne Søreide, for their inclusivity, guidance and support throughout my PhD.

This research was funded by the Norwegian Research Council (TerrACE; project number: 268458, PI A. Poste), the Fram Center Flagship "Fjord and Coast" grant (FreshFate; project number 132019, PI A. Poste), the Fram Center Flagship "Hazardous substances" grant (IcePOPs; project number: 772019, PI M. McGovern) and the Svalbard Science Forum's Arctic Field Grant (RIS number: 10914, PI M. McGovern).

I'd like to acknowledge my additional coauthors for their contribution to this body of work: Alexey Pavlov, Anne Deininger, Mats Granskog, Eva Leu (paper 1), Nick Warner, Pernilla Carlsson, Emelie Skogsberg, Guttorm Christensen and Anders Russ (paper 2), Michael Arts, Raul Primicerio, Eva Leu, Anna M. Dabrowska, Emilie Hernes Vereide and Paul Renaud (paper 3).

This thesis is based off of several sampling campaigns in Isfjorden, Svalbard, three in 2018 and two in 2019. I would like to thank TerrACE MSc students Emelie Skogsberg, Emilie Hernes Vereide, Nathalie Carrasco and Charlotte Pedersen Ugelstad for their substantial contributions to the fieldwork. I am thankful for additional support in the field provided by Eirik Aasmo Finne, Sverre Johansen, Connor McKnight, Hannah Miller, Anna Vader, Stuart Thompson, Tobias Vonnahme, Ulrike Dietrich, Uta Brandt, Cathrine Gundersen, Liv Sletten and Sarah Nelson. Thank you also to UNIS logistics, and the crew of the R/V Helmer Hanssen, Stig Henningsen at Henningsen Transport & Guiding with MS FARM, and the crew of *Clione* and the Czech station for their logistical support.

Thank you to UNIS, Akvaplan-niva and the University of Tromsø for allowing me to use their lab facilities for various analyses including stable isotope preparation, and sediment and POM chlorophyll-a analyses. I would also like to thank Nick Warner and Merete Miøen for guiding me through the POPs extractions and analyses at NILU lab in Tromsø. Thank you to Sofi Jonsson and Stockholm University for hosting me for MeHg analysis in water and Tina Bryntesen and NIVA lab in Oslo for hosting me for MeHg analysis in zooplankton. I am grateful for the additional labwork carried out at laboratories in Norway, North America and Europe. Water chemistry analyses were run at NIVA lab, facilitated by Elisabeth Hansen and Anne-Luise Ribeiro. DOM absorbance was run by Espen Lund at NIVA. Fatty acid analyses were run at Ryerson University in Toronto, CA by Dino Milotic and Ben Schultz overseen by Michael Arts. Stable isotope analyses were completed at UC-Davis stable isotope facility in USA. Taxonomic analysis of phytoplankton was completed by Anna Dabrowska at the Institute of Oceanology - Polish Academy of Science (IOPAS). I met Anna at her poster at the Gordon conference in Italy and I am very happy that we were able to turn that chance encounter into a concrete collaboration.

I would like to thank my fellow students at UiT, as well as NIVA section-317 for creating a warm and welcoming working environment. Thank you also to the ARCTOS and AMINOR networks for the many workshops, symposiums and social gatherings that bring together the research community here in Tromsø. I'd also like to thank the OsloR group and greater R community for being open and friendly and teaching me so much!

Finally, a heartfelt thank-you to my family and friends– in the office, at home and in the mountains: thank you for your kindness, patience and support, you made this PhD possible.

Supervisors

Dr. Amanda E. Poste // Norwegian Institute for Water Research, Tromsø, Norway

UiT: The Arctic University of Norway, Tromsø, Norway

Dr. Anita Evenset // Akvaplan-niva AS; Tromsø, Norway

Dr. Janne E. Søreide // University Centre in Svalbard, Longyearbyen, Norway

Prof. Katrine Borgå // Department of Biosciences, University of Oslo, Oslo, Norway

Centre for Biogeochemistry in the Anthropocene (CBA), University of Oslo, Oslo, Norway

Author contributions

	Paper 1	**Paper 2**	**Paper 3**
Concept & Idea (proposal lead)	AEP	AEP	AEP
Study design & Methods	MM, JES, AEP	MM, MA, KB, EL, PR, JES, AEP	MM, NAW, AE, KB,JES, AEP
Data gathering	MM, AD, JES, AEP	MM, MA, AMD, EHV, JES, AEP	MM, NAW, AE, PC, ES, JES, GC, AEP
Manuscript preparation	MM	MM	MM
Manuscript revisions & editing	MM, AP, AD, MG, EL, JES, AEP	MM, MA, KB, AMD, EL, RP, PR, JES, EHV, AEP	MM, NAW, KB, AE, PC, ES, JES, AR, GC, AEP

Abbreviations for authors:

Maeve McGovern (MM)
Alexey Pavlov (AP)
Anne Deininger (AD)
Mats Granskog (MG)
Eva Leu (EL)
Janne E Søreide (JES)
Amanda E Poste (AEP)

Michael Arts (MA)
Katrine Borgå (KB)
Anna M. Dąbrowska (AMB)
Raul Primicerio (RP)
Paul Renaud (PR)
Emilie H Vereide (EHV)

Nicholas A Warner (NW)
Anita Evenset (AE)
Pernilla Carlsson (PC)
Emelie Skogsberg (ES)
Anders Ruus (AR)
Guttorm Christensen (GC)

Abstract

Climate change driven increases in temperature are enhancing land-ocean connectivity in the coastal Arctic, with a range of implications for coastal food-webs and contaminant cycling. Terrestrial inputs are a direct source of carbon and legacy contaminants to coastal areas, but as a source of freshwater, nutrients and suspended inorganic sediments, they can also affect coastal food-webs and contaminant cycling indirectly through impacts on phytoplankton community structure and contaminant removal and burial. To investigate coastal responses to terrestrial inputs, we conducted a field study in a river- and glacier- influenced Arctic fjord system (Isfjorden, Svalbard), in May, June and August, 2018 with a follow-up study in 2019. Environmental data, zooplankton and benthos were collected from 17 fjord stations along transects from river estuaries and glacier fronts to the outer fjord. Fauna were analyzed for persistent organic pollutants and dietary carbon sources were assessed using a variety of biogeochemical tracer techniques, including fatty acid trophic markers and bulk stable isotopes. Our observations revealed a pervasive freshwater footprint in the inner fjord arms, the geochemical properties of which varied spatially and seasonally as the melt season progressed from snowmelt in June to glacial melt and permafrost runoff in August. Zooplankton fatty acid profiles were strongly coupled to fatty acid profiles of water column particulate organic matter, reflecting seasonal and spatial shifts in phytoplankton community structure, with elevated contributions of diatom fatty acids in May following the spring phytoplankton bloom, to dinoflagellate and terrestrial fatty acids in June and August when high sediment loads attenuate light in the nearshore. Persistent organic pollutant concentrations in coastal fauna were inversely related to terrestrial inputs spatially and seasonally, suggesting that freshwater and associated high rates of inorganic sedimentation act to dilute, bind and bury persistent organic pollutants in the inner fjord arms of Isfjorden. Our results highlight the physical, chemical and biological impact of terrestrial inputs on downstream coastal ecosystems in a rapidly changing Arctic environment.

List of papers

This thesis is based on the following three papers:

1. **McGovern M**, Pavlov A, Deininger A, Granskog M, Leu E, Søreide JE, Poste AE (2020). Terrestrial inputs drive seasonality in organic matter and nutrient biogeochemistry in a high Arctic fjord system (Isfjorden, Svalbard). *Frontiers in Marine Science.* 7:542563. doi: 10.3389/fmars.2020.542563

2. **McGovern M**, Arts M, Dąbrowska AM, Borgå K, Leu E, Primicerio R, Renaud P, Søreide JE, Vereide EH, Poste AE (Manuscript). Turbid meltwater plumes diminish the quality of particulate organic matter available for Arctic coastal food-webs. Advanced manuscript prepared for *Limnology & Oceanography*

3. **McGovern M**, Warner N, Borgå K, Evenset A, Carlsson P, Skogsberg E, Søreide JE, Ruus A, Christensen G, Poste AE (in review). Is glacial meltwater a secondary source of legacy contaminants to Arctic coastal food-webs? In review at *Environmental Science & Technology*

Other authored publications cited in this thesis:

McGovern M, Berge J, Szymczycha B, Węsławski JM, Renaud PE (2018). Hyperbenthic food-web structure in an Arctic fjord. *Marine Ecology Progress Series* 603:2946. doi.org/10.3354/meps12713

McGovern M, Evenset A, Borgå K, de Wit, HA, Braaten HFV, Hessen DO, Schultze S, Ruus A, Poste A (2019). Implications of Coastal Darkening for Contaminant Transport, Bioavailability, and Trophic Transfer in Northern Coastal Waters. *Environmental Science & Technology* 53 (13), 7180-7182. DOI: 10.1021/acs.est.9b03093

McGovern M, Poste AE, Oug E, Renaud PE, Trannum HC (2020). Riverine impacts on benthic biodiversity and functional traits: A comparison of two sub-Arctic fjords. *Estuarine, Coastal and Shelf Science* 240: 106774. doi.org/10.1016/j.ecss.2020.106774

McGovern M, Borgå K, Heimstad E, Ruus A, Christensen G, Evenset A (In Review). Small Arctic rivers transport legacy contaminants from thawing catchments to coastal areas in Kongsfjorden, Svalbard. In review at *Environmental Pollution*.

Delpech L-M, Vonnahme TR, **McGovern M**, Gradinger R, Præbel K and Poste AE (2021). Terrestrial Inputs Shape Coastal Bacterial and Archaeal Communities in a High Arctic Fjord (Isfjorden, Svalbard). Frontiers in Microbiology: 12:614634. doi: 10.3389/fmicb.2021.614634

Skogsberg E, **McGovern M**, Poste A, Jonsson S, Arts M, Varpe Ø, Borgå K (In Review). Effect of Seasonal Glacial Run-Off on Hg and Chlorinated POP Concentrations in Arctic Littoral Amphipods. In review at *Environmental Pollution*

1 Introduction

1.1 The Arctic land-ocean interface

The land-ocean interface, including fjords, and estuaries, are some of the worlds most productive and biologically diverse ecosystems (Talley et al. 2006; Winder et al. 2017). In the coastal zone, proximity to shore, and shallow depths allow for tight connectivity and transfer of organic matter (OM) and inorganic nutrients between terrestrial and marine systems and benthic and pelagic compartments.

Land-ocean connectivity is especially strong in the Arctic Ocean, which is surrounded by land and receives more than 10% of all continental runoff despite only containing 1% of global ocean volume (Macdonald 2000; McClelland et al. 2012). Functioning like one large estuary (Macdonald 2000; McClelland et al. 2012), the majority of runoff to the Arctic comes from large Arctic rivers with heterogenous catchments. River inputs, coastal erosion and diffuse runoff deliver freshwater, inorganic nutrients and OM to the coast (McClelland et al. 2008; Holmes et al. 2012), shaping water column structure and circulation (McClelland et al. 2008; Carmack et al. 2015), and contributing to phytoplankton production (Le Fouest et al. 2013; Terhaar et al. 2021). Strong land-ocean and pelagic-benthic connectivity also make coastal areas an important global carbon sink (Field et al. 1998; Smith et al. 2015; Cui et al. 2016).

Despite being recognized for important functions and ecosystem services, nearshore areas globally are particularly sensitive to human activities, and have suffered degradation over the past 100 years from overexploitation and habitat destruction with harmful impacts on coastal ecosystem structure and function (Lotze et al. 2006; Duarte et al. 2020). The Arctic is home to approximately 4 million people, 10% of whom are indigenous, with many relying on coastal areas for subsistence (Meredith et al. 2019). While much of the Arctic has remained relatively pristine, receding sea-ice may open-up previously untouched areas for fisheries, transport and resource extraction (Fauchald et al. 2021). These productive and important coastal areas of the Arctic are now facing an uncertain future in the face of rapid anthropogenic climate change (Arias et al. 2021).

1.2 Climate change driven increases in terrestrial inputs to coastal areas

While climate change affects the entire globe, it's occurring most rapidly in the Arctic, where increases in temperature are occurring at a rate that is more than twice the global average (Blunden and Arndt 2016; Meredith et al. 2019). Melting sea-ice and glaciers, thawing permafrost and extreme high temperatures are transforming the landscape and causing potentially irreversible changes (Meredith et al. 2019).

On land, climate change driven increases in temperature and the associated changes in the hydrological cycle (Rawlins et al. 2010) is leading to increases in precipitation, glacial melt, thawing permafrost and subsequently increased transport of freshwater and catchment-derived materials to coastal areas (Arias et al. 2021). Generally, these inputs are a source of carbon, nutrients, soils, and anthropogenic pollutants to the coastal zone (Holmes et al. 2012) where they are contributing to the *darkening* of northern coastlines (Konik et al. 2021) and have various implications for coastal ecosystem structure and function (Thrush et al. 2004; Aksnes et al. 2009; Frigstad et al. 2013; McGovern et al. 2019; Opdal et al. 2019).

Arctic coastal areas differ from other regions in their extreme seasonality in river discharge, with 90-95% of the total annual runoff occurring during summer (Macdonald et al. 1999; Macdonald 2000). The nature and magnitude of terrestrial inputs to coastal areas varies seasonally in relation to the progression of the melt season on land (Holmes et al. 2012), but also depends on catchment characteristics and local and regional variation in temperature and precipitation (Nowak and Hodson 2015; Giesbrecht et al. 2022). For example, land-ocean inputs from heavily glaciated landscapes on Greenland and Svalbard are generally more nutrient-poor compared to inputs from the permafrost dominated Russian and Canadian Arctic, where large rivers drain catchments reaching beyond the Arctic tundra to the boreal zone (Holmes et al. 2012; Hopwood et al. 2020). While the seasonal geochemistry of the 6 largest Arctic rivers is somewhat well-defined (Holmes et al. 2012), data from other parts of the heterogenous Arctic Ocean catchment are lacking, including more heavily glaciated fjords. Considering the ecological and societal importance of these systems, detailed characterization of terrestrial inputs and their subsequent impacts on the coastal zone, including how these processes are expected to respond to global climate change, are needed for future management of Arctic coastal areas.

1.3 Direct and indirect effects on coastal food-web carbon source

Terrestrial inputs affect coastal food-webs directly as a source of particulate and dissolved organic carbon (POC and DOC), which can be utilized as a carbon source at different levels of the food-web. However, terrestrial inputs can also impact coastal food-webs indirectly through impacts on light, temperature and nutrient availability (Mustaffa et al. 2020; Wollschläger et al. 2021).

Inputs of suspended sediments and terrestrial dissolved OM (tDOM) attenuate light needed for photosynthesis and also provide substrate for bacterial production (Jones 1992; Ask et al. 2009), potentially altering heterotrophic: autotrophic balance toward net heterotrophy (Vallières et al. 2008), leading to reduced food quality for ecologically important zooplankton and fish (Darnaude 2005), and enhancing remineralization of carbon to CO_2 in coastal systems (Ver et al. 1999).

Recent research has also highlighted the differences in meltwater characteristics and impacts for land- vs. marine-terminating glaciers (Hopwood et al. 2020). In fjords with marine-terminating glaciers, upwelling of sub-glacial discharge brings nutrient rich marine water to the surface, sustaining high productivity at glacier fronts (Meire et al. 2017; Hopwood et al. 2018; Kanna et al. 2018). In contrast, land-terminating glaciers are associated with nutrient poor, highly turbid and stratified river plumes which limit productivity in impacted fjords (Holding et al. 2019; Hopwood et al. 2020), findings which suggest dramatic changes in fjord functioning as marine-terminating glaciers retreat onto land (Lydersen et al. 2014).

The potential impacts on coastal ecosystems depend on characteristics of the meltwater, but also the characteristics of the receiving coastal system (e.g., which nutrients are limiting production). The timing of the inputs and their potential intersection with important seasonal processes in the water column also remains a substantial knowledge gap. The extreme seasonal variation in daylight drives strong seasonality in ecological processes in the water column, and shapes life history strategies for many important Arctic species. The spring phytoplankton bloom, which occurs during and after ice break-up, is driven by increased irradiation, nutrient supply and by stratification of the water column due to ice/snow melt (Sverdrup 1953; Leu et al. 2015). This annual event is timed perfectly with the growth and reproduction of key Arctic zooplankton, including *Calanus* spp., providing high quality FA to the Arctic marine food-web (Søreide et al. 2010; Daase et al. 2011, 2013). Thus, the melt season is intricately linked to seasonal ecological processes taking place in the nearshore, and changes in the timing, magnitude or geochemical nature of terrestrial inputs could have implications for Arctic ecosystem functioning.

1.4 Legacy POPs in a changing Arctic

1.4.1 Secondary sources

The melting Arctic terrestrial cryosphere is a potential source of environmental contaminants, including toxic persistent organic pollutants (POPs), to coastal areas. POPs are highly resistant towards degradation and can undergo long-range transport. They bioaccumulate and biomagnify in food chains and can cause adverse effects at low concentrations (Jørgensen et al. 2006; Johnson et al. 2013). Because of their adverse effects on humans and wildlife, international agreements have restricted the use of some of these compounds, including polychlorinated biphenyls (PCBs), hexachlorobenzene (HCB), dichlorodiphenyltrichloroethanes (DDTs), hexachlorocyclohexanes (HCHs) and chlordane pesticides (Stockholm Convention, 2013; Xu et al. (2013)]. However, decades of historical emissions by global industries have resulted in their widespread presence in the environment, even for POPs that are no longer produced or used ('legacy' POPs).

Legacy POPs in the atmosphere are declining across the Arctic (Wong et al. 2021), evidence of the effectiveness of regulatory measures in reducing primary emissions. However, the importance of secondary sources (i.e. media where POPs have been deposited in the past) is expected to increase with climate change (Macdonald et al. 2005; Kallenborn et al. 2012; Wöhrnschimmel et al. 2012, 2013; Gouin et al. 2013). These secondary sources include the reservoirs of legacy POPs which have accumulated in the Arctic environment over the past decades. These toxic compounds are transported via the atmosphere and oceanic currents from lower latitudes to the Arctic (Wania and Mackay 1993) where they have accumulated in ice, snow, permafrost, and surface soils (Hermanson et al. 2005; Aslam et al. 2019; Hermanson et al. 2020). Thus, with increased temperatures, terrestrial inputs can potentially transport these contaminants from the thawing Arctic landscape to coastal areas (Carlsson et al. 2012; Kallenborn et al. 2012; Johansen et al. 2021; McGovern et al. 2022a). These remobilized contaminants can then re-enter the atmosphere and global circulation, become buried in sediments (Hung et al. 2010; Ma et al. 2011; Bidleman et al. 2015), or potentially accumulate in coastal foods webs, which are important food sources for indigenous populations across the Arctic (Van Oostdam et al. 2005; Wania et al. 2017).

1.4.2 Accumulation in the coastal food-web

The movement of remobilized contaminants into and through coastal food webs depends on physical and environmental factors (e.g., presence of sea-ice, dissolved OM (DOM) and/or inorganic suspended sediments), food-web carbon source and structure, life history and physiology of coastal biota and the physical/chemical characteristics of the contaminants themselves (Borgå et al. 2004, 2022).

Environmental conditions, including temperature and the presence of sea-ice, can affect the mobility of POPs between environmental compartments. Increased temperatures and lack of sea-ice could facilitate volatilization of POPs to the atmosphere (Hargrave et al. 2000; Carlsson et al. 2016). Furthermore, OM and suspended sediments can affect contaminant bioavailability. For example, high concentrations of low-quality terrestrial DOM in the Baltic Sea has been shown to bind POPs, thus reducing their bioavailability for uptake in the food-web (Ripszam et al. 2015). These processes are also linked to the physical/chemical characteristics of the contaminants themselves. For example, hydrophilic PCB-52 is more easily dissolved in water and is likely to behave differently in the environment compared to hydrophobic PCB-153, which is more likely to be bound to OM or suspended sediments (Borgå et al. 2004).

Impacts of terrestrial inputs on primary carbon sources, trophic interactions and prey quality can lead to shifts in the bioavailability, accumulation and trophic transfer of contaminants (Larsson et al. 2000). For example, if terrestrial inputs are a substantial source of POPs, utilization of terrestrial OM as a food source could lead to enhanced uptake of hydrophobic POPs. Furthermore, shifts toward a microbial-based food web can lead to higher concentrations of biomagnifying contaminants in consumers because microbial food webs have additional trophic transfers compared with phytoplankton-based food webs, thus increasing the effective trophic level of consumers. Recent work from the Baltic Sea has shown that increased reliance on the microbial loop can lead to enhanced biomagnification of mercury (Hg) in estuarine zooplankton (Jonsson et al. 2017).

Terrestrial and microbial food sources also have lower nutritional value compared to high quality marine diatoms, which are rich in essential fatty acids (FA) like docosahexaenoic acid

(DHA) and eicosapentaenoic acid (EPA). Reductions in food quality and trophic efficiency in coastal food webs can subsequently lead to increases in contaminant uptake as organisms need to consume higher amounts of food to achieve the same level of growth (Karlsson et al. 2012, 2015; McGovern et al. 2019). Furthermore, a changing light environment due to high suspended sediment loads can hinder visual predators who may be unable to select for their preferred food choices (Aksnes et al. 2009). Observations from freshwater systems have revealed substantial impacts of these food-web shifts on production and contaminant loads in zooplankton and fish (Darnaude 2005; Poste et al. 2019). Recent studies have also reported other extensive ecological impacts of terrestrial runoff on fjord ecosystems, including restructuring of pelagic (Szeligowska et al. 2020; Trudnowska et al., 2020; Vereide 2019) and benthic communities (Ugelstad 2019; McGovern et al. 2020) in response to high sedimentation rates in the nearshore.

How these indirect effects of terrestrial run-off relate to contaminant dynamics is complex and poorly understood. Few studies have focused on these questions in coastal waters, especially in the Arctic. As these contaminants have a wide-range of environmental and human health effects, it is important to quantify concentrations in marine food-webs, and to understand how increased terrestrial inputs could impact their accumulation and trophic transfer.

1.5 Svalbard as a study location

Svalbard is a climate change hotspot in the rapidly warming Arctic, with annual air temperatures expected to increase by 7-10^{o}C and precipitation by 45-65% before 2100 (Hanssen-Bauer et al. 2019). Covered by 57% glaciers (Nuth et al. 2013), increased temperatures (Gjelten et al. 2016) and precipitation (Isaksen et al. 2017; Osuch and Wawrzyniak 2017), are already contributing to accelerated glacial melt (Błaszczyk et al. 2019; Pelt et al. 2021), and permafrost thaw (Wawrzyniak et al. 2016; Wawrzyniak and Osuch 2020). Associated increases in riverine discharge in most rivers (Killingtveit et al. 2003; Nowak et al. 2021) and coastal erosion (Sessford et al. 2015; Nicu et al. 2020) are enhancing the connectivity between thawing catchments and coastal waters. The transport of terrestrial organic matter (tOM) and suspended sediments from land to sea is affecting the fjord light climate (Pavlov et al. 2019; Konik et al. 2021) and phytoplankton communities (Halbach et al. 2019). However, the subsequent impacts on food-web carbon source and quality have received little attention. Furthermore, while studies have documented the presence of POPs in Svalbard ice cores (Hermanson et al. 2020), surface vegetation and sediments (Aslam et al. 2019; Johansen et al. 2021), and glacial streams (McGovern et al. 2022a), few studies have focused on accumulation at lower trophic levels in the recipient fjords (but see Hallanger et al. (2011a,b), especially in relation to the impacts of climate change on land-ocean interactions and fjord ecology.

2 Objectives and Hypotheses

This thesis investigates the influence of terrestrial inputs on the flow of energy and contaminants in coastal marine foods webs in Isfjorden, Svalbard. The project aims to evaluate riverine and glacial meltwater as a direct source of carbon and contaminants to coastal waters, as well as to assess the indirect effects of these terrestrial inputs on food-web carbon source and contamination. These overarching aims can be divided into three main research questions and hypothesis:

Research Question 1. What are the physical and chemical impacts of terrestrial inputs?

> **Hypothesis 1.** Terrestrial inputs create seasonal and spatial gradients in physical and chemical conditions in Isfjorden. Terrestrial inputs are a source of carbon and contaminants (POPs) to the Isfjorden system from melting glaciers and thawing permafrost.

Research Question 2. What are the direct and indirect impacts of terrestrial inputs on fjord zooplankton food source and quality?

> **Hypothesis 2.** Terrestrial inputs lead to reduced food quality, both directly where coastal fauna utilize tOM in the nearshore, and indirectly -as a source of inorganic nutrients and light attenuating particles- by increasing dietary reliance on the microbial loop in impacted areas of the fjord.

Research Question 3. How do the direct and indirect impacts on the physical environment and fjord food-web affect the accumulation of persistent organic pollutants (POPs) in coastal fauna?

> **Hypothesis 3.** Contaminant trophodynamics depend on basal carbon sources and food-web structure, but vary across different contaminant groups depending on their hydrophobicity. Hydrophobic POPs likely have reduced bioavailability in meltwater-impacted areas of the fjord due to sorption to tOM and inorganic particles. Meanwhile, hydrophilic POPs (including POPs from land) may exhibit higher bioavailability and uptake at the base of the coastal food web, as well as enhanced biomagnification, depending on degree of reliance on the microbial loop (hypothesis 2).

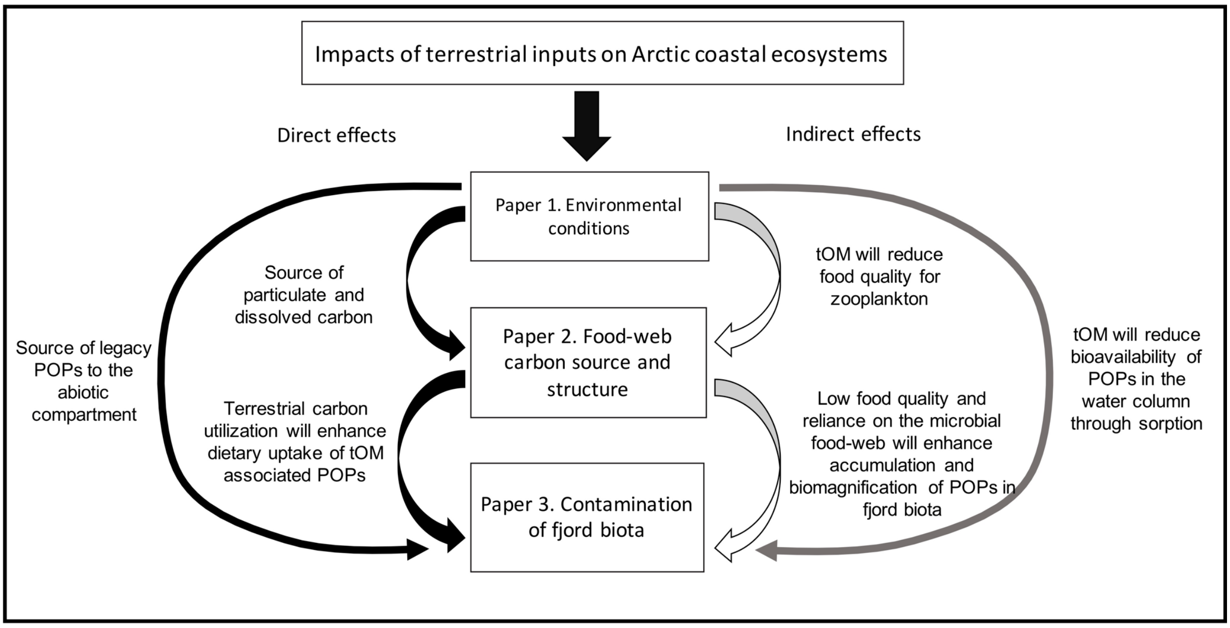

Figure 1. Expected direct and indirect effects of terrestrial inputs on Arctic coastal ecosystems.

3 Methods

3.1 Fieldwork

The main field season for this thesis work was in 2018, when we carried out field campaigns in May (10-18), June (14-25) and August (12-Sept 8) along transects in three fjord arms of Isfjorden (Adventfjorden, Tempelfjorden and Billefjorden; Figure 2) to capture gradients in terrestrial run-off. A follow-up campaign in June and August 2019 targeted one plume system in Adventfjorden, where we carried out high (horizontal and vertical) resolution gridded sampling.

We used both small and large boats, including small UNIS polarcirkle boats (*Flyer*, *Polaris, Kolga*) for sampling the shallow river estuary sites and larger vessels, including the RV *Helmer Hanssen, MS FARM* and *Clione,* for sampling offshore marine endpoint sites. To characterize the influence of river and glacier runoff on physicochemical conditions in the fjord, samples were collected from 17 stations in May, June and August 2018. In addition, vertical profiles of the water column were taken using a CTD (SAIV model 208; Bergen, Norway) and light meter (LI-192 Underwater Quantum Sensor, Li-191R quantum sensor and LI-1400 datalogger, LiCor, Germany). Water samples were collected from 15m depth and just below surface using a Niskin bottle (KC Denmark). Water was subsampled and preserved for a range of water chemistry analyses (DOC, DOM, dissolved nutrients) and filtered for analysis of particulate nutrients and stable isotopes and fatty acids of particulate OM (POM). A follow-up study was carried out in 2019 in Adventfjorden, a side fjord of Isfjorden, where environmental data were collected from a gridded sampling design from inner to outer fjord (see paper 1 for more details).

To determine the impacts of terrestrial inputs on coastal food-webs, extensive biological samples were collected at each station for food-web analysis and contaminant concentrations. At each station, zooplankton were collected using a variety of nets (60 µm, 200 µm, 1000 µm mesh sizes). Macrozooplankton (>20 mm) were sorted to genus, while mesozooplankton were pooled and divided into three size categories using 500 µm and 1000 µm sequential Nitex mesh screens. Subsamples were frozen at -20°C for stable isotopes analyses and -80°C for FA analyses. In addition a Van-veen grab was used to collect benthos from each station and gillnets were used to collect sculpin in the nearshore. Alongside subsamples from each individual or pooled zooplankton sample for dietary marker analysis, additional subsamples were collected for contaminant analyses (all frozen at -20°C). Targeted contaminants included PCBs (CB-28, 31, 52, 101, 118, 138, 153 and 180), and selected pesticides, including HCB, DDTs (o,p'- and p,p'-DDT) and their metabolites (o,p', p,p'-DDE and -DDD), as well as α-, β-, γ- HCH, cis- and trans isomers for chlordane and nonachlor, and mirex. In addition, zooplankton were further analyzed for enantiomeric fractions (EF = +/(+ &-)) of chiral α-HCH, trans- and cis-chlordane.

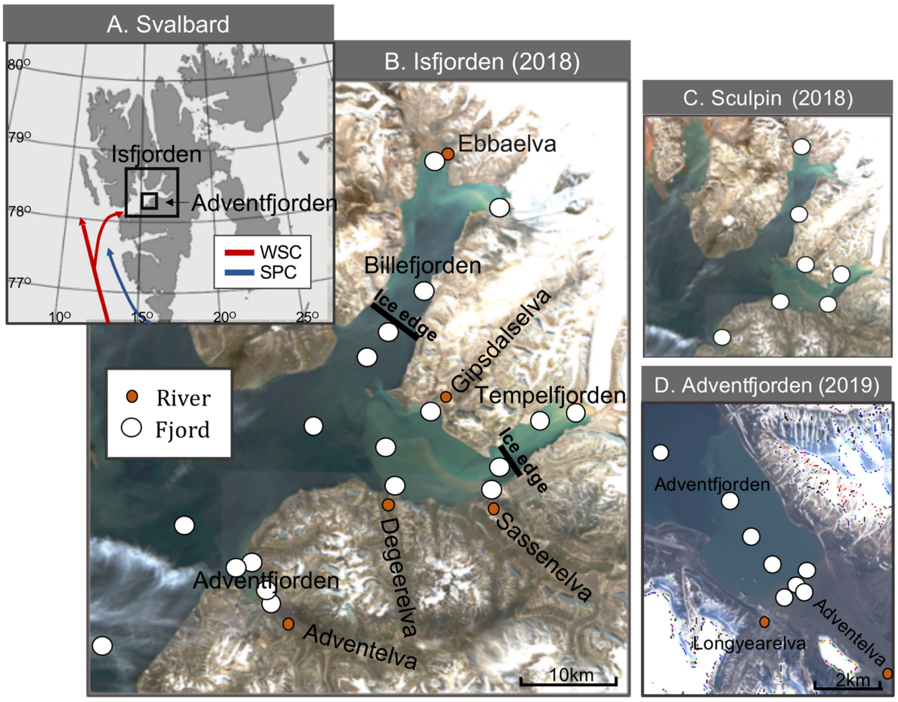

Figure 2. (A) Map of Svalbard showing the flow path of the West Spitsbergen Current (WSC) in red. (B) Station map (satellite image taken July 30, 2018; Sentinel-2 (https://scihub.copernicus.eu/) of Isfjorden illustrating where environmental variables and zooplankton were sampled in May, June and August 2018, and benthos in August, 2018. The ice edge in May 2018, when land-fast ice prevented sampling at the innermost stations is depicted in black. (C) Stations where sculpin were collected with gill nets in August, 2018 and (D) gridded sampling of the Adventfjord river estuary for environmental variables in 2019.

3.2 Approaches

A wide array of methods were used to target the research questions in this thesis. For evaluating the impacts of terrestrial runoff on coastal food webs, we used biogeochemical tracers including stable isotopes and FA. In addition, we targeted legacy contaminants whose usage are currently restricted, and used their structural characteristics (i.e. enantiomeric fractions) as tracers for glacial sources.

3.2.1 Stable isotopes of carbon and nitrogen

Stable isotopes of carbon ($\delta^{13}C$) and nitrogen ($\delta^{15}N$) reflect assimilated food sources over long time-scales (weeks/months) and are thus useful tools for food-web studies. The $\delta^{13}C$ values vary little (often within ~1 ‰) as carbon moves through marine food-webs, and are thus useful for determining dietary carbon source. Meanwhile, $\delta^{15}N$ values typically increase by 3-5 ‰ between trophic levels, and are often used for estimating trophic position (Peterson and Fry 1987).

In practice, $\delta^{13}C$ values are used to provide information about an organism's major carbon sources, based on assumptions regarding the ability to distinguish $\delta^{13}C$ signatures at the base of the food web (Søreide et al. 2006). Isotopic fractionation associated with carbon fixation varies between primary producers due to isotopic discrimination and local variation in the availability of CO_2 for photosynthesis. In aquatic plants, isotopic discrimination varies according to the thickness of diffusive boundary layers, which affect the rate of CO_2, or HCO_3 - diffusion and availability (Hobson et al. 1995). These boundary layers differ among species and among environments, with variation determined by depth and proximity to shore (France 1995).

The $\delta^{13}C$ values of primary producers are also strongly influenced by the $\delta^{13}C$ value of the available DIC pool. Therefore, spatial and seasonal variability in $\delta^{13}C$ at the base of the food web is also shaped by physical parameters including temperature and sources of $(CO_2)_{aq}$ which impact $\delta^{13}C$-DIC values (McMahon et al. 2013). For example, productive systems, like the coastal zone, where nutrient concentrations are higher than in the open ocean, are typically more ^{13}C enriched compared to offshore, pelagic systems (France 1995). Coastal systems also have a wider variety of carbon sources available, with tight land-ocean and benthic–pelagic coupling leading to the availability/utilization of ^{13}C-heavy benthic algae and C4 marsh plants (France 1995; McMahon et al. 2013). This diversity of carbon sources, paired with a high degree of spatial and temporal variability in coastal environmental conditions, can also complicate the determination of dietary carbon sources for coastal organisms (Canuel and Hardison 2016).

Values of $\delta^{15}N$ are typically used to determine the trophic level of a consumer, since tissues are predictably enriched in $\delta^{15}N$ by 3–4‰ relative to its diet due to urinary loss of $\delta^{15}N$ depleted ammonium and urea (Peterson and Fry 1987). However, variation at the base of the food-web, due to spatially and seasonally variable inorganic nitrogen sources and heterotrophic processes, often complicate the interpretation of $\delta^{15}N$ values, particularly for lower trophic level organisms and in systems impacted by high seasonal and spatial variability in inorganic nitrogen sources (Post 2002).

3.2.2 Fatty acids

FA can be used as indicators of food source and quality. The first steps of *de novo* FA synthesis involve acetyl-CoA and fatty acid synthase for carbon chain elongation, which produce the saturated FA (SFA) 16:0, which is typically the most common FA found in the environment. Further elongation and unsaturation produce mono- (MUFA) and poly-unsaturated FA (PUFA). FA form the building blocks of more complex lipid classes, whose diverse metabolic functions play an essential role for life in polar regions (Hirche and Kattner 1993; Lee et al. 2006). Polar lipids, including phospholipids, form the structural components in cell membranes, keeping them fluid at low temperatures (De Carvalho and Caramujo 2018). Nonpolar storage lipids, such as wax esters or triacylglycerols (TAG) are essential for organisms adapted to the short growing season at high latitudes (Guschina and Harwood 2009). Several essential PUFA, including eicosapentaenoic acid (EPA), docosahexaenoic acid (DHA), alpha-linolenic acid (ALA) and arachidonic acid (ARA), are synthesized *de novo* by microbial organisms at the base of the food-web and heterotrophs and higher trophic level consumers need to acquire these from their diet. These 'essential' FA (EFA) are high quality food for consumers, and contribute to important biochemical processes on the individual level (Twining et al. 2016). Furthermore, FA synthesis is, to some degree, taxon-specific (Jónasdóttir 2019). For example, diatoms are known to produce 16:1n-7 and EPA (20:5n-3) while dinoflagellates produce C18-PUFAs (e.g., 18:4n-3). Bacteria are known to synthesize odd chain FA (e.g., 17:0, 15:0) while terrestrial vegetation produce long unsaturated FA (e.g., 22:0, 24:0) (Dalsgaard et al. 2003; Kelly and Scheibling 2012). Thus, fatty acid compositions in consumers have be used to differentiate utilization of various primary producers (Søreide et al. 2008; Connelly et al. 2014; McGovern et al. 2018).

3.2.3 Chiral analysis

Some POPs, including α-HCH, trans- and cis-chlordane, are chiral compounds. Chirality is defined as having two stereoisomers, which are identical in the number of atoms and bindings, but have different molecular structures. These structural enantiomers are mirror images of each other and are therefore not superimposable (Borgå and Bidleman 2005). While enantiomers have identical physicochemical properties, including hydrophobicity and abiotic degradation rates, they display differing interactions with biological molecules (Wong and Warner 2009; Lu et al. 2014). The ratio of the two enantiomers in technical mixtures is racemic (i.e. 1:1). However, these proportions can change as the compounds enter the environment and interact with enantioselective biotic processes. Thus, previous studies have used enantiomeric fractions (EFs) as tracers of contaminant cycling, where they can distinguish fresh and degraded sources in the environment (Bidleman et al. 1998; Bidleman and Falconer 1999; Carlsson et al. 2014). Historically deposited pesticides stored in Arctic glaciers should be relatively protected from microbial degradation compared to other sources. Thus, EFs may be a useful tool for tracing pesticides recently released from melting glaciers (Carlsson et al. 2014) into coastal food-webs, especially for lower- trophic level zooplankton which should reflect the chiral signature of their surrounding environment (Warner et al. 2005).

3.3 Data analysis

All data analyses were performed using R (R version 4.0.2 (2020-06-22); R Core Team (2021)). Data preparation relied heavily on the *tidyverse* ecosystem (Wickham et al. 2019), whose usage of non-standard 'tidy' evaluation creates a low threshold environment for carrying out a diverse array of data manipulation and transformations (Wickham 2019). All plotting was carried out in *ggplot2* (Wickham 2016) and modeling in *vegan* (Oksanen et al. 2007) and *tidymodels* (Kuhn and Wickham 2020), often facilitated by functional programming using *purrr* (Henry and Wickham 2020) or *furrr* (Vaughan and Dancho 2021). Papers 2 and 3 were written with a fully reproducible workflow (Gandrud 2018) whereby raw datafiles are left untouched and all data preparation and analysis are completed using Rstudio (Allaire 2012) scripts with version control and back-up using git/github. In addition, these manuscripts (as well as this thesis) were written in RMarkdown (Allaire et al. 2021) with all statistics included via inline code. Raw data are published and openly available in line with open science practices (McGovern et al. 2022b).

This thesis project had a set of very clear research questions and hypotheses. However, where exploratory analyses were carried out, these were tempered and guided by theory (in the form of causal diagrams) and statistics (e.g., correcting for multiple comparisons). In addition, we took a ‘weight of evidence’ approach, which was carried out on multiple levels, both through verification of patterns using several methods of analysis and/or statistical tests, and also by the sheer breadth of our paired dataset which allows for multiple perspectives into each research question.

Prior to analysis, basic data exploration was carried out according to protocols outlined by Zuur et al. (2010) to remove outliers and test for normality. We mainly relied on frequentists methods, including both traditional statistics and computational data science. Traditional statistical methods used included univariate statistics such as Kruskal-Wallis rank sum tests with a pairwise posthoc Dunn’s test, and multivariate analyses including PCA and RDA. In light of our often restricted sample sizes, we present the raw data where possible, and use bootstrapped confidence intervals for summarizing group means (Greenacre 2016),

For paper 3, we used random forest classification and regression, a data-driven machine learning method well suited to complex datasets. Computational advances in recent years have made these methods accessible, accelerating the pace and quality of science (Thessen 2016). Random forests are more flexible and have fewer assumptions compared to other methods we could have used to meet the same ends (e.g., multiple linear regression assumes linearity). Random forests allow for modelling of complex, multidimensional and non-linear datasets with missing values, and were thus a powerful tool for exploring relationships between the paired environmental and ecological datasets in this study (Thessen 2016; Vabalas et al. 2019).

4 Key findings

4.1 Paper 1

Terrestrial inputs drive seasonality in organic matter and nutrient biogeochemistry in a high Arctic fjord system (Isfjorden, Svalbard)

Climate change driven increases in terrestrial inputs to coastal waters have the potential to impact the fjord physical and chemical environment. This paper characterizes the seasonal and spatial footprint of freshwater runoff and its impacts on fjord stratification, light attenuation, inorganic nutrients and OM characteristics.

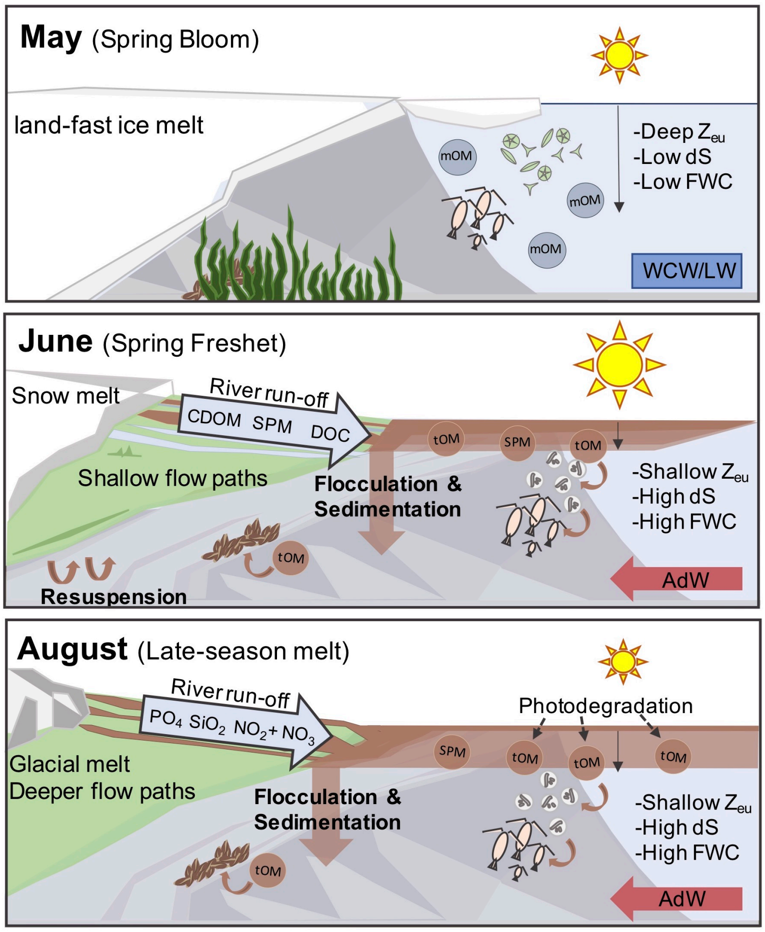

Figure 3. A conceptual diagram summarizing the article's main findings. This figure was borrowed from paper 1 (Figure 8).

Key findings:

1. In May, sea-ice covered the inner fjord arms of Isfjorden, and the majority of the region's rivers were frozen, with negligible freshwater runoff to the fjord. There was a deep euphotic zone (Zeu), and marine OM (mOM) was dominant in the water column following the spring phytoplankton bloom.

2. In June, the spring freshet was a source of CDOM and DOC to the fjord, with surprisingly high DOC concentrations (upwards of 1400 µmol/L) detected in river water samples. Freshwater-impacted areas were characterized by high concentrations of suspended particulate matter (SPM) and enhanced light attenuation. tOM was observed throughout the highly stratified (dS) and turbid fjord surface waters.

3. In August, glacier-fed rivers were a source of inorganic nutrients including nitrogen and phosphorus to Isfjorden. Highly stratified surface waters also had increased freshwater content (FWC) and degraded OM dominated throughout the fjord.

4.2 Paper 2

Turbid meltwater plumes diminish the quality of particulate organic matter available for Arctic coastal food-webs

Sediment-laden terrestrial inputs result in visible turbid meltwater plumes in Isfjorden. This paper investigates the relationships between meltwater-driven environmental gradients (paper 1) on the source and quality of fjord particulate organic matter (POM), and in turn zooplankton carbon sources using FA and stable isotopes.

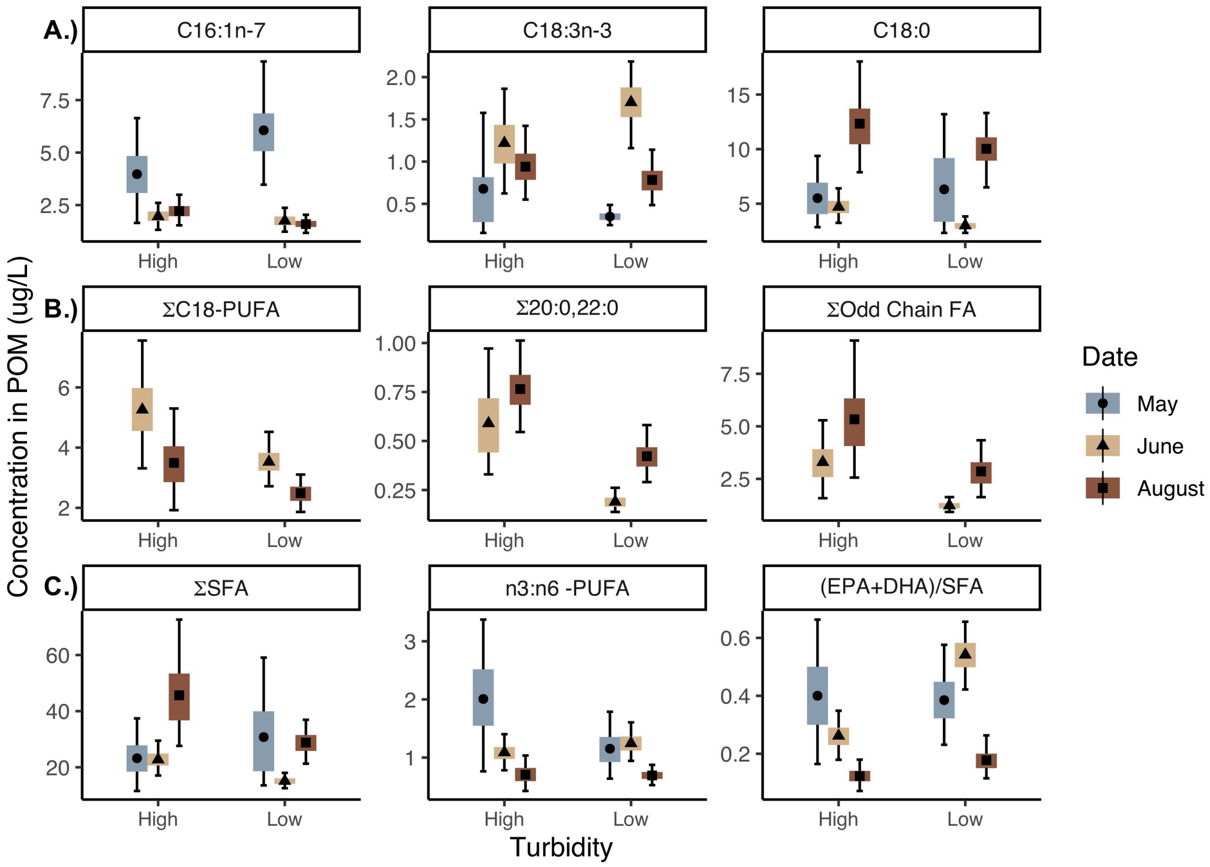

Figure 4. Confidence interval plots depicting (A) top 3 most important FA predictors of sampling month in the random forest classifier based on all FA in POM. (B) Important predictors of turbidity group (high (> 3 NTU) vs. low) in the random forest classifier for June and August POM. (C) OM-quality metrics for all samples. Black symbols indicate the sample mean, while the colored box represents the 50% bootstrapped confidence interval and the error bars the 95% bootstrapped confidence interval. This figure is borrowed from paper 2 (Figure 4).

Key findings

1. We observed seasonal variation in the composition and quality of potential food sources in Isfjorden surface waters. In the POM, the top three FA distinguishing the three sampling months were 16:1n-7, 18:3n-3 and 18:0, which summarize the observed seasonal transitions from the spring diatom bloom (16:1n-7) in May to the flagellate-dominated secondary bloom in June (18:3n-3), to late summer phytoplankton senescence (18:0). We also observed spatial differences in POM FA source and quality with turbid meltwater plumes associated with low quality FA and tOM in June and August.

2. Zooplankton FA profiles were strongly coupled to seasonal changes in water column POM, with profiles suggesting a shift from reliance on diatoms in May to flagellates and terrestrial material in June and August.

3. Strong spatial differences in June between high and low turbidity locations highlight the negative impacts of suspended sediments and associated light attenuation on food quality, but suggest that subsurface dinoflagellates and chrysophytes in the outer fjord are a source of high quality PUFA to fjord zooplankton in the weeks following the spring bloom.

4.3 Paper 3

Is glacial meltwater a secondary source of legacy contaminants to Arctic coastal food-webs?

The melting terrestrial cryosphere represents a potential secondary source of legacy contaminants to Arctic coastal areas. In this paper, POP concentrations in zooplankton and benthos are investigated in relation to meltwater-driven environmental gradients, food sources, and seasonal ecological processes in the water column.

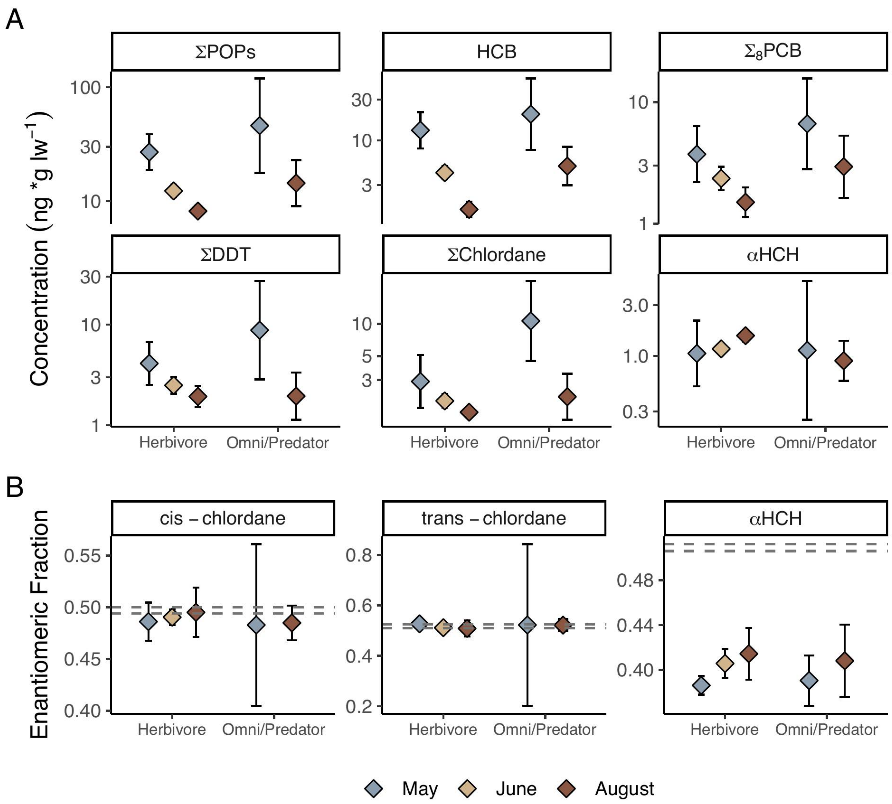

Figure 5. A) POP concentrations and (B) EFs in bulk zooplankton by month for each plankton type: Herbivorous zooplankton (*Calanus* spp., Meroplankton) and omnivorous and predator zooplankton (Macrozooplankton and Jellyplankton). Diamonds and error bars represent the bootstrapped mean and 95% confidence interval. $\sum_8$PCB is defined as the sum of all congeners, but CB-118, CB-138 and CB-180 were < LOD in zooplankton. The racemic ranges (determined using laboratory standards) are indicated as dashed gray lines. This figure is borrowed from paper 3 (Figure 2).

Key Findings:

1. Zooplankton contaminant concentrations were highest in May, when results of stable isotopes indicate dietary reliance on the spring phytoplankton bloom, highlighting the role of the spring bloom in the uptake of POPs into the marine food-web. Low concentrations in August were likely due to reduced exposure and lipid dilution as zooplankton accumulate storage lipids through the summer months.

2. While concentrations decreased from May to August for most contaminant groups, α-HCH, increased from May to June to August, alongside a more racemic enantiomeric fraction, suggesting that glacial meltwater is a source of α-HCH to Isfjorden biota.

3. While POPs in zooplankton responded primarily to seasonal variability in the water column, we did observe spatial patterns in the benthos in relation to terrestrial inputs and sources of local pollution. Benthos and sculpin (collected spatially only in August) in Billefjorden, which has a local source of PCBs, were more contaminated than those in Adventfjorden and Tempelfjorden, which have no local sources, and receive high loads of terrestrial inorganic sediments from glacial inputs.

5 Synthesis and perspectives

As permafrost thaws, and glaciers rapidly lose mass, the tight coupling between catchments and downstream ecosystems is expected to result in widespread impacts on Arctic coastal ecosystems. In Svalbard, the melt season progression on land and seasonal ecological processes in the water column resulted in strong seasonal variation in environmental conditions (paper 1), primary carbon source (paper 2) and contamination of coastal fauna (paper 3).

In Isfjorden, the terrestrial melt season spans from late May/June to September, with snow and glacial melt resulting in turbid meltwater plumes extending into the fjord. Remote sensing in Adventfjorden suggests tight coupling between plume extent and temperature-driven melting events in the catchment (Walch, in review). These temperature-driven meltwater plumes occur seasonally and spatially and shape the strong physicochemical gradients in the water column in June and August, with cascading effects on coastal food-webs. The breadth of the dataset collected from this field study allowed us to pair comprehensive data on environmental conditions with food-web and contaminant data in order to investigate the role of terrestrial inputs in shaping coastal food-webs and contamination.

5.1 Terrestrial inputs impact the fjord on seasonal and spatial gradients

The results of this work highlight the strong seasonal variation in physical and ecological processes in the high Arctic (Figure 6). The seasonal progression of the melt season on land is matched by strong seasonality in the water column where the extreme light regime at these high latitudes drives seasonal shifts in community structure and life history traits of resident coastal fauna (Leu et al., 2015; Søreide et al., 2010). These physical and ecological seasonal shifts also have implications for food source, quality and contamination of coastal food-webs. In particular, the spring bloom was a defining feature as a source of high quality OM (paper 1) and high quality particulate FA (paper 2) as well as a vector of POPs, including PCBs, HCB, DDTs, and chlordane pesticides, (paper 3) to fjord zooplankton. Subsequently, the snowmelt-driven spring freshet in June was a source of DOC to the fjord (paper 1), and glacial melt in August was a source of dissolved inorganic nutrients (paper 1), tOM (paper 2) and α-HCH (paper 3) to coastal areas.

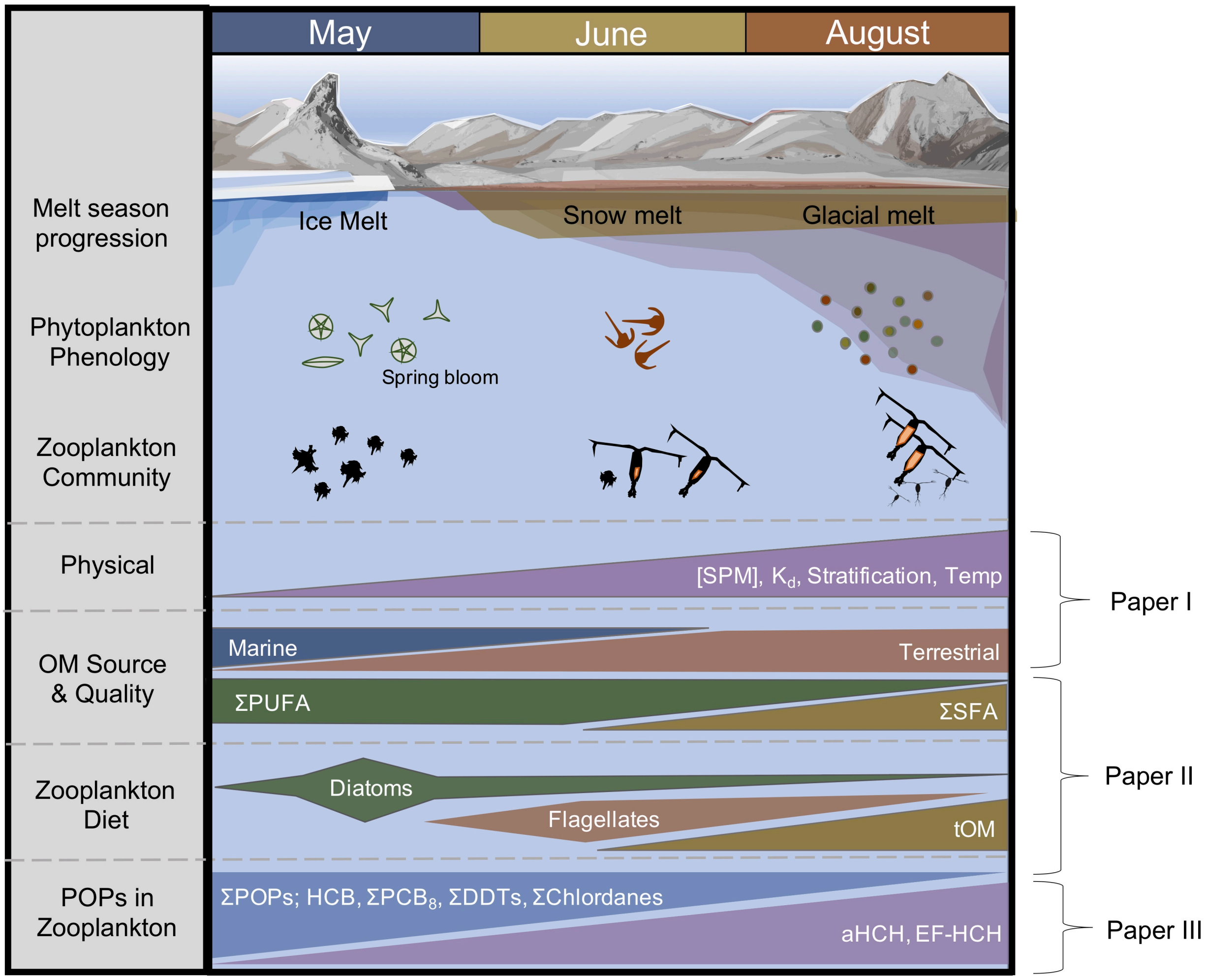

Figure 6. Conceptual diagram (adapted from paper 3) summarizing the seasonal variation in environmental conditions (paper 1), food-web carbon source (paper 2) and contamination of coastal fauna (paper 3) in relation to seasonal ecological processes in the water column.

The seasonal sampling carried out in 2018 was designed to target the seasonal variation in terrestrial inputs from before run-off (May) to spring freshet (June) to late seasonal glacial melt (August). However, we also positioned our sampling stations along the fjord gradient in an effort to capture a spatial gradient in freshwater inputs from (fresh) estuaries/glacier fronts to the outer (marine) fjord waters. Despite this sampling-design, we struggled to capture a continuous salinity gradient, with our samples rather falling on the two extremes: freshwater- or marine-dominated (paper 1). With very few previous studies investigating terrestrial inputs in Isfjorden, our 2018 study had a broad sampling design and scope. Based on results from the 2018 study, we carried out additional sampling in 2019 where we chose one estuary (Adventfjorden) and carried out a study using a gridded sampling design with high spatial and vertical resolution to better address the spatial gradient. From this follow-up study (paper 1) we observed strong gradients in environmental conditions, including light, OM and inorganic nutrients along the fjord axis in line with the same patterns observed at each extreme in 2018. While this additional study provided insight into the impacts of freshwater inputs on fjord biogeochemistry, we were not able to extend this study to food-web structure and contamination in the water column. Thus, our findings for papers 2 and 3 are dominated by seasonal trends with few strong spatial gradients. Because of this, interpretation of terrestrial impacts seasonally are intertwined with seasonal physical and ecological patterns in the water column. Nevertheless, with the help of the biogeochemical tracers used in this study, we were able to distinguish important impacts of terrestrial inputs on coastal food-web carbon source and contamination.

5.2 Impacts of terrestrial run-off on food-web carbon source

Terrestrial inputs were a direct source of tOM to the fjord in both particulate and dissolved forms. Results of stable isotopes and FA suggest that Isfjorden zooplankton utilized terrestrial carbon in June and August when high quality EFA, including EPA, were found in lower concentrations in the water column. Several other recent studies have also observed terrestrial carbon utilization along the Norwegian coast (McGovern et al. 2020) and in the Beaufort Sea Lagoons (Dunton et al. 2006, 2012; Bell et al. 2016; Mohan et al. 2016; Harris et al. 2018). Generally considered to be of low quality, these findings suggest that tOM is utilized when high quality food (e.g., diatoms) is not available. Utilization of terrestrial subsidies may be facilitated by the transformation and uptake of tOM by microbial communities, whose structure and functioning have been shown to shift in response to terrestrial inputs, with implications for the uptake of tOM into microbial food-webs (Sipler et al. 2017; Müller et al. 2018; Kellogg et al. 2019; Delpech et al. 2021). In this thesis project, we attempted to address this potential route of uptake in zooplankton using compound specific stable isotope analysis. In collaboration with Dr. Martin Kainz (WasserCluster Lunz), we extracted and analyzed odd-chain bacterial FA in POM and zooplankton with the hypothesis that these would demonstrate a more terrestrial carbon signature in June/August compared to May. However, these FA are found in very small concentrations, and we were unable to pool enough material to get a signal on the mass spectrophotometer. Thus, we are unable to draw a conclusion on whether terrestrial carbon is taken up directly by zooplankton (POC) or indirectly through the microbial loop (DOC). This is a topic that would be highly relevant for further study.

In addition to directly providing a terrestrial source of carbon to coastal biota, terrestrial inputs indirectly impacted zooplankton carbon source through impacts on light, nutrient availability, and temperature (Figure 7), which affect phytoplankton and bacterial community structure (Delpech et al., 2021), and in turn availability of essential PUFA in the water column. We observed a strong seasonal compositional shift from high quality PUFA in May to low quality SFA in August, reflecting typical seasonal trends from the spring phytoplankton bloom to nutrient-limited summer stratified periods (Leu et al. 2006; Mayzaud et al. 2013; Galloway and Winder 2015). While the overlap of seasonal phytoplankton phenology and impacts of the melt season are difficult to disentangle, the spatial differences observed in June highlight the negative impacts of terrestrial inputs on the availability of high quality FA. Turbid meltwater plumes, while a source of inorganic nutrients, rapidly attenuate light, reducing food quality, and availability of EFA, including EPA and DHA, for zooplankton in impacted surface waters.

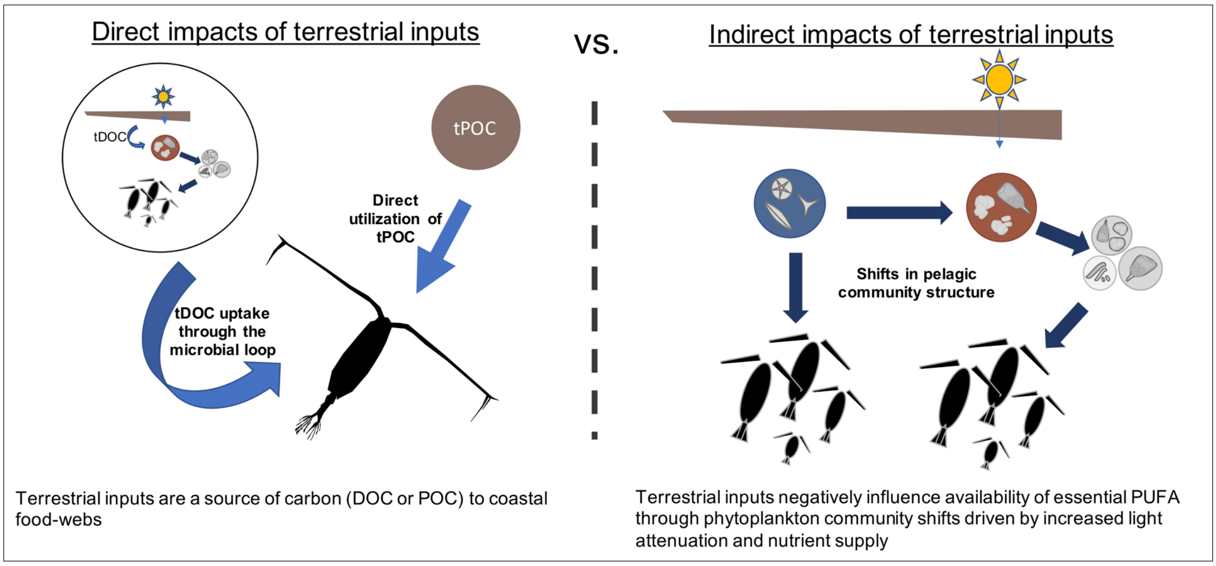

Figure 7. The direct and indirect effects of terrestrial runoff on zooplankton food-web structure.

5.3 Direct and indirect effects on contaminant trophodynamics

Contaminant dynamics in coastal ecosystems are governed by sources, the physical-chemical environment and characteristics of the contaminant of concern, as well as food-web carbon source and structure. Except for α-HCH, terrestrial inputs (as indicated by salinity and turbidity) were not related to increased concentrations of POPs in zooplankton and benthos. While we expected the rivers in Isfjorden to be a source of contamination (McGovern et al. 2022a), a parallel study suggests that riverine inputs may in fact have had the opposite effect, with their low contaminant and high sediment loads acting to dilute water column and sediment POP concentrations, and a potential for terrestrial particulate matter to bind and remove pollutants from the water column— potentially burying them on the sea-floor (Johansen et al. 2021). Thus, other source of POPs (Atlantic water inflow, local pollution, atmospheric deposition; Carlsson et al. (2018)) seem to be of greater importance to the contaminant load in coastal fauna than inputs of glacial meltwater in Isfjorden.

Food-web carbon source and structure were relevant to our results, but not in the way we expected. It was dietary reliance on marine phytoplankton (spring bloom) rather than terrestrial OM that led to enhanced accumulation of most contaminant groups measured (Figure 8). The spring bloom as a vector of contamination has been reported previously (Everaert et al. 2015; Ding et al. 2021) and could potentially lead to enhanced uptake of terrestrially derived contaminants if the timing of these events were to overlap in the future. For example, recent findings from Svalbard have pointed to snowmelt as a potential source of lower chlorinated PCBs (e.g., PCB-52) to coastal waters Johansen et al. (2021) which, if matched with the spring bloom, could facilitate uptake into the fjord food-web (Skogsberg et al. in review). We did not observe a relationship between terrestrial inputs and zooplankton reliance on microbial food sources, but in terms of shifts in food-web structure, we did find increased contributions of bacterial FA in zooplankton in May, which could partially explain the higher concentrations of POPs at that time. Environmental conditions suggest our sampling took place during a late-stage phytoplankton bloom. A different high-resolution seasonal study in Isfjorden in 2018 confirmed that the peak of the spring bloom occurred ~10 days prior to our sampling campaign (Nyeggen 2019). Thus, bacteria feeding on leftover high quality marine OM in the water column, and transferred into the pelagic food web via the microbial loop, may have provided additional trophic levels for biomagnification of POPs in the food-web.

Uncoupled from terrestrial inputs, we observed increased POP concentrations at higher trophic levels, as observed for other Svalbard studies on zooplankton (Hallanger et al. 2011b; Pouch et al. 2022). In addition, lipid dilution and changes in zooplankton community structure from May to August were likely strong drivers of the observed seasonal changes in contaminant concentrations.

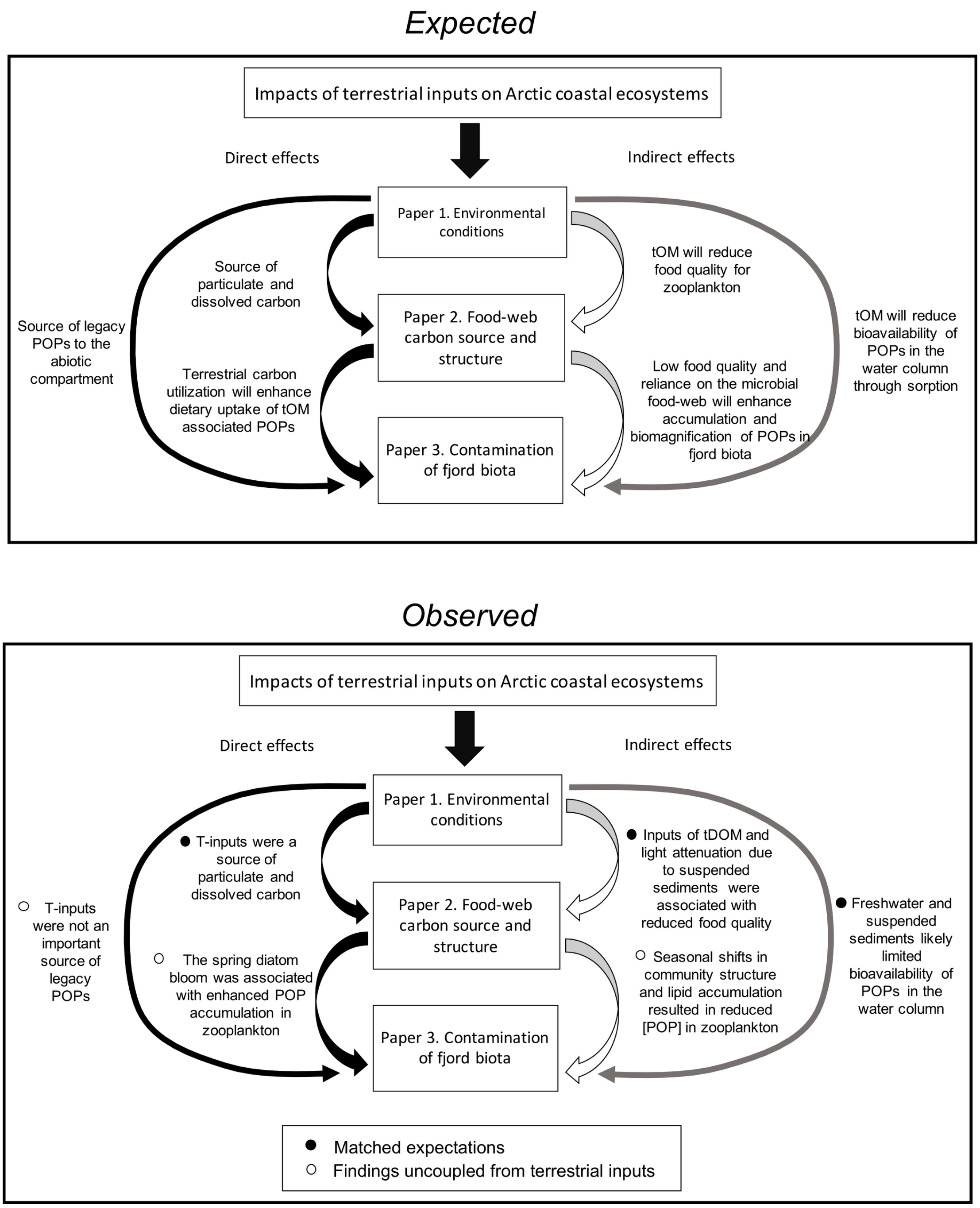

Figure 8. Expected and observed relationships between the direct and indirect effects of terrestrial inputs on environmental conditions (paper 1), and food-web carbon source (paper 2) and POPs in coastal zooplankton (paper 3).

5.4 Perspectives

This thesis provides a broad perspective on land-ocean interactions in a rapidly changing Arctic. Our results highlight the intense seasonality of high Arctic ecosystems, where the melt season on land intersects with seasonal ecological processes in the water column. The observed impacts of meltwater plumes from land-terminating glaciers on the fjord light climate and POM FA profiles suggest further coastal darkening due to increased tOM and suspended sediments loads will impact the quality of OM at the base of the food-web, with implications for pelagic and benthic communities.

While inputs from receding glaciers and thawing permafrost have extensive impacts on fjord biogeochemistry (paper 1) and the source and quality of OM supporting coastal food-webs (paper 2), our results suggest these inputs are not an important source of legacy contaminants to coastal fauna (paper 3). It is well established that POPs are present in the Svalbard terrestrial environment, however, they are transported from catchments to surface waters alongside high loads of freshwater and inorganic sediments, leading to low concentrations in runoff and terrestrial suspended particulate matter. However, the observed impacts of these turbid meltwater plumes on OM source and quality in the water column suggests that changes in terrestrial inputs likely do have implications for contaminant cycling, especially if those contaminants are coming from land. While meltwater was not an important source of legacy PCBs and pesticides to the Isfjorden system, this is not to say that it is not a source of other legacy pollutants that we did not measure, including mercury (Hg), a potent neurotoxin (Kim et al. 2016). In fact, recent findings from Isfjorden indicate terrestrial carbon in sediments is linked to increased abiotic Hg concentrations (Kim et al. 2020). Likewise, a parallel seasonal study in Adventfjord in 2018 links similar alterations in food-web carbon source, quality and structure to enhanced bioaccumulation of Hg in zooplankton during the melt season (Carrasco 2019).

Changes in sources and cycling of OM and contaminants in coastal areas due to increases in terrestrial run-off is relevant for coastal areas globally. In particular, Arctic coastlines, with their characteristic spring pulse of high primary productivity providing high quality FA to a lipid-based food-web, with excess production nurturing productive benthic ecosystems, could experience particularly strong alterations in ecosystem structure and functioning in the future due to enhanced land-ocean connectivity. In light of the vulnerability of coastal areas in the face of rapid climate change, and the potential impacts on coastal biogeochemical and commercial ecosystem services (CO_2 sink, seafood contamination), future work should consider the impacts of terrestrial inputs in order to predict and manage future changes and implications for society.

Works cited

Aksnes, D. L., N. Dupont, A. Staby, Ø. Fiksen, S. Kaartvedt, and J. Aure. 2009. Coastal water darkening and implications for mesopelagic regime shifts in norwegian fjords. Marine Ecology Progress Series **387**: 39–49.

Allaire, J. 2012. RStudio: Integrated development environment for r. Boston, MA **770**: 165–171.

Allaire, J., Y. Xie, J. McPherson, and others. 2021. Rmarkdown: Dynamic documents for r,.

Arias, P., N. Bellouin, E. Coppola, and others. 2021. Climate change 2021: The physical science basis. Contribution of working Group14 i to the sixth assessment report of the intergovernmental panel on climate change; technical summary.

Ask, J., J. Karlsson, L. Persson, P. Ask, P. Byström, and M. Jansson. 2009. Terrestrial organic matter and light penetration: Effects on bacterial and primary production in lakes. Limnology and Oceanography **54**: 2034–2040.

Aslam, S. N., C. Huber, A. G. Asimakopoulos, E. Steinnes, and Ø. Mikkelsen. 2019. Trace elements and polychlorinated biphenyls (PCBs) in terrestrial compartments of svalbard, norwegian arctic. Science of the Total Environment **685**: 1127–1138.

Bell, L. E., B. A. Bluhm, and K. Iken. 2016. Influence of terrestrial organic matter in marine food webs of the beaufort sea shelf and slope. Marine Ecology Progress Series **550**: 1–24.

Bidleman, T. F., and R. L. Falconer. 1999. Peer reviewed: Using enantiomers to trace pesticide emissions. Environmental science & technology **33**: 206A–209A.

Bidleman, T. F., L. M. Jantunen, H. Hung, J. Ma, G. A. Stern, B. Rosenberg, and J. Racine. 2015. Annual cycles of organochlorine pesticide enantiomers in arctic air suggest changing sources and pathways. Atmospheric Chemistry and Physics **15**: 1411–1420.

Blunden, J., and D. S. Arndt. 2016. State of the climate in 2015. Bulletin of the American Meteorological Society **97**: Si–S275.

Borgå, K., and T. F. Bidleman. 2005. Enantiomer fractions of organic chlorinated pesticides in arctic marine ice fauna, zooplankton, and benthos. Environmental science & technology **39**: 3464–3473.

Borgå, K., A. T. Fisk, P. F. Hoekstra, and D. C. Muir. 2004. Biological and chemical factors of importance in the bioaccumulation and trophic transfer of persistent organochlorine contaminants in arctic marine food webs. Environmental Toxicology and Chemistry: An International Journal **23**: 2367–2385.

Borgå, K., M. A. McKinney, H. Routti, K. J. Fernie, J. Giebichenstein, I. Hallanger, and D. C. Muir. 2022. The influence of global climate change on accumulation and toxicity of persistent organic pollutants and chemicals of emerging concern in arctic food webs. Environmental Science: Processes & Impacts.

Błaszczyk, M., D. Ignatiuk, A. Uszczyk, K. Cielecka-Nowak, M. Grabiec, J. Jania, M. Moskalik, and W. Walczowski. 2019. Freshwater input to the arctic fjord hornsund (svalbard).

Canuel, E. A., and A. K. Hardison. 2016. Sources, ages, and alteration of organic matter in estuaries. Annual Review of Marine Science **8**: 409–434.

Carlsson, P., K. Breivik, E. Brorström-Lundén, and others. 2018. Polychlorinated biphenyls (PCBs) as sentinels for the elucidation of arctic environmental change processes: A comprehensive review combined with ArcRisk project results. Environmental Science and Pollution Research **25**: 22499–22528.

Carlsson, P., J. Christensen, K. Borgå, R. Kallenborn, K. A. Pfaffhuber, J. Odland, L. Reiersen, and J. Pawlak. 2016. Influence of climate change on transport, levels, and effects of contaminants in northern areas. Arctic Monitoring and Assessment Programme.

Carlsson, P., G. Cornelissen, C. E. Bøggild, S. Rysgaard, J. Mortensen, and R. Kallenborn. 2012. Hydrology-linked spatial distribution of pesticides in a fjord system in greenland. Journal of Environmental Monitoring **14**: 1437–1443.

Carlsson, P., N. A. Warner, I. G. Hallanger, D. Herzke, and R. Kallenborn. 2014. Spatial and temporal distribution of chiral pesticides in calanus spp. From three arctic fjords. Environmental pollution **192**: 154–161.

Carmack, E., P. Winsor, and W. Williams. 2015. The contiguous panarctic riverine coastal domain: A unifying concept. Progress in Oceanography **139**: 13–23.

Carrasco, N. 2019. Seasonality in mercury bioaccumulation in particulate organic matter and zooplankton in a river-influenced arctic fjord (adventfjord, svalbard). Master’s thesis. UiT Norges arktiske universitet.

Connelly, T. L., D. Deibel, and C. C. Parrish. 2014. Trophic interactions in the benthic boundary layer of the beaufort sea shelf, arctic ocean: Combining bulk stable isotope and fatty acid signatures. Progress in Oceanography **120**: 79–92.

Cui, X., T. S. Bianchi, C. Savage, and R. W. Smith. 2016. Organic carbon burial in fjords: Terrestrial versus marine inputs. Earth and Planetary Science Letters **451**: 41–50.

Daase, M., S. Falk-Petersen, Ø. Varpe, and others. 2013. Timing of reproductive events in the marine copepod calanus glacialis: A pan-arctic perspective. Canadian journal of fisheries and aquatic sciences **70**: 871–884.

Daase, M., J. E. Søreide, and D. Martynova. 2011. Effects of food quality on naupliar development in calanus glacialis at subzero temperatures. Marine Ecology Progress Series **429**: 111–124.

Dalsgaard, J., M. S. John, G. Kattner, D. Müller-Navarra, and W. Hagen. 2003. Fatty acid trophic markers in the pelagic marine environment.

Darnaude, A. M. 2005. Fish ecology and terrestrial carbon use in coastal areas: Implications for marine fish production. Journal of Animal Ecology **74**: 864–876.

De Carvalho, C. C., and M. J. Caramujo. 2018. The various roles of fatty acids. Molecules **23**: 2583.

Delpech, L.-M., T. R. Vonnahme, M. McGovern, R. Gradinger, K. Præbel, and A. E. Poste. 2021. Terrestrial inputs shape coastal bacterial and archaeal communities in a high arctic fjord (isfjorden, svalbard). Frontiers in microbiology **12**: 295.

Ding, Q., X. Gong, M. Jin, X. Yao, L. Zhang, and Z. Zhao. 2021. The biological pump effects of phytoplankton on the occurrence and benthic bioaccumulation of hydrophobic organic contaminants (HOCs) in a hypereutrophic lake. Ecotoxicology and Environmental Safety **213**: 112017.

Duarte, C. M., S. Agusti, E. Barbier, and others. 2020. Rebuilding marine life. Nature **580**: 39–51.

Dunton, K. H., S. V. Schonberg, and L. W. Cooper. 2012. Food web structure of the alaskan nearshore shelf and estuarine lagoons of the beaufort sea. Estuaries and Coasts **35**: 416–435.

Dunton, K. H., T. Weingartner, and E. C. Carmack. 2006. The nearshore western beaufort sea ecosystem: Circulation and importance of terrestrial carbon in arctic coastal food webs. Progress in Oceanography **71**: 362–378.

Everaert, G., F. De Laender, P. L. Goethals, and C. R. Janssen. 2015. Multidecadal field data support intimate links between phytoplankton dynamics and PCB concentrations in marine sediments and biota. Environmental Science & Technology **49**: 8704–8711.

Fauchald, P., P. Arneberg, J. B. Debernard, S. Lind, E. Olsen, and V. H. Hausner. 2021. Poleward shifts in marine fisheries under arctic warming. Environmental Research Letters **16**: 074057.

Field, C. B., M. J. Behrenfeld, J. T. Randerson, and P. Falkowski. 1998. Primary production of the biosphere: Integrating terrestrial and oceanic components. science **281**: 237–240.

France, R. L. 1995. Differentiation between littoral and pelagic food webs in lakes using stable carbon isotopes. Limnology and Oceanography **40**: 1310–1313.

Frigstad, H., T. Andersen, D. O. Hessen, and others. 2013. Long-term trends in carbon, nutrients and stoichiometry in norwegian coastal waters: Evidence of a regime shift. Progress in Oceanography **111**: 113–124.

Galloway, A. W., and M. Winder. 2015. Partitioning the relative importance of phylogeny and environmental conditions on phytoplankton fatty acids. PloS one **10**: e0130053.

Gandrud, C. 2018. Reproducible research with r and RStudio, Chapman; Hall/CRC.

Giesbrecht, I. J. W., S. E. Tank, G. W. Frazer, and others. 2022. Watershed classification predicts streamflow regime and organic carbon dynamics in the northeast pacific coastal temperate rainforest. Global Biogeochemical Cycles e2021GB007047.

Gjelten, H. M., Ø. Nordli, K. Isaksen, and others. 2016. Air temperature variations and gradients along the coast and fjords of western spitsbergen. Polar Research **35**: 29878.

Gouin, T., J. M. Armitage, I. T. Cousins, D. C. Muir, C. A. Ng, L. Reid, and S. Tao. 2013. Influence of global climate change on chemical fate and bioaccumulation: The role of multimedia models. Environmental Toxicology and Chemistry **32**: 20–31.

Greenacre, M. 2016. Data reporting and visualization in ecology. Polar Biology **39**: 2189–2205.

Guschina, I. A., and J. L. Harwood. 2009. Algal lipids and effect of the environment on their biochemistry, p. 1–24. *In* Lipids in aquatic ecosystems. Springer.

Halbach, L., M. Vihtakari, P. Duarte, and others. 2019. Tidewater glaciers and bedrock characteristics control the phytoplankton growth environment in a fjord in the arctic. Frontiers in Marine Science **6**: 254.

Hallanger, I. G., A. Ruus, N. A. Warner, D. Herzke, A. Evenset, M. Schøyen, G. W. Gabrielsen, and K. Borgå. 2011a. Differences between arctic and atlantic fjord systems on bioaccumulation of persistent organic pollutants in zooplankton from svalbard. Science of the Total Environment **409**: 2783–2795.

Hallanger, I. G., N. A. Warner, A. Ruus, A. Evenset, G. Christensen, D. Herzke, G. W. Gabrielsen, and K. Borgå. 2011b. Seasonality in contaminant accumulation in arctic marine pelagic food webs using trophic magnification factor as a measure of bioaccumulation. Environmental Toxicology and Chemistry **30**: 1026–1035.

Hanssen-Bauer, I., E. Førland, H. Hisdal, S. Mayer, A. Sandø, and A. Sorteberg. 2019. Climate in svalbard 2100. A knowledge base for climate adaptation.

Hargrave, B. T., G. A. Phillips, W. P. Vass, P. Bruecker, H. E. Welch, and T. D. Siferd. 2000. Seasonality in bioaccumulation of organochlorines in lower trophic level arctic marine biota. Environmental science & technology **34**: 980–987.

Harris, C. M., N. D. McTigue, J. W. McClelland, and K. H. Dunton. 2018. Do high arctic coastal food webs rely on a terrestrial carbon subsidy? Food Webs **15**: e00081.

Henry, L., and H. Wickham. 2020. Purrr: Functional programming tools,.

Hermanson, M. H., E. Isaksson, D. Divine, C. Teixeira, and D. C. Muir. 2020. Atmospheric deposition of polychlorinated biphenyls to seasonal surface snow at four glacier sites on svalbard, 2013–2014. Chemosphere **243**: 125324.

Hermanson, M., K. Matthews, G. Johnson, E. Isaksson, C. Teixeira, D. C. Muir, and R. S. Van Wal. 2005. Historic PCB congener profiles in an ice core from svalbard, norway.

Hirche, H.-J., and G. Kattner. 1993. Egg production and lipid content of calanus glacialis in spring: Indication of a food-dependent and food-independent reproductive mode. Marine Biology **117**: 615–622.

Hobson, K. A., W. G. Ambrose Jr, and P. E. Renaud. 1995. Sources of primary production, benthic-pelagic coupling, and trophic relationships within the northeast water polynya: Insights from δ13C and δ15N analysis. Marine Ecology Progress Series **128**: 1–10.

Holding, J. M., S. Markager, T. Juul-Pedersen, M. L. Paulsen, E. F. Møller, L. Meire, and M. K. Sejr. 2019. Seasonal and spatial patterns of primary production in a high-latitude fjord affected by greenland ice sheet run-off. Biogeosciences **16**: 3777–3792.

Holmes, R. M., J. W. McClelland, B. J. Peterson, and others. 2012. Seasonal and annual fluxes of nutrients and organic matter from large rivers to the arctic ocean and surrounding seas. Estuaries and Coasts **35**: 369–382.

Hopwood, M. J., D. Carroll, T. Browning, L. Meire, J. Mortensen, S. Krisch, and E. P. Achterberg. 2018. Non-linear response of summertime marine productivity to increased meltwater discharge around greenland. Nature Communications **9**: 1–9.

Hopwood, M. J., D. Carroll, T. Dunse, and others. 2020. How does glacier discharge affect marine biogeochemistry and primary production in the arctic? The Cryosphere **14**: 1347–1383.

Hung, H., R. Kallenborn, K. Breivik, and others. 2010. Atmospheric monitoring of organic pollutants in the arctic under the arctic monitoring and assessment programme (AMAP): 1993–2006. Science of The Total Environment **408**: 2854–2873. doi:https://doi.org/10.1016/j.scitotenv.2009.10.044

Isaksen, K., E. Førland, A. Dobler, R. Benestad, J. Haugen, and A. Mezghani. 2017. Klimascenarioer for longyearbyen-området, svalbard. MET Norway Report **14**: 2017.

Johansen, S., A. Poste, I. Allan, A. Evenset, and P. Carlsson. 2021. Terrestrial inputs govern spatial distribution of polychlorinated biphenyls (PCBs) and hexachlorobenzene (HCB) in an arctic fjord system (isfjorden, svalbard). Environmental Pollution **281**: 116963.

Johnson, L. L., B. F. Anulacion, M. R. Arkoosh, and others. 2013. Effects of legacy persistent organic pollutants (POPs) in fish—current and future challenges. Fish Physiology **33**: 53–140.

Jones, R. I. 1992. The influence of humic substances on lacustrine planktonic food chains. Hydrobiologia **229**: 73–91.

Jonsson, S., A. Andersson, M. B. Nilsson, U. Skyllberg, E. Lundberg, J. K. Schaefer, S. Åkerblom, and E. Björn. 2017. Terrestrial discharges mediate trophic shifts and enhance methylmercury accumulation in estuarine biota. Science Advances **3**: e1601239.

Jónasdóttir, S. H. 2019. Fatty acid profiles and production in marine phytoplankton. Marine drugs **17**: 151.

Jørgensen, E. H., M. M. Vijayan, J.-E. A. Killie, N. Aluru, Ø. Aas-Hansen, and A. Maule. 2006. Toxicokinetics and effects of PCBs in arctic fish: A review of studies on arctic charr. Journal of Toxicology and Environmental Health, Part A **69**: 37–52.

Kallenborn, R., C. Halsall, M. Dellong, and P. Carlsson. 2012. The influence of climate change on the global distribution and fate processes of anthropogenic persistent organic pollutants. Journal of Environmental Monitoring **14**: 2854–2869.

Kanna, N., S. Sugiyama, Y. Ohashi, D. Sakakibara, Y. Fukamachi, and D. Nomura. 2018. Upwelling of macronutrients and dissolved inorganic carbon by a subglacial freshwater driven plume in bowdoin fjord, northwestern greenland. Journal of Geophysical Research: Biogeosciences **123**: 1666–1682.

Karlsson, J., Berggren,M., Ask, J., Byström, P., Jonsson, A., Laudon, H., et al., 2012. Terrestrial organic matter support of lake food webs: evidence from lake metabolism and stable hydrogen isotopes of consumers. Limnol. Oceanogr. 57, 1042–1048.

Karlsson, J., Bergström, A.-K., Byström, P., Gudasz, C., Rodríguez, P., Hein, C., 2015. Terrestrial organic matter input suppresses biomass production in lake ecosystems. Ecology 96, 2870–2876.

Kellogg, C. T., J. W. McClelland, K. H. Dunton, and B. C. Crump. 2019. Strong seasonality in arctic estuarine microbial food webs. Frontiers in microbiology 2628.

Kelly, J. R., and R. E. Scheibling. 2012. Fatty acids as dietary tracers in benthic food webs. Marine Ecology Progress Series **446**: 1–22.

Killingtveit, Å., L.-E. Pettersson, and K. Sand. 2003. Water balance investigations in svalbard. Polar Research **22**: 161–174.

Kim, H., S. Y. Kwon, K. Lee, and others. 2020. Input of terrestrial organic matter linked to deglaciation increased mercury transport to the svalbard fjords. Scientific reports **10**: 1–11.

Kim, K.-H., E. Kabir, and S. A. Jahan. 2016. A review on the distribution of hg in the environment and its human health impacts. Journal of hazardous materials **306**: 376–385.

Konik, M., M. Darecki, A. K. Pavlov, S. Sagan, and P. Kowalczuk. 2021. Darkening of the svalbard fjords waters observed with satellite ocean color imagery in 1997–2019. Frontiers in Marine Science.

Kuhn, M., and H. Wickham. 2020. Tidymodels: A collection of packages for modeling and machine learning using tidyverse principles. Boston, MA, USA.[(accessed on 10 December 2020)].

Larsson, P., A. Andersson, D. Broman, J. Nordbäck, and E. Lundberg. 2000. Persistent organic pollutants (POPs) in pelagic systems. AMBIO: A Journal of the Human Environment **29**: 202–209.

Le Fouest, V., M. Babin, and J.-É. Tremblay. 2013. The fate of riverine nutrients on arctic shelves. Biogeosciences **10**: 3661–3677.

Lee, R. F., W. Hagen, and G. Kattner. 2006. Lipid storage in marine zooplankton. Marine Ecology Progress Series **307**: 273–306.

Leu, E., S. Falk-Petersen, S. Kwaśniewski, A. Wulff, K. Edvardsen, and D. O. Hessen. 2006. Fatty acid dynamics during the spring bloom in a high arctic fjord: Importance of abiotic factors versus community changes. Canadian Journal of Fisheries and Aquatic Sciences **63**: 2760–2779.

Leu, E., C. Mundy, P. Assmy, K. Campbell, T. Gabrielsen, M. Gosselin, T. Juul-Pedersen, and R. Gradinger. 2015. Arctic spring awakening–steering principles behind the phenology of vernal ice algal blooms. Progress in Oceanography **139**: 151–170.

Lotze, H. K., H. S. Lenihan, B. J. Bourque, and others. 2006. Depletion, degradation, and recovery potential of estuaries and coastal seas. Science **312**: 1806–1809.

Lu, Z., A. T. Fisk, K. M. Kovacs, and others. 2014. Temporal and spatial variation in polychlorinated biphenyl chiral signatures of the greenland shark (somniosus microcephalus) and its arctic marine food web. Environmental pollution **186**: 216–225.

Lydersen, C., P. Assmy, S. Falk-Petersen, and others. 2014. The importance of tidewater glaciers for marine mammals and seabirds in svalbard, norway. Journal of Marine Systems **129**: 452–471.

Ma, J., H. Hung, C. Tian, and R. Kallenborn. 2011. Revolatilization of persistent organic pollutants in the arctic induced by climate change. Nature Climate Change **1**: 255–260.

Macdonald, R. 2000. Arctic estuaries and ice: A positive—negative estuarine couple, p. 383–407. *In* The freshwater budget of the arctic ocean. Springer.

Macdonald, R., E. Carmack, and D. Paton. 1999. Using the δ18O composition in landfast ice as a record of arctic estuarine processes. Marine Chemistry **65**: 3–24.

Macdonald, R., T. Harner, and J. Fyfe. 2005. Recent climate change in the arctic and its impact on contaminant pathways and interpretation of temporal trend data. Science of the total environment **342**: 5–86.

Mayzaud, P., M. Boutoute, M. Noyon, F. Narcy, and S. Gasparini. 2013. Lipid and fatty acids in naturally occurring particulate matter during spring and summer in a high arctic fjord (kongsfjorden, svalbard). Marine biology **160**: 383–398.

McClelland, J. W., R. Holmes, K. Dunton, and R. Macdonald. 2012. The arctic ocean estuary. Estuaries and Coasts **35**: 353–368.

McClelland, J. W., R. M. Holmes, B. J. Peterson, and others. 2008. Development of a pan-arctic database for river chemistry. Eos, Transactions American Geophysical Union **89**: 217–218.

McGovern, M., J. Berge, B. Szymczycha, J. M. Węsławski, and P. E. Renaud. 2018. Hyperbenthic food-web structure in an arctic fjord. Marine Ecology Progress Series **603**: 29–46.

McGovern, M., K. Borgå, Heimstad Eldbjørg, A. Russ, G. Christensen, and A. Evenset. 2022a. Small arctic rivers transport legacy contaminants from thawing catchments to coastal areas in kongsfjorden, svalbard. Environmental Pollution revised.

McGovern, M., A. Evenset, K. Borgå, and others. 2019. Implications of coastal darkening for contaminant transport, bioavailability, and trophic transfer in northern coastal waters. Environmental Science and Technology.

McGovern, M., A. E. Poste, E. Oug, P. E. Renaud, and H. C. Trannum. 2020. Riverine impacts on benthic biodiversity and functional traits: A comparison of two sub-arctic fjords. Estuarine, Coastal and Shelf Science **240**: 106774.

McGovern, M., N. A. Warner, and A. E. Poste. 2022b. Replication Data for: Is glacial meltwater a secondary source of legacy contaminants to Arctic coastal food-webs?doi:10.18710/KYIZOQ

McMahon, K. W., L. L. Hamady, and S. R. Thorrold. 2013. A review of ecogeochemistry approaches to estimating movements of marine animals. Limnology and oceanography **58**: 697–714.

Meire, L., J. Mortensen, P. Meire, and others. 2017. Marine-terminating glaciers sustain high productivity in greenland fjords. Global Change Biology **23**: 5344–5357.

Meredith, M., M. Sommerkorn, S. Cassota, and others. 2019. Polar regions.

Mohan, S. D., T. L. Connelly, C. M. Harris, K. H. Dunton, and J. W. McClelland. 2016. Seasonal trophic linkages in arctic marine invertebrates assessed via fatty acids and compound-specific stable isotopes. Ecosphere **7**: e01429.

Mustaffa, N. I. H., L. Kallajoki, J. Biederbick, F. I. Binder, A. Schlenker, and M. Striebel. 2020. Coastal ocean darkening effects via terrigenous DOM addition on plankton: An indoor mesocosm experiment. Frontiers in Marine Science.

Müller, O., L. Seuthe, G. Bratbak, and M. L. Paulsen. 2018. Bacterial response to permafrost derived organic matter input in an arctic fjord. Frontiers in Marine Science **5**: 263.

Nicu, I. C., K. Stalsberg, L. Rubensdotter, V. V. Martens, and A.-C. Flyen. 2020. Coastal erosion affecting cultural heritage in svalbard. A case study in hiorthhamn (adventfjorden)—an abandoned mining settlement. Sustainability **12**: 2306.

Nowak, A., R. Hodgkins, A. Nikulina, and others. 2021. From land to fjords: The review of svalbard hydrology from 1970 to 2019 (SvalHydro).

Nowak, A., and A. Hodson. 2015. On the biogeochemical response of a glacierized high arctic watershed to climate change: Revealing patterns, processes and heterogeneity among micro-catchments. Hydrological Processes **29**: 1588–1603.

Nuth, C., J. Kohler, M. König, A. Von Deschwanden, J. Hagen, A. Kääb, G. Moholdt, and R. Pettersson. 2013. Decadal changes from a multi-temporal glacier inventory of svalbard. The Cryosphere **7**: 1603–1621.

Nyeggen, M. U. 2019. Seasonal zooplankton dynamics in svalbard coastal waters: The shifting dominance of mero-and holoplankton and timing of reproduction in three species of copepoda. Master's thesis. The University of Bergen.

Oksanen, J., R. Kindt, P. Legendre, B. O'Hara, M. H. H. Stevens, M. J. Oksanen, and M. Suggests. 2007. The vegan package. Community ecology package **10**: 719.

Opdal, A. F., C. Lindemann, and D. L. Aksnes. 2019. Centennial decline in north sea water clarity causes strong delay in phytoplankton bloom timing. Global change biology **25**: 3946–3953.

Osuch, M., and T. Wawrzyniak. 2017. Inter-and intra-annual changes in air temperature and precipitation in western spitsbergen. International Journal of Climatology **37**: 3082–3097.

Pavlov, A. K., E. Leu, D. Hanelt, and others. 2019. The underwater light climate in kongsfjorden and its ecological implications, p. 137–170. *In* The ecosystem of kongsfjorden, svalbard. Springer.

Pelt, W. J. van, T. V. Schuler, V. A. Pohjola, and R. Pettersson. 2021. Accelerating future mass loss of svalbard glaciers from a multi-model ensemble. Journal of Glaciology **67**: 485–499.

Peterson, B. J., and B. Fry. 1987. Stable isotopes in ecosystem studies. Annual review of ecology and systematics **18**: 293–320.

Post, D. M. 2002. Using stable isotopes to estimate trophic position: Models, methods, and assumptions. Ecology **83**: 703–718.

Poste, A. E., C. S. Hoel, T. Andersen, M. T. Arts, P.-J. Færøvig, and K. Borgå. 2019. Terrestrial organic matter increases zooplankton methylmercury accumulation in a brown-water boreal lake. Science of the Total Environment **674**: 9–18.

Pouch, A., A. Zaborska, A. M. Dąbrowska, and K. Pazdro. 2022. Bioaccumulation of PCBs, HCB and PAHs in the summer plankton from west spitsbergen fjords. Marine Pollution Bulletin **177**: 113488.

R Core Team. 2021. R: A language and environment for statistical computing, R Foundation for Statistical Computing.

Rawlins, M. A., M. Steele, M. M. Holland, and others. 2010. Analysis of the arctic system for freshwater cycle intensification: Observations and expectations. Journal of Climate **23**: 5715–5737.

Ripszam, M., J. Paczkowska, J. Figueira, C. Veenaas, and P. Haglund. 2015. Dissolved organic carbon quality and sorption of organic pollutants in the baltic sea in light of future climate change. Environmental science & technology **49**: 1445–1452.

Sessford, E. G., M. G. Bæverford, and A. Hormes. 2015. Terrestrial processes affecting unlithified coastal erosion disparities in central fjords of svalbard. Polar Research **34**: 24122.

Sipler, R. E., C. T. Kellogg, T. L. Connelly, Q. N. Roberts, P. L. Yager, and D. A. Bronk. 2017. Microbial community response to terrestrially derived dissolved organic matter in the coastal arctic. Frontiers in microbiology **8**: 1018.

Skogsberg, E., M. McGovern, A. E. Poste, S. Jonsson, M. Arts, Ø. Varpe, and K. Borgå. in review. Seasonal pollutant levels in littoral high-arctic amphipods in relation to food sources and terrestrial run-off. Environmental Pollution.

Smith, R. W., T. S. Bianchi, M. Allison, C. Savage, and V. Galy. 2015. High rates of organic carbon burial in fjord sediments globally. Nature Geoscience **8**: 450–453.

Sverdrup, H. 1953. On conditions for the vernal blooming of phytoplankton. J. Cons. Int. Explor. Mer **18**: 287–295.

Szeligowska, M., E. Trudnowska, R. Boehnke, A. M. Dąbrowska, J. M. Wiktor, S. Sagan, and K. Błachowiak-Samołyk. 2020. Spatial patterns of particles and plankton in the warming arctic fjord (isfjorden, west spitsbergen) in seven consecutive mid-summers (2013–2019). Frontiers in Marine Science **7**: 584.

Søreide, J. E., S. Falk-Petersen, E. N. Hegseth, H. Hop, M. L. Carroll, K. A. Hobson, and K. Blachowiak-Samolyk. 2008. Seasonal feeding strategies of calanus in the high-arctic svalbard region. Deep Sea Research Part II: Topical Studies in Oceanography **55**: 2225–2244.

Søreide, J. E., E. V. Leu, J. Berge, M. Graeve, and S. Falk-Petersen. 2010. Timing of blooms, algal food quality and calanus glacialis reproduction and growth in a changing arctic. Global change biology **16**: 3154–3163.

Søreide, J. E., T. Tamelander, H. Hop, K. A. Hobson, and I. Johansen. 2006. Sample preparation effects on stable c and n isotope values: A comparison of methods in arctic marine food web studies. Marine Ecology Progress Series **328**: 17–28.

Talley, D. M., G. R. Huxel, and M. Holyoak. 2006. Connectivity at the land-water interface. CONSERVATION BIOLOGY SERIES-CAMBRIDGE- **14**: 97.

Terhaar, J., R. Lauerwald, P. Regnier, N. Gruber, and L. Bopp. 2021. Around one third of current arctic ocean primary production sustained by rivers and coastal erosion. Nature Communications **12**: 1–10.

Thessen, A. 2016. Adoption of machine learning techniques in ecology and earth science. One Ecosystem **1**: e8621.

Thrush, S., J. Hewitt, V. Cummings, J. Ellis, C. Hatton, A. Lohrer, and A. Norkko. 2004. Muddy waters: Elevating sediment input to coastal and estuarine habitats. Frontiers in Ecology and the Environment **2**: 299–306.

Trudnowska, E., A. Dąbrowska, R. Boehnke, M. Zajączkowski, and K. Blachowiak-Samolyk. 2020. Particles, protists, and zooplankton in glacier-influenced coastal Svalbard waters. Estuarine, Coastal and Shelf Science 242: 106842.

Twining, C. W., J. T. Brenna, N. G. Hairston Jr, and A. S. Flecker. 2016. Highly unsaturated fatty acids in nature: What we know and what we need to learn. Oikos **125**: 749–760.

Ugelstad, C. P. 2019. Riverine and glacier influence on infaunal benthic communities in isfjorden, svalbard. Master's thesis. UiT Norges arktiske universitet.

Vabalas, A., E. Gowen, E. Poliakoff, and A. J. Casson. 2019. Machine learning algorithm validation with a limited sample size. PloS one **14**: e0224365.

Vallières, C., L. Retamal, P. Ramlal, C. L. Osburn, and W. F. Vincent. 2008. Bacterial production and microbial food web structure in a large arctic river and the coastal arctic ocean. Journal of Marine Systems **74**: 756–773.

Van Oostdam, J., S. G. Donaldson, M. Feeley, and others. 2005. Human health implications of environmental contaminants in arctic canada: A review. Science of the total environment **351**: 165–246.

Vaughan, D., and M. Dancho. 2021. Furrr: Apply mapping functions in parallel using futures,.

Ver, L. M. B., F. T. Mackenzie, and A. Lerman. 1999. Carbon cycle in the coastal zone: Effects of global perturbations and change in the past three centuries. Chemical Geology **159**: 283–304.

Vereide, E. H. 2019. Seasonal zooplankton community patterns along a gradient from land to sea in isfjorden, svalbard. Master's thesis.

Walch DMR, Singh RK , Søreide JE, Lantuit H, Poste A (in review) Spatio-temporal variability of suspended particulate matter in a high-Arctic estuary (Adventfjorden, Svalbard). using Sentinel-2 timeseries. Remote Sensing.

Wania, F., M. J. Binnington, and M. S. Curren. 2017. Mechanistic modeling of persistent organic pollutant exposure among indigenous arctic populations: Motivations, challenges, and benefits. Environmental Reviews **25**: 396–407.

Wania, F., and D. Mackay. 1993. Global fractionation and cold condensation of low volatility organochlorine compounds in polar regions. Ambio 10–18.

Warner, N. A., R. J. Norstrom, C. S. Wong, and A. T. Fisk. 2005. Enantiomeric fractions of chiral polychlorinated biphenyls provide insights on biotransformation capacity of arctic biota. Environmental Toxicology and Chemistry: An International Journal **24**: 2763–2767.

Wawrzyniak, T., and M. Osuch. 2020. A 40-year high arctic climatological dataset of the polish polar station hornsund (SW spitsbergen, svalbard). Earth System Science Data **12**: 805–815.

Wawrzyniak, T., M. Osuch, J. Napiórkowski, and S. Westermann. 2016. Modelling of the thermal regime of permafrost during 1990–2014 in hornsund, svalbard. Polish Polar Research 219–242.

Wickham, H. 2016. ggplot2: Elegant graphics for data analysis, Springer-Verlag New York.

Wickham, H. 2019. Advanced r, chapman; hall/CRC.

Wickham, H., M. Averick, J. Bryan, and others. 2019. Welcome to the tidyverse. Journal of Open Source Software **4**: 1686. doi:10.21105/joss.01686

Winder, M., J. Carstensen, A. W. Galloway, H. H. Jakobsen, and J. E. Cloern. 2017. The land–sea interface: A source of high-quality phytoplankton to support secondary production. Limnology and Oceanography **62**: S258–S271.

Wollschläger, J., P. J. Neale, R. L. North, M. Striebel, and O. Zielinski. 2021. Climate change and light in aquatic ecosystems: Variability & ecological consequences. Frontiers in Marine Science **8**: 506.

Wong, C. S., and N. A. Warner. 2009. Chirality as an environmental forensics tool, John Wiley & Sons, Ltd: Chichester, UK.

Wong, F., H. Hung, H. Dryfhout-Clark, and others. 2021. Time trends of persistent organic pollutants (POPs) and chemicals of emerging arctic concern (CEAC) in arctic air from 25 years of monitoring. Science of the Total Environment **775**: 145109.

Wöhrnschimmel, H., M. MacLeod, and K. Hungerbuhler. 2012. Global multimedia source-receptor relationships for persistent organic pollutants during use and after phase-out. Atmospheric Pollution Research **3**: 392–398.

Wöhrnschimmel, H., M. MacLeod, and K. Hungerbuhler. 2013. Emissions, fate and transport of persistent organic pollutants to the arctic in a changing global climate. Environmental science & technology **47**: 2323–2330.

Xu, W., X. Wang, and Z. Cai. 2013. Analytical chemistry of the persistent organic pollutants identified in the stockholm convention: A review. Analytica Chimica Acta **790**: 1–13.

Zuur, A. F., E. N. Ieno, and C. S. Elphick. 2010. A protocol for data exploration to avoid common statistical problems. Methods in ecology and evolution **1**: 3–14.

Paper 1

frontiers in Marine Science

ORIGINAL RESEARCH
published: 08 September 2020
doi: 10.3389/fmars.2020.542563

Terrestrial Inputs Drive Seasonality in Organic Matter and Nutrient Biogeochemistry in a High Arctic Fjord System (Isfjorden, Svalbard)

Maeve McGovern[1,2,3], Alexey K. Pavlov[4,5], Anne Deininger[1,6], Mats A. Granskog[7], Eva Leu[4], Janne E. Søreide[3] and Amanda E. Poste[1]**

[1] Norwegian Institute for Water Research, Oslo, Norway, [2] Department of Arctic and Marine Biology, UiT: The Arctic University of Norway, Tromsø, Norway, [3] University Centre in Svalbard, Longyearbyen, Norway, [4] Akvaplan-niva, Fram Centre, Tromsø, Norway, [5] Institute of Oceanology, Polish Academy of Sciences, Sopot, Poland, [6] Center for Coastal Research, University of Agder, Kristiansand, Norway, [7] Norwegian Polar Institute, Fram Centre, Tromsø, Norway

OPEN ACCESS

Edited by:
Susana Agusti,
King Abdullah University of Science and Technology, Saudi Arabia

Reviewed by:
Maria Lund Paulsen,
Aarhus University, Denmark
Rainer M. W. Amon,
Texas A&M University, United States

***Correspondence:**
Maeve McGovern
maeve.mcgovern@niva.no
Amanda E. Poste
amanda.poste@niva.no

Specialty section:
This article was submitted to Global Change and the Future Ocean, a section of the journal Frontiers in Marine Science

Received: *13 March 2020*
Accepted: *17 August 2020*
Published: *08 September 2020*

Citation:
McGovern M, Pavlov AK, Deininger A, Granskog MA, Leu E, Søreide JE and Poste AE (2020) Terrestrial Inputs Drive Seasonality in Organic Matter and Nutrient Biogeochemistry in a High Arctic Fjord System (Isfjorden, Svalbard). Front. Mar. Sci. 7:542563. doi: 10.3389/fmars.2020.542563

Climate-change driven increases in temperature and precipitation are leading to increased discharge of freshwater and terrestrial material to Arctic coastal ecosystems. These inputs bring sediments, nutrients and organic matter (OM) across the land-ocean interface with a range of implications for coastal ecosystems and biogeochemical cycling. To investigate responses to terrestrial inputs, physicochemical conditions were characterized in a river- and glacier-influenced Arctic fjord system (Isfjorden, Svalbard) from May to August in 2018 and 2019. Our observations revealed a pervasive freshwater footprint in the inner fjord arms, the geochemical properties of which varied spatially and seasonally as the melt season progressed. In June, during the spring freshet, rivers were a source of dissolved organic carbon (DOC; with concentrations up to 1410 μmol L^{-1}). In August, permafrost and glacial-fed meltwater was a source of inorganic nutrients including $NO_2 + NO_3$, with concentrations 12-fold higher in the rivers than in the fjord. While marine OM dominated in May following the spring phytoplankton bloom, terrestrial OM was present throughout Isfjorden in June and August. Results suggest that enhanced land-ocean connectivity could lead to profound changes in the biogeochemistry and ecology of Svalbard fjords. Given the anticipated warming and associated increases in precipitation, permafrost thaw and freshwater discharge, our results highlight the need for more detailed seasonal field sampling in small Arctic catchments and receiving aquatic systems.

Keywords: climate change, coastal biogeochemistry, dissolved organic matter, freshwater inputs, glacier runoff, light climate, permafrost, land-ocean interactions

INTRODUCTION

Recent climate change driven increases in air temperature and precipitation are changing the timing, magnitude and geochemical nature of freshwater runoff with unknown implications for Arctic coastal waters. The observed changes in climate have been distinct in the high-Arctic Svalbard archipelago (e.g., Adakudlu et al., 2019; van Pelt et al., 2019) where marine and land-terminating glaciers are shrinking in size (van Pelt et al., 2019) and where the upper layer of permafrost, where large amounts of organic carbon are stored (Tarnocai et al., 2009) is warming (Grosse et al., 2016; Biskaborn et al., 2019), and active layer depth is increasing (Christiansen et al., 2005). Together with increased precipitation and freshwater discharge (Peterson et al., 2002; McClelland et al., 2006; Adakudlu et al., 2019), the thawing terrestrial cryosphere is expected to lead to the mobilization and transport of dissolved and particulate organic and inorganic matter from Arctic watersheds to coastal waters (Parmentier et al., 2017).

In central Svalbard, snowmelt typically occurs in June (van Pelt et al., 2016) alongside high river discharge (Hodson et al., 2016). The permafrost active layer is deepest in August (Christiansen et al., 2005), a typically low discharge period (Hodson et al., 2016) when glacial-meltwater has higher residence time in the catchment. Seasonal changes in catchment hydrology have implications for the transport and bioavailability of carbon and nutrients in glacial meltwater on Svalbard (Nowak and Hodson, 2015; Koziol et al., 2019) and elsewhere in the Arctic (Neff et al., 2006; Holmes et al., 2008; Spencer et al., 2008). For example, carbon delivered during spring freshet in Alaskan rivers is more labile compared to aged, microbially reworked carbon delivered later in the summer (Holmes et al., 2008). While seasonal changes in river physicochemistry have been well documented for the Great Arctic rivers (e.g., Holmes et al., 2011), seasonal data from small Arctic catchments are scarce, making it difficult to assess potential impacts on receiving near-shore and coastal waters.

Arctic fjord estuaries are biogeochemical hotspots for the cycling of organic matter (OM) (Bianchi et al., 2020) and burial of carbon (Smith et al., 2015; Bianchi et al., 2018). The fate of terrestrial materials in the marine system is linked to physical and biological processes in the water column. Flocculation and sedimentation at the land-ocean interface (Meslard et al., 2018), and photodegradation and mineralization can act to remove OM from the water column while uptake by coastal biota can integrate terrestrial OM into the marine food-web (Parsons et al., 1989; Harris et al., 2018). Turbid freshwater plumes can also stratify the water column and inhibit nutrient-rich deep water renewal (Torsvik et al., 2019), while also rapidly attenuating light critical for photosynthesis (Murray et al., 2015; Holinde and Zielinski, 2016; Pavlov et al., 2019), with implications for the autotrophic: heterotrophic balance in nearshore areas (Wikner and Andersson, 2012). Despite the rapid warming documented in the high Arctic (IPCC, 2014; Adakudlu et al., 2019), little is known regarding how these changes will affect the quantity and quality of materials transported to and through near-shore, fjord and coastal systems and thus their potential impacts on local and regional biogeochemical cycles (Parmentier et al., 2017).

To address these knowledge gaps, we studied the impacts of inputs from marine terminating glaciers and rivers on light, stratification, nutrient and OM dynamics in Isfjorden (Svalbard). To evaluate seasonal changes in runoff and associated impacts (snow melt vs. glacial melt/permafrost erosion), we targeted three stages of the melt season (1) pre-freshet in May, (2) spring freshet in June, and (3) late-summer runoff in August. Specifically, we aimed to identify the spatial and seasonal response in fjord physicochemical conditions and OM characteristics and evaluate how these might change with the future projected changes in freshwater runoff on Svalbard.

MATERIALS AND METHODS

Sampling Location

Fieldwork took place in 2018 and 2019 in Isfjorden, the largest fjord system on the West coast of Spitsbergen, Svalbard (**Figures 1a,b**). Isfjorden exchanges waters with the west Spitsbergen shelf, where the West Spitsbergen Current (WSC) and the Spitsbergen Polar Current (SPC) bring Atlantic and Arctic waters, which enter the fjord along the southern shore and exit the fjord along the northern coastline (Nilsen et al., 2016; **Figure 1c**). Isfjorden has several fjord arms (e.g., Fraser et al., 2018). Tempelfjorden and Billefjorden and the northern side of Isfjorden have marine terminating glaciers, which are absent from the southern side of Isfjorden, including Adventfjorden (**Figure 1b**). Of the sampled fjord arms, only Billefjorden has a shallow sill (50 m) at the entrance, which typically inhibits water mass exchange with adjacent (or central) parts of Isfjorden (Nilsen et al., 2008). The intrusion of warm and saline Atlantic water from the WSC (Fraser et al., 2018) facilitates the melting of Svalbard glaciers (Luckmann et al., 2015). In turn, runoff from glaciers and rivers contribute to estuarine circulation in the fjord (Torsvik et al., 2019). The rivers sampled in this study have catchments ranging from (55–725 km^2) in size with varying degrees of glacial cover (10–51%; pers. com. Guerrero, 2019).

Sample Collection and Processing

In 2018, samples were collected in May (10th–11th), June (18th–24th), and August (16th–24th), from a total of 17 different stations in Isfjorden along gradients from rivers and glaciers to the outer fjord (**Figure 1a**). The number of stations sampled each month varied due to presence of ice in May (**Figure 1a**), when additional fjord transect stations were sampled at the land-fast ice edge in the fjord arms, and where the innermost stations were not accessible. In 2019, the same sampling techniques were used in Adventfjorden with a higher spatial resolution, during June (15th–17th) and August (7th–9th; **Figure 1b**). Samples were collected from 8 stations in Adventfjorden as well as 2 rivers (Adventelva and Longyearelva). At each fjord station, water samples were collected from up to 5 depths (surface, 2 m, 5 m, 15 m, and 30 m) depending on station depth.

In both sampling years, a CTD profiler (SD204, SAIV A/S or Seabird SBE 911) was used to collect vertical profiles of salinity, temperature and chlorophyll fluorescence. Secchi depth was measured and light measurements were made using optical sensors. In 2018, a PAR cosine-corrected sensor was used to obtain vertical profiles of photosynthetically active radiation (PAR, 400–700 nm) while in 2019, TrioS Ramses ACC-VIS hyperspectral radiometers (one for profiling, one as a surface reference) were used to obtain downwelling planar irradiance profiles. At all stations, water was collected from the surface and 15 m using a Niskin bottle. At stations shallower than 17 m,

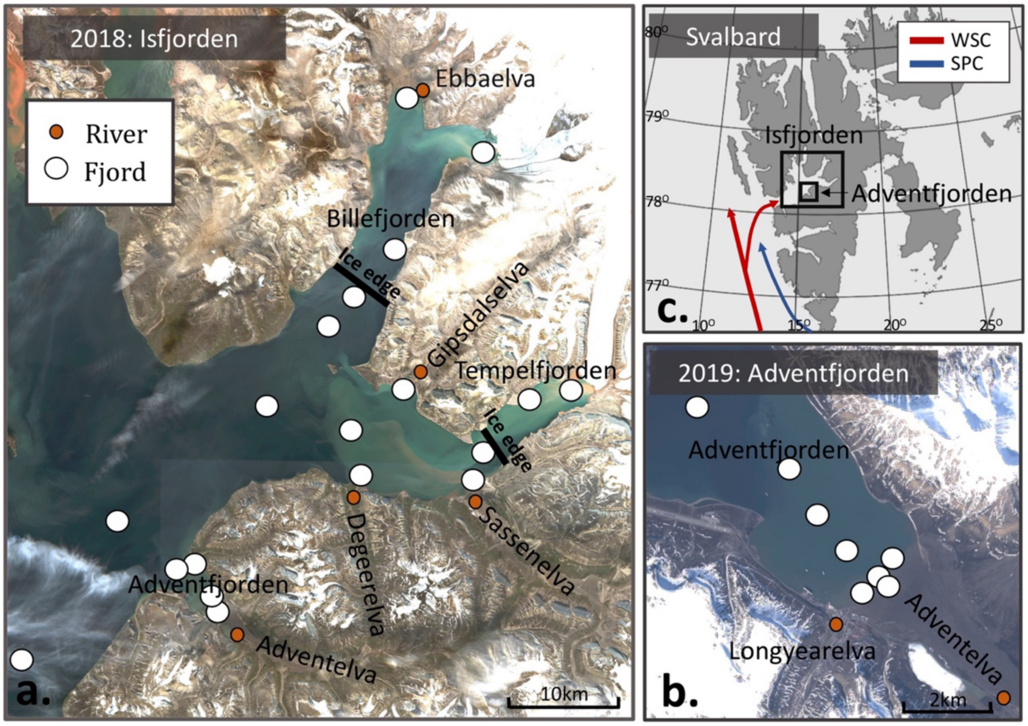

FIGURE 1 | (a) Station map of Isfjorden (sampled in 2018), and **(b)** Adventfjorden (sampled in 2019), superimposed on satellite images taken from the same week as sampling [August 20, 2018 and June 14th, 2019; Sentinel-2 (https://scihub.copernicus.eu/)]. The location of the ice edge in May 2018, when land-fast ice covered the inner fjord arms, is indicated in black. **(c)** Map of Svalbard with the West Spitsbergen Current (WSC) and Spitsbergen Polar Current (SPC) depicted in red and blue respectively.

water was collected from the surface and from 2 m above the bottom. A multiparameter sensor (Hanna instruments, HI 98195) and handheld turbidity meter (Thermo Scientific Eutech TN-100) were used in the field to record temperature, salinity, pH, conductivity and turbidity for each sample in a well-mixed bucket of sample water immediately after collection. Water was collected directly from the Niskin bottle into 20 liter jugs for further processing at the University Centre in Svalbard (UNIS).

Samples for analysis of dissolved organic carbon (DOC), dissolved nutrients [ammonium (NH_4), phosphate (PO_4), nitrite + nitrate ($NO_2 + NO_3$), and silica (SiO_2)] were filtered through 0.2 μm polycarbonate membrane filters and preserved with 4M H_2SO_4 (final concentration of 1% by volume) in 100 mL pre-cleaned amber glass bottles (DOC) or 100 mL acid-washed HDPE bottles (dissolved nutrients). Samples were stored in the dark at 4°C until analysis. For characterization of chromophoric dissolved organic matter (cDOM), water was filtered through 0.2 um polycarbonate filters and stored in 100 mL amber glass bottles in the dark at 4°C. To determine the concentration of suspended particulate matter (SPM), water was filtered onto pre-combusted and pre-weighed glass fiber filters (Whatman GF/F, nominal pore size 0.7 μm). For particulate organic carbon (POC) and particulate nitrogen (PartN) and analysis of stable carbon and nitrogen isotopes (SIA), up to 1.5L of water was filtered onto pre-combusted 25 mm GF/F filters. Particulate phosphorus (PartP) and chlorophyll *a* (Chla) samples were filtered onto a non-combusted GF/F filters. All filters were stored frozen at −20°C until analysis.

Laboratory Analyses

Nutrient, DOC, and PartP analyses were carried out at the Norwegian Institute for Water Research (NIVA, Oslo, Norway) using standard and accredited methods (as described in Kaste et al., 2018). Filters for SPM were dried and reweighed to determine SPM concentrations. Chlorophyll *a* was determined fluorometrically on a Turner 10-AU fluorometer after methanol extraction (Parsons, 2013). Pheophytin was measured on the same samples following acidification with 3 drops of 1M HCl. Stable isotope analysis of particulate organic matter (POM) was carried out at the University of California, Davis (UC Davis Stable Isotope Facility, United States). For PartN, filters were dried and packed into tin capsules for analysis. For POC, filters were fumigated for 24–48 h in a desiccator with concentrated HCl to remove inorganic carbonates prior to encapsulation. $\delta^{13}C$, $\delta^{15}N$, as well as total C and N content were measured using an elemental analyzer interfaced to an isotope ratio mass spectrometer. Run-specific standard deviations at UC Davis were ± 0.09‰ for ^{13}C and 0.05‰ for ^{15}N in 2018 and ± 0.08‰ for ^{13}C and 0.05‰ for ^{15}N in 2019. Stable carbon and nitrogen isotope values are presented using delta notation, relative to international standards (Vienna PeeDee Belemnite for C, and atmospheric N for nitrogen) (Peterson and Fry, 1987). For analysis of cDOM properties (**Table 1**), absorbance was measured at 1 nm intervals across a wavelength range of 200–900 nm with a Perkin-Elmer Lambda 40P UV/VIS Spectrophotometer using a cuvette with a 5 cm path-length. Absorbance values were blank corrected (Milli-Q) and the average absorbance from 700–900 nm was subtracted from the spectra to correct for possible absorption offset (Helms et al., 2008). Values were converted to Naperian absorption coefficients by multiplying the raw absorbance values by 2.303 and dividing by the pathlength (m) (Hu et al., 2002). Spectral slopes (S) (**Table 1**), which serve as proxies for the composition and source of DOM, with steeper $S_{275-295}$ and increasing slope ratio ($S_{R;}$ $S_{275-295}$:$S_{350-400}$) indicative of marine, low molecular weight OM (Helms et al., 2008), were calculated from the spectral absorption data. Meanwhile, specific UV absorbance at 254 nm ($SUVA_{254}$), which is positively related to aromaticity of DOM (Weishaar et al., 2003), was calculated by dividing absorbance at 254 nm by the DOC concentration (Weishaar et al., 2003).

Light and Stratification

Spectral irradiance obtained using TriOS Ramses ACC-VIS sensors in 2019 was integrated over the PAR range (400–700 nm). The diffuse attenuation coefficient K_d(PAR) (m-1) was calculated in the top 1 m using the following equation (Kirk, 2010), which assumes the exponential attenuation of light with depth (Beer's Law):

$$K_d(PAR) = \frac{1}{Z} \ln\left(\frac{E_d(PAR, 0)}{E_d(PAR, Z)}\right)$$

where Ed(PAR, 0) and Ed(PAR, Z) represent the downwelling irradiance just below the surface and at depth Z, respectively.

The euphotic depth (Z_{eu}) was calculated as 1% of surface values (just below the water surface) based on irradiance profiles. In cases when Z_{eu} exceeded the station depth, light profiles were extrapolated using the best exponential fit to estimate Z_{eu}.

Freshwater content (FWC) relative to a salinity of 34.7 in the top 10 m was calculated from CTD profiles at all stations using the following equation (Proshutinsky et al., 2009):

$$FWC = \int_{z}^{0} \frac{Sref - S}{Sref} dz$$

The reference salinity, S_{ref} is taken as 34.7, which represents the boundary between surface waters and advected waters in Isfjorden (Nilsen et al., 2008). S is the water salinity at depth z. Change in FWC is a measure of how much liquid freshwater has accumulated or been lost from the ocean column bounded by the 34.7 isohaline. In this study, FWC in the surface layer is used as an indicator of degree of freshwater influence in Isfjorden. In addition, a difference in salinity (dS) between the surface and 10 m is used as a simple indicator of water column stratification at the time of sampling.

Data Analysis

All statistical analyses were carried out using R (version 3.4.3, R Core Team, 2017). Temperature-Salinity (TS) diagrams were made using the PlotSvalbard package (Vihtakari, 2019). Water mass determinations were made based on Nilsen et al. (2008); Surface waters (SW) = Sal < 34, T > 1°C, intermediate waters (IW) = 34 < Sal < 34.7, T > 1°C, Atlantic waters (AW) = Sal > 34.9, T > 3°C), transformed Atlantic water (TAW) = Sal > 34.7, T > 1°C, Arctic water (ArW) = 34.4 < Sal < 34.8, −1.5 > T < 1°C, winter cooled

TABLE 1 | Optical characteristics of cDOM based on absorption spectra.

DOM absorption metric	Equation	Interpretation	References
a_{CDOM} (375)	Absorption coefficient (a) at 375 nm	Quantity of cDOM	Stedmon and Markager, 2001
$SUVA_{254}$	a_{CDOM} (254):DOC	Indicates aromaticity of DOM (humic content)	Weishaar et al., 2003
$S_{275-295}$	Non-linear slope of absorption between 275 and 295 nm	High = Marine, Low = Terrestrial	Helms et al., 2008
$S_{350-400}$	Non-linear slope of absorption between 350 and 400 nm	High molecular weight and aromaticity	Helms et al., 2008
S_R	Slope ratio $S_{275-295}$:$S_{350-400}$	Low molecular weight and aromaticity	Helms et al., 2008

TABLE 2 | Key water chemistry parameters (averages ± SD) of river water, fjord surface water (SW), and fjord advected water (AdW) samples from 2018 to 2019 for each month.

Month	Sample	*n*	SPM (mg L^{-1})	$NO_2 + NO_3$ (μmol L^{-1})	PO_4 (μmol L^{-1})	DOC (μmol L^{-1})	POC (μmol L^{-1})	δ^{13}C-POC (‰)
May	River	1	110.5	3.27	0.06	980	205.65	−26.5
	Fjord SW	7	27.1 (± 9.2)	0.36 (± 0.14)	0.11 (± 0.03)	206 (± 170)	28.5 (± 11.0)	−24.0 (± 0.8)
	Fjord AdW	20	32.3 (± 6.8)	0.88 (± 0.96)	0.18 (± 0.07)	161 (± 127)	29.5 (± 5.8)	−23.8 (± 0.8)
June	River	7	348.5 (± 288.0)	7.78 (± 2.56)	0.04 (± 0.03)	604 (± 550)	549.4 (± 604.6)	−26.5 (± 1.1)
	Fjord SW	48	29.4 (± 7.5)	1.27 (± 1.39)	0.44 (± 0.67)	196 (± 193)	41.8 (± 24.2)	−26.2 (± 2.1)
	Fjord AdW	7	26.1 (± 3.5)	0.55 (± 0.26)	0.17 (± 0.05)	139 (± 139)	25.4 (± 11.0)	−27.4 (± 1.3)
August	River	7	170.0 (± 91.6)	12.03 (± 7.45)	0.56 (± 0.67)	43 (± 19)	789.1 (± 1412.5)	−26.5 (± 1.0)
	Ford SW	44	46.5 (± 41.7)	0.93 (± 2.06)	0.22 (± 0.09)	71 (± 17)	65.4 (± 99.9)	−26.4 (± 0.8)
	Fjord AdW	14	24.2 (± 11.3)	0.72 (± 0.45)	0.26 (± 0.07)	77 (± 11)	19.1 (± 8.1)	−27.3 (± 0.9)

A complete overview of measured parameters can be found in ***Supplementary Table S1****.*

water (WCW) = Sal > 34.74, T < −0.5°C) and local water (LW) = T < 1°C. For **Table 2**, discrete waters samples are grouped by fjord surface water (salinity < 34.7) and fjord advected water (salinity ≥ 34.7). Spearman rank correlations were used to evaluate relationships between water chemistry parameters and salinity (**Supplementary Figure S1**).

Redundancy analysis (RDA) was performed on scaled data using the vegan package (Oksanen et al., 2018) to test whether terrestrial inputs explain variation in water chemistry parameters as well as the source and quality of OM. Explanatory variables included salinity, turbidity, temperature and sampling month. To avoid overestimation of the explained variation, constraining variables were selected using forward model selection with a double-stopping criterion (Blanchet et al., 2008). For the water chemistry RDA, salinity, turbidity, temperature and sampling month were chosen via forward selection and all explained a significant amount of variation. For the organic matter RDA, turbidity was not significant, and instead salinity, temperature and sampling month were chosen for the RDA model.

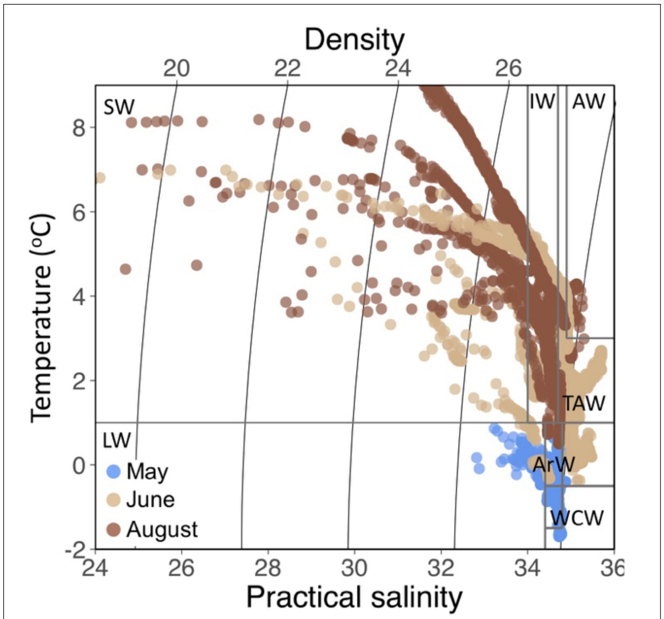

FIGURE 2 | TS diagram based on all CTD profiles by sampling month. Water masses were determined using categories specific to Isfjorden (Nilsen et al., 2008).

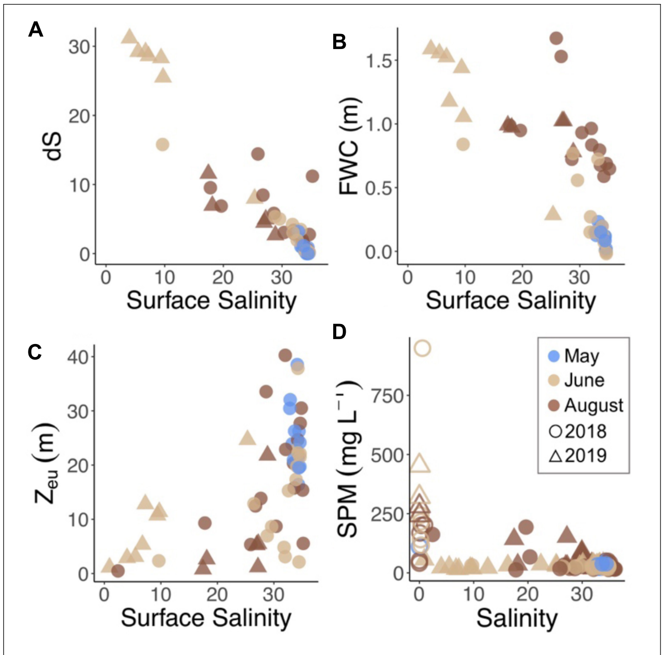

FIGURE 3 | **(A)** Difference in salinity (dS) between surface and 10 m, **(B)** fresh water content (FWC) between surface and 10 m, **(C)** depth of euphotic zone (Z_{eu}), and **(D)** suspended particulate matter (SPM) by year (symbol) and month (color). River samples are further distinguished by open symbols.

RESULTS

Freshwater Inputs and Seasonal Water Mass Transformation

In May, sampling took place when land-fast ice still covered much of inner Billefjorden and Tempelfjorden (**Figure 1**). Of the six rivers sampled in this study, only one (Adventelva) was running in May, and the water column at all sampling stations comprised of WCW and LW (**Figure 2**). In June and August, freshwater input from all of the rivers, as well as glacial melt and diffuse runoff along the coast, resulted in extensive freshening of surface waters in both years (**Figure 2**). This freshening was accompanied by increased stratification (based on dS) and fresh water content (FWC) between the surface and 10 m in June and August (**Figures 3A,B**). Riverine and glacial inputs delivered high concentrations of SPM to nearshore waters in Isfjorden (**Figure 3D**), resulting in turbid freshwater plumes associated with increased light attenuation, and thus a decreased depth of the euphotic zone (Z_{eu}) in affected areas of the fjord (**Figure 3C**). Meanwhile, in the deeper waters, the intrusion of cold saline ArW and warmer saline TAW from the shelf was observed at the outer Isfjorden stations in June and August (**Figure 2**).

Runoff as a Source of Carbon and Nutrients to Fjord Waters

River samples had high concentrations of carbon early in the melt season (**Figure 4A**). In May, the DOC concentration in Adventelva was 980 μmol L^{-1}. In June, DOC in Adventelva was much lower (40 μmol L^{-1}) while the other rivers sampled had concentrations ranging from 670 to 1410 μmol L^{-1} (average 604 ± 550 μmol L^{-1}; **Table 2**). All rivers had much lower concentrations of DOC in August, similar to those of Adventelva in June (range: 30–80 μmol L^{-1}; average: 43 ± 19 μmol L^{-1}). POC was also highly variable between rivers (**Figure 4B**) and was much higher than concentrations observed for advected water (**Table 2**). Results of $\delta^{13}C$-POC (**Figure 4C**) indicate that marine phytoplankton dominated the particulate matter pool in May during the spring phytoplankton bloom ($\delta^{13}C$: −23.9 ± 0.8‰). Meanwhile, terrestrial carbon dominated POC in June ($\delta^{13}C$:

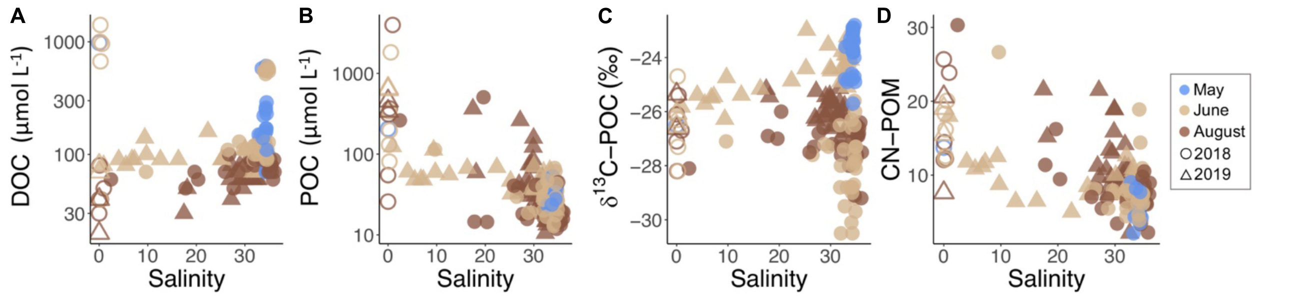

FIGURE 4 | Concentrations of **(A)** DOC, **(B)** POC, and **(C)** δ^{13}C-POC and **(D)** CN ratio of POM vs. salinity for each water sample by year (symbol) and month (color). River samples are further distinguished by open symbols.

−26.4 ± 2.0‰) and August (δ^{13}C: −26.6 ± 0.9‰) at all fjord sampling locations. CN ratios (**Figure 4D**) increased from May to June to August in both the rivers and the water column and decreased across the salinity gradient.

Concentrations of $NO_2 + NO_3$ and SiO_2 were highest in the river samples and decreased across the salinity gradient (**Figure 5**). These nutrients had high spatial and seasonal variability in Isfjorden with increasing concentrations from May to August at the near-shore stations (**Figure 5**). In May, 2018, sampling occurred during the end of the spring bloom. Concentrations of $NO_2 + NO_3$ in surface waters averaged 0.36 ± 0.14 µmol L^{-1} in SW, and 0.88 ± 0.96 µmol L^{-1} in AdW (**Table 2**). In June and August, nutrient concentrations were more strongly related to freshening when rivers and glaciers were a source of dissolved (**Figure 5A**) and particulate (**Figure 5D**) nitrogen (N) to Isfjorden. The partitioning of the N pool between particulate and dissolved phases also varied along the freshwater-marine gradient. In June and August, partN made up 60 ± 23 and 53 ± 28% of the total N pool in river samples and 30 ± 8 and 28 ± 14% in fjord SW and 23 ± 12 and 21 ± 12% of the total N pool in AdW respectively.

Rivers were also a source of phosphorus (P) in August (**Figure 5B** and **Table 2**). Mean concentrations of PO_4 were 0.56 ± 0.67 µmol L^{-1} in river water samples, 0.22 ± 0.09 in fjord SW and 0.26 ± 0.07 µmol L^{-1} in AdW. Rivers had high concentrations of partP in both June and August, which were exponentially higher than concentrations in Fjord SW (**Figure 5E**). Similar to N, P concentrations were higher in the particulate fraction in rivers, but then partitioned more toward the dissolved phase across the salinity gradient. In June and August, partP made up 97 ± 3 and 70 ± 26% of total P in river samples and 38 ± 20 and 42 ± 23% in fjord SW and 19 ± 10 and 19 ± 11% of total P in AdW respectively.

DOM Properties

Seasonal changes in DOM properties overwhelmed spatial differences within the fjord. In May, steep spectral slopes ($S_{275-295}$) and high S_R (**Figure 6**) indicated marine-derived, low molecular weight mDOM in the fjord. In both June and August, DOM properties in fjord waters were consistent between river and glacier-influenced parts of the fjord where low $S_{275-295}$ values indicated the dominance of terrestrially derived OM (**Figure 6**). However, despite terrestrial OM dominating in both freshwater-influenced months, there was a distinct difference between tDOM in June and August, largely driven by differing concentrations of $a_{CDOM}(375)$ and slope ratio (S_R). The higher levels of $a_{CDOM}(375)$ and $S_{350-400}$ in June indicated that terrestrial cDOM dominated the DOM pool at all fjord stations. High concentrations of DOC in several high salinity samples in the outer fjord in June (**Figure 4A**) were accompanied by low values of δ^{13}C (**Figure 4D**), high $S_{350-400}$ (**Figure 6D**), and low S_R (**Figure 6E**) values similar to river samples (**Figure 6F**). Meanwhile, in August, DOM properties reflected a terrestrial (low $S_{275-295}$), aromatic (high $SUVA_{254}$) source of DOM, which was of low molecular weight (high $S_{R;}$ **Figure 6E**) across all fjord stations.

Results of redundancy analysis illustrated the importance of salinity, turbidity, sampling month and temperature in explaining variation in water chemistry parameters and sampling month, temperature and salinity for explaining variation in OM source and quality in both sampling years (**Figure 7**). Of the constraining variables, salinity and turbidity explained 31% of the total variation in the water chemistry parameters while sampling month explained the greatest amount of variation in the OM dataset (19% of the total variation; **Figure 7**).

DISCUSSION

We observed seasonal changes in organic matter properties and water column structure from May to August along the terrestrial to marine gradient (**Figure 8**). Changes in water column structure can be attributed to two main drivers: freshwater discharge from land and the advection of Atlantic and Arctic water masses from the shelf into the fjord (**Figure 2**). In Isfjorden, the main source of freshwater is from melting marine-terminating glaciers, and river runoff sustained by land-terminating glacial meltwater and snow melt (Nilsen et al., 2008). Meanwhile, TAW and AW, largely driven by local wind conditions, enter the fjord in the deep and subsurface waters from the shelf. These two endmembers (terrestrial inputs and marine advected water) as well as local autochthonous production, represent the main sources of OM and inorganic nutrients to Isfjorden. The terrestrial endmember, represented here by river samples,

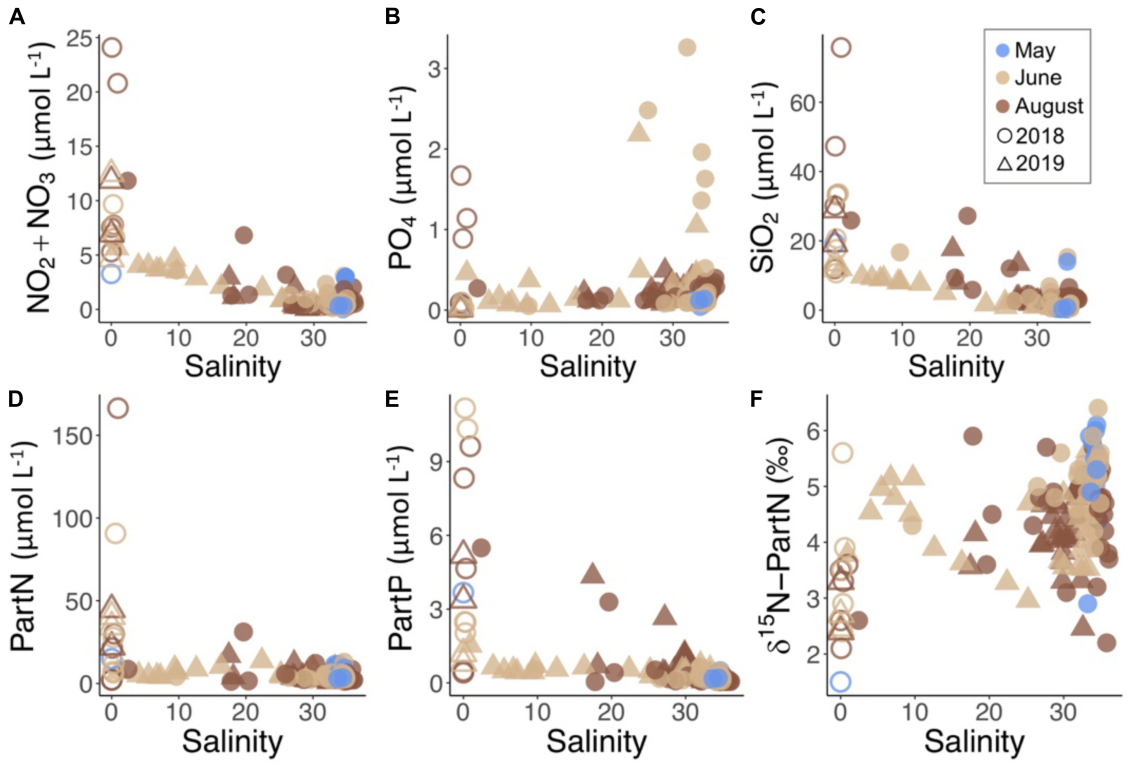

FIGURE 5 | Concentrations of dissolved nutrients **(A)** NO_2 + NO_3, **(B)** PO_4, **(C)** SiO_2 and particulate nutrients **(D)** particulate nitrogen (PartN), **(E)** particulate phosphorus (PartP), and **(F)** δ^{15}N-PartN vs. salinity for each water sample by year (symbol) and month (color). River samples are further distinguished by open symbols.

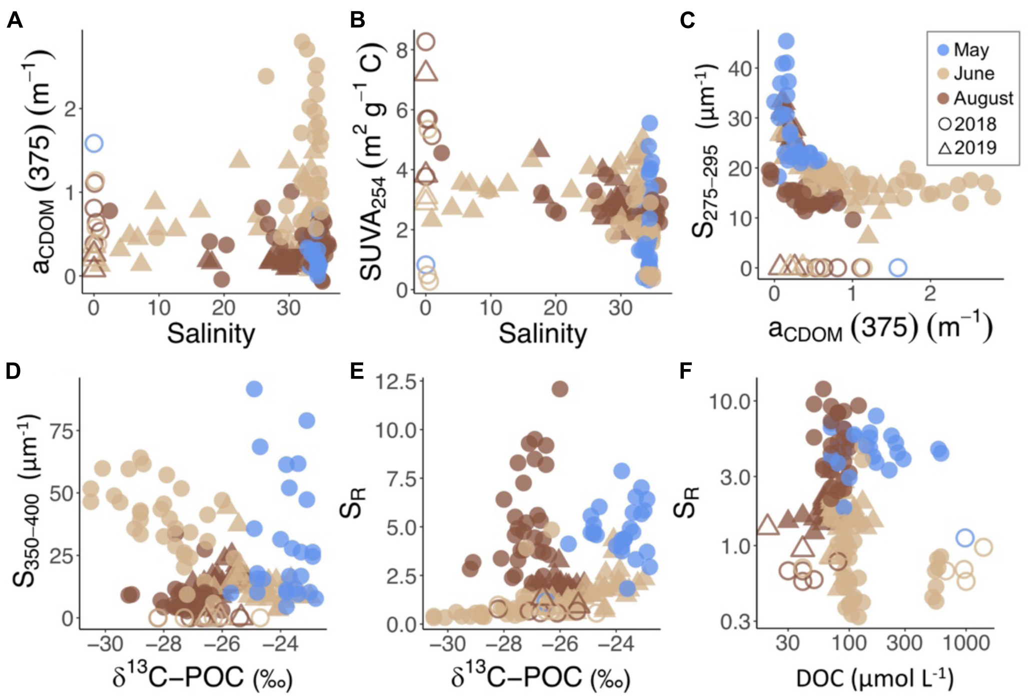

FIGURE 6 | cDOM absorption characteristics including **(A)** $a_{CDOM}(375)$ and **(B)** $SUVA_{254}$ vs. salinity, **(C)** $S_{275-295}$ vs. $a_{CDOM}(375)$ and **(D)** $S_{350-400}$ and **(E)** slope ratio (S_R) vs. δ^{13}C-POC and **(F)** S_R vs. DOC for all water samples by year (symbol) and month (color). River samples are further distinguished by open symbols.

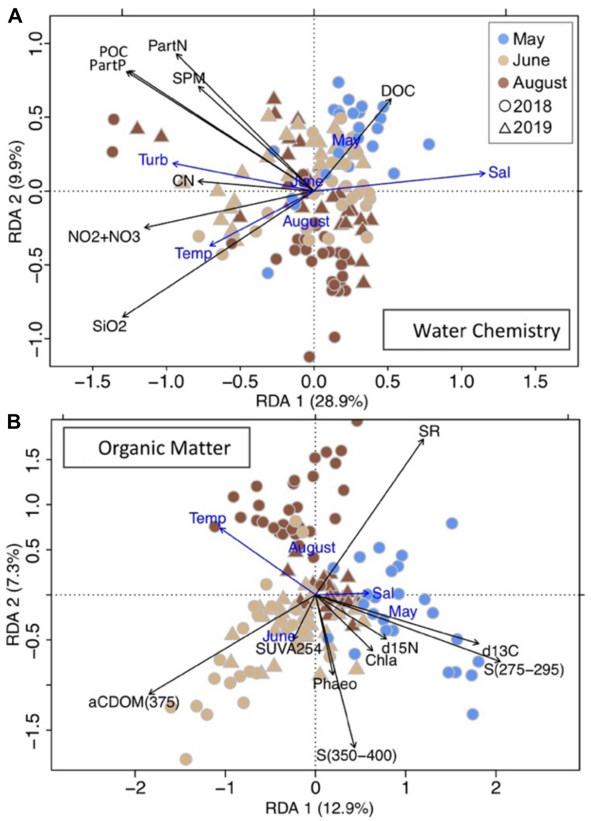

FIGURE 7 | Redundancy analyses (RDA) of **(A)** water chemistry parameters constrained by salinity, turbidity, temperature and sampling month (in blue), and **(B)** organic matter properties constrained by salinity, temperature and sampling month (in blue). Response variables unrelated to main axes (p > 0.05) are not shown.

shifted seasonally, with high DOC concentrations in June and high dissolved nutrient ($NO_2 + NO_3$ and PO_4) concentrations measured in August. Thus, from the spring phytoplankton bloom in May to spring freshet in June and late-season melt in August, we observed strong seasonal changes in nutrients and OM properties in the fjord, with potential implications for coastal biogeochemistry and carbon pathways. The fate of these terrestrial carbon and nutrients in the marine system is likely linked to the physical effects of freshwater, including light attenuation and stratification, as well as the bioavailability of the delivered terrestrial material to marine biological communities.

River Water Chemistry Changes Seasonally

Seasonal variation in river water chemistry from May through August reflects changing flow paths in the catchments. River samples collected during the spring freshet in May/June had concentrations of DOC similar to values observed during spring freshet for permafrost dominated catchments in the Siberian and North American Arctic (Holmes et al., 2011; Amon et al., 2012), and much higher than observations from glacier-dominated catchments elsewhere on Svalbard (Zhu et al., 2016) and in Greenland (Paulsen et al., 2017). In fact, concentrations in Sassenelva (a river draining a permafrost-rich valley; **Figure 1**) in June reached 1400 μmol L^{-1} while samples from Gipsdalselva and Ebbaelva (both heavily glaciated catchments) were as high as 670 and 1000 μmol L^{-1}, respectively. Adventelva was the only river with low concentrations of DOC in June (40 μmol L^{-1}), but this river was flowing already in May, with a DOC concentration of 980 μmol L^{-1} at that time (**Table 2**), confirming that the melt progression occurred earlier in Adventdalen. These high concentrations of riverine DOC draining into Isfjorden in June are consistent with other studies in the Arctic that show that approximately half of Arctic river DOC flux occurs during snow melt (Finlay et al., 2006) and high flow events (Rember and Trefry, 2004; Raymond et al., 2007; Raymond and Saiers, 2010; Coch et al., 2018) when surficial and shallow flow paths (Barnes et al., 2018) and high catchment connectivity (Johnston et al., 2019) help to flush modern, plant-derived OM (Feng et al., 2013) into aquatic systems. Permafrost also plays an important role in mobilization and transport of DOC from C-rich surface soils during snowmelt by sustaining near surface water tables and inhibiting deep percolation (Carey, 2003). Moreover, high discharge periods lead to reduced residence time in the catchment, reducing the potential for processing of DOC during transport from the catchment to coastal areas (Koch et al., 2013; Raymond et al., 2016). Thus, the high concentrations of DOC and increased cDOM observed throughout fjord surface waters in June is likely a result of increased transport of terrestrial OM during the spring freshet.

On Svalbard, late-season run-off is driven by glacial melt (Nowak and Hodson, 2015), which was characterized by much lower concentrations of DOC, but higher concentrations of N and P. Decreases in DOC post-freshet has also been found for the Yukon river (Striegl et al., 2005) and Siberian rivers (Neff et al., 2006) as flow paths deepen. Depending on the geology of the catchment, deeper flow paths can potentially drain nutrient-rich mineral soils, transporting N and P to aquatic systems (Barnes et al., 2018). Alternatively, microbial processes, including nitrification, on catchment glaciers have also been linked to N and P -rich meltwater (Hodson et al., 2004; Telling et al., 2011; Wadham et al., 2016). It is estimated that approximately half of glacially exported N is sourced from microbial activity within glacial sediments at the surface and bed of the ice, doubling N fluxes in runoff (Wadham et al., 2016). However, both glacial and soil-derived nutrients may also be heavily sediment bound (P; Hodson et al., 2004), or retained in the catchment through further microbial processing or uptake by terrestrial vegetation (N; Nowak and Hodson, 2015). Even so, concentrations of $NO_2 + NO_3$ in our river samples (sampled close to the river outlet) reached 24 μmol L^{-1} in August, with estuary surface waters still high at 11.8 μmol L^{-1}. Concentrations of PO_4 were also high, reaching 1.7 μmol L^{-1} in river samples in August. These concentrations are higher than concentrations measured from AW advected from the shelf (maximum of 2 μmol L^{-1} for $NO_2 + NO_3$ and 0.4 μmol L^{-1} for PO_4 in this study, but other observations from Svalbard show 6–11 μmol L^{-1} for N and 0.8 μmol L^{-1} for P (Chierici et al., 2019; Halbach et al., 2019). While SiO_2 has been associated with glacial meltwater from contact with silica-rich bedrock in Isfjorden (Fransson et al., 2015), Kongsfjorden (Halbach et al., 2019) and Greenland fjords (Meire et al., 2016; Kanna et al., 2018; Hendry et al., 2019), N and P have been linked primarily to advected deep water. In contrast to glacial meltwaters in Kongsfjorden (Halbach et al., 2019) and Greenland (Paulsen et al., 2017), the rivers sampled in our study had comparably high concentrations of N and P in addition to SiO_2. While these increased solute concentrations were observed during a relatively low discharge period, the extensive freshwater presence in the fjord in late summer and associated physical effects on the water column could enhance their importance for biological processes.

Physical Effects of Freshwater Runoff Indirectly Affect Fate of Terrestrial OM in Surface Waters

The physical effects of freshwater and suspended sediments associated with glacial and riverine inputs have implications for the fate of terrestrial OM in the marine system. When river inputs meet the coast, the slowing of the current can cause large particles, including sediment-associated particulate nutrients, to settle out of the water column. In addition, increased salinity causes flocculation and sedimentation of finer particles and dissolved components (Sholkovitz, 1976). These processes are reflected in the exponential decrease in SPM, carbon and nutrients from rivers to estuary stations observed in this study. In the Adventelva estuary, this has been known to lead to the rapid removal of 25% of the suspended sediments from surface waters to the benthos, where hyperpycnal flows transport sediment along the bottom (Zajączkowski, 2008). Despite these losses, concentrations of nutrients in terrestrially influenced surface waters were higher than in subsurface fjord waters, which suggests that these nutrients could support excess coastal production.

Freshwater runoff to surface waters combined with warm, saline water masses transported from the shelf in the deeper waters resulted in seasonally increasing stratification throughout Isfjorden in 2018 and 2019 (**Figure 5**). As noted in previous studies, strong stratification weakens vertical mixing of the water column and in extreme cases can prevent bottom water renewal (Boone et al., 2017; Torsvik et al., 2019), which can lead to nutrient limitation, especially when nutrients from advected deep waters are important (Bergeron and Tremblay, 2014; Coupel et al., 2015; Yun et al., 2016; Holding et al., 2019). However, in this study, surface waters were influenced by nutrient-rich terrestrial runoff, so the stratification could be an effective physical barrier keeping these nutrients suspended in the euphotic zone, and thus available for primary production. While the fresh surface layer was very thin (and very fresh) in June, mixing of this layer with deeper water can occur through tidal or wind action (Cottier et al., 2010). In August, the fresh surface layer had mixed with the upper water column, resulting in a higher FWC. The deeper mixed layer in August is likely important for the biological utilization of the associated terrestrial nutrients delivered during this period.

High concentrations of SPM are not unusual for coastal waters influenced by runoff from heavily glaciated catchments, where these particles rapidly attenuate light needed for photosynthesis (Murray et al., 2015; Pavlov et al., 2019). In this study, the shallowest mean euphotic depth was observed at estuary stations, where the rapid attenuation of light (max $K_{d\ PAR}$ in the top 1 m was 5.40 m^{-1}) resulted in euphotic depths of just over 5 m in June, and 1.55 m in August. Meanwhile, the finer particles, which can remain suspended and, in some cases, can be transported several kilometers from the meltwater plumes (Cowan and Powell, 1991; Meslard et al., 2018), are likely responsible for the far-reaching effects on light attenuation, which reached the fjord transect stations in June. At outer fjord stations, the lowest mean K_d(PAR) was 0.27–0.38 m^{-1} in August, which is comparable to K_d(PAR) values previously reported in surface waters of WSC in autumn (Pavlov et al., 2015). These corresponded to mean Z_{eu} exceeding 25–30 m. Thus, in August, increased FWC but reduced turbidity may allow for increased photodegradation of terrestrial OM in surface waters. Thus, the fate of transported terrestrial OM is closely tied to the physical effects of terrestrial runoff. Terrestrial carbon and nutrients can be exported to the sediments when reaching the marine system, or transported further out into the fjord where they are largely confined to the mixed layer due to stratification and could potentially be photodegraded or utilized for primary production where turbidity is low enough that sufficient light is available.

Seasonal Changes in Source and Quality of Organic Matter in Isfjorden

The fate of terrestrial OM in the coastal system is also linked to its nutritional value and bioavailability for microbial communities. The seasonality in OM composition observed in this study is linked to the progression from a spring phytoplankton bloom (before spring freshet) to impacts of terrestrial inputs, the geochemical nature of which shifted from freshet to late summer. These seasonal changes, in both the rivers and the fjord, had strong effects on the quality and quantity of DOM throughout the entire fjord and provide insights into the potential for processing of terrestrial carbon in the water column.

In May, the quantity and quality of OM is related to the spring phytoplankton bloom. Monthly chlorophyll *a* concentrations measured in outer Adventfjorden in 2018 confirm that the spring bloom occurred in early May, roughly a week before the sampling for this study was carried out (Nyeggen, 2019). While the spring bloom was over in the nearshore stations (low concentrations of N and Chl *a*), the outer fjord stations were characterized by high abundances of *Phaeocystis* (pers. com; Dąbrowska, 2020). High $\delta^{13}C$ values indicate that POC was dominated by marine phytoplankton, and DOM properties (**Table 1**) also reflect a predominantly marine source of OM. The high $S_{275-295}$ and S_R (Helms et al., 2008) indicate that this freshly produced marine mDOM is of low molecular weight, and is presumably quite bioavailable to bacterial communities. This is in line with a recent study in Isfjorden which highlighted the importance of marine OM, and ice algae for bacterial production following the spring phytoplankton bloom (Holding et al., 2017).

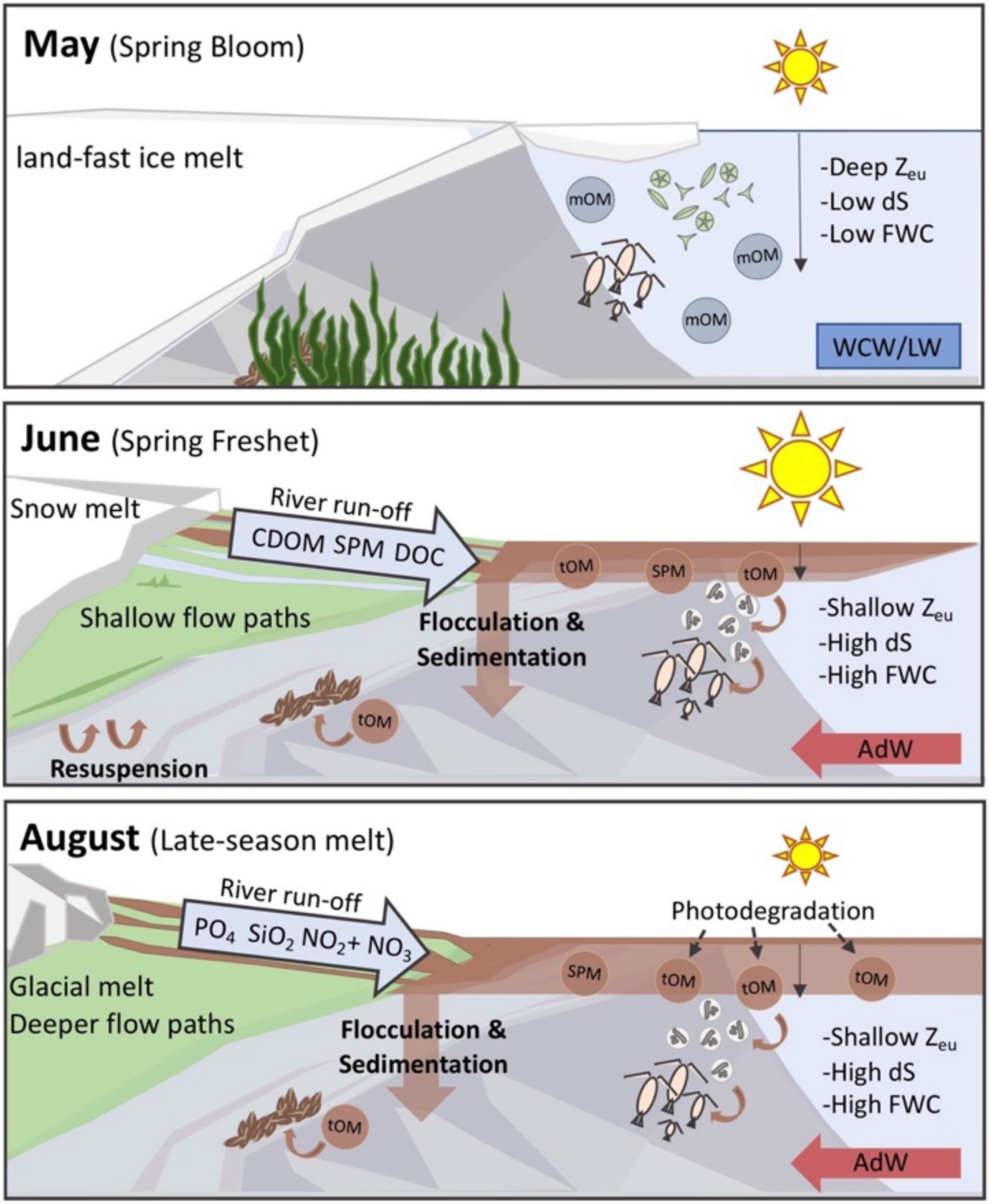

FIGURE 8 | A conceptual diagram summarizing main findings and future perspectives. In May, ice still covered the inner fjord arms of Isfjorden and marine OM (mOM) was present throughout the water column following the spring phytoplankton bloom, when there was a deep euphotic zone (Z_{eu}). The spring freshet in June was a source of terrestrial DOC and SPM to Isfjorden, and while some of these materials were removed from the water column through flocculation and sedimentation, terrestrial OM (tOM) was observed throughout the highly stratified (dS) and turbid fjord surface waters. In August, glacier-fed rivers with deeper flowpaths were a source of nutrients including nitrogen and phosphorus to Isfjorden. Surface waters also had increased fresh water content (FWC) and degraded OM dominated throughout the fjord in August.

Meanwhile, in June, terrestrially derived OM dominated surface waters throughout the fjord. High DOC concentrations in the rivers in June were found alongside increased $a_{CDOM}(375)$ at all fjord stations, even for more saline samples collected from the outer fjord. Results of stable isotope analysis confirm that the POM at the highly turbid estuary and glacier stations was dominated by terrestrial particles. In fact, terrestrially derived POC was present even in the outer fjord. Surprisingly, while δ^{13}C-POC values from river samples ranged from −24 to −28 ‰, estuary and outer fjord stations had values as low as −30.5 ‰ in June, 2018. Studies in Kongsfjorden have also reported similarly low δ^{13}C values for POC (Kędra et al., 2012; Calleja et al., 2017; Jain et al., 2019), which no clear explanation. We suggest that the low δ^{13}C-POC values here could represent the finer organic fraction of terrestrial POC transported farther from glacial fronts and river outlets, or the transport of material from diffuse runoff, coastal erosion and sediment resuspension in the nearshore (Zajączkowski, 2008). While the outer fjord stations were further from the glacier fronts and river outlets, they were still in close proximity to shore (**Figure 1**). The low δ^{15}N values of PartN also imply a terrestrial source of POM (**Figure 5F**). DOM absorption properties for these outer fjord samples with low δ^{13}C-POC further support a terrestrial origin for OM at these sites. As also observed in Kongsfjorden (Calleja et al., 2017), low δ^{13}C values were found alongside steep spectral slopes at the longer wavelengths ($S_{350-400}$) and low S_R (**Figure 6**), both indications of high molecular weight terrestrial material (Weishaar et al., 2003; Helms et al., 2008). On the other hand, Jain et al. (2019), suggest that low δ^{13}C values can also be observed for marine POC on Svalbard, where increased lipids (which are depleted in ^{13}C) due to the presence of cryophytes in the water column, lead to lower δ^{13}C values in the POM. While cryptophytes and other lipid-rich plankton were present in the water column in June, 2018 (pers. com. Dąbrowska, 2020), no relationship was found between lipid content of POM and δ^{13}C values for POC in our dataset (M. McGovern, unpublished data).

In August, river runoff is driven by glacial meltwater, which was characterized by low DOC concentrations, similar to concentrations found in Bayelva in Kongsfjorden (Zhu et al., 2016). DOM absorption characteristics of these samples reflected a terrestrial yet highly aromatic (high $SUVA_{254}$) source of DOM (Weishaar et al., 2003). While a high proportion of ancient, glacial OM can be quite labile (Hood et al., 2009) and thus an important resource for microbial processing as glaciers recede, our study indicates that for Isfjorden, terrestrial OM mobilized during freshet (high concentrations of presumably modern, plant-derived DOM from surficial flowpaths), may be more important when considering coastal processes. In fjord surface waters, DOM absorption characteristics in August indicate that while the DOM was terrestrial (and humic), it was also of low molecular weight. Low S_R values in August are consistent with previously observed changes in DOM properties associated with photochemical or microbial processing in the marine environment (Moran et al., 2000; Granskog et al., 2012; Asmala et al., 2018). In fact, the decrease in $SUVA_{254}$ from river to fjord in August, and in $S_{350-400}$ from June to August in surface waters indicate that photochemical degradation of terrestrial OM, presumably from freshet, could be largely responsible for the observed changes in S_R from June to August (Hansen et al., 2016). This photochemical alteration of DOM from larger molecules to smaller labile photoproducts impacts the potential cycling of DOM (Hansen et al., 2016) in Isfjorden, as it could lead to the removal of DOM by volatilization or microbial utilization (Wetzel et al., 1995; Moran and Zepp, 1997). This is in line with the rapid photodegradation of freshet OM to a more bioavailable form readily remineralized by microbial communities in the Mackenzie delta (Gareis and Lesack, 2018) and Kolyma river basin (Mann et al., 2012), and thus may represent an important pathway driving remineralization of terrestrial OM delivered to Isfjorden during freshet.

Future Perspectives

With air temperatures projected to increase upwards of 10°C by 2100, Svalbard, which is covered by more than 53% glaciers (Nuth et al., 2013), is facing rapid changes (Adakudlu et al., 2019), and the effects are already evident. Pronounced glacier mass loss, changes in precipitation patterns, permafrost warming, and subsequent increases in freshwater runoff have been documented in the last decades (Adakudlu et al., 2019; Błaszczyk et al., 2019; van Pelt et al., 2019) and are expected to continue during this century. The results of this study highlight the spatial and seasonal variability in riverine runoff as a source of OM and inorganic nutrients to Isfjorden, and suggest that in Svalbard, terrestrial DOC inputs could be systematically underestimated due to lack of field sampling during freshet, or following increasingly frequent intense rainfall events (Adakudlu et al., 2019). Since these high DOC concentrations in the river samples are likely due to the flushing of vegetative layer with snow melt, this young terrigenous carbon is presumably semi-bioavailable to fjord microbial communities (Raymond et al., 2007). Moreover, expected increases in vegetative biomass (Myneni et al., 1997; Ju and Masek, 2016) will likely enhance DOC export during periods of high discharge while further permafrost degradation will likely lead to increased POC (Guo and Macdonald, 2006) and nutrient export later in the summer. Higher sediment loads in rivers across the Arctic, including in Adventelva tributaries (Bogen and Bønsnes, 2003) are also expected due to increased erosion with amplified discharge (Syvitski, 2002). Thus, expected future changes in Arctic catchments paired with increased runoff will likely lead to enhanced land-ocean connectivity and increased transport of carbon, nutrients and SPM to coastal areas (**Figure 8**).

In Svalbard fjords, changes in the timing and geochemical nature of freshwater inputs are occurring alongside increases in Atlantic water advection (Spielhagen et al., 2011), and the disappearance of sea-ice (Muckenhuber et al., 2016) and associated ice algae. Thus, increased freshwater inputs are likely to both limit marine production as the turbid melt season may eventually overlap with the spring phytoplankton bloom, while also providing a potential terrestrial carbon subsidy to marine food-webs. With greener catchments and reductions in sea-ice, terrestrial carbon could become increasingly important for coastal zooplankton and benthos, especially in heavily impacted parts of the fjord where increased light attenuation could limit phytoplankton and macroalgal growth. However, more detailed characterization of the terrestrial DOM pool both seasonally and also between glacial and riverine/permafrost sources is required to better predict the fate of terrestrial material in the marine system. If bioavailable, terrestrial OM can provide heterotrophic bacteria with substrate that allows them to out-compete phytoplankton for nutrients (Sipler et al., 2017), driving shifts in lower food-web structure (Joli et al., 2018; Kellogg et al., 2019) and autotrophic: heterotrophic balance (Wikner and Andersson, 2012). Thus, increasingly persistent and turbid freshwater plumes could lead to changes in basal production, food-web structure and carbon balance in Isfjorden and other Arctic areas facing enhanced land-ocean connectivity (**Figure 8**).

While it's evident that terrestrial inputs have profound physical, chemical and biological implications for the fjord, these freshwater plumes are highly variable in space and time. The spatial extent of freshwater plumes is driven by freshwater discharge, the Coriolis effect, tides, ice cover, and the wind direction and strength (Granskog et al., 2005; Forwick et al., 2010). Observed changes in extent and duration of sea ice in Isfjorden (Muckenhuber et al., 2016), and the expected future reduction in sea ice, will also affect the spatial extent of freshwater plumes (Granskog et al., 2005), especially in spring in combination with earlier snow melt (Adakudlu et al., 2019). However, considering the strong explanatory power of turbidity when constraining physicochemical parameters for both sampling years, our results indicate that the use of ocean color data from satellite or airborne platforms has great potential for assessing and quantifying the spatial extent and associated impacts of terrestrial inputs on coastal surface waters. However, the importance of seasonality for constraining OM quality and quantity also emphasizes the need for high temporal resolution data to capture seasonal changes as well as dynamic local events in the catchments and water column.

CONCLUSION

Seasonality in the magnitude and geochemistry of terrestrial inputs drive strong gradients in light availability, nutrient concentrations, and DOM properties in Isfjorden (**Figure 8**). Large differences between glacial rivers and marine surface water concentrations indicate that flocculation and sedimentation is an efficient removal pathway for particulate and dissolved carbon and nutrients associated with riverine and glacial SPM. Despite high removal at the land-ocean interface, terrestrial OM was observed throughout Isfjorden's surface waters in June and August. The physical effects of freshwater on the water column, including retention of terrestrial carbon and nutrients within the euphotic zone due to stratification, may indicate that riverine OM and inorganic nutrients are particularly biologically relevant in coastal systems where vertical mixing is limited during the most productive season. Seasonal shifts in optical properties of DOM further suggest that the photodegradation of terrestrial OM delivered during the spring freshet could lead to increased bioavailability for microbial communities. Climate-change driven increases in freshwater discharge can be expected to lead to increased suspended sediment loads, and the mobilization and transport of terrestrial carbon and nutrients from thawing and greening watersheds, with important implications for future Arctic coastal ecosystems.

DATA AVAILABILITY STATEMENT

The datasets generated for this study are available on request to the corresponding author.

AUTHOR CONTRIBUTIONS

AEP and MM developed the study design. MM, JS, AEP, and AD carried out fieldwork in 2018 and 2019. AKP performed calculations of K_d, FWC, and dS. MM analyzed the data, made the figures, and wrote the manuscript with contributions from all co-authors. All authors contributed to the article and approved the submitted version.

FUNDING

This research was supported by the Norwegian Research Council (TerrACE; project number: 268458), the Fram Center Flagship "Fjord and Coast" grant (FreshFate; project number 132019), and the Svalbard Science Forum's Arctic Field Grant (RIS number: 10914).

ACKNOWLEDGMENTS

We thank Espen Lund and Emelie Skogsberg for running the cDOM samples and the NIVA lab (especially Anne Luise Ribeiro and Tina Brytensen) for water chemistry analyses. We would like to thank the students and fellow scientists who helped us with the fieldwork including Uta Brandt, Nathalie Carrasco, Ulrike Dietrich, Cathrine Gundersen, Sverre Johansen, Hannah Miller, Sarah Nelson, Emelie Skogsberg, Liv Sletten, Tobias Vonnahme, and Emilie Hernes Vereide. We also thank Laura de Steur for a discussion about freshwater content calculations. Additional gratitude goes to UNIS logistics and the crew of the RV *Helmer Hansen* and *Clione* for their help during the field campaigns.

SUPPLEMENTARY MATERIAL

The Supplementary Material for this article can be found online at: https://www.frontiersin.org/articles/10.3389/fmars.2020.542563/full#supplementary-material

REFERENCES

Adakudlu, M., Andresen, J., Bakke, J., Beldring, S., Benestad, R., Bilt, W., et al. (2019). *Climate in Svalbard 2100 – A Knowledge Base for Climate Adaptation*. Norway: Norwegian Environmental Agency.

Amon, R., Rinehart, A., Duan, S., Louchouarn, P., Prokushkin, A., Guggenberger, G., et al. (2012). Dissolved organic matter sources in large arctic rivers. *Geochim. Cosmochim. Acta* 94, 217–237. doi: 10.1016/j.gca.2012.07.015

Asmala, E., Haraguchi, L., Markager, S., Massicotte, P., Riemann, B., Staehr, P. A., et al. (2018). Eutrophication leads to accumulation of recalcitrant autochthonous organic matter in coastal environment. *Glob. Biogeochem. Cycles* 32, 1673–1687. doi: 10.1029/2017GB005848

Barnes, R. T., Butman, D. E., Wilson, H. F., and Raymond, P. A. (2018). Riverine export of aged carbon driven by flow path depth and residence time. *Environ. Sci. Technol.* 52, 1028–1035. doi: 10.1021/acs.est.7b04717

Bergeron, M., and Tremblay, J.-E. (2014). Shifts in biological productivity inferred from nutrient drawdown in the southern Beaufort Sea (2003–2011) and the northern Baffin Bay (1997–2011), Canadian Arctic. *Geophys. Res. Lett.* 41, 3979–3987. doi: 10.1002/2014GL059649

Bianchi, T. S., Arndt, S., Austin, W. E. N., Benn, D. I., Bertrand, S., Cui, X., et al. (2020). Fjords as aquatic critical zones (ACZs). *Earth Sci. Rev.ews* 203:103145. doi: 10.1016/j.earscirev.2020.103145

Bianchi, T. S., Cui, X., Blair, N. E., Burdige, D. J., Eglinton, T. I., and Galy, V. (2018). Centers of organic carbon burial and oxidation at the land-ocean interface. *Organ. Geochem.* 115, 138–155. doi: 10.1016/j.orggeochem.2017.09.008

Biskaborn, B. K., Smith, S. L., Noetzli, J., Matthes, H., Vieira, G., Streletskiy, D. A., et al. (2019). Permafrost is warming at a global scale. *Nat. Commun.* 10:264. doi: 10.1038/s41467-018-08240-4

Blanchet, F. G., Legendre, P., and Borcard, D. (2008). Forward selection of explanatory variables. *Ecology* 89, 2623–2632. doi: 10.1890/07-0986.1

Błaszczyk, M., Ignatiuk, D., Uszczyk, A., Cielecka-Nowak, K., Grabiec, M., Jania, J. A., et al. (2019). Freshwater input to the Arctic fjord Hornsund (Svalbard). *Polar Res.* 38:3506. doi: 10.33265/polar.v38.3506

Bogen, J., and Bønsnes, T. E. (2003). Erosion and sediment transport in high arctic rivers, Svalbard. *Polar Res.* 22, 175–189. doi: 10.1111/j.1751-8369.2003.tb00106.x

Boone, W., Rysgaard, S., Kirillov, S., Dmitrenko, I., Bendtsen, J., Mortensen, J., et al. (2017). Circulation and fjord-shelf exchange during the ice-covered period in young sound-Tyrolerfjord, Northeast Greenland (74° N). *Estuar. Coast. Shelf Sci.* 194, 205–216. doi: 10.1016/j.ecss.2017.06.021

Calleja, M. L., Kerhervé, P., Bourgeois, S., Kędra, M., Leynaert, A., Devred, E., et al. (2017). Effects of increase glacier discharge on phytoplankton bloom dynamics and pelagic geochemistry in a high Arctic fjord. *Prog. Oceanogr.* 159, 195–210. doi: 10.1016/j.pocean.2017.07.005

Carey, S. K. (2003). Dissolved organic carbon fluxes in a discontinuous permafrost subarctic alpine catchment. *Permafrost Periglac. Process.* 14, 161–171. doi: 10.1002/ppp.444

Chierici, M., Vernet, M., Fransson, A., and Børsheim, K. Y. (2019). Net community production and carbon exchange from winter to summer in the Atlantic water inflow to the Arctic Ocean. *Front. Mar. Sci.* 6:528. doi: 10.3389/fmars.2019.00528

Christiansen, H. H., French, H. M., and Humlum, O. (2005). Permafrost in the Gruve-7 mine, Adventdalen, Svalbard. *Norwegian J. Geogr.* 59, 109–115. doi: 10.1080/00291950510020592

Coch, C., Lamoureux, S. F., Knoblauch, C., Eischeid, I., Fritz, M., Obu, J., et al. (2018). Summer rainfall dissolved organic carbon, solute, and sediment fluxes in a small Arctic coastal catchment on Herschel Island (Yukon Territory, Canada). *Arctic Sci.* 4, 750–780. doi: 10.1139/as-2018-0010

Cottier, F. R., Nilsen, F., Skogseth, R., Tverberg, V., SkarÐhamar, J., and Svendsen, H. (2010). Arctic fjords: a review of the oceanographic environment and dominant physical processes. *Geol. Soc. Lond. Spec. Publ.* 344, 35–50. doi: 10.1144/SP344.4

Coupel, P., Ruiz-Pino, D., Sicre, M. A., Chen, J. F., Lee, S. H., Schiffrine, N., et al. (2015). The impact of freshening on phytoplankton production in the Pacific Arctic Ocean. *Prog. Oceanogr.* 131, 113–125. doi: 10.1016/j.pocean.2014.12.003

Cowan, E. A., and Powell, R. D. (1991). "Ice-proximal sediment accumulation rates in a temperate glacial fjord, southeastern Alaska," in *Glacial Marine Sedimentation: Paleoclimatic Significance*, eds J. B. Anderson and G. M. Ashley (Boulder, CO: Geological Society America), 61–73. doi: 10.1130/spe261-p61

Dąbrowska, A. M. (2020). *Institute of Oceanology, Polish Academy of Sciences Sopot, Poland*. Spring: Personal communication.

Feng, X., Vonk, J. E., Van Dongen, B. E., Gustafsson, Ö, Semiletov, I. P., Dudarev, O. V., et al. (2013). Differential mobilization of terrestrial carbon pools in Eurasian Arctic river basins. *Proc. Natl. Acad. Sci. U.S.A.* 110, 14168–14173. doi: 10.1073/pnas.1307031110

Finlay, J., Neff, J., Zimov, S., Davydova, A., and Davydov, S. (2006). Snowmelt dominance of dissolved organic carbon in high-latitude watersheds: implications for characterization and flux of river DOC. *Geophys. Res. Lett.* 33:L10401. doi: 10.1029/2006GL025754

Forwick, M., Vorren, T. O., Hald, M., Korsun, S., Roh, Y., Vogt, C., et al. (2010). Spatial and temporal influence of glaciers and rivers on the sedimentary environment in Sassenfjorden and Tempelfjorden, Spitsbergen. *Geol. Soc. Lond. Spec. Publ.* 344, 163–193. doi: 10.1144/sp344.13

Fransson, A., Chierici, M., Nomura, D., Granskog, M. A., Kristiansen, S., Martma, O., et al. (2015). Effect of glacial drainage water on the CO2 system and ocean acidification state in an Arctic tidewater-glacier fjord during two contrasting years. *J. Geophys. Res. Ocean.* 120, 2413–2429. doi: 10.1002/2014JC010320

Fraser, N. J., Skogseth, R., Nilsen, F., and Inall, M. E. (2018). Circulation and exchange in abroad Arctic fjord using glider-based observations. *Polar Res.* 37:1485417. doi: 10.1080/17518369.2018.1485417

Gareis, J. A., and Lesack, L. F. (2018). Photodegraded dissolved organic matter from peak freshet river discharge as a substrate for bacterial production in a lake-rich great Arctic delta. *Arctic Sci.* 4, 557–583. doi: 10.1139/as-2017-0055

Granskog, M. A., Ehn, J., and Niemelä, M. (2005). Characteristics and potential impacts of under-ice river plumes in the seasonally ice-covered Bothnian Bay (Baltic Sea). *J. Mar. Syst.* 53, 187–196. doi: 10.1016/j.jmarsys.2004.06.005

Granskog, M. A., Stedmon, C. A., Dodd, P. A., Amon, R. M., Pavlov, A. K., de Steur, L., et al. (2012). Characteristics of colored dissolved organic matter (CDOM) in the Arctic outflow in the Fram Strait: assessing the changes and fate of terrigenous CDOM in the Arctic Ocean. *J. Geophys. Res. Oceans* 117:C12021. doi: 10.1029/2012JC008075

Grosse, G., Goetz, S., McGuire, A. D., Romanovsky, V. E., and Schuur, E. A. (2016). Changing permafrost in a warming world and feedbacks to the Earth system. *Environ. Res. Lett.* 11:040201. doi: 10.1088/1748-9326/11/4/040201

Guerrero, J. L. (2019). *Norwegian Institute for Water Research*. Oslo: Personal communication related to Isfjorden catchments.

Guo, L., and Macdonald, R. W. (2006). Source and transport of terrigenous organic matter in the upper Yukon River: evidence from isotope (d13C,D14C, and d15N) composition of dissolved, colloidal, and particulate phases. *Glob. Biogeochem. Cycles* 20:GB2011. doi: 10.1029/2005GB002593

Halbach, L., Assmy, P., Vihtakari, M., Hop, H., Duarte, P., Wold, A., et al. (2019). Tidewater glaciers and bedrock characteristics control the phytoplankton growth environment in an Arctic fjord. *Front. Mar. Sci.* 6:254. doi: 10.3389/fmars.2019.00254

Hansen, A. M., Kraus, T. E. C., Pellerin, B. A., Fleck, J. A., Downing, B. D., Bergamaschi, and B. A. (2016). Optical properties of dissolved organic matter (DOM): effects of biological and photolytic degradation. *Limnol. Oceanogr.* 61, 1015–1032. doi: 10.1002/lno.10270

Harris, C. N., McTigue, N. D., McClelland, J. W., and Dunton, K. H. (2018). Do high Arctic coastal food webs rely on a terrestrial carbon subsidy? *Food Webs* 15, 2352–2496.

Helms, J. R., Stubbins, A., Ritchie, J. D., Minor, E. C., Kieber, D. J., and Mopper, K. (2008). Absorption spectral slopes and slope ratios as indicators of molecular weight, source, and photobleaching of chromophoric dissolved organic matter. *Limnol. Oceanogr.* 53, 955–969. doi: 10.4319/lo.2008.53.3.0955

Hendry, K. R., Huvenne, V. A. I., Robinson, L. F., Annett, A., Badger, M., Jacobel, A. W., et al. (2019). The biogeochemical impact of glacial meltwater from Southwest Greenland. *Prog. Oceanogr.* 176:102126. doi: 10.1016/j.pocean.2019.102126

Hodson, A., Mumford, P., and Lister, D. (2004). Suspended sediment and phosphorus in proglacial rivers: bioavailability and potential impacts upon the P status of ice-marginal receiving waters. *Hydrol. Process.* 18, 2409–2422. doi: 10.1002/hyp.1471

Hodson, A., Nowak, A., and Christiansen, H. (2016). Glacial and periglacial floodplain sediments regulate hydrologic transfer of reactive iron to a high arctic fjord. *Hydrol. Process.* 30, 1219–1229. doi: 10.1002/hyp.10701

Holding, J. M., Duarte, C. M., Delgado-Huertas, A., Soetaert, K., Vonk, J. E., Agustí, S., et al. (2017). Autochthonous and allochthonous contributions of organic carbon to microbial food webs in Svalbard fjords. *Limnol. Oceanography* 62, 1307-1323. doi: 10.1002/lno.10526

Holding, J. M., Markager, S., Juul-Pedersen, T., Paulsen, M. L., Moller, E. F., Meire, L., et al. (2019). Seasonal and spatial patterns of primary production in a high-latitude fjord affected by Greenland Ice Sheet run-off. *Biogeosciences* 16, 3777–3792. doi: 10.5194/bg-16-3777-2019

Holinde, L., and Zielinski, O. (2016). Bio-optical characterization and light availability parameterization in Uummannaq Fjord and Vaigat-Disko Bay (West Greenland). *Ocean Sci.* 12, 117–128. doi: 10.5194/os-12-117-2016

Holmes, R. M., McClelland, J. W., Peterson, B. J., Tank, S. E., Bulygina, E., Eglinton, T. I., et al. (2011). Seasonal and annual fluxes of nutrients and organic matter from large rivers to the Arctic Ocean and surrounding seas. *Estuar. Coasts* 35, 369–382. doi: 10.1007/s12237-011-9386-6

Holmes, R. M., McClelland, J. W., Raymond, P. A., Frazer, B. B., Peterson, B. J., and Stieglitz, M. (2008). Lability of DOC transported by Alaskan rivers to the Arctic Ocean. *Geophys. Res. Lett.* 35:L03402. doi: 10.1029/2007GL032837

Hood, E., Fellman, J., Spencer, R. G. M., Hernes, P. J., Edwards, R., D'Amore, D., et al. (2009). Glaciers as a source of ancient and labile organic matter to the marine environment. *Nature* 462, 1044–1047. doi: 10.1038/nature08580

Hu, C., Muller-Karger, F. E., and Zepp, R. G. (2002). Absorbance, absorption coefficient, and apparent quantum yield: a comment on common ambiguity in the use of these optical concepts. *Limnol. Oceanogr.* 47, 1261–1267. doi: 10.4319/lo.2002.47.4.1261

IPCC (2014). "Climate change 2014: synthesis report," in *Proceedings of the Contribution of Working Groups I, II and III to the Fifth Assessment Report of the Intergovernmental Panel on Climate Change[Core Writing Team]*, eds R. K. Pachauri and L. A. Meyer (Geneva: IPCC).

Jain, A., Krishnan, K. P., Singh, A., Thomas, F. A., Begum, N., Tiwari, M., et al. (2019). Biochemical composition of particles shape particle-attached bacterial community structure in a high Arctic fjord. *Ecol. Indic.* 102, 581–592. doi: 10.1016/j.ecolind.2019.03.015

Johnston, S. E., Bogard, M. J., Rogers, J. A., Butman, A., Striegl, R. G., Dornblaser, et al. (2019). Constraining dissolved organic matter sources and temporal variability in a model sub-Arctic lake. *Biogeochemistry* 146, 271–292. doi: 10.1007/s10533-019-00619-9

Joli, N., Gosselin, M., Ardyna, M., Babin, M., Onda, D. F., Tremblay, J. E., et al. (2018). Need for focus on microbial species following ice melt and changing freshwater regimes in a Janus Arctic Gateway. *Sci. Rep.* 8:9405. doi: 10.1038/s41598-018-27705-6

Ju, J., and Masek, J. G. (2016). The vegetation greenness trend in Canada and US Alaska from 1984–2012 Landsat data. *Remote Sens. Environ.* 176, 1–16. doi: 10.1016/j.rse.2016.01.001

Kanna, N., Sugiyama, S., Ohashi, Y., Sakakibara, D., Fukamachi, Y., and Nomura, D. (2018). Upwelling of macronutrients and dissolved inorganic carbon by a subglacial freshwater driven plume in Bowdoin Fjord, northwestern Greenland. *J. Geophys. Res. Biogeosci.* 123, 1666–1682. doi: 10.1029/2017jg004248

Kaste, Ø, Skarbøvik, E., Greipsland, I., Gundersen, C. B., Austnes, K., Skancke, L. B., et al. (2018). *The Norwegian River Monitoring Programme–Water Quality Status and Trends 2017. NIVA-Repport M-no* 1168. Norway: Miljødirektoratet.

Kędra, M., Kuliński, K., Walkusz, W., and Legeżyńska, J. (2012). The shallow benthic food web structure in the high Arctic does not follow seasonal changes in the surrounding environment. *Estuar. Coast. Shelf Sci.* 114, 183–191. doi: 10.1016/J.ECSS.2012.08.015

Kellogg, C. T. E., McClelland, J. W., Dunton, K. H., and Crump, B. C. (2019). Strong seasonality in arctic estuarine microbial food webs. *Front. Microbiol.* 10:2628. doi: 10.3389/fmicb.2019.02628

Kirk, J. T. O. (2010). *Light and Photosynthesis in Aquatic Ecosystems*. Cambridge: Cambridge University Press.

Koch, J. C., Runkel, R. L., Striegl, R., and McKnight, D. M. (2013). Hydrologic controls on the transport and cycling of carbon and nitrogen in a boreal catchment underlain by continuous permafrost. *J. Geophys. Res. Biogeo.* 118, 698–712. doi: 10.1002/jgrg.20058

Koziol, K. A., Moggridge, H. L., Cook, J. M., and Hodson, A. J. (2019). Organic carbon fluxes of a glacier surface: a case study of Foxfonna, a small Arctic glacier. *Earth Surf. Process. Landf.* 44, 405–416. doi: 10.1002/esp.4501

Luckmann, A., Benn, D. I., Cottier, F., Bevan, S., Nilsen, F., and Inall, M. (2015). Calving rates at tidewater glaciers vary strongly with oceantemperature. *Nat. Comm.* 6:8566. doi: 10.1038/ncomms9566

Mann, P. J., Davydova, A., Zimov, N., Spencer, R. G. M., Davydov, S., Bulygina, E., et al. (2012). Controls on the composition and lability of dissolved organic matter in Siberia's Kolyma River basin. *J. Geophys. Res.* 117:G01028. doi: 10.1029/2011jg001798

McClelland, J. W., Déry, S. J., Peterson, B. J., Holmes, R. M., and Wood, E. F. (2006). A pan-arctic evaluation of changes in river discharge during the latter half of the 20th century. *Geophys. Res. Lett.* 33:L06715. doi: 10.1029/2006gl025753

Meire, L., Mortensen, J., Rysgaard, S., Bendtsen, J., Boone, W., Meire, P., et al. (2016). Spring bloom dynamics in a subarctic fjord influenced by tidewater outlet glaciers (Godthåbsfjord, SW Greenland). *J. Geophys. Res. Biogeosci.* 121, 1581–1592. doi: 10.1002/2015JG003240

Meslard, F., Bourrin, F., Many, G., and Kerhervé, P. (2018). Suspended particle dynamics and fluxes in an Arctic fjord (Kongsfjorden, Svalbard). *Estuar. Coast. Shelf Sci.* 204, 212–224. doi: 10.1016/j.ecss.2018.02.020

Moran, M. A., Sheldon, W. M. Jr., and Zepp, R. G. (2000). Carbon loss and optical property changes during long-term photochemical and biological degradation of estuarine dissolved organic matter. *Limnol. Oceanogr.* 45, 1254–1264. doi: 10.4319/lo.2000.45.6.1254

Moran, M. A., and Zepp, R. G. (1997). Role of photoreactions in the formation of biologically labile compounds from dissolved organic matter. *Limnol. Oceanogr.* 42, 1307–1316. doi: 10.4319/lo.1997.42.6.1307

Muckenhuber, S., Nilsen, F., Korosov, A., and Sandven, S. (2016). Sea ice cover in Isfjorden and Hornsund, Svalbard (2000–2014) from remote sensing data. *Cryosphere* 10, 149–158. doi: 10.5194/tc-10-149-2016

Murray, C., Markager, S., Stedmon, C. A., Juul-Pedersen, T., Sejr, M. K., and Bruhn, A. (2015). The influence of glacial melt water on bio-optical properties in two contrasting Greenlandic fjords. *Estuar. Coast. Shelf Sci.* 163, 72–83. doi: 10.1016/j.ecss.2015.05.041

Myneni, R. B., Keeling, C. D., Tucker, C. J., Asrar, G., and Nemani, R. R. (1997). Increased plant growth in the northern high latitudes from 1981-1991). *Nature* 386, 698–701. doi: 10.1038/386698a0

Neff, J. C., Finaly, J. C., Zimov, S. A., Davydov, S. P., Carrasco, J. J., Schuur, E. A. G., et al. (2006). Seasonal changes in the age and structure of dissolved organic carbon in Siberian rivers and streams. *Geophy. Res. Lett.* 33:L10401. doi: 10.1029/2006GL028222

Nilsen, F., Cottier, F., Skogseth, R., and Mattsson, S. (2008). Fjord-shelf exchanges controlled by ice and brine production: the interannual variation of Atlantic Water in Isfjorden, Svalbard. *Contin. Shelf Res.* 28, 1838–1853. doi: 10.1016/j.csr.2008.04.015

Nilsen, F., Skogseth, R., Vaardal-Lunde, J., and Inall, M. (2016). A simple shelf circulation model: intrusion of Atlantic Water on the West Spitsbergen Shelf. *J. Phys. Oceanogr.* 46, 1209–1230. doi: 10.1175/jpo-d-15-0058.1

Nowak, A., and Hodson, A. (2015). On the biogeochemical response of a glacierized High Arctic watershed to climate change: revealing patterns, processes and heterogeneity among micro-catchments. *Hydrol. Process.* 29, 1588–1603. doi: 10.1002/hyp.10263

Nuth, C., Kohler, J., König, M., von Deschwanden, A., Hagen, J. O., and Kääb, A. (2013). Decadal changes from a multi-temporal glacier inventory of Svalbard. *Cryosphere* 7, 1603–1621. doi: 10.5194/tc-7-1603-2013

Nyeggen, M. U. (2019). *Seasonal Zooplankton Dynamics in Svalbard Coastal Waters: The Shifting Dominance of Mero- and Holoplankton and Timing of Reproduction in Three Species of Copepoda*. Master thesis. Bergen: University of Bergen.

Oksanen, J., Blanchet, F. G., Friendly, M., Kindt, R., Legendre, P., McGlinn, D., et al. (2018). *vegan: Community Ecology Package. R Package Version 2.5-2. 2018*.

Parmentier, F. J. W., Christensen, T. R., Rysgaard, S., Bendtsen, J., Glud, R. N., Else, B., et al. (2017). A synthesis of the arctic terrestrial and marine carbon cycles under pressure from a dwindling cryosphere. *Ambio* 46, S53–S69. doi: 10.1007/s13280-016-0872-8

Parsons, T. R. (2013). *A Manual of Chemical & Biological Methods for Seawater Analysis*. Kent: Elsevier.

Parsons, T. R., Webb, D. G., Rokeby, B. E., Lawrence, M., Hopkey, G., and Chiperzak, D. (1989). Autotrophic and heterotrophic production in the Mackenzie River/Beaufort Sea estuary. *Polar Biol.* 9, 261–266. doi: 10.1007/bf00263774

Paulsen, M. L., Nielsen, S. E. B., Müller, O., Møller, E. F., Stedmon, C. A., Juul-Pedersen, T., et al. (2017). Carbon bioavailability in a high arctic fjord influenced by glacial meltwater, NE Greenland. *Front. Mar. Sci.* 4:176. doi: 10.3389/fmars.2017.00176

Pavlov, A. K., Granskog, M. A., Stedmon, C. A., Ivanov, B. V., Hudson, S. R., and Falk-Petersen, S. (2015). Contrasting optical properties of surface waters across the Fram Strait and its potential biological implications. *J. Mar. Syst.* 143, 62–72. doi: 10.1016/j.jmarsys.2014.11.001

Pavlov, A. K., Leu, E., Hanelt, D., Bartsch, I., Karsten, U., Hudson, S. R., et al. (2019). "The underwater light climate in Kongsfjorden and its ecological implications," in *The Ecosystem of Kongsfjorden, Svalbard*, eds H. Hop and C. Wiencke (Cham: Springer International Publishing), 137–170. doi: 10.1007/978-3-319-46425-1_5

Peterson, B. J., and Fry, B. (1987). Stable isotopes in ecosystem studies. *Annu. Rev. Ecol. Syst.* 18, 293–320. doi: 10.1146/annurev.es.18.110187.001453

Peterson, B. J., Holmes, R. M., McClelland, J. W., Vörösmarty, C. J., Lammers, R. B., Shiklomanov, A. I., et al. (2002). Increasing river discharge to the Arctic Ocean. *Science* 298, 2171–2173. doi: 10.1126/science.1077445

Proshutinsky, A., Krishfield, R., Timmermans, M.-L., Toole, J., Carmack, E., McLaughlin, F., et al. (2009). Beaufort gyre freshwater reservoir: state and variability from observations. *J. Geophys. Res. Oceans* 114:C00A10. doi: 10.1029/2008jc005104

R Core Team (2017). *R: A Language and Environment for Statistical Computing*. Vienna: R Foundation for Statistical Computing.

Raymond, P., Saiers, J., and Sobczak, W. (2016). Hydrological and biogeochemical controls on watershed dissolved organic matter transport: pulse-shunt concept. *Ecology* 97, 5–16. doi: 10.1890/14-1684.1

Raymond, P. A., McClelland, J. W., Holmes, R. M., Zhulidov, A. V., Mull, K., Peterson, B. J., et al. (2007). Flux and age of dissolved organic carbon exported to the Arctic Ocean: a carbon isotopic study of the five largest arctic rivers. *Glob. Biogeochem. Cycles* 21:GB401. doi: 10.1029/2007gb002934

Raymond, P. A., and Saiers, J. E. (2010). Event controlled DOC export from forested watersheds. *Biogeochemistry* 100, 197–209. doi: 10.1007/s10533-010-9416-7

Rember, R. D., and Trefry, J. H. (2004). Increased concentrations of dissolved trace metals and organic carbon during snowmelt in rivers of the Alaskan Arctic. *Geochim. Cosmochim. Acta* 68, 477–489. doi: 10.1016/s0016-7037(03)00458-7

Sholkovitz, E. R. (1976). Flocculation of dissolved organic and inorganic matter during the mixing of river water and seawater. *Geochim. Cosmochim. Acta* 40, 831–845. doi: 10.1016/0016-7037(76)90035-1

Sipler, R. E., Kellogg, C. T. E., Connelly, T. L., Roberts, Q. N., Yager, P. L., and Bronk, D. A. (2017). Microbial community response to terrestrially derived dissolved organic matter in the coastal Arctic. *Front. Microbiol.* 8:1018. doi: 10.3389/fmicb.2017.01018

Smith, R. W., Bianchi, T. S., Allison, M., Savage, C., and Galy, V. (2015). High rates of organic carbon burial in fjord sediments globally. *Nat. Geosci.* 8, 450–U446. doi: 10.1038/ngeo2421

Spencer, R. G. M., Aiken, G. R., Wickland, K. P., Striegl, R. G., and Hernes, P. J. (2008). Seasonal and spatial variability in dissolved organic matter quantity and composition from the Yukon River basin, Alaska. *Glob. Biogeochem. Cycles* 22:GB4002. doi: 10.1029/2008gb003231

Spielhagen, R. F., Werner, K., Sørensen, S. A., Zamelczyk, K., Kandiano, E., Budeus, G., et al. (2011). Enhanced modern heat transfer to the arctic by warm atlantic water. *Science* 331, 450–453. doi: 10.1126/science.1197397

Stedmon, C., and Markager, S. (2001). The optics of chromophoric dissolved organic matter (CDOM) in the Greenland Sea: an algorithm for differentiation between marine and terrestrially derived organic matter. *Limnol. Oceanogr.* 46, 2087–2093. doi: 10.4319/lo.2001.46.8.2087

Striegl, R. G., Aiken, G. R., Dornblaser, M. M., Raymond, P. A., and Wickland, K. P. (2005). A decrease in discharge-normalized DOC export by the Yukon River during summer through autumn. *Geophys. Res. Lett.* 32:L21413. doi: 10.1029/2005GL024413

Syvitski, J. P. M. (2002). Sediment discharge variability in Arctic rivers: implications for a warmer future. *Polar Res.* 21:323. doi: 10.3402/polar.v21i2.6494

Tarnocai, C., Canadell, J. G., Schuur, E. A. G., Kuhry, P., Mazhitova, G., and Zimov, S. (2009). Soil organic carbon pools in the northern circumpolar permafrost region. *Glob. Biogeochem. Cycles* 23:GB2023. doi: 10.1029/2008gb003327

Telling, J., Anesio, A. M., Tranter, M., Irvine-Fynn, T., Hodson, A., Butler, C., et al. (2011). Nitrogen fixation on Arctic glaciers, Svalbard. *J. Geophys. Res. Biogeosci.* 116:G03039. doi: 10.1029/2010jg001632

Torsvik, T., Albretsen, J., Sundfjord, A., Kohler, J., Sandvik, A. D., Skarðhamar, J., et al. (2019). Impact of tidewater glacier retreat on the fjord system: modeling present and future circulation in Kongsfjorden, Svalbard. *Estuar. Coast. Shelf Sci.* 220, 152–165. doi: 10.1016/j.ecss.2019.02.005

van Pelt, W., Pohjola, V. A., Pettersson, R., Marchenko, S., Kohler, J., Luks, B., et al. (2019). A long-term dataset of climatic mass balance, snow conditions, and runoff in Svalbard (1957-2018). *Cryosphere* 13, 2259–2280. doi: 10.5194/tc-13-2259-2019

van Pelt, W. J. J., Pohjola, V. A., and Reijmer, C. H. (2016). The changing impact of snow conditions and refreezing on the mass balance of an idealized Svalbard Glacier. *Front. Earth Sci.* 4:102. doi: 10.3389/feart.2016.00102

Vihtakari, M. (2019). *PlotSvalbard: PlotSvalbard – Plot Research Data From Svalbard on Maps. Rpackage version* 0.8.5.

Wadham, J. L., Hawkings, J., Telling, J., Chandler, D., Alcock, J., O'Donnell, E., et al. (2016). Sources, cycling and export of nitrogen on the Greenland Ice Sheet. *Biogeosciences* 13, 6339–6352. doi: 10.5194/bg-13-6339-2016

Weishaar, J. L., Aiken, G. R., Bergamaschi, B. A., Fram, M. S., Fujii, R., and Mopper, K. (2003). Evaluation of specific ultraviolet absorbance as an indicator of the chemical composition and reactivity of dissolved organic carbon. *Environ. Sci. Technol.* 37, 4702–4708. doi: 10.1021/es030360x

Wetzel, R. G., Hatcher, P. G., and Bianchi, T. S. (1995). Natural photolysis by ultraviolet irradiance of recalcitrant dissolved organic matter to simple substrates for rapid bacterial metabolism. *Limnol. Oceanogr.* 40, 1369–1380. doi: 10.4319/lo.1995.40.8.1369

Wikner, J., and Andersson, A. (2012). Increased freshwater discharge shifts the trophic balance in the coastal zone of the northern Baltic Sea. *Glob. Chang. Biol.* 18, 2509–2519. doi: 10.1111/j.1365-2486.2012.02718.x

Yun, M. S., Whitledge, T. E., Stockwell, D., Son, S. H., Lee, J. H., Park, J. W., et al. (2016). Primary production in the Chukchi Sea with potential effects of freshwater content. *Biogeosciences* 13, 737–749. doi: 10.5194/bg-13-737-2016

Zajączkowski, M. (2008). Sediment supply and fluxes in glacial and outwash fjords, Kongsfjorden and Adventfjorden, Svalbard. *Polish Polar Res.* 29, 59–72.

Zhu, Z., Wu, Y., Liu, S., Wenger, F., Hu, J., Zhang, J., et al. (2016). Organic carbon flux and particulate organic matter composition in Arctic valley glaciers: examples from the Bayelva River and adjacent Kongsfjorden. *Biogeosciences* 13, 975–987. doi: 10.5194/bg-13-975-2016

Conflict of Interest: The authors declare that the research was conducted in the absence of any commercial or financial relationships that could be construed as a potential conflict of interest.

Table S1. Physical and chemical characteristics of water samples (means ±SD) for each month and water type. Categories include physical and chemical parameters and organic matter.

	May			June			August		
	River	**Fjord SW**	**Fjord AW**	**River**	**Fjord SW**	**Fjord AdW**	**River**	**Fjord SW**	**Fjord AdW**
Number of samples	1	7	20	7	53	10	7	44	14
Water Mass	N/A	SW	ArW	N/A	SW/IW	TAW/ArW	N/A	SW/IW	AW
PHYSICAL									
Salinity	N/A	33.5 ±0.6	34.4 ±0.2	N/A	27.6 ±9.9	34.7 ±0.3	N/A	28.6 ±6.0	35.3 ±0.5
Temp (ºC)	N/A	0.3 ±0.4	-0.2 ±0.4	5.5 ±1.3	4.6 ±1.7	1.8 ±0.6	N/A	7.7 ±1.7	4.5 ±0.8
Turbidity (NTU)	N/A	2.9 ±2.4	2.0 ±2.7	303.0 ±166.2	7.0 ±9.7	2.6 ±1.1	485.2 ±194.5	20.7 ±62.2	6.2 ±10.0
SPM (mg L^{-1})	110.5	27.1 ±9.2	32.3 ±6.8	348.5 ±288.0	29.4 ±7.6	26.1 ±3.5	170.0 ±91.7	46.5 ±41.7	24.2 ±11.3
CHEMICAL									
NO_2+NO_3 (μmol L^{-1})	3.27	0.36 ±0.14	0.88 ±0.96	7.78 ±2.56	1.27 ±1.39	0.55 ±0.26	12.03 ±7.45	0.93 ±2.06	0.72 ±0.45
NH_4 (μmol L^{-1})	1.91	0.96 ±0.57	1.08 ±0.39	1.18 ±0.50	1.08 ±0.54	0.95 ±0.49	1.43 ±1.05	1.13 ±0.53	1.25 ±0.54
PO_4 (μmol L^{-1})	0.06	0.11 ±0.03	0.18 ±0.07	0.04 ±0.03	0.44 ±0.67	0.17 ±0.05	0.56 ±0.67	0.22 ±0.09	0.26 ±0.07
SiO_2 (μmol L^{-1})	19.31	0.58 ±0.26	1.29 ±3.03	20.14 ±9.63	3.15 ±4.00	0.99 ±0.49	35.20 ±21.09	4.89 ±5.82	3.50 ±0.98
PartN (μmol L^{-1})	14.99	5.85 ±3.97	4.65 ±1.48	31.28 ±29.44	4.76 ±2.32	4.02 ±3.18	41.25 ±57.17	5.20 ±5.14	2.91 ±2.02
PartP (μmol L^{-1})	3.67	0.17 ±0.02	0.23 ±0.10	4.35 ±4.42	0.37 ±0.24	0.15 ±0.09	4.58 ±3.55	0.66 ±1.13	0.12 ±0.09
ORGANIC MATTER									
DOC (μmol L^{-1})	980	206 ±170	161 ±127	604 ±550	95 ±21	101 ±15	43 ±19	71 ±17	77 ±11
POC (μmol L^{-1})	205.7	28.5 ±11.0	29.5 ±5.8	549.4 ±604.6	41.8 ±24.2	25.4 ±11.0	789.1 ±1412.5	65.4 ±99.9	19.1 ±8.1
C:N (molar ratio)	13.7	6.1 ±2.5	6.6 ±1.3	16.3 ±3.1	9.0 ±3.8	7.2 ±2.2	16.7 ±6.8	10.5 ±5.5	7.5 ±2.0
Chl *a* (mg/m^3)	N/A	0.29 ±0.20	1.51 ±1.75	N/A	0.80 ±0.80	1.46 ±0.94	N/A	0.89 ±0.54	0.96 ±0.43
$\delta^{13}C$ (‰)	-26.5	-24.0 ±0.8	-23.8 ±0.8	-26.5 ±1.1	-26.2 ±2.1	-27.4 ±1.3	-26.5 ±1.0	-26.4 ±0.8	-27.3 ±0.9
$\delta^{15}N$ (‰)	1.5	5.0 ±1.0	5.3 ±0.4	3.4 ±1.1	4.6 ±0.7	4.9 ±0.7	3.0 ±0.6	4.3 ±0.8	4.3 ±0.8
$a_{CDOM}(375)$ (1/m)	1.58	0.30 ±0.11	0.24 ±0.20	0.53 ±0.36	1.04 ±0.71	0.93 ±0.39	0.54 ±0.35	0.30 ±0.21	0.35 ±0.22
$SUVA_{254}$ (m^2/gC)	0.83	1.54 ±0.74	2.59 ±1.55	2.42 ±2.10	2.81 ±1.14	1.71 ±0.81	5.65 ±1.65	2.86 ±0.67	2.52 ±0.39
$S_{275-295}$	0.02	23.95 ±3.21	28.45 ±8.74	0.01 ±0.0	17.55 ±3.48	17.23 ±2.22	0.01 ±0.01	22.13 ±6.95	14.36 ±2.22
$S_{350-400}$	0.02	18.29 ±9.82	33.66 ±26.64	0.02 ±0.0	25.15 ±17.58	32.86 ±17.30	0.02 ±0.01	12.12 ±6.19	8.94 ±7.72
S_R	1.1	4.4 ±1.4	5.0 ±1.3	0.8 ±0.1	1.3 ±0.9	1.3 ±1.3	0.8 ±0.3	3.4 ±2.5	4.8 ±2.4

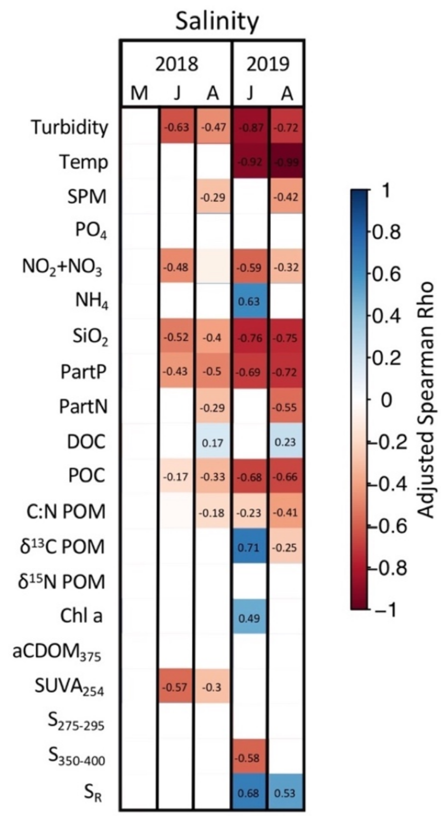

Figure S1. Spearman's rank correlation coefficients for each variable vs. salinity for each sampling month (M = May, J = June, A = August) in both sampling years. Color represents the correlation coefficients on a scale from 1 to -1. Coefficients with $p > 0.05$ (after Bonferroni correction) are not shown.

Paper 2

Turbid Meltwater Plumes Diminish the Quality of Particulate Organic Matter available for Arctic Coastal Food-webs

Maeve McGovern[1,2,3]*, Michael T Arts[4], Katrine Borgå[5,6] Anna M Dąbrowska[7], Eva Leu[8], Raul Primicerio[2], Paul Renaud[8,3], Janne E Søreide[3], Emilie H Vereide[9], Amanda E Poste[1,2]

[1]Norwegian Institute for Water Research, Tromsø, Norway; [2]Department of Arctic Marine Biology, UiT: The Arctic University of Norway, Tromsø, Norway; [3]University Centre in Svalbard, Longyearbyen, Norway; [4]Ryerson University, Toronto, M5B 2K3, Canada; [5]Department of Biosciences, University of Oslo, Oslo, Norway; [6]Centre for Biogeochemistry in the Anthropocene (CBA), University of Oslo, Oslo, Norway; [7]Institute of Oceanology, Polish Academy of Sciences, Sopot, Poland; [8]Akvaplan-niva, Fram Centre, Tromsø, Norway; [9]Institute of Marine Research, Bergen, Norway

Corresponding Author: Maeve McGovern (maeve.mcgovern@niva.no)

Abstract

Climate change driven increases in sediment-laden terrestrial inputs to coastal areas are impacting the base of Arctic food-webs, and potentially altering the quality of organic material available for consumers. In the High Arctic, coastal ecosystem responses to increased meltwater transport from melting glaciers and permafrost occur alongside strong seasonal changes in water column structure and productivity, and zooplankton life history strategies. We investigated spatial and seasonal variations in source and quality of zooplankton food sources using bulk stable isotopes (SI) and fatty acid (FA) trophic markers. Zooplankton and water samples were collected along transects from glacier fronts and river estuaries to the outer fjord before the melt season (May), during spring freshet (June) and in late summer (August). Fatty acid content and composition are investigated in relation to physical and chemical environmental forcing and shifts in relative composition of different phytoplankton groups. Elevated diatom FA 16:1n-7 in May POM coincided with the spring phytoplankton bloom, which provides zooplankton with essential nutrients.

In June, turbid, glacier-impacted waters were characterized by reduced food quality while at stations beyond the reach of these visible meltwater plumes, high-quality EPA and DHA were observed alongside a mixed flagellate community. August FA profiles were dominated by low quality saturated fatty acids characteristic of late summer conditions. Zooplankton FA profiles were strongly coupled with water column POM, demonstrating strong seasonal shifts from elevated contributions of diatom FATM in May, to flagellate and terrestrial FATMs in June and August. Results highlight the importance of terrestrial inputs and associated light-attenuating suspended sediments on phytoplankton community composition, driving shifts in the quality of fatty acids available for uptake into the food-web at the land-ocean interface.

Keywords: Climate change, fatty acids, stable isotopes, organic matter quality, land ocean interactions, machine learning, biogeochemical tracers

1. Introduction

Arctic fjords represent the dynamic interface between land and sea, and thus are affected by climate-driven changes in terrestrial catchments as well as marine waters. On land, increased temperatures and precipitation are leading to increases in vegetative biomass (Goetz et al. 2005; Epstein et al. 2008), permafrost thaw (Biskaborn et al. 2019), glacial melt (Tepes et al. 2021) and riverine discharge (Ahmed et al. 2020; Stadnyk et al. 2021). At sea, increases in sediment-laden freshwater inputs stratify and darken impacted surface waters (Sagan and Darecki 2018; Konik et al. 2021), driving increased light attenuation in coastal waters across the Arctic (Hylander et al. 2011).

In Isfjorden, in central Spitsbergen, Svalbard, climate-change driven increases in temperature have been profound (Isaksen et al. 2016). On land, this region has the warmest permafrost for its latitude (Strand et al. 2021). Increases in temperature (Hanssen-Bauer et al. 2019) are leading to reductions in sea-ice and glacial mass balance (Dahlke et al. 2020; Morris et al. 2020). Inputs of freshwater from marine and land-terminating glaciers further enhance estuarine circulation, facilitating advection of warm, saline water from the shelf (Fraser et al. 2018), which transport nutrient-rich water, as well as zooplankton (Walczyńska et al. 2019) into the fjord.

At high latitudes, these climate-driven changes occur against the backdrop of extreme variations in daylight, with polar day lasting from April to August and polar night from October to February. This unwavering seasonal solar cycle drives strong seasonal variations in phytoplankton production with implications for food availability and quality for coastal zooplankton (Leu et al. 2011). Life history strategies of resident zooplankton, and the calanoid copepod *Calanus* spp. in particular, are thus adapted to rely on the short, intense spring phytoplankton bloom (Søreide et al. 2010). In Svalbard, the annual spring bloom typically occurs between April and May, and provides high-quality food, including various essential algal-produced fatty acids (EFA) to zooplankton. Zooplankton effectively incorporate these FA into various lipid classes, whose diverse metabolic functions play essential roles (e.g. membrane fluidity, energy storage) for life in the High Arctic (Hirche and Kattner 1993; Lee et al. 2006).

Algae, or more precisely particulate organic matter, is considered to be of high quality if it contains specific PUFA, including the n-3 FA and n-6 essential fatty acids (EFA; e.g. eicosapentaenoic acid (EPA; 20:5n-3), docosahexaenoic acid (DHA; 22:6n-3), and a-linolenic acid (ALA; 18:3n-3), and arachidonic acid (ARA; 20:4n-6)). These PUFA are synthesized primarily by phytoplankton, macrophytes and plants. Consumers, including zooplankton, fish and humans, must acquire these critical nutrients from their diet (Parrish 2009; Galloway and Winder 2015).

Availability of these EFA is important for the growth and development of zooplankton and higher trophic level predators (Jónasdóttir et al. 2002; Daase et al. 2011). n-3 PUFA in particular, are directly linked to ecosystem health, with n-3 limitation resulting in ecological implications at the individual, population, food web, and ecosystem scales (Mayzaud et al. 2013; Twining et al. 2016). Thus, a large body of research has focused on taxa-specific production of these EFA, which allows us to use these FA as biomarkers for the presence of certain phytoplankton in the diets of grazers and higher trophic level organisms (Dalsgaard et al. 2003; Budge et al. 2006). However, studies have also shown the impacts of environmental stressors, like temperature, and light and nutrient limitation on phytoplankton production of FA, demonstrating the plasticity of FA synthesis (Harrison et al. 1990; Reitan et al. 1994; Leu et al. 2006b; Hixson and Arts 2016).

Increases in sediment-and OM-laden terrestrial inputs have the potential to alter phytoplankton growth and community composition through impacts on light availability, nutrients, salinity and temperature (Hylander et al. 2011; Calleja et al. 2017; Halbach et al. 2019; Szeligowska et al. 2020; Dunse et al. 2021). Since FA production is phylum-specific (Jónasdóttir 2019), these indirect impacts of terrestrial inputs may subsequently affect the production of EFA, with cascading effects for coastal ecosystems structure and function. Terrestrial inputs also provide a direct source of organic carbon to coastal food-webs in the particulate and dissolved forms. Terrestrial carbon can be taken up into the food-web directly through consumption of POC, or indirectly through the microbial loop (Cole et al. 2006; Hiltunen et al. 2017). Lower food quality has consequences for Arctic zooplankton who rely on the summer season for accumulation of storage lipids which allow them to survive longer periods without food (Lee et al. 2006).

In this study, we investigate the interaction between the summer melt season on land and seasonality in the water column and how these drivers manifest in FA source and quality available for and utilized by Isfjorden zooplankton. We use machine learning as a novel approach to evaluate the connectivity between FA source and quality in relation to environmental forcing and phytoplankton biomass. Our objective is to determine how the effects of terrestrial inputs, including impacts on stratification, nutrients, light and temperature, affect organic matter source and quality, and in turn, zooplankton carbon sources, at the land-ocean interface.

2. Methods

2.1 Field sampling

Zooplankton and water samples were collected from 17 stations in Isfjorden, Svalbard in June 18th-24, and August 16th-24, 2018. During 10-11 May, only 12 stations were sampled since land-fast ice prevented access to the innermost fjord stations (Fig. 1). Zooplankton were sampled using 60 and 200 μm WP2 nets (both with a diameter of 0.25 m^2) and a larger and coarser 1000 μm WP3 net (with a diameter of 1 m^2). All net contents were pooled and macrozooplankton were removed prior to size-fractionation with sequential Nitex mesh screens (mesh sizes: 1000 μm, 500 μm, 200 μm, and 50 μm). Subsamples of size fractions were frozen for stable isotope (-20°C), and FA (-80°C) analyses. In addition, a subsample from each size fraction was fixed (10% Formalin) for determination of relative species composition.

Water samples were collected from the surface (0 m) and subsurface (15 m) using a 12 L Niskin bottle. Water samples were sieved to remove zooplankton (200 µm mesh) and stored in cold and dark conditions while being transported to the lab. Subsamples for phytoplankton community analyses were collected in 250 mL dark containers and fixed with a lugol-glutaraldehyde solution. Within a 24 h period, water samples were filtered (500-1000 mL) and POM collected on 0.2 µm QMA filters, which were folded and tucked into a 1.8 mL cryovial and frozen at -80°C. Collection of physicochemical data, including light and CTD profiles as well as discrete measurements of salinity, turbidity, temperature, particulate and dissolved nutrients, and $\delta^{13}C$ and $\delta^{15}N$-POM are reported in a parallel study (McGovern et al. 2020).

2.2 Bulk stable isotope analysis

Stable isotope ($\delta^{13}C$ and $\delta^{15}N$) analysis of zooplankton was carried out at the University of California, Davis (UC Davis Stable Isotope Facility, USA). Prior to analysis, zooplankton samples (n = 114) were freeze-dried for 24-48 h and homogenized using an agate mortar and pestle. Since $\delta^{13}C$ measurements are influenced by carbonate content, and $\delta^{15}N$ measurements by carbonate removal methods (Søreide and Nygård 2012), a subset of acidified (1N HCl) samples (n= 16), were used to test for effects of acidification on zooplankton $\delta^{13}C$ (Carrasco 2019). Subsamples were weighed to the nearest 1 µg and packed in aluminium capsules. Zooplankton $\delta^{13}C$ and $\delta^{15}N$ were analyzed using a PDZ Europa ANCA-GSL elemental analyser interfaced to a PDZ Europa 20-20 continuous flow isotope ratio mass spectrometer (IRMS), (Sercon Ltd., Cheshire, UK). Mean standard deviation for reference materials was ±0.04 for δ13C, and ±0.07 for $\delta^{15}N$. $\delta^{13}C$ and $\delta^{15}N$ values are expressed in units of per thousand (‰). Internal standards were Pee Dee Belemnite and Atmospheric N_2.

2.3 Fatty acid analysis

Fatty acid (FA) analysis of 42 FA was carried out on zooplankton (n = 60) and POM (n = 86) at Ryerson University (Toronto, Canada). Total lipids were extracted (Folch et al. 1957) with 4 mL of 2:1 chloroform:methanol. An 18 μg aliquot of Tricosanoic acid (23:0) was added to each tube as an internal standard in order determine recovery and methylation efficiency (mean ~80%). The extracts were then dried with non-reactive nitrogen gas. For the methylation of FA, 2 mL of hexanes was added to each of the tubes after which two 100 μL aliquots of the lipid solution was removed from each tube and placed in cast tin cups. After evaporation of the solvent, tubes were placed on a heating block for 90 min at 90°C. A Shimadzu GC-2010 plus, with an AOC-20i/s auto sampler and twin auto injectors, with Shimadzu LabSolutions software, was used to quantify FA. Column temperature was set to hold at 140°C for 5 min, ramping up to 240°C at 2°C/min for 50 min, and then holding at 240°C for the final 10 min. FA in the samples were identified and quantified by referencing them to the retention times of FA and using a series of calibration standards (GLC 463, GLC 68E, and 23:0, NuChek Prep., Waterville, MN, USA), respectively.

2.4 Protist identification and enumeration

Seawater subsamples of 200 mL were immediately fixed with an acidic Lugol's solution-glutaraldehyde (GA) mixture (1-2 % of final concentration), recommended for preservation of cells and colonies in protistan biomass studies (Rousseau et al. 1990). The subsamples were qualitatively and quantitatively analyzed according to the protocols described by Utermöhl (1958) and modified by Edler (1979). For this purpose, 10–50-mL subsamples were poured into the sedimentation chambers for 24 h, and then the protists were counted under an inverted microscope equipped with phase and interference contrasts (Nikon Eclipse TE-300). Nanoplanktonic cells (3–20 μm) were counted at 400× magnification by moving the field of view along the length of three transverse transects. We counted up to 50 specimens for the most numerous taxa, and the number of fields of view was considered individually. According to the taxonomic system presented in the World Register of Marine Species (WoRMS), taxes were identified to the lowest possible taxonomic level. Except for the indeterminate flagellates (Flagellate indet.: classified as mono- and biflagellates, up to 13 μm), each taxon was classified as one major taxonomic group (class or phylum). The total abundances (calculated per cubic meter) was converted to biomass (expressed as carbon content) using the database produced by the HELCOM Phytoplankton Expert Group (PEG; Olenina (2006)), based on the volume-to-biomass formulas developed by Menden-Deuer and Lessard (Menden-Deuer and Lessard 2000). Because ciliates require a specific method of fixation and preparation (the Quantitative Protargol Technique (QPS), e.g., Montagnes and Lynn (1987)) to avoid considerable cell shrinkage and distortion (Stoecker et al. 1994), and since Lugol's dark brown staining causes difficulties in optical microscope analyses, biomass was calculated only for the taxa identified to the species or genus level, which morphology makes it easily recognizable (repeatable within the samples) and, in terms of loricate ciliates, a shell-like protective outer covering gives the cell some resistance to deformation during fixation and handling. We are aware, however, that the estimated biomass of this group may be biased, and thus, it is treated with caution.

2.5 Data Analysis

Statistical analyses were performed using R (R version 4.0.2 (2020-06-22); R Core Team (2021)). The relative biomass of taxonomic groups in zooplankton size-fractions were calculated by matching species abundances with taxon-specific estimates of dry weights for individuals of Arctic zooplankton (Blachowiak-Samolyk et al. 2008). Zooplankton $\delta^{13}C$ values were lipid-corrected based on CN ratios (according to Pomerleau et al. 2014) to account for seasonality and interspecific variation in concentrations of $\delta^{13}C$ depleted lipids (Parker 1964). POM values were not corrected because in our glacier-impacted study system, CN ratios reflect high inorganic sediment loads rather than high lipid content. There was no relationship between lipid content and CN, or with $\delta^{13}C$ for POM (McGovern et al. 2020).

POM FA were analyzed based on concentrations and on relative composition while zooplankton FA were analyzed based only on relative composition only. Only FA which were detected in > 70 % of the samples were selected for analysis, and remaining non-detects were replaced with zeros. Sums and FATM were calculated from the remaining dataset. Relationships between FA and sampling date, depth and turbidity were investigated with a Kruskal-Wallis rank sum test and the *post hoc* Dunn's test (Dunn 1964) to account for non-normal distributions ($p < 0.05$, Shapiro-Wilk's test; Conover (1998)). P-values were adjusted for multiple comparisons using the Bonferroni correction (Bland and Altman 1995). In consideration of our small sample sizes and skewed data, results are presented as bootstrapped means with 95% confidence intervals (Greenacre 2016).

We used machine learning classification and regression algorithms for investigating broad patterns and relationships to environmental variables and phytoplankton biomass (Vabalas et al. 2019). While more typically used for big data, iterative, data-driven machine learning workflows, especially non-parametric methods like random forest, have advantages over traditional statistical methods for small ecological datatsets since they can infer missing values, and are free from strict assumptions including independent observations and collinearity. This allows for modelling of highly dimensional and non-linear data with complex interactions and missing values, issues that are commonplace in ecological studies (Thessen 2016).

To elucidate broad patterns of FA profiles across all samples and to identify FA that drive variability in our dataset, we used random forest models for classifying FA profiles based on sampling month and sample turbidity. The selected turbidity cut-off (3 NTU), was chosen based on optimization of the random forest model. Multidimensional scaling (MDS) was used to visualize variations in model proximities. Confidence interval plots were then constructed based on the most important FA differentiating sampling month and turbidity.

Variations in POM food quality and specific FA in response to environmental gradients and phytoplankton biomass were investigated using random forest regressions, which were built, tuned and assessed using the *tidymodels* ecosystem in R (Kuhn and Wickham 2020). Environmental variables included in the model were temperature, salinity, turbidity, NO_2+NO_3, DOC, CDOM, $S_{275-295}$, and secchi depth. Phytoplankton groups included Bacillariophyceae, Dinophyceae, Crytophyceae, Chrysophyceae, Oligotrichea and Prymnesiophyceae. Data were centered and scaled prior to analysis and missing values were imputed. Models were run on randomly split (70:30) training and test datasets, used for model training and prediction respectively. To increase the reliability of model estimates in light of our small sample size, we performed data splitting iteratively and present bootstrapped estimates, including the root mean square error (RMSE) and coefficient of determination (R^2) as means and confidence intervals of 100 iterations (Eischeid et al. 2021). Variable importance was evaluated by ranking the percentage of variance explained by each predictor variable in the final fitted model. Partial dependence plots were constructed to examine the marginal effects of each of the predictors on the response variables.

3. Results

3.1 Environmental characteristics of the water column

Physciochemical characteristics of the water column are reported in a parallel study (McGovern et al. 2020). Briefly, Isfjorden's inner fjord arms (Tempelfjorden and Billefjorden) were ice covered in May, when local and winter-cooled water dominated. Rivers were open and running with snowmelt in June during spring freshet, while August run-off was primarily driven by glacial meltwater. Surface water temperatures ranged from (-0.9 to 0.9°C) in May to (3.7 to 8.9°C) in August, and salinities ranged from (2.4 to 36.1) over the entire study period, with the lowest salinities measured in August. Atlantic water advection was detected in deeper waters in June and August. Chlorophyll *a* was generally low (< 1.2 (1—1.4) mg L^{-1}), with the highest values recorded in May. Values for bulk δ^{13}C-POC were highest in May (-23.9 (-24.1 to -23.6)) and lowest in June (-28 (-28.5 to -27.6)). Values did not differ spatially or vertically within each month ($p > 0.05$). Values of δ^{15}N were higher in May compared to June and August ($p > 0.05$) and were generally higher at 15 m compared to surface ($p < 0.05$; Fig. S1).

Total biomass of phytoplankton was higher in May (66.4; 47.9—86.1 mg C/m3) and June (62.6; 33.3—96.8 mg C/m3) compared to August (4.1; 2.6—5.6 mg C/m3). Community composition indicated a seasonal transition from microplankton dominance in May to nanoplankton dominance in August (Fig. 5). Bacillariophyceae contributed to 12.9 (5.2—21.9)% of total biomass in May, when Oligotrichea and Dinophyceae were also observed in high concentrations. Raphidophyceae, Chrysophyceae and Oligotrichea dominated in June, while Dinophyceae and Crytophyceae dominated what little phytoplankton biomass was present in August.

3.2 Seasonal and spatial patterns in POM SI and FA.

Total particulate lipid concentrations in surface waters remained consistent across months (58.6, 95% CI: 47.4—71.4 µg/L), but demonstrated seasonal and spatial variations in composition (Fig. 2). ΣPUFA concentrations were consistently higher at 15 m compared to the surface waters, but FA composition was generally uniform between depths, and thus depths were combined for further analysis (Table S1). ΣSFA contributed a greater percentage of total FA at high vs. low turbidity, with relative contribution increasing from May (40.2; 37—43.4%) and June (36.5; 33.8—39.7%) to August (51.6; 48.4—54.6%), when it dominated total FA in all samples. In contrast, ΣPUFA was higher at low turbidity in all months ($p < 0.05$), with highest concentrations in June (40.1; 36.4—43.6%) and May (34.8; 30.7—38.5%) and lowest in August (30.5; 26.8—34.3%).

Random forest classification was 84 % accurate, with a 16 % out of bag error rate, in sorting samples by sampling month based on all 36 FA (Fig. 3a). The most important FA for differentiating sampling month were 16:1n-7, 18:3n-3 and 18:0. Palmitoleic acid (16:1n-7) was higher in May compared to June and August ($p < 0.05$) while 18:3n-3 was higher in June ($p < 0.05$; Table 1), and 18:0 was highest in August (16.5; 14.2—18.8%) compared to June (7.6; 6.4—9%) and May (7.9; 6.8—9.1%; $p < 0.05$; Fig. 4a).

Random forest classification of June and August samples between high and low turbidity was 66 % accurate, with a 33.9 % out of bag error rate (Fig. 3b, S4). The most important FA for differentiating high and low turbidity were 22:0, 14:0, 22:6n-3, 18:3n-6 and 17:0. With further investigation, 22:0 + 20:0 (used previously as a terrestrial biomarker; Budge et al., 2001) was higher in turbid samples in June and August, Σodd-chain FA were higher in high turbidity samples, and ΣC18-PUFA was higher in samples with low turbidity (Fig. 4b).

Food quality, defined by ((EPA+DHA)/ΣSFA), was higher in May and June compared to August (Table 1; Fig. 4c). n-3 PUFA, including 20:5n-3 and 22:6n-3, peaked in June (10.9; 8.7—13.2 µg/L), while n-6 PUFA, including 20:4n-6, 18:3n-6 and 20:3n-6, were highest in August (11.6; 9—15.3 µg/L), especially at higher turbidity (Fig. 4c).

3.3 Relationships between POM FA and phytoplankton carbon and environmental variables

Results of random forest regression models indicate that environmental variables (RMSE: 0.2 (0.2—0.3); R^2: 0.4 (0.3—0.4)) were better at predicting food quality (defined as ((EPA + DHA)/SFA) compared to phytoplankton community composition (RMSE: 0.3 (0.3—0.3); R^2: 0.2 (0.1—0.2)) in both absolute (RMSE) and relative (R^2) terms based on 100 iterations of each ML algorithm. The most important environmental variables for predicting food quality were CDOM, NO_2 + NO_3, SiO_2, Turbidity and Secchi depth while important phytoplankton included Chrysophyceae, Prymnesiophyceae, Dinophyceae, Oligotrichia and Bacillariophyceae (Fig. 6). Partial dependence plots illustrate the relationships between the most important variables and food quality. Turbidity, as well as dissolved nutrients (NO_2 + NO_3, SiO_2) demonstrated a negative nonlinear relationship with food quality while secchi depth and CDOM had a positive relationship (Fig. 7).

3.4 Zooplankton SIA and FA profiles.

The relative composition of mesozooplankton taxa in size fractions shifted seasonally from Cirripedia nauplii dominance in May to *Calanus* spp. and Cirripedia cyprid larvae in June to *Calanus* spp, *Oithona* spp. and other small copepods in August (Fig. S3). Lipid-corrected bulk δ^{13}C values decreased seasonally in zooplankton from May (-19.8 (-20.3 to -19.3)) to June to August (-23.4 (-23.8 to -23); Fig. 8, Table 1), but did not differ spatially within each month ($p < 0.05$). Values of δ^{15}N were higher in May (9.6 (7.9 to 11.8)) compared to

June and August (7.4 (6.9 to 7.8); $p < 0.05$). Values for bulk δ^{13}C-POC were highest in May (-23.9 (-24.1 to -23.6)) and lowest in June (-28 (-28.5 to -27.6); McGovern et al. (2020)). Values did not differ spatially within each month ($p > 0.05$). Values of δ^{15}N were higher in May compared to June and August ($p > 0.05$; Fig. 8).

The dominant FA for all zooplankton included 16:0, 22:6n-3, and 20:5n-3 which together accounted for 55.8 (51.9—60.5) % of the total FA composition in zooplankton (Fig. S7). Diatom FATM (16:1n-7) was highest in May, contributing to 14 (11.3—16.7) of TFA (Table 1). Mean percentages of bacterial FA (Σodd-chain FA) were also higher in May compared to June and August (Table 1; Fig. 9). Meanwhile, flagellate FATM (ΣC18 PUFA) was highest in June and August and lowest in May (Table 1). Terrestrial FATM was overall very low in zooplankton, with the highest contribution observed in August (0.2 (0.1—0.3); Fig. 9).

4. Discussion:

We observed seasonal changes in food source composition and quality in the Isfjorden system. For POM, the top three FA differentiating the three sampling months were 16:1n-7, 18:3n-3 and 18:0. These three FA summarize the observed seasonal transformations from the spring diatom bloom in May to the flagellate-dominated bloom in June, to late summer. These findings are in line with previous studies which detail the Arctic seasonal FA-progression from the diatom bloom to late summer senescence (Leu et al. 2006a; Mayzaud et al. 2013; Galloway and Winder 2015; Connelly et al. 2016).

In Isfjorden, environmental conditions vary seasonally in the fjord and on land. The melt season extends from June to September, with snow and glacial melt delivering high suspended particle loads to the fjord, creating turbid meltwater plumes visible to the naked eye. A recent study using remote sensing in Adventfjorden, a branch of the Isfjorden system, revealed tight relationships between plume extent and temperature-driven melting events in the catchment (Walch in prep). These temperature-driven meltwater plumes transport catchment-derived materials (McGovern et al. 2020), and can have extensive impacts on the underwater light climate in the fjord (Halbach et al. 2019; Pavlov et al. 2019; Hopwood et al. 2020). Both of these factors are key drivers of the spatial patterns we observed in FA source and quality in June and August. In the POM, the top FA for differentiating high and low turbidity areas of the fjord were terrestrial FA (22:0 +20:0), bacterial FA, and saturated FA, reflecting low quality degraded sources, and material of terrestrial origin. The chosen food quality index ((EPA+DHA)/ΣSFA), first proposed by Derieux et al. (1998) as an index of organic matter 'freshness,' reflects these seasonal and spatial trends, with low food quality in areas impacted by the freshwater plume. However, high concentrations of EFA at the outer stations in June indicates there may be a 'sweet spot' for production of EFA in stratified areas receiving terrestrially-derived carbon and nutrients. Here, terrestrial runoff delivers nutrients and enhances stratification in areas where much of the suspended sediments have dispersed or settled out.

The strength of this study is the breadth of the dataset, which allows us to pair extensive environmental variables and phytoplankton community abundances with POM FA contents and composition. This allows for evaluation of the quantity and quality of OM available for zooplankton, and potential identification of spatial and seasonal EFA limitation. In addition, the paired phytoplankton dataset allows for validation of previously reported FATM for our study system which can then be applied to zooplankton collected from the same stations. Here, we present zooplankton as pooled samples of several size fractions. Dominated by suspension feeders, the taxonomic composition of these size fractions shifted seasonally from Cirripedia nauplii in May to *Calanus* spp. and *Oithona* spp. dominance in June and August. Thus, seasonality in food source and quality occurs alongside variations in zooplankton community structure and associated life history traits, with varying ecosystem implications at each stage in the melt season.

4.1 The spring bloom as a source of diatoms for zooplankton nauplii

In May 2018, sea-ice was still present in Isfjorden and rivers were frozen with minimal runoff to the fjord. FA profiles in May were representative of a typical late-stage spring phytoplankton bloom. High concentrations of palmitoleic acid (16:1n-7), were present alongside the highest biomass of Bacillariophyceae (diatoms) observed over the sampling period. The strong positive relationship between the two support the use of this FA as a biomaker for diatoms, as has been previously reported across the Arctic (Parrish et al. 2005; Pepin et al. 2011; Leu et al. 2020; Marmillot et al. 2021)

Previous studies have illustrated the important role the diatom-dominated spring bloom in Arctic fjords for fueling the Arctic food-web (Leu et al. 2011), with the highest concentrations of high-quality PUFA present during the early phase of spring bloom (Parrish et al. 2005; Leu et al. 2006a). PUFA concentrations observed in this study (3.8 to 60.1 µg/L) were similar to values reported for other Arctic spring bloom events (Reuss and Poulsen 2002; Leu et al. 2006a). Zooplankton FA profiles also reflected elevated contributions of diatoms and bacterial FA during this time, with size fractions dominated by Cirripedia and copepod nauplii. Food quality plays an important role in naupliar development (Daase et al. 2011). Cirripedia planktotrophic nauplii (likely *Balanus balanus;* Walczyńska et al. 2019), were found in high concentrations in nearshore Isfjorden in May (Vereide 2019). These feed extensively on the phytoplankton bloom (Stübner et al. 2016) before evolving into lecithotrophic cypris larvae (dominant here in June) and settling to the benthos (Weydmann-Zwolicka et al. 2021), actively transporting high-quality pelagic carbon to depth.

Alongside diatom FA, we also observed evidence of nutrient limitation (McGovern et al. 2020), and elevated contributions of saturated and odd-chain FA, alongside elevated $\delta^{15}N$, in some areas of the fjord. While $\delta^{15}N$ can be high in early spring in offspring and overwintering stages, the high values here are likely due to reliance on the microbial food-web, as indicated by increased contributions of odd-chain FA and 18:1n-7, typically associated with bacterial resource use (Howell et al. 2003; Kelly and Scheibling 2012). The spatial variation in FA profiles in May is unrelated to terrestrial inputs, but rather reflects the patchiness in spring bloom progression between nearshore (low turbidity) and outer fjord (high turbidity) areas. While there was nutrient limitation in the nearshore, a deeper mixed layer in the outer fjord supported an ongoing *Phaeocystis pouchetii* bloom. These observations suggest that May sampling occurred towards the end of the spring bloom in Isfjorden, a hypothesis supported by high resolution chlorophyll-*a* sampling in Adventfjord, which puts the peak of the spring bloom ~10 days prior to our sample collection (Nyeggen 2019). The relatively high contributions of saturated and bacterial FA are likely due to microbial degradation of the remains of the high-quality marine production in the water column.

4.2 Light availability shapes food quality along the fjord gradient

Previous studies have suggested the importance of terrestrial inputs and associated nutrient supply for the production of high-quality FA in coastal areas (Winder et al. 2017). However, in the Arctic, and especially in glacial fjords, these inputs are often accompanied by high concentrations of suspended sediments, which rapidly attenuate light in the nearshore. Our results emphasize this negative impact of terrestrial inputs on the production of EFA in Isfjorden. This is best represented by the spatial patterns observed in June, with strong differences between high and low turbidity areas. High turbidity was associated with reduced food quality, and meltwater plumes were both low in EFA like EPA and DHA, but also high in saturated FA. Compositionally, C18-PUFA were more dominant, which is a finding typical of nutrient-limited summer stratified periods which facilitate flagellate production (Mayzaud et al. 2013).

Intriguingly, despite the negative impact of these freshwater plumes, the highest food quality over the studied period was observed in the outer fjord in June, the month with the most extensive freshwater footprint. While these stations were characterized by low turbidity relative to the inner fjord stations, terrestrial material was still observed in the water column. In 2018, June sampling took place during the spring freshet, when high concentrations of DOC were observed in rivers draining into Isfjorden (McGovern et al. 2020). While meltwater transported SPM and associated particulates settle out relatively quickly, dissolved carbon and nutrients can be transported further from shore (Hyndes et al.

2014), and potentially accumulate in the outer fjord (Skogseth et al. 2020). High concentrations of ALA, EPA and DHA were also present in the outer fjord beyond the reach of the suspended sediments. EPA, typically associated with diatoms (Viso and Marty 1993; Dalsgaard et al. 2003; Connelly et al. 2016), was highest in June with a significant negative relationship with diatom biomass, but positive relationships with cryptophytes, dinoflagellates and chrysophytes.

Results of ML models suggest the key environmental driver of food quality as well as EPA and DHA concentrations individually was $a_{CDOM}(375)$, which was highest at these outer stations and tightly correlated with low $\delta^{13}C$-POC, suggesting the presence of terrestrial OM. Food quality was also positively correlated with secchi depth and DOC, variables which were also higher at these stations. The high $a_{CDOM}(375)$ and DOC concentrations in the outer fjord may be driven by the degradation of terrestrial POC, a process which releases humic substances (Brogi et al. 2019). These materials, together with meltwater-driven stratification and Atlantic water advection of nutrients, have been suggested to contribute to increased relative abundance of copiotrophic bacteria, including *Sulfitobacter* and the heterotrophic *Octadecabacter* at these stations (Delpech et al. 2021). While the high food quality observed here could be due to marine autotrophic production, these other environmental variables may indicate the importance of heterotrophic processes and potential trophic upgrading of terrestrial DOC to high-quality PUFA (Bec et al. 2003).

In addition to positive relationships with CDOM, DOC and Secchi depth, model results also reveal the negative relationship between food quality and turbidity and NO_2+NO_3 and SiO_2. While collinearity does not affect the strength of the model, it can potentially lead to misinterpretation of the results. It is therefore essential to thoroughly understand the linkages between predictor variables and keep in mind the theoretical causal linkages (Fig. S2). In Isfjorden and other glacial fjords, dissolved nutrients, including NO_2+NO_3 and SiO_2, are strongly associated with glacial meltwater in midsummer (Fransson et al. 2015; McGovern et al. 2020; Szeligowska et al. 2021), and in our model, these two predictors are collinear with turbidity as additional tracers of glacial melt. However, the observed nonlinear relationship between food quality and nutrient concentrations does suggest the complex interplay between nutrient and light availability in waters impacted by glacial meltwater. While highly impacted areas of the fjord are characterized by reduced food quality, terrestrial inputs may indirectly fuel high-quality FA production outside the immediate freshwater plume where light is available, driving strong variations in food quality across the fjord gradient. This high-quality production could be an important source of EFA for zooplankton like *Calanus* spp., especially in midsummer when zooplankton accumulate storage lipids in preparation for winter.

4.3. Terrestrial carbon utilization in the nearshore

In contrast to the high-quality POM available in May and June, August FA profiles were dominated by SFA and odd-chain FA with high contributions of 18:0, a FA typical of refractory material dominating winter-time POM in the Arctic (Mayzaud et al. 2013; Connelly et al. 2016). Low phytoplankton biomass, and dominance of small flagellates further illustrate the low food availability at the end of the summer season. While we observed strong coupling between POM FA and phytoplankton community structure in May and June, very little phytoplankton biomass was present in the water column in August. The dearth of phytoplankton indicates that POM, which in reality represents a heterogenous sample of material ranging in size from 0.2 to 200um, is likely reflecting a mix of detritus, small flagellates and terrestrial particles.

Terrestrial FA in the POM was indeed high in August compared to May and June, especially within the turbid meltwater plumes. This is reflected in the zooplankton, where lower $\delta^{13}C$ and increased contributions of terrestrial FA suggests that terrestrial carbon utilization may supplement zooplankton diets in late summer when other high-quality food is unavailable. Previous studies have reported similar utilization of terrestrial carbon by coastal zooplankton and benthos in the Mackenzie River delta and Beaufort Sea lagoons (Connelly et al. 2015; Mohan et al. 2016; Harris et al. 2018) using stable isotopes and terrestrial FATM.

At this point in the season, *Calanus* copepods are no long feeding at the same intensity as earlier in the summer, and small copepods like *Oithona* have a greater contribution to the zooplankton community (Balazy et al. 2021). It may be that smaller, indiscrimminant filter feeders are more likely to consume terrestrial material compared to selective feeders who can select for higher quality food sources. Furthermore, *Oithona* do not demonstrate clear vertical migration in late summer, and their low swimming ability may contribute to their inability to avoid or escape coastal plumes.

4.4 Conclusions

Our observations suggest that terrestrial inputs shape food quality in coastal waters during the High Arctic melt season through impacts on light availability in the water column. Areas of immediate and acute impact with high suspended sediment loads are characterized by reduced food quality, however, terrestrially derived dissolved carbon and nutrients transported beyond the turbid plume, may (together with AW transport) act to fuel heterotrophic and mixotrophic processes, facilitating the production of high-quality EFA for uptake into the fjord food-web. Zooplankton FA profiles in May and June generally reflected the same seasonal shifts from diatoms in May to flagellates and terrestrial material in June and August, highlighting the tight coupling between primary producers and first order consumers. Our results highlight the interaction between the melt season on land and spring bloom phenology and suggest that future increases in the spatial extent of turbid meltwater pumes could constrain EFA production in the nearshore, with implications for Arctic coastal food-webs.

Data availability

Raw data for stable isotopes and fatty acids will be openly available in the UiT data archive Dataverse upon publication. In addition, a full analysis and presentation of protistan community abundances will be published separately in Dąbrowska et al. in prep.

Acknowledgements

This research was funded by the Norwegian Research Council (TerrACE; project number: 268458) and the Svalbard Science Forum's Arctic Field Grant (RIS number: 10914, year: 2018). We thank the students and fellow scientists who helped us with the fieldwork including Anne Deininger, Nathalie Carrasco, Eirik Aasmo Finne, Sverre Johansen, Hannah Miller, Emelie Skogsberg and Charlotte Pedersen Ugelstad. We acknowledge Dino Milotic and Ben Schultz (Ryerson University) for fatty acid analyses, Anita Evenset for inputs to the study design and general supervision, as well as Nathalie Carrasco for preliminary analysis of Adventfjord zooplankton.

Author contributions:

MM: Study design, fieldwork, data analysis and writing; **MA:** Study design, FA analysis and guidance; **KB:** Study design, critical revision; **AD:** Phytoplankton taxonomy and biomass conversions; **EL**: Study design and interpretation of FA results; **RP:** Statistics guidance and critical revision; **PR**: Study design and critical revision; **JS:** Study design, fieldwork and interpretation of zooplankton FA and SIA results; **EHV:** Fieldwork and zooplankton taxonomy and biomass conversion; **AP**: Study design, fieldwork, supervision, project lead, funding acquisition, critical revision.

References

Ahmad, N., H. Bihs, M. A. Chella, Ø. A. Arntsen, and A. Aggarwal. 2017. Numerical modelling of arctic coastal erosion due to breaking waves impact using REEF3D. *The 27th international ocean and polar engineering conference*. OnePetro.

Ahmed, R., T. Prowse, Y. Dibike, B. Bonsal, and H. O'Neil. 2020. Recent trends in freshwater influx to the arctic ocean from four major arctic-draining rivers. Water **12**: 1189.

Balazy, K., R. Boehnke, E. Trudnowska, J. E. Søreide, and K. Błachowiak-Samołyk. 2021. Phenology of oithona similis demonstrates that ecological flexibility may be a winning trait in the warming arctic. Scientific reports **11**: 1–13.

Bec, A., C. Desvilettes, A. Véra, C. Lemarchand, D. Fontvieille, and G. Bourdier. 2003. Nutritional quality of a freshwater heterotrophic flagellate: Trophic upgrading of its microalgal diet for daphnia hyalina. Aquatic Microbial Ecology **32**: 203–207.

Biskaborn, B. K., S. L. Smith, J. Noetzli, and others. 2019. Permafrost is warming at a global scale. Nature communications **10**: 1–11.

Blachowiak-Samolyk, K., J. E. Søreide, S. Kwasniewski, A. Sundfjord, H. Hop, S. Falk-Petersen, and E. N. Hegseth. 2008. Hydrodynamic control of mesozooplankton abundance and biomass in northern svalbard waters (79–81 n). Deep Sea Research Part II: Topical Studies in Oceanography **55**: 2210–2224.

Bland, J. M., and D. G. Altman. 1995. Multiple significance tests: The bonferroni method. Bmj **310**: 170.

Brogi, S. R., J. Y. Jung, S.-Y. Ha, and J. Hur. 2019. Seasonal differences in dissolved organic matter properties and sources in an arctic fjord: Implications for future conditions. Science of the Total Environment **694**: 133740.

Budge, S. M., S. J. Iverson, and H. N. Koopman. 2006. Studying trophic ecology in marine ecosystems using fatty acids: A primer on analysis and interpretation. Marine Mammal Science **22**: 759–801.

Budge, S., C. Parrish, and C. Mckenzie. 2001. Fatty acid composition of phytoplankton, settling particulate matter and sediments at a sheltered bivalve aquaculture site. Marine Chemistry **76**: 285–303.

Calleja, M. L., P. Kerhervé, S. Bourgeois, M. Kędra, A. Leynaert, E. Devred, M. Babin, and N. Morata. 2017. Effects of increase glacier discharge on phytoplankton bloom dynamics and pelagic geochemistry in a high arctic fjord. Progress in Oceanography **159**: 195–210.

Carrasco, N. 2019. Seasonality in mercury bioaccumulation in particulate organic matter and zooplankton in a river-influenced arctic fjord (adventfjord, svalbard). Master's thesis. UiT Norges arktiske universitet.

Cole, J. J., S. R. Carpenter, M. L. Pace, M. C. Van de Bogert, J. L. Kitchell, and J. R. Hodgson. 2006. Differential support of lake food webs by three types of terrestrial organic carbon. Ecology Letters **9**: 558–568.

Connelly, T. L., T. N. Businski, D. Deibel, C. C. Parrish, and P. Trela. 2016. Annual cycle and spatial trends in fatty acid composition of suspended particulate organic matter across the beaufort sea shelf. Estuarine, Coastal and Shelf Science **181**: 170–181.

Connelly, T. L., J. W. McClelland, B. C. Crump, C. T. Kellogg, and K. H. Dunton. 2015. Seasonal changes in quantity and composition of suspended particulate organic matter in lagoons of the alaskan beaufort sea. Marine Ecology Progress Series **527**: 31–45.

Conover, W. J. 1998. Practical nonparametric statistics, John Wiley & Sons.

Daase, M., J. E. Søreide, and D. Martynova. 2011. Effects of food quality on naupliar development in calanus glacialis at subzero temperatures. Marine Ecology Progress Series **429**: 111–124.

Dahlke, S., N. E. Hughes, P. M. Wagner, S. Gerland, T. Wawrzyniak, B. Ivanov, and M. Maturilli. 2020. The observed recent surface air temperature development across svalbard and concurring footprints in local sea ice cover. International Journal of Climatology **40**: 5246–5265.

Dalsgaard, J., M. S. John, G. Kattner, D. Müller-Navarra, and W. Hagen. 2003. Fatty acid trophic markers in the pelagic marine environment.

Delpech, L.-M., T. R. Vonnahme, M. McGovern, R. Gradinger, K. Præbel, and A. E. Poste. 2021. Terrestrial inputs shape coastal bacterial and archaeal communities in a high arctic fjord (isfjorden, svalbard). Frontiers in microbiology **12**: 295.

Derieux, S., J. Fillaux, and A. Saliot. 1998. Lipid class and fatty acid distributions in particulate and dissolved fractions in the north adriatic sea. Organic Geochemistry **29**: 1609–1621.

Dunn, O. J. 1964. Multiple comparisons using rank sums. Technometrics **6**: 241–252.

Dunse, T., K. Dong, K. S. Aas, and L. C. Stige. 2021. Regional-scale phytoplankton dynamics and their association with glacier meltwater runoff in svalbard. Biogeosciences Discussions 1–30.

Edler, L. 1979. Recommendations on methods for marine biological studies in the baltic sea. Phytoplankton and chlorophyll. Publication-Baltic Marine Biologists BMB (Sweden).

Eischeid, I., E. M. Soininen, J. J. Assmann, and others. 2021. Disturbance mapping in arctic tundra improved by a planning workflow for drone studies: Advancing tools for future ecosystem monitoring. Remote Sensing **13**. doi:10.3390/rs13214466

Epstein, H. E., D. A. Walker, M. K. Raynolds, G. J. Jia, and A. M. Kelley. 2008. Phytomass patterns across a temperature gradient of the north american arctic tundra. Journal of Geophysical Research: Biogeosciences **113**.

Folch, J., M. Lees, and G. S. Stanley. 1957. A simple method for the isolation and purification of total lipides from animal tissues. Journal of biological chemistry **226**: 497–509.

Fransson, A., M. Chierici, D. Nomura, M. A. Granskog, S. Kristiansen, T. Martma, and G. Nehrke. 2015. Effect of glacial drainage water on the CO 2 system and ocean acidification state in an a rctic tidewater-glacier fjord during two contrasting years. Journal of Geophysical Research: Oceans **120**: 2413–2429.

Fraser, N. J., R. Skogseth, F. Nilsen, and M. E. Inall. 2018. Circulation and exchange in a broad arctic fjord using glider-based observations. Polar Research **37**: 1485417.

Galloway, A. W., and M. Winder. 2015. Partitioning the relative importance of phylogeny and environmental conditions on phytoplankton fatty acids. PloS one **10**: e0130053.

Goetz, S. J., A. G. Bunn, G. J. Fiske, and R. A. Houghton. 2005. Satellite-observed photosynthetic trends across boreal north america associated with climate and fire disturbance. Proceedings of the National Academy of Sciences **102**: 13521–13525.

Greenacre, M. 2016. Data reporting and visualization in ecology. Polar Biology **39**: 2189–2205.

Halbach, L., M. Vihtakari, P. Duarte, and others. 2019. Tidewater glaciers and bedrock characteristics control the phytoplankton growth environment in a fjord in the arctic. Frontiers in Marine Science **6**: 254.

Hanssen-Bauer, I., E. Førland, H. Hisdal, S. Mayer, A. Sandø, and A. Sorteberg. 2019. Climate in svalbard 2100. A knowledge base for climate adaptation.

Harris, C. M., N. D. McTigue, J. W. McClelland, and K. H. Dunton. 2018. Do high arctic coastal food webs rely on a terrestrial carbon subsidy? Food Webs **15**: e00081.

Harrison, P., P. Thompson, and G. Calderwood. 1990. Effects of nutrient and light limitation on the biochemical composition of phytoplankton. Journal of Applied Phycology **2**: 45–56.

Hiltunen, M., M. Honkanen, S. Taipale, U. Strandberg, and P. Kankaala. 2017. Trophic upgrading via the microbial food web may link terrestrial dissolved organic matter to daphnia. Journal of Plankton Research **39**: 861–869.

Hirche, H.-J., and G. Kattner. 1993. Egg production and lipid content of calanus glacialis in spring: Indication of a food-dependent and food-independent reproductive mode. Marine Biology **117**: 615–622.

Hixson, S. M., and M. T. Arts. 2016. Climate warming is predicted to reduce omega-3, long-chain, polyunsaturated fatty acid production in phytoplankton. Global Change Biology **22**: 2744–2755.

Hopwood, M. J., D. Carroll, T. Dunse, and others. 2020. How does glacier discharge affect marine biogeochemistry and primary production in the arctic? The Cryosphere **14**: 1347–1383.

Howell, K. L., D. W. Pond, D. S. Billett, and P. A. Tyler. 2003. Feeding ecology of deep-sea seastars (echinodermata: Asteroidea): A fatty-acid biomarker approach. Marine Ecology Progress Series **255**: 193–206.

Hylander, S., T. Jephson, K. Lebret, and others. 2011. Climate-induced input of turbid glacial meltwater affects vertical distribution and community composition of phyto-and zooplankton. Journal of Plankton Research **33**: 1239–1248.

Hyndes, G. A., I. Nagelkerken, R. J. McLeod, R. M. Connolly, P. S. Lavery, and M. A. Vanderklift. 2014. Mechanisms and ecological role of carbon transfer within coastal seascapes. Biological Reviews **89**: 232–254.

Isaksen, K., Ø. Nordli, E. J. Førland, E. Łupikasza, S. Eastwood, and T. Niedźwiedź. 2016. Recent warming on spitsbergen—influence of atmospheric circulation and sea ice cover. Journal of Geophysical Research: Atmospheres **121**: 11–913.

Jónasdóttir, S., H. Gudfinnsson, A. Gislason, and O. Astthorsson. 2002. Diet composition and quality for calanus finmarchicus egg production and hatching success off south-west iceland. Marine Biology **140**: 1195–1206.

Jónasdóttir, S. H. 2019. Fatty acid profiles and production in marine phytoplankton. Marine drugs **17**: 151.

Kelly, J. R., and R. E. Scheibling. 2012. Fatty acids as dietary tracers in benthic food webs. Marine Ecology Progress Series **446**: 1–22.

Konik, M., M. Darecki, A. K. Pavlov, S. Sagan, and P. Kowalczuk. 2021. Darkening of the svalbard fjords waters observed with satellite ocean color imagery in 1997-2019. Frontiers in Marine Science 1576.

Kuhn, M., and H. Wickham. 2020. Tidymodels: A collection of packages for modeling and machine learning using tidyverse principles.,.

Lee, R. F., W. Hagen, and G. Kattner. 2006. Lipid storage in marine zooplankton. Marine Ecology Progress Series **307**: 273–306.

Leu, E., T. A. Brown, M. Graeve, and others. 2020. Spatial and temporal variability of ice algal trophic markers—with recommendations about their application. Journal of Marine Science and Engineering **8**: 676.

Leu, E., S. Falk-Petersen, S. Kwaśniewski, A. Wulff, K. Edvardsen, and D. O. Hessen. 2006a. Fatty acid dynamics during the spring bloom in a high arctic fjord: Importance of abiotic factors versus community changes. Canadian Journal of Fisheries and Aquatic Sciences **63**: 2760–2779.

Leu, E., J. Søreide, D. Hessen, S. Falk-Petersen, and J. Berge. 2011. Consequences of changing sea-ice cover for primary and secondary producers in the european arctic shelf seas: Timing, quantity, and quality. Progress in Oceanography **90**: 18–32.

Leu, E., S.-Å. Wängberg, A. Wulff, S. Falk-Petersen, J. B. Ørbæk, and D. O. Hessen. 2006b. Effects of changes in ambient PAR and UV radiation on the nutritional quality of an arctic diatom (thalassiosira antarctica var. borealis). Journal of Experimental Marine Biology and Ecology **337**: 65–81.

Luckman, A., D. I. Benn, F. Cottier, S. Bevan, F. Nilsen, and M. Inall. 2015. Calving rates at tidewater glaciers vary strongly with ocean temperature. Nature communications **6**: 1–7.

Marmillot, V., C. C. Parrish, J.-É. Tremblay, M. Gosselin, and J. F. MacKinnon. 2021. Environmental and biological determinants of algal lipids in western arctic and subarctic seas. Biogeochemical Consequences of Climate-Driven Changes in the Arctic.

Mayzaud, P., M. Boutoute, M. Noyon, F. Narcy, and S. Gasparini. 2013. Lipid and fatty acids in naturally occurring particulate matter during spring and summer in a high arctic fjord (kongsfjorden, svalbard). Marine biology **160**: 383–398.

McGovern, M., A. K. Pavlov, A. Deininger, M. A. Granskog, E. Leu, J. E. Søreide, and A. E. Poste. 2020. Terrestrial inputs drive seasonality in organic matter and nutrient biogeochemistry in a high arctic fjord system (isfjorden, svalbard). Frontiers in Marine Science **7**: 747.

Menden-Deuer, S., and E. J. Lessard. 2000. Carbon to volume relationships for dinoflagellates, diatoms, and other protist plankton. Limnology and oceanography **45**: 569–579.

Mohan, S. D., T. L. Connelly, C. M. Harris, K. H. Dunton, and J. W. McClelland. 2016. Seasonal trophic linkages in arctic marine invertebrates assessed via fatty acids and compound-specific stable isotopes. Ecosphere **7**: e01429.

Montagnes, D., and D. Lynn. 1987. A quantitative protargol stain(QPS) for ciliates: Method description and test of its quantitative nature. Mar. Microb. Food Webs. **2**: 83–93.

Morris, A., G. Moholdt, and L. Gray. 2020. Spread of svalbard glacier mass loss to barents sea margins revealed by CryoSat-2. Journal of Geophysical Research: Earth Surface **125**: e2019JF005357.

Nyeggen, M. U. 2019. Seasonal zooplankton dynamics in svalbard coastal waters: The shifting dominance of mero-and holoplankton and timing of reproduction in three species of copepoda. Master's thesis. The University of Bergen.

Olenina, I. 2006. Biovolumes and size-classes of phytoplankton in the baltic sea.

Parker, P. L. 1964. The biogeochemistry of the stable isotopes of carbon in a marine bay. Geochimica et Cosmochimica Acta **28**: 1155–1164.

Parrish, C. C. 2009. Essential fatty acids in aquatic food webs, p. 309–326. *In* Lipids in aquatic ecosystems. Springer.

Parrish, C. C., R. J. Thompson, and D. Deibel. 2005. Lipid classes and fatty acids in plankton and settling matter during the spring bloom in a cold ocean coastal environment. Marine Ecology Progress Series **286**: 57–68.

Pavlov, A. K., E. Leu, D. Hanelt, and others. 2019. The underwater light climate in kongsfjorden and its ecological implications, p. 137–170. *In* The ecosystem of kongsfjorden, svalbard. Springer.

Pepin, P., C. C. Parrish, and E. J. Head. 2011. Late autumn condition of calanus finmarchicus in the northwestern atlantic: Evidence of size-dependent differential feeding. Marine Ecology Progress Series **423**: 155–166.

Pomerleau, C., G. Winkler, A. Sastri, R. J. Nelson, and W. J. Williams. 2014. The effect of acidification and the combined effects of acidification/lipid extraction on carbon stable isotope ratios for sub-arctic and arctic marine zooplankton species. Polar Biology **37**: 1541–1548.

R Core Team. 2021. R: A language and environment for statistical computing, R Foundation for Statistical Computing.

Reitan, K. I., J. R. Rainuzzo, and Y. Olsen. 1994. Effect of nutrient limitation on fatty acid and lipid content of marine microalgae 1. Journal of Phycology **30**: 972–979.

Reuss, N., and L. Poulsen. 2002. Evaluation of fatty acids as biomarkers for a natural plankton community. A field study of a spring bloom and a post-bloom period off west greenland. Marine Biology **141**: 423–434.

Rousseau, V., S. Mathot, and C. Lancelot. 1990. Calculating carbon biomass of phaeocystis sp. From microscopic observations. Marine Biology **107**: 305–314.

Sagan, S., and M. Darecki. 2018. Inherent optical properties and particulate matter distribution in summer season in waters of hornsund and kongsfjordenen, spitsbergen. Oceanologia **60**: 65–75.

Skogseth, R., L. L. Olivier, F. Nilsen, and others. 2020. Variability and decadal trends in the isfjorden (svalbard) ocean climate and circulation–an indicator for climate change in the european arctic. Progress in Oceanography **187**: 102394.

Stadnyk, T. A., A. Tefs, M. Broesky, and others. 2021. Changing freshwater contributions to the arctic: A 90-year trend analysis (1981–2070). Elem Sci Anth **9**: 00098.

Stoecker, D. K., D. J. Gifford, and M. Putt. 1994. Preservation of marine planktonic ciliates: Losses and cell shrinkage during fixation. Marine Ecology Progress Series 293–299.

Strand, S. M., H. H. Christiansen, M. Johansson, J. Åkerman, and O. Humlum. 2021. Active layer thickening and controls on interannual variability in the nordic arctic compared to the circum-arctic. Permafrost and Periglacial Processes **32**: 47–58.

Stübner, E., J. Søreide, M. Reigstad, M. Marquardt, and K. Blachowiak-Samolyk. 2016. Year-round meroplankton dynamics in high-arctic svalbard. Journal of Plankton Research **38**: 522–536.

Szeligowska, M., E. Trudnowska, R. Boehnke, A. M. Dąbrowska, K. Dragańska-Deja, K. Deja, M. Darecki, and K. Błachowiak-Samołyk. 2021. The interplay between plankton and particles in the isfjorden waters influenced by marine-and land-terminating glaciers. Science of The Total Environment **780**: 146491.

Szeligowska, M., E. Trudnowska, R. Boehnke, A. M. Dąbrowska, J. M. Wiktor, S. Sagan, and K. Błachowiak-Samołyk. 2020. Spatial patterns of particles and plankton in the warming arctic fjord (isfjorden, west spitsbergen) in seven consecutive mid-summers (2013–2019). Frontiers in Marine Science **7**: 584.

Søreide, J. E., E. V. Leu, J. Berge, M. Graeve, and S. Falk-Petersen. 2010. Timing of blooms, algal food quality and calanus glacialis reproduction and growth in a changing arctic. Global change biology **16**: 3154–3163.

Søreide, J. E., and H. Nygård. 2012. Challenges using stable isotopes for estimating trophic levels in marine amphipods. Polar biology **35**: 447–453.

Tepes, P., N. Gourmelen, P. Nienow, M. Tsamados, A. Shepherd, and F. Weissgerber. 2021. Changes in elevation and mass of arctic glaciers and ice caps, 2010–2017. Remote Sensing of Environment **261**: 112481.

Thessen, A. 2016. Adoption of machine learning techniques in ecology and earth science. One Ecosystem **1**: e8621.

Trudnowska, E., A. Dąbrowska, R. Boehnke, M. Zajączkowski, and K. Blachowiak-Samolyk. 2020. Particles, protists, and zooplankton in glacier-influenced coastal svalbard waters. Estuarine, Coastal and Shelf Science **242**: 106842.

Twining, C. W., J. T. Brenna, P. Lawrence, J. R. Shipley, T. N. Tollefson, and D. W. Winkler. 2016. Omega-3 long-chain polyunsaturated fatty acids support aerial insectivore performance more than food quantity. Proceedings of the National Academy of Sciences **113**: 10920–10925.

Utermöhl, H. 1958. Zur vervollkommnung der quantitativen phytoplankton-methodik: Mit 1 tabelle und 15 abbildungen im text und auf 1 tafel. Internationale Vereinigung für theoretische und angewandte Limnologie: Mitteilungen **9**: 1–38.

Vabalas, A., E. Gowen, E. Poliakoff, and A. J. Casson. 2019. Machine learning algorithm validation with a limited sample size. PloS one **14**: e0224365.

Vereide, E. H. 2019. Seasonal zooplankton community patterns along a gradient from land to sea in isfjorden, svalbard. Master's thesis.

Viso, A.-C., and J.-C. Marty. 1993. Fatty acids from 28 marine microalgae. Phytochemistry **34**: 1521–1533.

Walch, S., D. M. R. in prep. Using a redefined SPM algorithm on sentinel-2 time series analysis of spatio-temporal variability of turbid sediment plumes in the arctic adventfjorden estuary, svalbard. Remote Sensing.

Walczyńska, K. S., J. E. Søreide, A. Weydmann-Zwolicka, M. Ronowicz, and T. M. Gabrielsen. 2019. DNA barcoding of cirripedia larvae reveals new knowledge on their biology in arctic coastal ecosystems. Hydrobiologia **837**: 149–159.

Weydmann-Zwolicka, A., P. Balazy, P. Kuklinski, J. E. Søreide, W. Patuła, and M. Ronowicz. 2021. Meroplankton seasonal dynamics in the high arctic fjord: Comparison of different sampling methods. Progress in Oceanography **190**: 102484.

Winder, M., J. Carstensen, A. W. Galloway, H. H. Jakobsen, and J. E. Cloern. 2017. The land–sea interface: A source of high-quality phytoplankton to support secondary production. Limnology and Oceanography **62**: S258–S271.

Tables and Figures

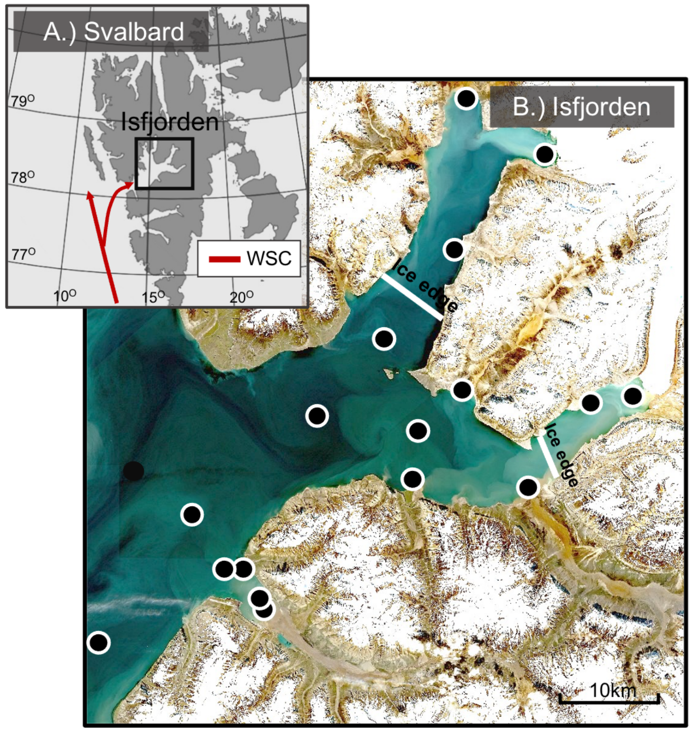

Fig 1. (A) Map of Svalbard showing the flow path of the West Spitsbergen Current (WSC) in red. (B) Station map (satellite image taken July 30, 2018; Sentinel-2 (https://scihub.copernicus.eu/) of Isfjorden illustrating where zooplankton were sampled in May, June and August 2018, and the position of the ice edge in May 2018, when land-fast ice prevented sampling at the innermost stations.

Table 1. Summaries (mean and 95 % CI) of stable isotopes and key fatty acids for particulate organic matter (POM) and zooplankton (Zoo) within each month in Isfjorden, Svalbard. Fatty acids (FA) are presented in µg/L for POM, and in % total FA for zooplankton. Zooplankton samples were lipid corrected prior to $\delta^{13}C$ anlaysis.

	POM-May	POM-June	POM-Aug	Zoo-May	Zoo-June	Zoo-Aug
nSIA	27	33	31	40	39	35
$\delta^{13}C$ (‰)	-23.9 (-24.1 to -23.6)	-28 (-28.5 to -27.6)	-27.2 (-27.5 to -27)	-19.8 (-20.3 to -19.3)	-21.7 (-22.1 to -21.3)	-23.4 (-23.8 to -23)
$\delta^{15}N$ (‰)	5.2 (5 to 5.4)	5 (4.8 to 5.2)	4.5 (4.2 to 4.7)	9.6 (7.9 to 11.8)	7.7 (7.5 to 7.9)	7.4 (6.9 to 7.8)
nFA	27	29	30	13	29	22
16:1n-7	5.3 (3.5—7.7)	1.9 (1.4—2.3)	1.9 (1.5—2.5)	14 (11.3—16.7)	7.6 (6.1—9.4)	5 (4.4—5.7)
20:5n-3	3.5 (1.7—6.2)	2.9 (2.2—3.5)	2.2 (1.5—2.9)	21.7 (19.7—23.9)	14.9 (13.8—16)	13.4 (11.9—15.1)
22:6n-3	3 (1.8—4.3)	3.8 (3.1—4.6)	1.9 (1.3—2.6)	11.6 (9.6—13.4)	14.7 (13.3—16.1)	16.2 (13.1—19.2)
18:4n-3	0.6 (0.3—1)	2 (1—3.1)	0.9 (0.4—1.7)	3.3 (2.8—3.8)	11.3 (10.1—12.5)	10.7; 9—12.5 %

18:3n-3	0.4 (0.2—0.6)	1.5 (1.1—1.9)	0.9 (0.6—1.2)	1.2 (1.1—1.2)	2.2 (2—2.3)	2.3 (2—2.5)
ΣC18PUFA	2.6 (1.6—4.2)	4.4 (3.3—5.6)	3.1 (2.1—4.2)	5.8 (5—6.7)	18.1 (15.7—20.6)	15.8 (13.7—17.7)
Σ20,22	0.7 (0.3—1.5)	0.4 (0.2—0.6)	0.6 (0.5—0.8)	0.2 (0.1—0.3)	0.2 (0.1—0.2)	0.2 (0.1—0.3)
Σodd-chain	5.9 (2.4—11.5)	2.2 (1.4—3.3)	4.3 (2.5—6.6)	4.8 (3.9—5.6)	3 (2.6—3.6)	2.6 (2—3.4)
ΣPUFA	16.2 (12—20.9)	20.5 (17.4—23.9)	18.1 (14.8—22.1)	41.5 (39.5—43.2)	57.9 (50.1—66.3)	51.7 (47—57)
Σn-3PUFA	8.2 (5—12.2)	10.9 (8.7—13.2)	6.5 (4.7—8.5)	38.9 (36.5—41.1)	53.9 (46.9—61.5)	47.5 (42.9—52.8)
Σn-6PUFA	8 (6.2—10.1)	9.7 (8.3—11.1)	11.6 (9—15.3)	2.5 (1.8—3.4)	4 (3.4—4.7)	4.2 (3.7—4.8)
EPA + DHA ΣSFA	0.4 (0.2—0.5)	0.4 (0.3—0.5)	0.1 (0.1—0.2)			
ΣFA	58.8 (37—96.3)	49 (41.8—57.8)	67.6 (51.1—91.1)			

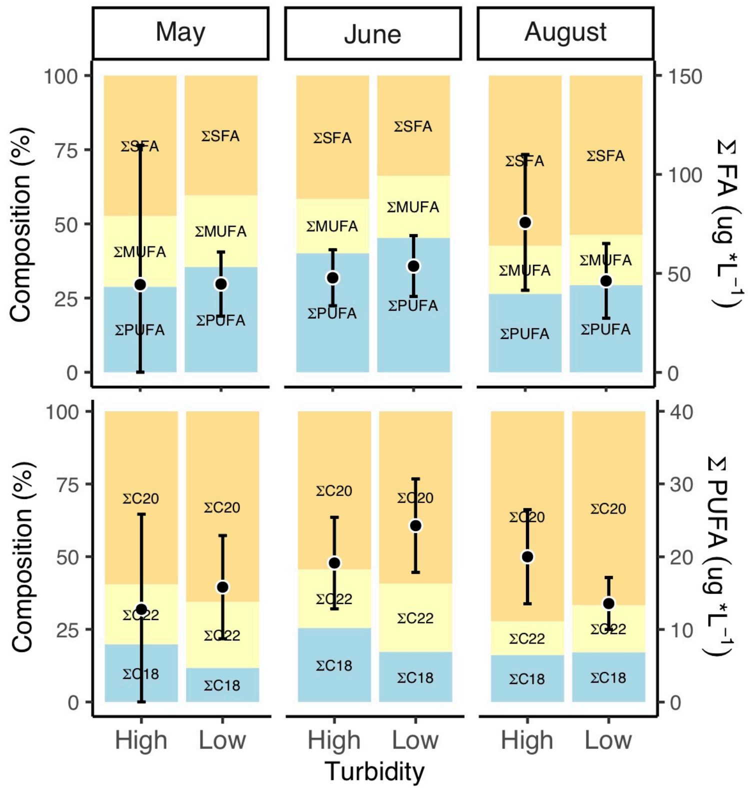

Fig 2. Composition (bars) and concentration (2nd y-axis, points/error bars)) of fatty acids (FA) and essential polyunsaturated fatty acids (PUFA) for high (> 3 NTU) and low (< 3NTU) turbidity samples within each month.

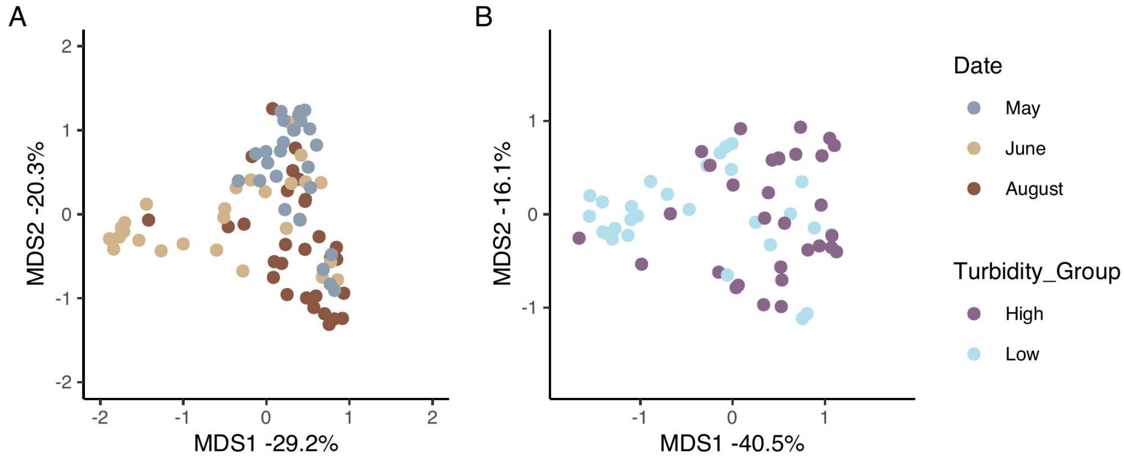

Fig 3. MDS plot using 1- Random Forest Proximities based concentrations of all POM-FA classified by month (A) and turbidity group for June and August (B). The model predicting sampling month had a 25.6% error rate, and the model predicting turbidity group (high vs. low) had a 33.9% error rate. POM concentrations were log transformed prior to analysis.

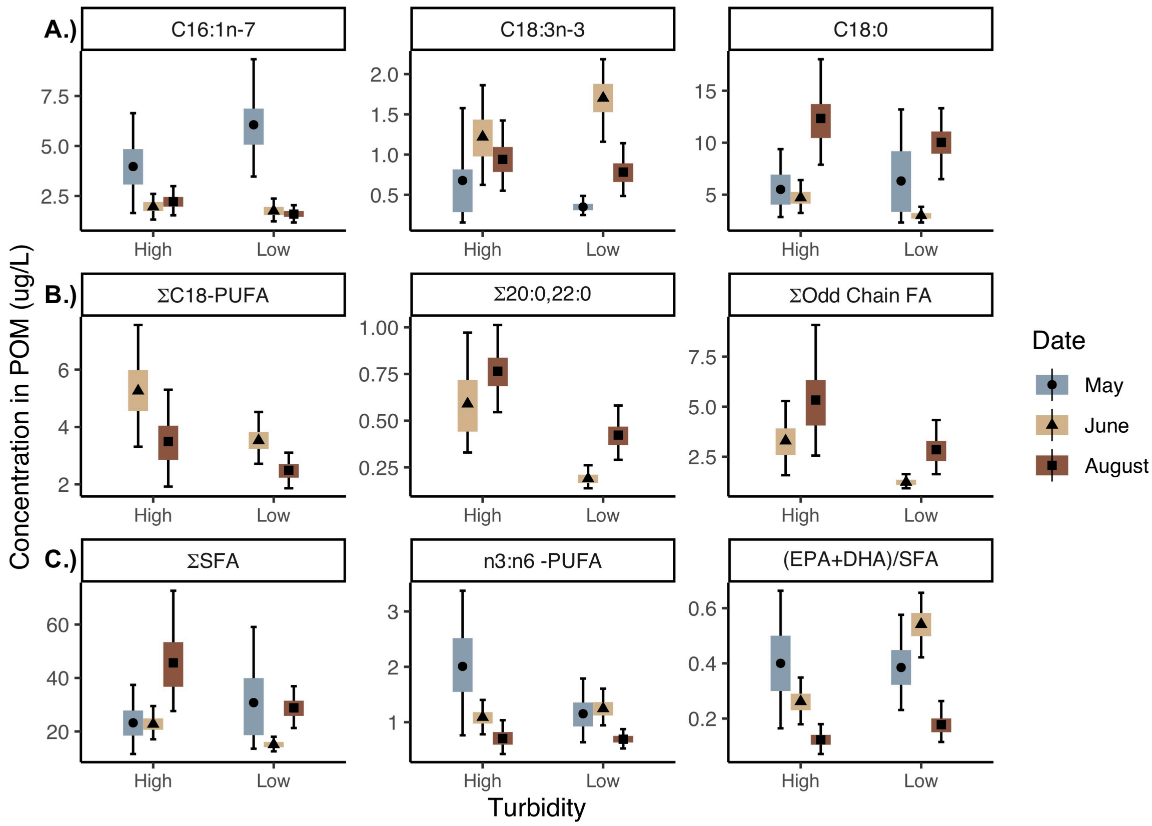

Fig 4. Confidence interval plots depicting (A) top 3 most important predictors of sampling month in the random forest classifier based on all FA in POM. (B) Important predictors of turbidity group (high (> 3NTU) vs. low) in the random forest classifier for June and August POM. (C) OM-quality metrics for all samples. Black symbols indicate the sample mean, while the colored box represents the 50% bootstrapped confidence interval and the error bars the 95% bootstrapped confidence interval.

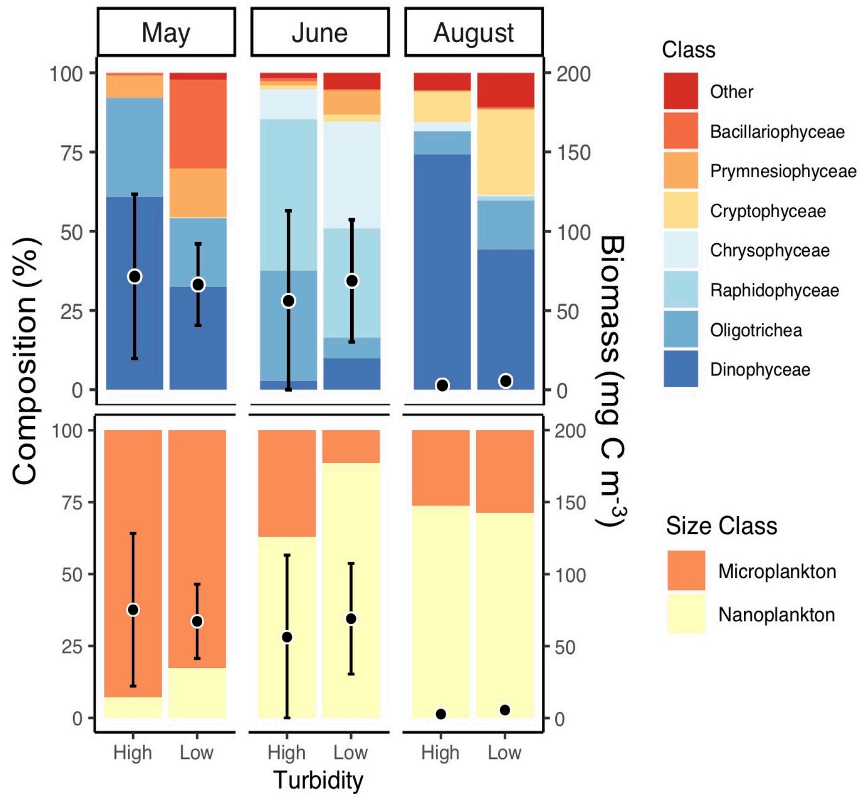

Fig 5. Phytoplankton composition (bars) and biomass (points with standard deviation) by class and size in low and high (> 3 NTU) turbidity samples within each month.

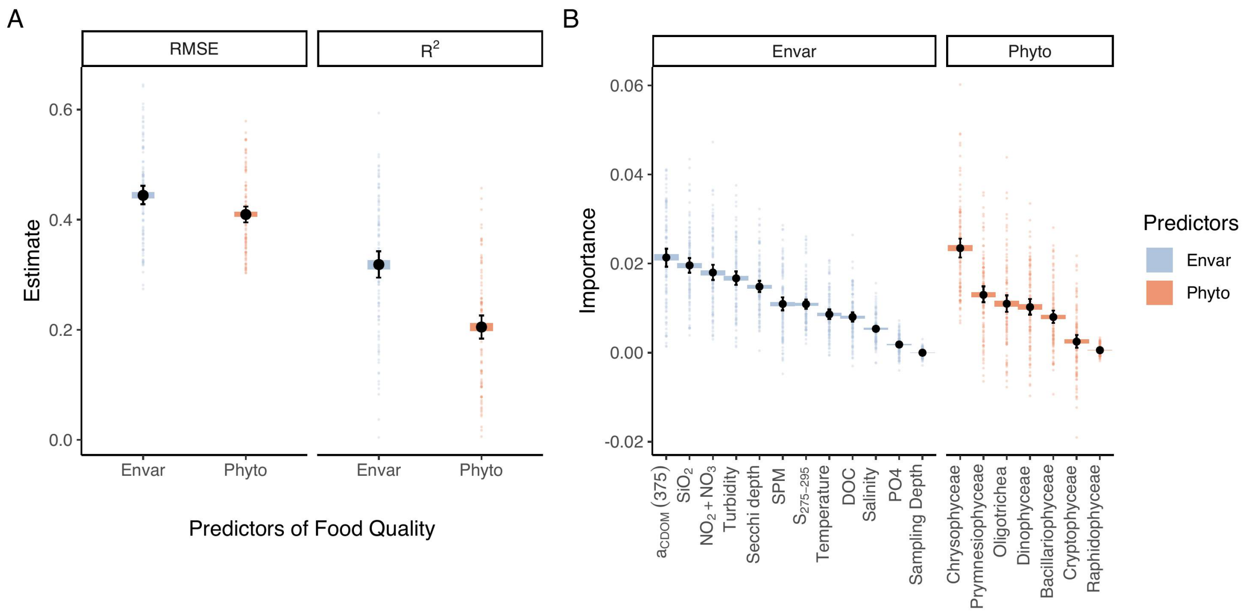

Fig 6. Results of random forest regressions predicting food quality ((EPA+DHA)/ΣSFA) based on environmental drivers (Envar) and biomass of phytoplankton groups (Phyto) showing (a) model estimates (root mean square error and R^2) and (B) variable importance plots from random forest ensemble. Algorithms were run on split data (70 training/30 validation), so results are presented as the bootstrapped mean and confidence intervals (50% & 95%) of 100 permutations of the data splitting step in order to provide more robust estimates with our small dataset. Predictors and response variables were normalized prior to analysis.

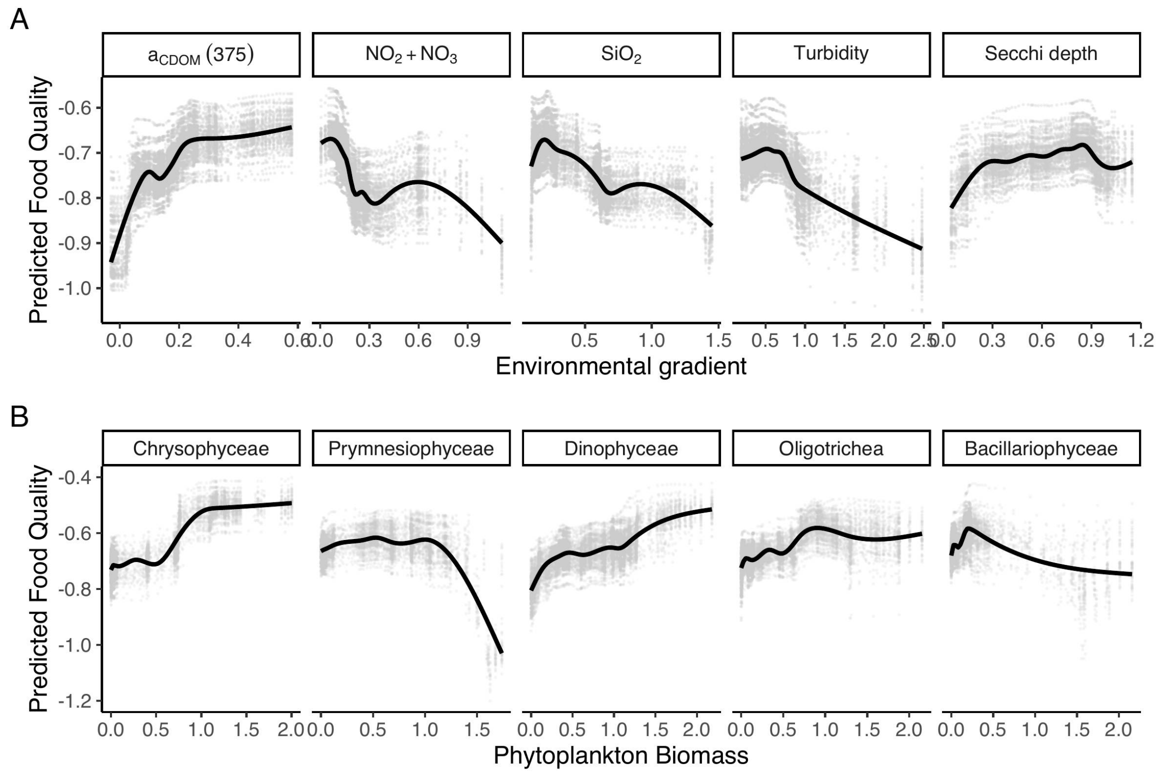

Fig 7. Partial dependence plots show the nonlinear relationships between the top 5 variables in the random forest regression and predicted food quality ((EPA +DHA)/SFA). All 100 iterations are shown in grey, and a general additive model (gam, in black) is used as a smoother across all results.

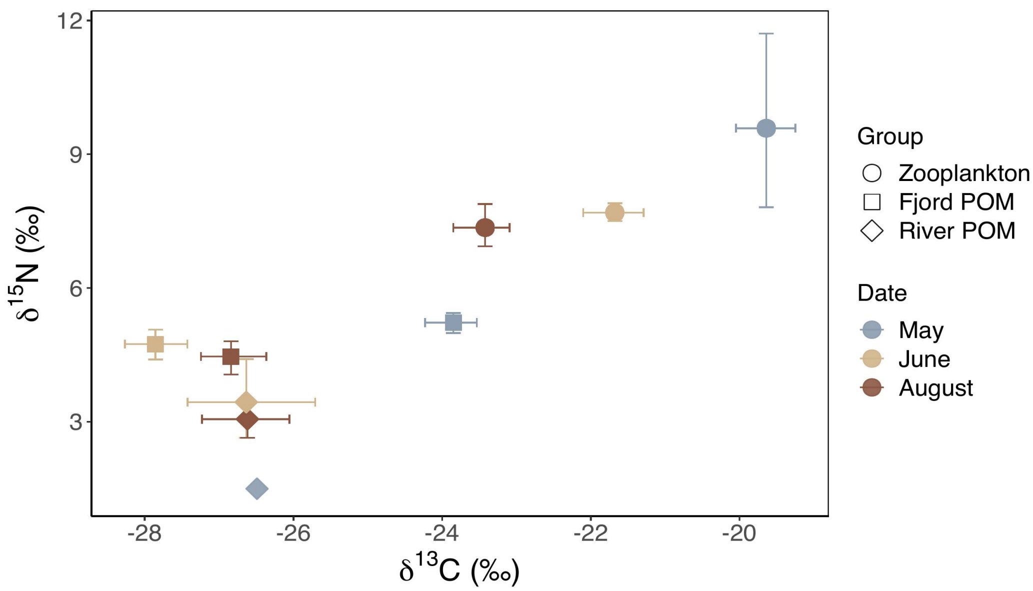

Fig 8. Bootstrapped means and 95% confidence intervals of $\delta^{13}C$ vs $\delta^{15}N$ values for POM and zooplankton within each month. POM data from rivers and fjord have been previously published in McGovern et al. (2020).

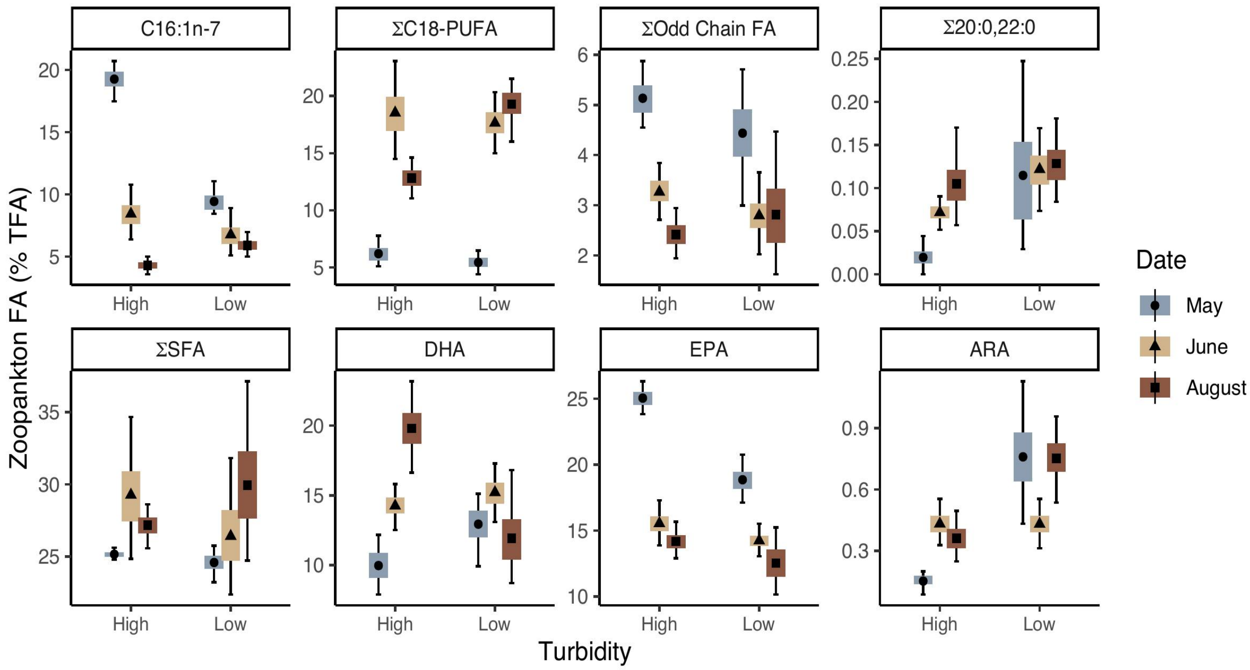

Fig 9. Key FATM in size fractionated zooplankton (% TFA) for each month and turbidity group (high > 3 NTU).

Supplemental Materials:

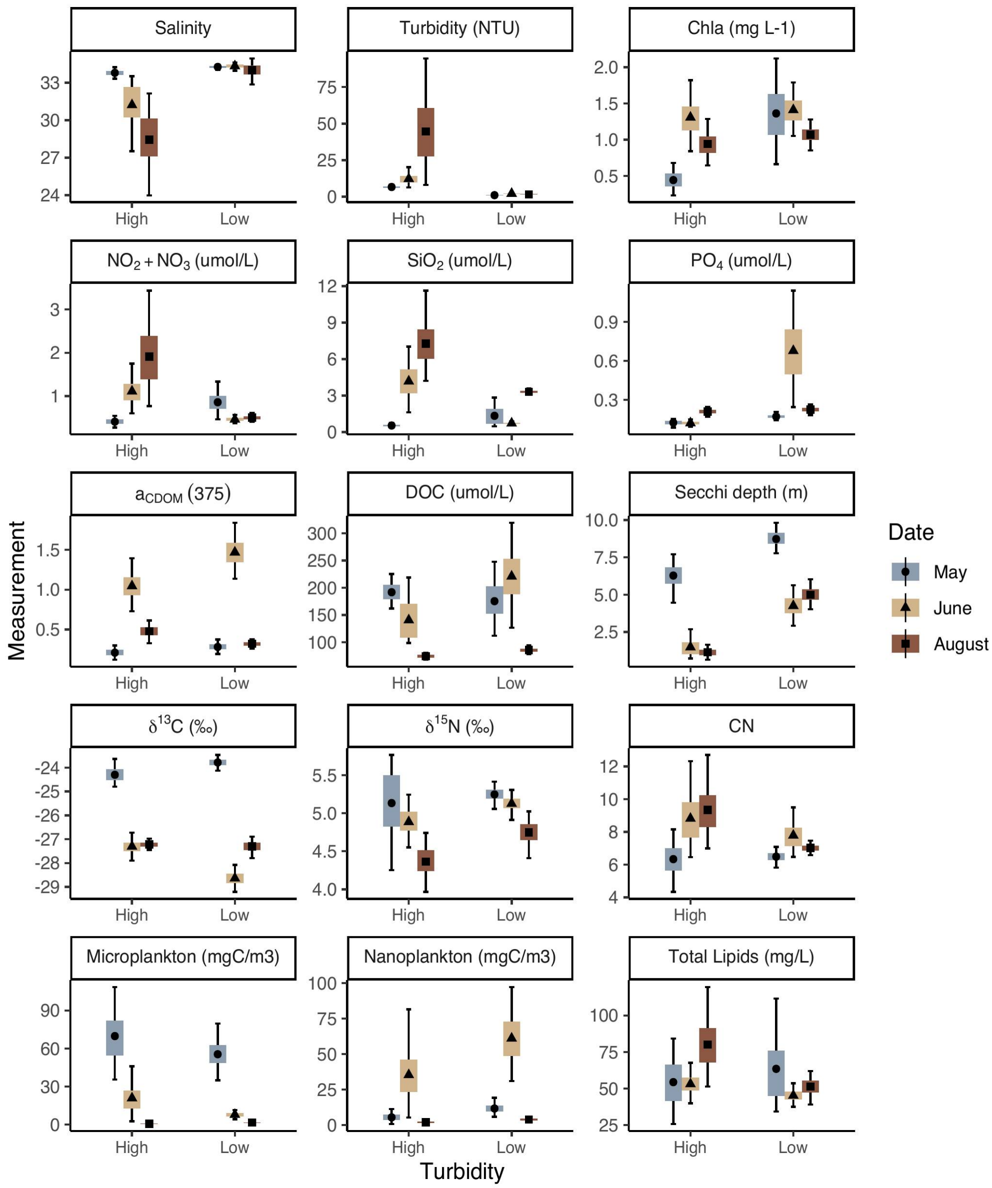

Fig S1. Environmental variables (data provided by McGovern et al., (2020)), as well as phytoplankton biomass and total lipids between high and low turbidity locations in May, June and August.

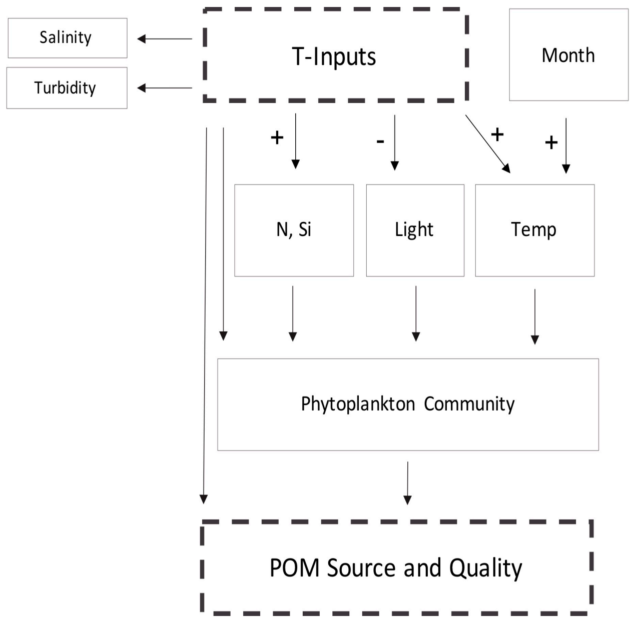

Fig S2. Causal diagram which was used to guide statistical analyses.

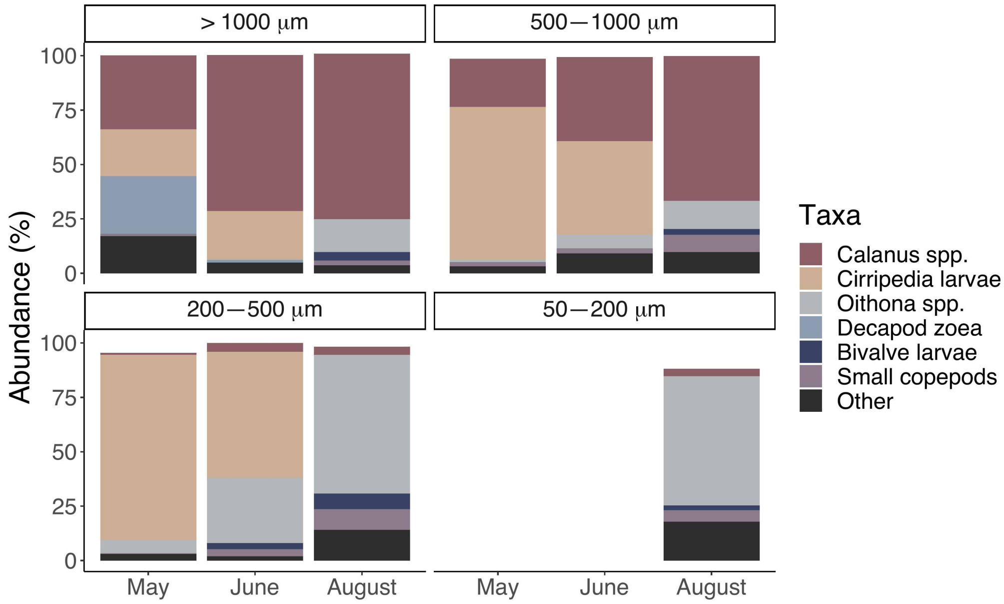

Fig S3. Community composition of zooplankton size fractions. Composition is reported as the mean percentage of abundance within each sampling month.

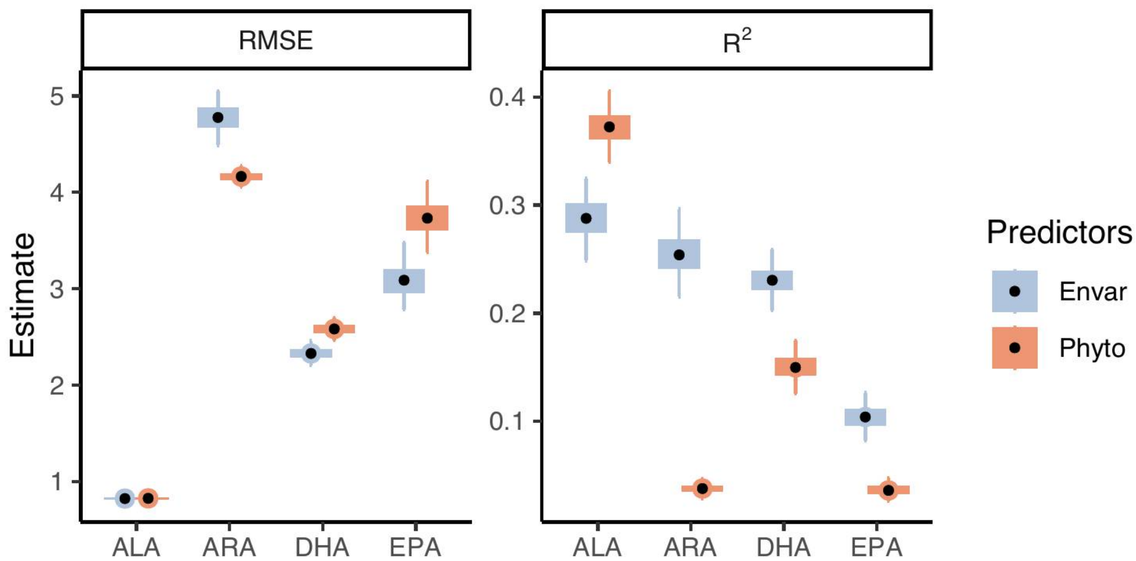

Fig S4. Estimates for random forest models build using environmental drivers and phytoplankton biomass.

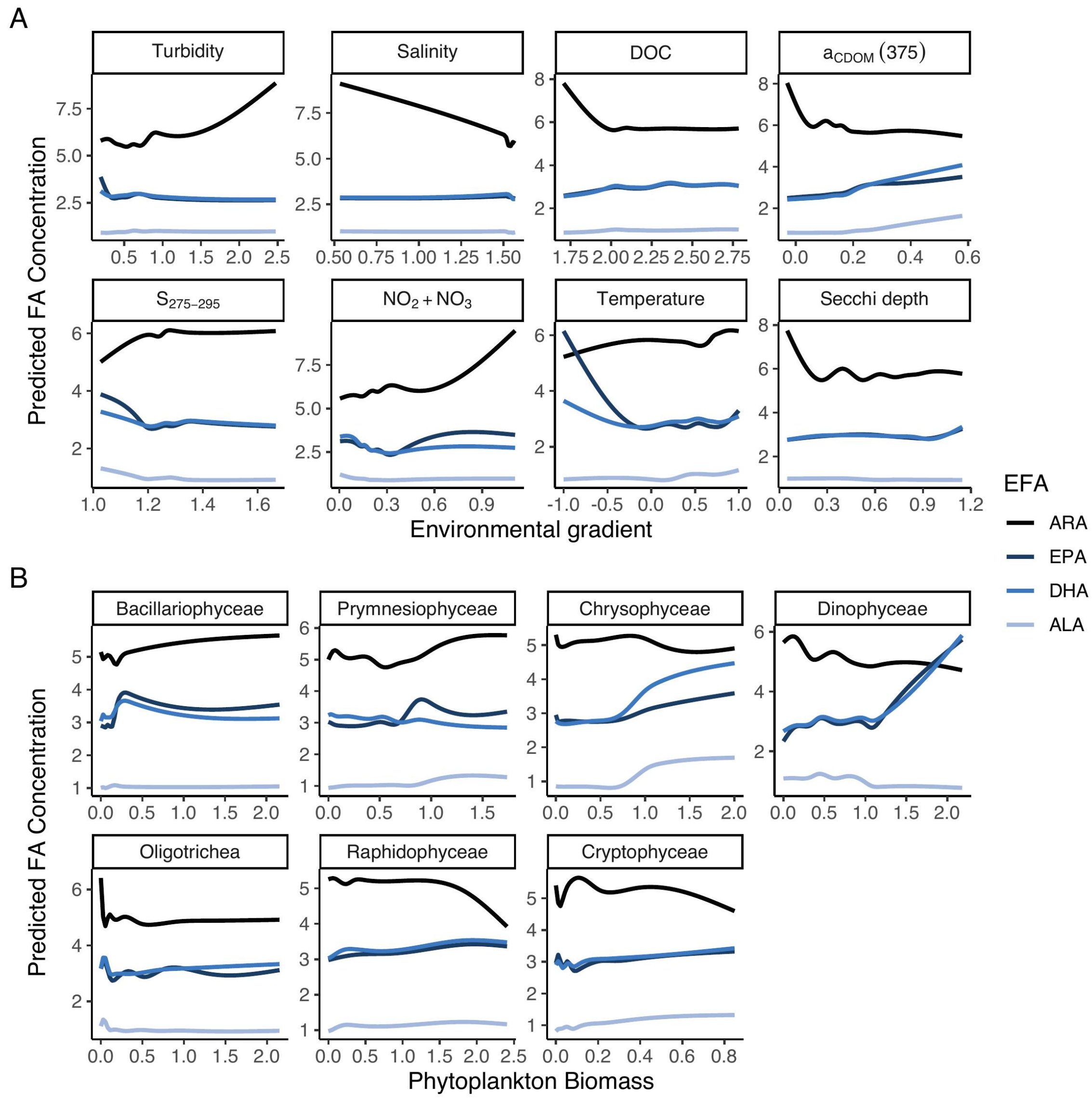

Fig S5. Partial dependence plots summarizing random forest ensemble models for predicted FA concentrations vs each key FA.

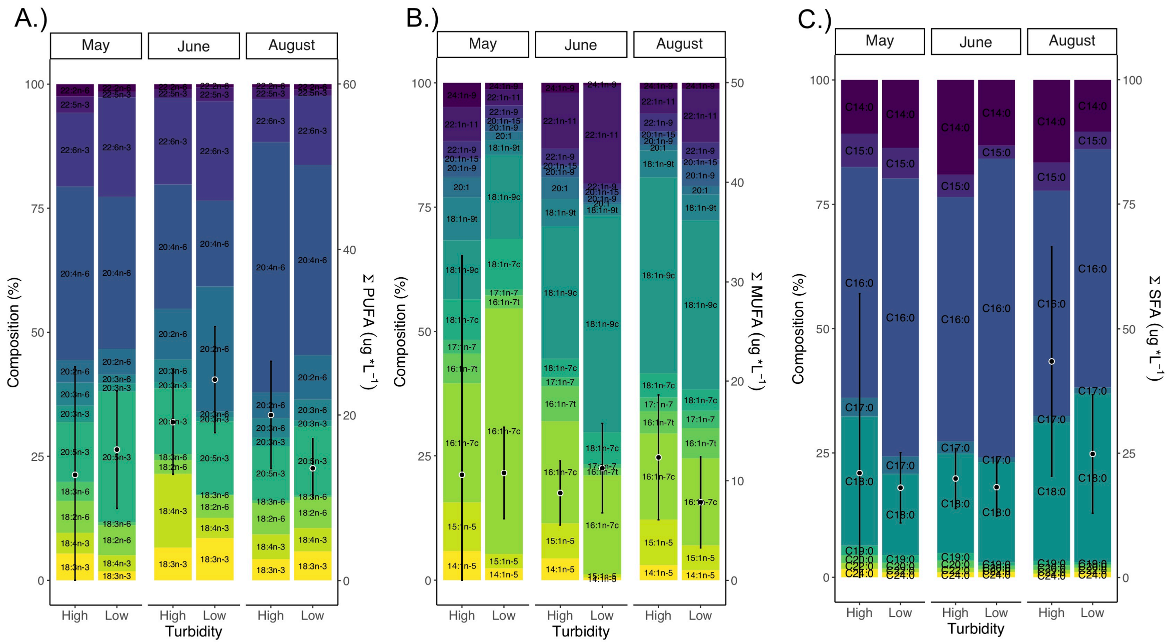

Fig S6. Detailed overview of FA composition in POM.

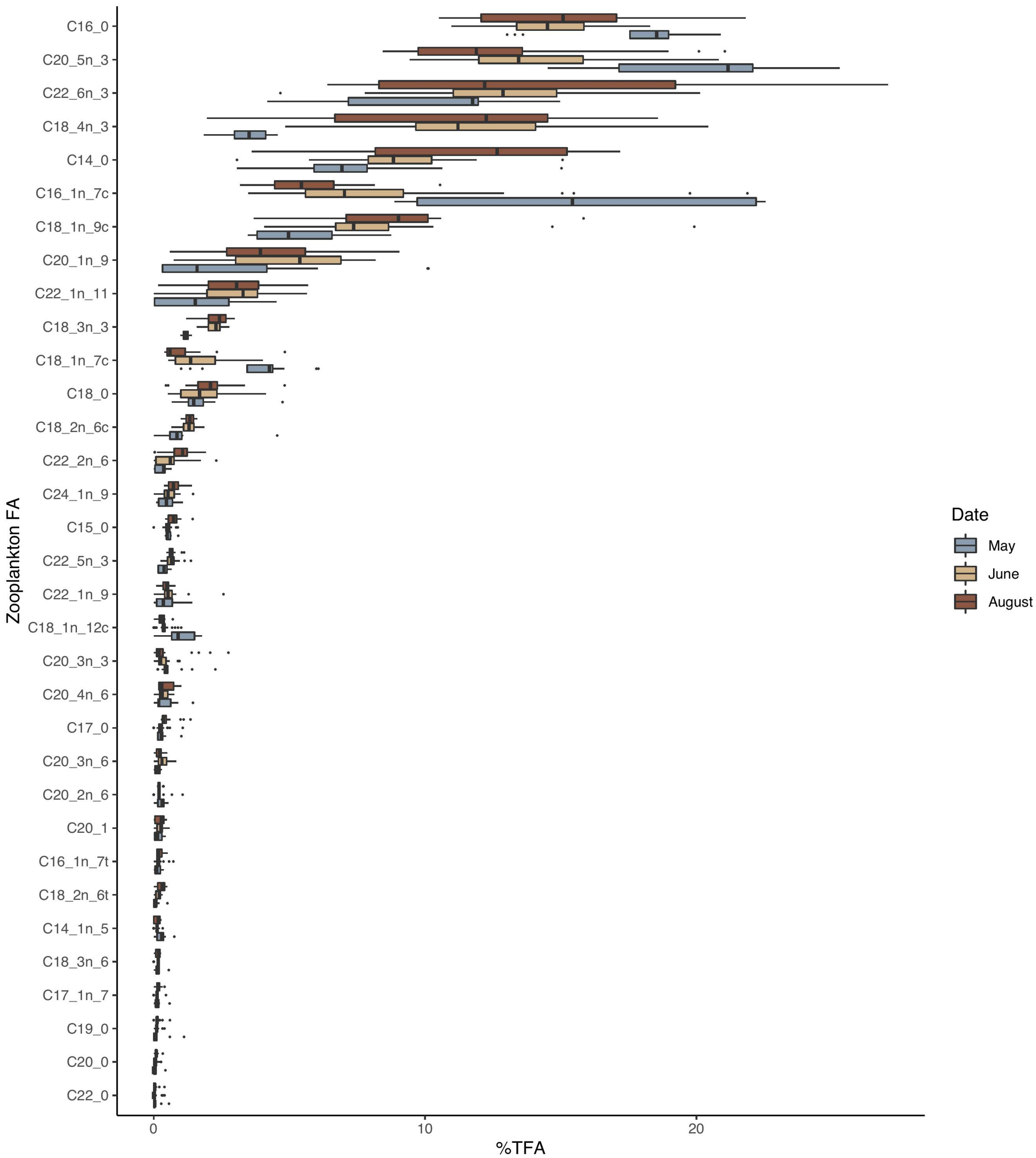

Fig S7. Overview of all FA in zooplankton

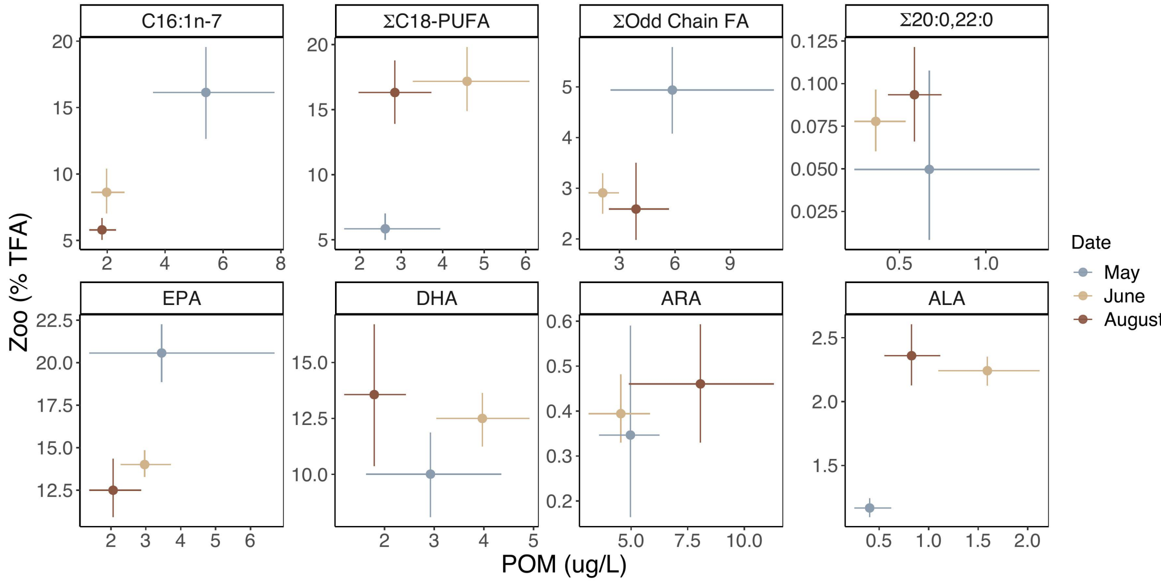

Fig S8. Key FATM in zooplankton vs. concentrations measured in POM for each month.

Paper 3

Is glacial meltwater a secondary source of legacy contaminants to Arctic coastal food-webs?

Maeve McGovern[1,2,3]*, Nicholas A. Warner[4,5,6], Katrine Borgå[7,8], Anita Evenset[2,9], Pernilla Carlsson[1], Emelie Skogsberg[10,11], Janne E. Søreide[3], Anders Ruus[7,11], Guttorm Christensen[9], Amanda E. Poste[1,2]

[1]Norwegian Institute for Water Research, 9007 Tromsø, Norway,
[2]Department of Arctic Marine Biology, UiT, The Arctic University of Norway, 9019 Tromsø, Norway,
[3]University Centre on Svalbard, 9170 Longyearbyen, Norway,
[4]NILU-Norwegian Institute for Air Research, The Fram Centre, 9007 Tromsø, Norway,
[5]Department of Chemistry, UiT, The Arctic University of Norway, 9019 Tromsø, Norway,
[6] Thermo Fischer Scientific, 28199 Bremen, Germany
[7]Department of Biosciences, University of Oslo, 0316 Oslo, Norway,
[8]Centre for Biogeochemistry in the Anthropocene (CBA), University of Oslo, 0316 Oslo, Norway,
[9]Akvaplan-niva, Fram Centre, 9007 Tromsø, Norway,
[10]Norwegian University of Life Sciences, Faculty of Environmental Sciences and Natural Resource Management, 1430 Ås, Norway,
[11]Norwegian Institute for Water Research, 0579 Oslo, Norway

Corresponding Author: Maeve McGovern

Graphical abstract:

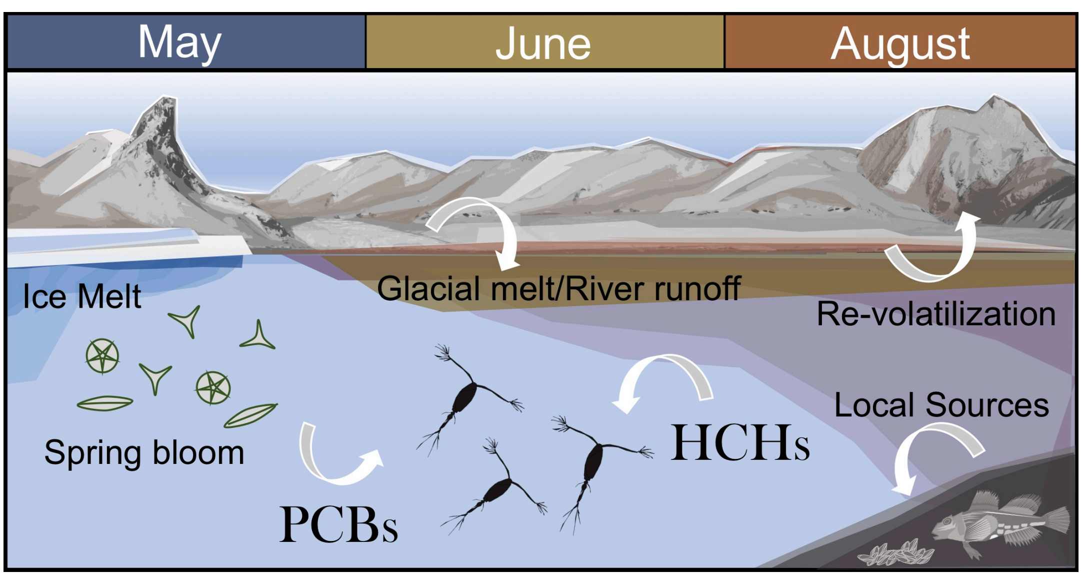

Abstract

Climate change-driven increases in air and sea temperatures are rapidly thawing the Arctic cryosphere with potential for remobilization and accumulation of legacy persistent organic pollutants (POPs) in adjacent coastal food-webs. Here, we present concentrations of selected POPs in zooplankton (spatially and seasonally), as well as benthos and sculpin (spatially) from Isfjorden, Svalbard. Herbivorous zooplankton contaminant concentrations were highest in May (e.g ∑Polychlorinated biphenyls ($_8$PCB); 4.43, 95% CI: 2.72–6.3 ng/g lipid weight), coinciding with the final stages of the spring phytoplankton bloom, and lowest in August ($\sum_8$PCB; 1.6, 95% CI: 1.29–1.92 ng/g lipid weight) when zooplankton lipid content was highest, and the fjord was heavily impacted by sediment-laden terrestrial inputs. Slightly increasing concentrations of alpha hexachlorocyclohexane (α-HCH) in zooplankton from June (1.18, 95% CI: 1.06–1.29 ng/g lipid weight) to August (1.57, 95% CI: 1.44–1.71 ng/g lipid weight), alongside a higher percentage of α-HCH enantiomeric fractions closer to racemic ranges, indicate that glacial meltwater is a secondary source of α-HCH to fjord zooplankton in late summer. Except for α-HCH, terrestrial inputs were generally associated with reduced POP concentrations in zooplankton, suggesting that increased glacial melt is not likely to significantly increase exposure of legacy POPs in coastal fauna.

Keywords: Climate change, persistent organic pollutants, chiral pesticides, zooplankton, zoobenthos, sculpin, stable isotopes, Svalbard

Synopsis: Glacial meltwater is not an important secondary source of legacy contaminants to coastal zooplankton and zoobenthos in Isfjorden, Svalbard.

1. Introduction

The Arctic cryosphere is melting at an unprecedented rate,[1,2] yet little information exists on the potential role of melting glaciers and thawing permafrost as secondary sources of legacy contaminants to coastal food-webs. In Svalbard, annual runoff has increased more than 35% since 1980, mainly due to enhanced glacial melt, transferring high quantities of meltwater to coastal areas.[3,4] Glaciers, snow caps, and Arctic tundra contain stores of contaminants,[5] including persistent organic pollutants (POPs), that have been atmospherically-transported from lower latitudes[6] and deposited on the Arctic environment.[7–10] Runoff from these systems potentially represents a secondary source of legacy contaminants, including hexachlorobenzene (HCB), Polychlorinated biphenyls (PCBs), Dichlorodiphenyltrichloroethane (DDTs), hexachlorocyclohexane (HCHs) and chlordane pesticides, to the coastal zone.[11–15]

In addition to remobilization of these legacy POPs, climate-change driven impacts on biogeochemistry and ecology are likely to have implications for the accumulation and trophic transfer of contaminants in the coastal environment.[2,16–19] Increased temperatures and diminished sea-ice may lead to enhanced volatilization of POPs across the air-water interface, resulting in reduced dissolved concentrations available for uptake.[20] Phytoplankton and high biomass-events, like the spring bloom, can facilitate the uptake of dissolved POPs into the food-web, or their removal from the water column.[21] Similarly, the high load of suspended particles associated with riverine and glacial runoff on Svalbard[22] may effectively remove POPs with high particle affinity from the water column.[23] Furthermore, shifts in carbon source and food-web structure can lead to changes in contaminant pathways in marine food-webs.[24] Recent studies suggest that terrestrially derived organic matter may provide an additional energy source to littoral amphipods and marine zooplankton in Isfjorden, Svalbard, during the melt season.[25,26] Such terrestrial carbon utilization could alter exposure and potential trophic transfer of POPs in coastal ecosystems. Many of these expected changes also occur seasonally in the Isfjorden system, with sea-ice present from December to May, presenting the opportunity to investigate these physical and ecological impacts on contaminant dynamics. Given the potential for climate-driven increases in inputs of POPs from secondary sources,[27] it is important to elucidate the various biogeochemical and ecological processes affecting accumulation and trophic transfer of POPs in the seasonally dynamic coastal zone in the High Arctic in order to assess the potential for increased contamination of coastal food webs.

Chiral compounds exist as enantiomers that have the same physical-chemical properties but can display different affinity/interaction with biological molecules (e.g. enzymes). These differences can give rise to enantiomer enrichment through biological enantiomer-selective processes.[28,29] Enantiomeric fractions (EFs) of chiral pesticides allow for relative differentiation between fresh and degraded sources of contaminants to receiving marine systems.[30] Previous studies have used EFs in Svalbard zooplankton[31,32] to distinguish contaminant sources in relation to ice melt, water mass transport and biological processes in the water column (e.g., spring bloom).

In the present study, we target several POP groups, covering a broad range of physicochemical properties together with isomeric and enantioselective analysis.[31,33] We pair these results with environmental data and stable isotope analysis of carbon (for assessing carbon source) and nitrogen (trophic position) to determine the relative importance of terrestrial runoff to contaminant loads in coastal fauna in Isfjorden, Svalbard. Zooplankton, which drift with water masses and represent a key link between the base of the food web and higher trophic levels, were chosen to reflect seasonal variations in contamination, while the more stationary benthic invertebrates and sculpin were selected to study temporally integrated spatial differences among the sampled fjord-arms. For zooplankton, we targeted three key time points in the high Arctic summer: the spring bloom in May, the snowmelt period in June, and late-summer glacial melt in August. Through examination of contaminant dynamics together with spatial and seasonal physical and ecological processes, we aim to gain a better understanding of contaminant sources and pathways in the dynamic High Arctic coastal zone.

2. Methods

2.1 Field sampling

Zooplankton, benthic invertebrates and sculpin, as well as temperature and salinity profiles and surface water samples, were collected from 17 stations in Isfjorden (Adventfjorden, Tempelfjorden and Billefjorden) in 2018 (Figure 1). Zooplankton were sampled spatially and seasonally, in May (10–11), June (18–24), and August (16–24), while benthic invertebrates and sculpin were sampled spatially in late summer (August 24-September 1). Fjord stations were positioned along gradients from river estuaries and glacier fronts to the outer fjord (Figure 1). Glacier front stations in Billefjorden and Tempelfjorden were inaccessible in May due to the presence of land-fast ice. Methods for collection and analysis of environmental data, including water mass determination, salinity, temperature, and turbidity, are described, along with results, in a parallel study.[22]

A range of vertical plankton net (WP) sizes were used for zooplankton collection, including WP2 (0.25 m^2 diameter with 60 and 200 µm mesh size) and a larger and coarser WP3 (1 m^2 diameter with 1000 µm mesh size). Net contents were pooled and macrozooplankton were selectively removed and frozen separately. The rest of the pooled zooplankton were size-fractionated through 500 µm and 1000 µm sequential Nitex mesh screens.

Benthic invertebrates were sampled using a Van Veen grab from the same fjord stations as the zooplankton (Figure 1a), while sculpin were sampled from river estuaries and other near-shore stations using gill nets deployed at 10-15 m depth (Figure 1b). Samples were homogenized and subsamples of macro- and size-fractionated zooplankton, benthic invertebrates (whole organisms), and sculpin (dorso-lateral muscle tissue) were frozen (-20°C) separately for contaminant (in solvent-rinsed, pre-combusted (450 °C, 6h) glass containers) and stable isotope ($\delta^{13}C$ and $\delta^{15}N$) analyses. In addition, subsamples of zooplankton size-fractions were fixed (4% buffered formaldehyde-seawater solution) for species identification and abundance-based compositional determination (Figure S1).

2.3 Stable isotope analysis

Bulk stable isotope (SI) analysis of carbon and nitrogen (δ^{13}C, δ^{15}N) was carried out on zooplankton (n = 44) and benthic invertebrates (n = 24) at the University of California, Davis (UC Davis Stable Isotope Facility, USA) while sculpin (n = 27) samples were analysed at the University of Oslo (UiO Stable Isotope Laboratory). All samples were freeze-dried, homogenized, weighed and packed in tin capsules prior to analysis. Samples were not lipid extracted. Subsamples of benthic organisms expected to have high calcium carbonate content (mollusks and echinoderms) were acidified to remove inorganic carbon. Due to potential impacts of acidification on δ^{15}N values,[34] acidified samples (used for δ^{13}C values) were analyzed in parallel with unacidified samples (used for δ^{15}N values). δ^{13}C and δ^{15}N were measured using an elemental analyzer interfaced to an isotope ratio mass spectrometer.[35] Long-term standard deviations at UC Davis are 0.2 ‰ for δ^{13}C and 0.3 ‰ for δ^{15}N. Run-specific standard deviations at UiO were 0.04 ‰ for δ^{13}C and 0.02 ‰ for δ^{15}N. Stable carbon and nitrogen isotope values are expressed using delta notation, relative to international standards (Vienna PeeDee Belemnite for C, and atmospheric N for nitrogen).[36]

2.4 Contaminant analysis

Contaminant analyses were carried out at the Norwegian Institute for Air Research's (NILU) laboratory in Tromsø, Norway. Zooplankton (n = 44), benthic invertebrates (n = 26) and sculpin (n = 35) were analyzed for HCB and PCBs (CB-28, 31, 52, 101, 118, 138, 153 and 180). In addition, all zooplankton (n=44) and several benthic invertebrates (n=10) were analyzed for DDTs (*o,p'*- and *p,p'*-DDT) and their metabolites (*o,p'*, *p,p'*-DDE and -DDD), as well as α-, β-, γ- HCH, *cis*- and *trans* isomers for chlordane and nonachlor, and mirex. CB-28 and 31 co-eluted, and are treated together. In addition, all zooplankton samples were further analyzed for enantiomeric fractions (EF = +/(+ &-)) of chiral α-HCH, *trans*- and *cis*-chlordane.

All equipment was pre-combusted and solvent-washed. All chemicals were SupraSolv grade (Merck). Zooplankton, benthic invertebrates and sculpin samples were extracted and analyzed according to previously described methods.[37] Briefly, samples were homogenized, weighed and freeze dried in 1:3 (w/w) Na_2SO_4 (pre-combusted at 600 °C) overnight. The following day, ^{13}C-labeled internal standards (HCB, PCB-28, PCB -31, PCB -52, PCB -101, PCB -118, PCB -138, PCB -153, PCB -180, α-HCH, β-HCH, γ-HCH, *p,p'*-DDE, *p,p'*-DDD, *p,p'*-DDT, *trans*-chlordane, *cis*-chlordane, *trans*-nonachlor) were added to the samples before 15 min of ultrasonic extraction with 3:1 (v/v) cyclohexane/acetone. The solvent phase was isolated and evaporated in pre-weighed vials for gravimetric lipid determination. Lipids were then removed using solid phase extraction (EZ-POP columns (Supelco/Merck) eluted with acetonitrile) and additional clean-up using pre-combusted florisil (450 °C). Samples were then evaporated and transferred to a GC-vial and the recovery standard (^{13}C- labeled CB-159) was added. Target analytes were analyzed using gas chromatography high-resolution accurate mass spectrometry (GC-HRAM) using a GC-Q-Exactive Orbitrap mass analyzer (Thermo Scientific, UK). Cold splitless injection using programmable temperature vaporization (PTV) with a 1-µL injection volume was performed. The PTV injector was held at 90°C for 0.15 min, ramped to 320°C at 5°C/min with a hold time of 5 min. Details surrounding chromatographic separation and mass spectrometer settings are previously described by Warner & Cojocariu.[38]

Quality assurance of the analytical method was assessed through measurements of laboratory blanks (15 procedural blanks) and standard reference material (contaminated fish; EDF-2524, Cambridge Isotope Laboratories, UK). Samples were blank corrected. The limit of detection (LOD) and quantification (LOQ) were defined as 3 and 10 times the standard deviation of the blank replicates for each extraction batch, respectively. LOD ranged from 0.01 pg g^{-1} to 47.0 pg g^{-1} ww for POPs analyzed (Table S1) and average recovery for the ^{13}C- labeled compounds ranged from 9.6 to 110.1 % for biota samples and from 11.9 to 68.3 % for standard reference material (Table S2).

Enantiomer selective analysis of α-HCH and *cis*- and *trans*-chlordane in zooplankton samples was performed using a chiralsil-dex column (12.5 m x 0.25 mm x 0.25 µm (Agilent (chrompack), USA) connected in tandem with a TG5-SILMS (12.5 m x 0.25 mmx 0.25 µm (Thermo Scientific, UK)). Analysis was performed on a TSQ 9000 GC-MS/MS (Thermo Scientific, UK) using a 2 µL injection volume with conditions described previously using PTV injection. Ion transitions with collision energies, chromatograph separation and mass spectrometer conditions are described in Table S3 of the supporting information. The baseline racemic range was defined as the average EF ± the standard deviation (SD) of the standards; α-HCH (0.51–0.51), *trans*-chlordane (0.51-0.52) and *cis*-chlordane (0.49–0.50).

2.5 Data analyses

Statistical analyses were performed using R version 4.0.2 (R Development Core Team, 2020). Individual compounds that were detected in less than 60% of the samples (CB-118, CB-138, CB-180, *o,p'*-DDT and mirex for zooplankton, CB-28/31, CB-101 and CB-118 for sculpin and γ-HCH, *o,p'*-DDT, and *p,p'*-DDD for benthic invertebrates) were removed from analysis. For the remaining congeners, non-detects were replaced with values (assuming a beta distribution; $\alpha = 5$, $\beta = 1$) conditioned to fall between 0 and LOD using a multiple imputation method.[39] Replaced values represent 12% (for PCBs/HCB) and 8% (other analysed pesticides) of the zooplankton values, 24% (PCBs/HCB) and 19% (other pesticides) of the benthic invertebrate values and 16% (PCBs/HCB) of the sculpin values.

To investigate the relationships between POP concentrations and stable isotopes, lipids, sampling date, taxonomic grouping, and sampling location, Wilcoxon rank sum tests or Kruskal-Wallis rank sum test with the *post hoc* Dunn's test[40] were performed to account for non-normal distributions ($p < 0.05$, Shapiro-Wilk's test).[41] P-values were adjusted for multiple comparisons using the Bonferroni correction.[42] In consideration of our small sample sizes and skewed data, results are presented as bootstrapped means with 95% confidence intervals.[43] Seasonality in zooplankton contaminant loads occur alongside seasonal changes in lipid content, so results are given in ng/g lipid weight (lw) for zooplankton. Sculpin and benthic invertebrates, however, were only sampled spatially. Thus, due to unusually low gravimetrically-determined lipid weights from Adventfjorden sculpin, results for both sculpin and benthic invertebrates are provided on a wet weight (ww) basis for better comparison among fjords.

Water chemistry data collected from two depths (surface and 15 m)[22] were averaged for each station to be used in relation to zooplankton collected from the entire water column. To account for seasonal variation in lipid content (range: 0.2–6.4 %), zooplankton $\delta^{13}C$ values were lipid-corrected based on their CN ratios (range: 2.2–7.6), using the model proposed by Pomerleau et al. (2014)[44]. Sculpin and benthic invertebrates had low lipid content (< 3 %), so $\delta^{13}C$ values were not lipid corrected for these groups.[45]

Redundancy analysis (RDA) was carried out in the R package 'vegan'[46] to evaluate the importance of physical and ecological drivers for explaining variance in contaminant concentrations in zooplankton, sculpin and benthic invertebrates separately. Prior to RDA analyses, contaminant mass fractions were log-transformed to reduce skewness and the influence of abundant congeners on the outcome of the ordination. For herbivorous zooplankton, partial RDA was carried out on the sums of contaminant groups with lipid content included as a covariable. Scaled explanatory variables were grouped according to four likely seasonal drivers of contaminant accumulation: (1) terrestrial inputs were represented by salinity, (2) carbon source by zooplankton $\delta^{13}C$, (3) seasonal atmosphere-volatilization by surface water temperature. To check for multicollinearity among explanatory variables, variance inflation factors were calculated to confirm that VIFs were < 5.[47] Variance partitioning was then carried out using a series of partial RDAs, in order to better understand the degree of overlapping variance among the four drivers (terrestrial inputs, carbon source, temperature and changes in lipid content).

For benthic invertebrates, partial RDA was carried out using lipid content (which was significant for explaining variance in zoobenthos POP content) as a covariable. Explanatory variables included $\delta^{13}C$ and $\delta^{15}N$, feeding habit, taxonomic group, fjord and sampling location (to represent distance to rivers/glaciers). To test the impact of local contaminant loads on invertebrate contaminant concentrations, sediment $\sum_8$PCB and HCB concentrations (using published data from the same fjords; from Johansen et al.),[23] were included as explanatory variables. For sculpin, partial RDA was carried out with fish length included as a covariable. Both fjord and location (estuary vs. nearshore) were included as environmental variables, $\delta^{13}C$ and $\delta^{15}N$ as food-web tracers, and sediment $\sum_8$PCB and HCB content as indicators of local contamination. With variance explained by covariables removed, partial RDA models fit the leftover explanatory variables to the residual variance. To test the significance of these models, permutation tests (Monte-Carlo, 10,000 permutations; significance level of $p \leq 0.05$) were run on the model residuals.

3. Results

3.1 Characteristics of sampled fauna

Zooplankton collected for POP analysis included both size-fractionated samples ('size fractions') and individual taxa. Zooplankton size-fractions were dominated by herbivorous zooplankton. In May, size fractions were dominated by *Cirripedia nauplii* and decapoda larvae (zoea), while copepodites of *Calanus* spp. prevailed in June and August (Figure S1). Individual macrozooplankton taxa consisted of predator chaetognaths (*Parasagitta elegans* and *Eukrohnia hamata*), the small fish *Leptoclinus maculatus* as well as the omnivorous euphausiid *Thysanoessa* spp in May and June. In August, predator jellyplankton, including *Mertensia ovum*, *Beroe cucumis* and *Cyanea capillata,* were also present.

Lipid content in herbivorous zooplankton increased from May (1.63, CI: 1.21–2.07 % ww) to August (3.19, CI: 2.11–4.15 % ww; Dunn's: $p = 0.05$), while lipids in omnivorous/predator zooplankton remained similar between months (Wilcoxon: $p = 0.121$). Lipid corrected $\delta^{13}C$ values decreased seasonally in herbivorous zooplankton, indicating a shift from marine to terrestrial carbon from May (-19.68, CI: -20.45 to -18.98 ‰) to June (-21.77, CI: -22.44 to -21.2 ‰; Dunn's: $p = 0.005$), to August (-24.31, CI: -24.71 to -23.84

‰; Dunn's: $p = 0.005$; Figure S2, Table1)[36]. Values of $\delta^{15}N$ were higher in omnivorous/predator zooplankton (9.8, CI: 8.72–11.03 ‰) than herbivorous zooplankton (7.73, CI: 7.45–8.03 ‰; Wilcoxon: $p = 0.001$), but did not differ among months within each feeding group (Kruskal-Wallis: $p > 0.05$, Figure S2).

Sampled benthic taxa included filter/suspension feeders (the bivalves *Astarte* spp., *Cilliatocardium cilliatum*, *Serripes groenlandicus*, *Mya arenaria* and ascidians), surface-deposit and deep-deposit feeders (bivalve *Macoma calcarea* and polychate *Maldane sarsi* respectively), predators (polychaete *Nephtys* sp., and decapods *Pandalus borealis* and *Sabinea septemcarinata*) and scavengers (seastar *Leptasterias muelleri*, and crab *Hyas araneus*). Due to a lack of adequate replication on the species level, benthic invertebrates were grouped by these feeding strategies for comparison among and within fjords. Lipid content (0.9; CI: 0.64–1.17 %) and $\delta^{13}C$ values (-20.53; CI: -21.07 to -20.05 ‰) in benthic invertebrates did not differ among fjords or feeding groups (Kruskal-Wallis: $p > 0.05$) except for in Adventfjorden, where sampled ascidians had relatively low lipid content. Values of $\delta^{15}N$ were higher in predator species (11.09, CI: 10.58–11.61 ‰) compared to filter feeders and surface deposit feeders (8.18, CI: 7.27–9.13 ‰; Wilcoxon: $p < 0.001$; Figure S3).

For shorthorn sculpin (*Myoxocephalus scorpius*), individuals collected from gillnets were mostly female (32 female, 3 male) with a mean length of 19.9 cm (CI: 19.1–20.7) and mean weight of 165 g (CI: 142.5–188.3). Sculpin lipid content was lower in Adventfjorden (0.02, CI: 0.01—0.02 %) than Billefjorden (0.5, CI: 0.2—0.9 %) and Tempelfjorden (0.4, CI: 0.1—0.8 %). Values of $\delta^{13}C$ (-19.24, CI: -19.5 to -19.01 ‰) did not differ among fjords (Kruskal-Wallis: $p > 0.05$). Values of $\delta^{15}N$ were higher in Billefjorden (14.27, CI: 14–14.61 ‰) compared to Adventfjorden (13.39, CI: 13.11–13.59 ‰; Dunn's: $p = 0.048$) and Tempelfjorden (13.41, CI: 13.03–13.81 ‰; Dunn's: $p = 0.01$; Figure S4).

3.2 POP concentrations in Isfjorden biota

HCB concentrations (on a wet weight basis) in zooplankton ranged from 0.03–0.59 ng/g ww (May: 0.27, CI: 0.18–0.35 ng/g ww, June: 0.06, CI: 0.05–0.07 ng/g ww, August: 0.07, CI: 0.04–0.12 ng/g ww). After lipid normalization, HCB concentrations ranged from 1.28–31.70 ng/g lw (May: 16.67, CI: 12.44–20.93 ng/g lw; June: 4.47, CI: 3.84–5.07 ng/g lw; August: 4.57, CI: 2.61–7.36 ng/g lw). $\sum_8$PCB concentrations (on a wet weight basis) in zooplankton ranged from 0.01–0.19 ng/g ww (May: 0.08, CI: 0.05–0.11 ng/g ww, June: 0.04, CI: 0.03–0.05 ng/g ww, August: 0.05, CI: 0.03–0.07 ng/g ww). After lipid normalization, $\sum_8$PCB concentrations ranged from 0.96–26.06 ng/g lw (May: 5.11, CI: 3.62–6.80 ng/g lw; June: 2.52, CI: 2.09–2.99 ng/g lw; August: 3.45, CI: 1.82–6.23 ng/g lw).

To facilitate interpretation, data were pooled by feeding group for further statistical analysis and visualization (*Calanus* spp.-, Cirripedia nauplii- and decapod zoea- dominated size fractions as herbivores and individual macrozooplankton and jellyplankton as omnivore/predators). Contaminant concentrations did not differ among taxa within each feeding group by month (Kruskal-Wallis: $p > 0.05$). In addition, no spatial trends were observed in contaminant concentrations by feeding group within each month (Kruskal-Wallis tests among fjords within each month: $p > 0.05$; Figure S5). While herbivorous and predatory zooplankton both exhibited similar seasonal trends for each POP group, concentrations were consistently higher in predatory zooplankton (Figure 2a; Wilcoxon rank sum tests for each contaminant group: $p < 0.05$).

Lipid adjusted $\sum$POPs in zooplankton decreased from May to August for most contaminant groups (Figure 2a). HCB was the dominant contaminant and demonstrated a seasonal decrease in herbivorous zooplankton from May (14.9, CI: 10.24–18.9 ng/g lw) to June (4.47, CI: 3.87–5.09 ng/g lw) to August (1.62, CI: 1.4–1.89 ng/g lw ; Dunn's: $p < 0.001$; Figure 2a). Similar downward trends were visible for $\sum_8$PCB, $\sum$DDTs and $\sum$Chlordane pesticides from May to August for both herbivorous and omni/predator zooplankton (Figures 2a and S6; Table 1). This decrease from May to June/August was also apparent on a wet weight basis for both feeding groups (Figures S7 and S8). In contrast, α-HCH concentrations increased from June (1.18, CI: 1.06–1.29 ng/g lw) to August (1.57, CI: 1.44–1.72 ng/g lw) in herbivorous zooplankton (Wilcoxon: $p = 0.004$; Figure 2a, Table 1). An increase from May/June to August was also observed on a wet weight basis for herbivorous zooplankton. In addition, EFs of α-HCH were significantly closer to the racemic range in August (0.41, CI: 0.4–0.43) compared to May (0.39, CI: 0.38–0.39; Wilcoxon: $p = 0.02$; Figure 2b).

∑POPs were higher in scavenger and predator benthic invertebrates compared to filter- and deposit- feeders (Wilcoxon: $p = 0.002$), especially for the higher chlorinated PCBs (Figure S9). For surface deposit feeding and filter-feeding zoobenthos, $\sum_8$PCB was higher at the outer Isfjorden stations (0.25, CI: 0.16–0.37 ng/g ww) compared to the inner fjord arms (Billefjorden: 0.1, CI: 0.04–0.2 ng/g ww, Adventfjorden: 0.13, CI: 0.04–0.3 ng/g ww and Tempelfjorden: 0.06, CI: 0.04–0.09 ng/g ww; Table 2). $\sum_8$PCB and HCB were highest in sculpin collected from Billefjorden ($\sum_8$PCB: 0.22, CI: 0.14–0.33 ng/g ww; HCB: 0.1, CI: 0.08–0.12 ng/g ww), with concentrations significantly higher than those from Tempelfjorden ($\sum_8$PCB: 0.09, CI: 0.06–0.13 ng/g ww; HCB: 0.06, CI: 0.05–0.08 ng/g ww; Wilcoxon: $p < 0.25$; Figure 4; Table 2).

3.3 Physical and ecological drivers of contaminant concentrations

Seasonality in the physical-chemical environment in Isfjorden is reported in a parallel study (Figure S10).[22] Briefly, land-fast sea-ice was present in Billefjorden and Tempelfjorden in May, and many stations were dominated by local and winter-cooled water (Temperature <1; Salinity < 35; Figure S11). High concentrations of chlorophyll-a in the water column, coinciding with low nutrient concentrations, suggest that May sampling took place approximately one week after the peak of the spring phytoplankton bloom.[22,48] In June, freshwater from river run-off and glacier-front ablation was detected in surface waters throughout Isfjorden. In August, freshwater inputs to surface waters, alongside Atlantic Water (Figure S11) advection from the West Spitsbergen Current (WSC; Figure 1a,c), resulted in stratification of the water column. In Isfjorden, marine- and land- terminating glaciers deliver freshwater to the fjord, transporting high suspended sediment loads, terrestrial organic matter and inorganic nutrients to the fjord.[22]

In the zooplankton RDA, constraining variables explained a significant amount of the residual variance in herbivorous zooplankton contaminant concentrations (41.0 %, permutation test: $p = 0.001$; Figure 3) when variance due to lipid content (20.6 %) was removed. The first axis, which separates May from June and August and represents overlapping seasonal and freshwater gradients, explained 38.1 % of the variance (permutation test: $p = 0.001$). The second axis, which captures the within season spatial variability, explained only 2.8 % of the variance in zooplankton contaminant concentrations, and was not significant (permutation test: $p > 0.05$; Figure 3). Results of variance partitioning illustrate the extensive overlapping variance of the explanatory variables (Figure S12). For benthic invertebrates, lipid content explained 30.7% of the variance in contaminant concentrations (permutation test: $p = 0.001$). When variance due to lipid content was accounted for, only taxonomic grouping was significant, explaining 55% of the residual variance. For sculpin, fjord and fjord sediment concentrations of $\sum_8$PCB were the best predictors of contaminant concentrations, explaining 15.5 % and 13.8 % of the residual variance, respectively, when variance due to fish length (6.7 %) was removed. Other variables, including sampling location in the fjord, and $\delta^{13}C$ and $\delta^{15}N$ values, were not significant.

4. Discussion

4.1 Terrestrial inputs are associated with lower concentrations of ∑POPs in Isfjorden biota

Climate change driven increases in temperature are leading to enhanced glacial melt. Here, we investigated the role of glacial meltwater as a secondary source of POPs to coastal food-webs along spatial and seasonal gradients in glacial influence. In Isfjorden, extreme seasonal variations in day length drive seasonal changes on land, where the melt season progresses from snow melt in May and June to glacier melt and permafrost thaw in July and

August.[49,50] This seasonal progression is associated with the delivery of increasingly warm, and sediment-laden meltwater to coastal waters either directly, through glacier-front ablation, or through riverine inputs.[22]

In our study, decreasing water column salinity, increased turbidity, and zooplankton terrestrial carbon utilization were associated with reduced contaminant concentrations, contradicting our hypothesis that glacier meltwater inputs are an important secondary source of legacy POPs to Isfjorden biota. These findings stand in contrast to previous studies on Svalbard which have attributed increased POP exposure in sediment compartments to meltwater inputs.[51–53] However, our observations are in agreement with recent findings from Isfjorden, which found that high sediment loads from marine-terminating glaciers and rivers may act to scavenge and/or dilute contaminant concentrations in coastal waters and sediments.[23]

4.2 Glacier meltwater inputs may be source of α-HCH to coastal zooplankton

While we observed a general decrease in zooplankton contaminant concentrations through the melt season for most POP groups, this was not the case for HCHs. In fact, contaminant profiles demonstrate a clear transition from HCB-dominance in May, to HCH dominance in August, with α-HCH representing the most prevalent isomer. HCH has a lower octanol water partitioning coefficient (K_{ow}) and therefore higher solubility in water compared to the higher K_{ow} HCB and PCBs, which are more likely to be bound to inorganic sediments and therefore not as bioavailable for zooplankton in glacial meltwaters.

Enantioselective analysis of α-HCH illustrates the potential role of glaciers as a secondary source of α-HCH to the fjord in late summer. EF signatures in zooplankton were more racemic in August, when the fjord was most impacted by glacial melt, especially at the glacier fronts and river estuary stations.[22] Historically deposited α-HCH stored in glaciers are not subject to substantial microbial degradation. Thus, in theory, fresh inputs should reflect an EF closer to that of the racemic (equal amounts of left- and right-handed enantiomers) industrial product while biologically degraded compounds deviate from a racemic signature.[54] While macrozooplankton degrade chiral POPs enantiomer-selectively,[55] EFs in lower- trophic level zooplankton, including *Calanus* spp. and meroplankton, should reflect the chiral signature of the surrounding environment.[31,56]

Thus, the change in α-HCH EFs in zooplankton towards a more racemic signature in August indicates fresh inputs of α-HCH to the fjord from glacial meltwater. Atlantic-water advection in August may also be a source of racemic oceanic α-HCH to zooplankton.[31] However, considering the spatial gradient investigated within this study, EFs were closer to racemic in estuarine zooplankton compared to the outer fjord, and the correlations with salinity and turbidity suggest that freshwater inputs from melting glaciers are likely the main driver of the observed patterns. While atmospheric concentrations of HCH have declined since 1990 in Svalbard and the Canadian Arctic,[57,58] our results suggest that exposure trends to coastal fauna may be spatially dependent and deviate from atmospheric trends with continued glacial meltwater release of HCHs into Arctic coastal waters.

4.3 Physical and biological processes explain seasonal decrease in zooplankton contaminant concentrations.

POP concentrations in zooplankton were similar or lower compared to previous studies in Svalbard,[59] the Canadian Arctic[60,61] and the marginal sea-ice zone.[32] Total contaminant concentrations (∑POPs) decreased seasonally in all taxa. However, concentrations in omnivorous/predatory zooplankton were consistently higher compared to herbivorous zooplankton, indicating biomagnification of POPs through the zooplankton food web, as previously described for Arctic zooplankton.[59,62–64]

While glacial inputs were likely a source of α-HCH, all other contaminant groups demonstrated clear and significant seasonal decreases. This seasonal decrease is likely due to seasonality in several processes acting in concert that affect primary production and lipid content in zooplankton, which in turn influence the seasonal availability and uptake of POPs in the food-web.[20,24,59,63] The highest concentrations of POPs in zooplankton were observed in May, during ice break-up, alongside higher $\delta^{13}C$ values, indicating reliance on marine carbon from the spring phytoplankton bloom.[36] These findings are in line with previously documented seasonal processes in the Arctic.[65] During the Arctic polar night, cold temperatures and sea-ice can act chemically and physically to prevent outgassing of POPs from the water column, resulting in increased dissolved concentrations.[20] This is particularly true for highly volatile compounds, like HCB, which has had relatively stable concentrations in the Svalbard atmosphere since 1990,[58] and which dominated zooplankton contaminant profiles in May. Subsequently, with the return of the sun in spring, ice-algae and pelagic phytoplankton blooms commence as surficial snow melts and the sea-ice is broken up.[66] This rapid increase in biomass in the water column provides increased surface area for POPs to adsorb to, a process driven by their high affinity for organic matter.[67,68] Thus, zooplankton grazing on the spring phytoplankton bloom in May are exposed to higher concentrations of POPs within the water column, as well as through their diet. Similar findings have been reported for littoral amphipods in Adventfjorden[69].

The decrease in POP concentrations from May to June was observed on both a lipid weight and wet-weight basis, suggesting reduced exposure following ice melt and the spring phytoplankton bloom. In contrast, the decrease in contaminant concentrations from June to August on a lipid weight basis was not observed on a wet weight basis. For herbivorous zooplankton, May and June communities were dominated by meroplankton and the lipid-depleted overwintering population of *Calanus* spp. The seasonal increase in relative abundance of *Calanus* spp. in August size fractions, together with accumulation of storage lipids through the summer feeding season, suggests that lower contaminant concentrations from June to August can be attributed to changes in species composition and lipid dilution.[70,71]

4.4 Zoobenthos reflect impacts of local sources and inorganic sedimentation

Zoobenthos, including the higher trophic-level sculpin, provide a time-integrated perspective on contamination on annual and multi-year time scales. Thus, stationary infauna as well as sculpin, known to be a territorial fish with a small home-range,[72] should reflect the signal in the location collected. While benthic invertebrates and sculpin showed similar concentrations of POPs to previous studies for Svalbard zoobenthos,[69,73,74] the spatial patterns across the Isfjorden system highlight the importance of inputs from local point-sources and effects of fjord-specific physical processes, like varying sedimentation rates, on exposure to the benthic environment.

The sampling design employed here targeted the contrast between river estuaries and marine-influenced areas of the fjord with the aim of distinguishing impacts of river runoff and associated shifts in carbon source on contaminant loads. However, no difference between within-fjord sampling locations was detected, and spatial differences in $\delta^{13}C$ values in biota had no effect on PCBs or HCB concentrations. Instead, the sampled fjord was the most important explanation for HCB and PCB contamination in sculpin and lower trophic level benthic invertebrates (filter and surface deposit feeders). The high POP concentrations in Billefjorden fauna reflect the impact of the previously described point-source from the Russian mining settlement Pyramiden, which was closed in 1997.[23,75–78] POP concentrations in Billefjorden sediments sampled adjacent to Pyramiden are 5-fold higher than Adventfjorden and Tempelfjorden sediments.[23] In contrast, Adventfjorden and Tempelfjorden do not contain significant local sources of PCBs, and lower concentrations match the lower contaminant load in sediments samples collected from the same stations (Figure 4)[23,68]. In addition, Tempelfjorden has a marine-terminating glacier which delivers high inorganic suspended sediment loads to the fjord. In fact, the highest concentrations in benthic invertebrates were measured from outer Isfjorden, suggesting oceanic transport of legacy POPs is likely more important than sources associated with glacial meltwater. High sedimentation rates accompanying glacial melt likely act to dilute sediment contaminant concentrations, creating a spatial gradient along the fjord axis, a process supported by previously reported patterns in sediment concentrations.[23]

4.5 Future Perspectives

As temperatures increase globally and glacier mass balance is significantly reduced,[79] there is concern that coastal areas will increasingly receive inputs of remobilized legacy contaminants from melting cryospheric compartments,[5,12] especially in Arctic regions, where contaminants accumulate due to global distillation processes.[80] While ice profiles from Svalbard glaciers have illustrated the storage of legacy POPs through the decades,[8,9] our results do not indicate that the these glaciers are an important source of legacy contaminants to coastal fauna. For the benthic compartment, glacial inputs of contaminants are diluted by high rates of inorganic sedimentation, which also likely act to bury local contamination. In the water column, we found indications of accumulation of remobilized α-HCH in coastal zooplankton, but the resulting concentrations were low. All other POP groups, including PCBs, Chlordanes and DDTs were not associated with glacial meltwater and demonstrated clear seasonal declines in coastal zooplankton following the spring phytoplankton bloom. For these heavily glaciated Svalbard fjords, other physical and ecological processes, including increased inorganic sediment loads and seasonal lipid accumulation in zooplankton, result in lower contaminant loads during the melt season, outweighing any inputs from glacial melt.

Data availability

Contaminant data are openly available on DataverseNO (UiT Open Research Data).[81] The supporting environmental data are published by McGovern et al. (2020).[22]

Supporting Information

Additional results and figures can be found in supporting information.

Acknowledgments

This research was funded by the Norwegian Research Council (TerrACE; project number: 268458), the Fram Center Flagship "Hazardous substances" grant (IcePOPs; project number: 772019, year: 2020), and the Svalbard Science Forum's Arctic Field Grant (RIS number: 10914, year: 2018). We thank the students and fellow scientists who helped us with the fieldwork including Nathalie Carrasco, Anne Deininger, Eirik Aasmo Finne, Sverre Johansen, Hannah Miller, Paul Renaud, Charlotte Pedersen Ugelstad, and Emilie Hernes Vereide. We also thank UNIS logistics and Stig Henningsen at Henningsen Transport & Guiding with MS FARM for their help during the field campaigns and Merete Miøen for assistance in the laboratory.

References

(1) Mercier, D. Climate Change and the Melting Cryosphere. In *Spatial impacts of climate change*; John Wiley & Sons, Ltd, 2021; pp 21–41. https://doi.org/https://doi.org/10.1002/9781119817925.ch2.

(2) AMAP. Arctic Climate Change Update 2021: Key Trends and Impacts. Summary for Policy-Makers. **2021**.

(3) Hanssen-Bauer, I.; Førland, E.; Hisdal, H.; Mayer, S.; Sandø, A.; Sorteberg, A. Climate in Svalbard 2100, a Knowledge Base for Climate Adaptation. *Norwegian Centre for Climate Services (NCCS) for Norwegian Environment Agency (Miljødirektoratet)* **2019**, 208.

(4) Tepes, P.; Gourmelen, N.; Nienow, P.; Tsamados, M.; Shepherd, A.; Weissgerber, F. Changes in Elevation and Mass of Arctic Glaciers and Ice Caps, 2010–2017. *Remote Sensing of Environment* **2021**, *261*, 112481.

(5) Bogdal, C.; Schmid, P.; Zennegg, M.; Anselmetti, F. S.; Scheringer, M.; Hungerbühler, K. Blast from the Past: Melting Glaciers as a Relevant Source for Persistent Organic Pollutants. *Environmental science & technology* **2009**, *43* (21), 8173–8177.

(6) Pacyna, J. M.; Oehme, M. Long-Range Transport of Some Organic Compounds to the Norwegian Arctic. *Atmospheric Environment (1967)* **1988**, *22* (2), 243–257.

(7) Hermanson, M. H.; Isaksson, E.; Hann, R.; Teixeira, C.; Muir, D. C. Atmospheric Deposition of Organochlorine Pesticides and Industrial Compounds to Seasonal Surface Snow at Four Glacier Sites on Svalbard, 2013–2014. *Environmental Science & Technology* **2020**, *54* (15), 9265–9273.

(8) Ruggirello, R. M.; Hermanson, M. H.; Isaksson, E.; Teixeira, C.; Forsström, S.; Muir, D. C.; Pohjola, V.; Wal, R. van de; Meijer, H. A. Current Use and Legacy Pesticide

Deposition to Ice Caps on Svalbard, Norway. *Journal of Geophysical Research: Atmospheres* **2010**, *115* (D18), 308.

(9) Garmash, O.; Hermanson, M. H.; Isaksson, E.; Schwikowski, M.; Divine, D.; Teixeira, C.; Muir, D. C. Deposition History of Polychlorinated Biphenyls to the Lomonosovfonna Glacier, Svalbard: A 209 Congener Analysis. *Environmental science & technology* **2013**, *47* (21), 12064–12072.

(10) Aslam, S. N.; Huber, C.; Asimakopoulos, A. G.; Steinnes, E.; Mikkelsen, Ø. Trace Elements and Polychlorinated Biphenyls (PCBs) in Terrestrial Compartments of Svalbard, Norwegian Arctic. *Science of the Total Environment* **2019**, *685*, 1127–1138.

(11) AMAP. Snow, Water, Ice and Permafrost in the Arctic (SWIPA); Summary for Policy-Makers. **2017**.

(12) Grannas, A. M.; Bogdal, C.; Hageman, K. J.; Halsall, C.; Harner, T.; Hung, H.; Kallenborn, R.; Klán, P.; Klánová, J.; Macdonald, R. W.; others. The Role of the Global Cryosphere in the Fate of Organic Contaminants. *Atmospheric Chemistry and Physics* **2013**, *13* (6), 3271–3305.

(13) Noyes, P. D.; McElwee, M. K.; Miller, H. D.; Clark, B. W.; Van Tiem, L. A.; Walcott, K. C.; Erwin, K. N.; Levin, E. D. The Toxicology of Climate Change: Environmental Contaminants in a Warming World. *Environment international* **2009**, *35* (6), 971–986.

(14) Kallenborn, R.; Halsall, C.; Dellong, M.; Carlsson, P. The Influence of Climate Change on the Global Distribution and Fate Processes of Anthropogenic Persistent Organic Pollutants. *Journal of Environmental Monitoring* **2012**, *14* (11), 2854–2869.

(15) Carlsson, P.; Cornelissen, G.; Bøggild, C. E.; Rysgaard, S.; Mortensen, J.; Kallenborn, R. Hydrology-Linked Spatial Distribution of Pesticides in a Fjord System in Greenland. *Journal of Environmental Monitoring* **2012**, *14* (5), 1437–1443.

(16) Carlsson, P.; Breivik, K.; Brorström-Lundén, E.; Cousins, I.; Christensen, J.; Grimalt, J. O.; Halsall, C.; Kallenborn, R.; Abass, K.; Lammel, G.; others. Polychlorinated Biphenyls (PCBs) as Sentinels for the Elucidation of Arctic Environmental Change Processes: A Comprehensive Review Combined with ArcRisk Project Results. *Environmental Science and Pollution Research* **2018**, *25* (23), 22499–22528.

(17) McGovern, M.; Evenset, A.; Borgå, K.; Wit, H. A. de; Braaten, H. F. V.; Hessen, D. O.; Schultze, S.; Ruus, A.; Poste, A. Implications of Coastal Darkening for Contaminant Transport, Bioavailability, and Trophic Transfer in Northern Coastal Waters. *Environmental science & technology*, 2019, *53*, 7180–7182.

(18) Hung, H.; Halsall, C.; Ball, H.; Bidleman, T.; Dachs, J.; De Silva, A.; Hermanson, M.; Kallenborn, R.; Muir, D.; Sühring, R.; Wang, X.; Wilson, S. Climate Change Influence on the Levels and Trends of Persistent Organic Pollutants (POPs) and Chemicals of Emerging Arctic Concern (CEACs) in the Arctic Physical Environment – a Review. *Environ Sci: Proc Imp.* **2022**.

(19) Borgå, K.; McKinney, M.; Routti, H.; Fernie, K.; Giebichenstein, J.; Hallanger, I.; Muir, D. The Influence of Global Climate Change on Accumulation and Toxicity of Persistent Organic Pollutants and Chemicals of Emerging Arctic Concern in Arctic Food Webs. *Environmental Science: Processes & Impacts* **2022**.

(20) Hargrave, B. T.; Phillips, G. A.; Vass, W. P.; Bruecker, P.; Welch, H. E.; Siferd, T. D. Seasonality in Bioaccumulation of Organochlorines in Lower Trophic Level Arctic Marine Biota. *Environmental science & technology* **2000**, *34* (6), 980–987.

(21) Nizzetto, L.; Gioia, R.; Li, J.; Borgå, K.; Pomati, F.; Bettinetti, R.; Dachs, J.; Jones, K. C. Biological Pump Control of the Fate and Distribution of Hydrophobic Organic Pollutants in Water and Plankton. *Environmental science & technology* **2012**, *46* (6), 3204–3211.

(22) McGovern, M.; Pavlov, A. K.; Deininger, A.; Granskog, M.; Leu, E. S.; Søreide, J.; Poste, A. Terrestrial Inputs Drive Seasonality in Organic Matter and Nutrient Biogeochemistry in a High Arctic Fjord System (Isfjorden, Svalbard). **2020**.

(23) Johansen, Sverre; Poste, A. E.; Allan, I.; Evenset, A.; Carlsson, P. Terrestrial Inputs Govern Spatial Distribution of Polychlorinated Biphenyls (PCBs) and Hexachlorobenzene (HCB) in an Arctic Fjord System (Isfjorden, Svalbard). *Environmental Pollution* **2021**, 116963.

(24) Borgå, K.; Fisk, A.; Hoekstra, P.; Muir, D. Biological and Chemical Factors of Importance in the Bioaccumulation and Trophic Transfer of Persistent Organochlorine Contaminants in Arctic Marine Food Webs. *Environmental Toxicology and Chemistry: An International Journal* **2004**, *23* (10), 2367–2385.

(25) Carrasco, N. Seasonality in Mercury Bioaccumulation in Particulate Organic Matter and Zooplankton in a River-Influenced Arctic Fjord (Adventfjord, Svalbard). Master's thesis, UiT Norges arktiske universitet, 2019.

(26) Skogsberg, S. L. E. Effects of Seasonal Riverine Run-Off on Contaminant Accumulation in Arctic Littoral Amphipods. Master's thesis, The University of Oslo, 2019.

(27) Wong, F.; Hung, H.; Dryfhout-Clark, H.; Aas, W.; Bohlin-Nizzetto, P.; Breivik, K.; Mastromonaco, M. N.; Lundén, E. B.; Ólafsdóttir, K.; Sigursson, Á.; others. Time Trends of Persistent Organic Pollutants (POPs) and Chemicals of Emerging Arctic Concern (CEAC) in Arctic Air from 25 Years of Monitoring. *Science of the Total Environment* **2021**, *775*, 145109.

(28) Wong, C. S.; Warner, N. A. *Chirality as an Environmental Forensics Tool*; John Wiley & Sons, Ltd: Chichester, UK, 2009.

(29) Lu, Z.; Fisk, A. T.; Kovacs, K. M.; Lydersen, C.; McKinney, M. A.; Tomy, G. T.; Rosenburg, B.; McMeans, B. C.; Muir, D. C.; Wong, C. S. Temporal and Spatial Variation

in Polychlorinated Biphenyl Chiral Signatures of the Greenland Shark (Somniosus Microcephalus) and Its Arctic Marine Food Web. *Environmental pollution* **2014**, *186*, 216–225.

(30) Lehmler, H.-J.; Harrad, S. J.; Hühnerfuss, H.; Kania-Korwel, I.; Lee, C. M.; Lu, Z.; Wong, C. S. Chiral Polychlorinated Biphenyl Transport, Metabolism, and Distribution: A Review. *Environmental science & technology* **2010**, *44* (8), 2757–2766.

(31) Carlsson, P.; Warner, N. A.; Hallanger, I. G.; Herzke, D.; Kallenborn, R. Spatial and Temporal Distribution of Chiral Pesticides in Calanus Spp. From Three Arctic Fjords. *Environmental pollution* **2014**, *192*, 154–161.

(32) Borgå, K.; Bidleman, T. Enantiomer Fractions of Organic Chlorinated Pesticides in Arctic Marine Ice Fauna, Zooplankton, and Benthos. *Environmental science & technology* **2005**, *39* (10), 3464–3473.

(33) Dickhut, R. M.; Cincinelli, A.; Cochran, M.; Ducklow, H. W. Atmospheric Concentrations and Air- Water Flux of Organochlorine Pesticides Along the Western Antarctic Peninsula. *Environmental science & technology* **2005**, *39* (2), 465–470.

(34) Søreide, J. E.; Tamelander, T.; Hop, H.; Hobson, K. A.; Johansen, I. Sample Preparation Effects on Stable c and n Isotope Values: A Comparison of Methods in Arctic Marine Food Web Studies. *Marine Ecology Progress Series* **2006**, *328*, 17–28.

(35) UC Davis Stable Isotope Facility. Carbon and Nitrogen in Solids. *https://stableisotopefacility.ucdavis.edu/carbon-and-nitrogen-solids*, 2020, 1.

(36) Peterson, B. J.; Fry, B. Stable Isotopes in Ecosystem Studies. *Annual review of ecology and systematics* **1987**, *18* (1), 293–320.

(37) Hitchcock, D. J.; Andersen, T.; Varpe, Ø.; Loonen, M. J.; Warner, N. A.; Herzke, D.; Tombre, I. M.; Griffin, L. R.; Shimmings, P.; Borgå, K. Potential Effect of Migration

Strategy on Pollutant Occurrence in Eggs of Arctic Breeding Barnacle Geese (Branta Leucopsis). *Environmental science & technology* **2019**, *53* (9), 5427–5435.

(38) Warner, N. A.; Cojocariu, C. I. Versatility of GC-Orbitrap Mass Spectrometry for the Ultra-Trace Detection of Persistent Organic Pollutants in Penguin Blood from Antarctica. *Thermo Fisher Scientific* **2018**, 1–8.

(39) Baccarelli, A.; Pfeiffer, R.; Consonni, D.; Pesatori, A. C.; Bonzini, M.; Patterson Jr, D. G.; Bertazzi, P. A.; Landi, M. T. Handling of Dioxin Measurement Data in the Presence of Non-Detectable Values: Overview of Available Methods and Their Application in the Seveso Chloracne Study. *Chemosphere* **2005**, *60* (7), 898–906.

(40) Dunn, O. J. Multiple Comparisons Using Rank Sums. *Technometrics* **1964**, *6* (3), 241–252.

(41) Conover, W. J. *Practical Nonparametric Statistics*; John Wiley & Sons, 1998; Vol. 350, pp 428–433.

(42) Bland, J. M.; Altman, D. G. Multiple Significance Tests: The Bonferroni Method. *Bmj* **1995**, *310* (6973), 170.

(43) Greenacre, M. Data Reporting and Visualization in Ecology. *Polar Biology* **2016**, *39* (11), 2189–2205.

(44) Pomerleau, C.; Winkler, G.; Sastri, A.; Nelson, R. J.; Williams, W. J. The Effect of Acidification and the Combined Effects of Acidification/Lipid Extraction on Carbon Stable Isotope Ratios for Sub-Arctic and Arctic Marine Zooplankton Species. *Polar Biology* **2014**, *37* (10), 1541–1548.

(45) Post, D. M.; Layman, C. A.; Arrington, D. A.; Takimoto, G.; Quattrochi, J.; Montana, C. G. Getting to the Fat of the Matter: Models, Methods and Assumptions for Dealing with Lipids in Stable Isotope Analyses. *Oecologia* **2007**, *152* (1), 179–189.

(46) Oksanen, J.; Blanchet, F. G.; Friendly, M.; Kindt, R.; Legendre, P.; McGlinn, D.; Minchin, P. R.; O'Hara, R. B.; Simpson, G. L.; Solymos, P.; Stevens, M. H. H.; Szoecs, E.; Wagner, H. *Vegan: Community Ecology Package*; 2019; p 1.

(47) Kock, N.; Lynn, G. Lateral Collinearity and Misleading Results in Variance-Based SEM: An Illustration and Recommendations. *Journal of the Association for information Systems* **2012**, *13* (7).

(48) Nyeggen, M. U. Seasonal Zooplankton Dynamics in Svalbard Coastal Waters: The Shifting Dominance of Mero-and Holoplankton and Timing of Reproduction in Three Species of Copepoda. Master's thesis, The University of Bergen, 2019.

(49) Killingtveit, Å.; Pettersson, L.-E.; Sand, K. Water Balance Investigations in Svalbard. *Polar Research* **2003**, *22* (2), 161–174.

(50) Nowak, A.; Hodgkins, R.; Nikulina, A.; Osuch, M.; Wawrzyniak, T.; Kavan, J.; Łepkowska, E.; Majerska, M.; Romashova, K.; Vasilevich, I.; others. From Land to Fjords: The Review of Svalbard Hydrology from 1970 to 2019 (SvalHydro). **2021**.

(51) Pouch, A.; Zaborska, A.; Pazdro, K. Concentrations and Origin of Polychlorinated Biphenyls (PCBs) and Polycyclic Aromatic Hydrocarbons (PAHs) in Sediments of Western Spitsbergen Fjords (Kongsfjorden, Hornsund, and Adventfjorden). *Environmental monitoring and assessment* **2017**, *189* (4), 175.

(52) Pouch, A.; Zaborska, A.; Pazdro, K. The History of Hexachlorobenzene Accumulation in Svalbard Fjords. *Environmental monitoring and assessment* **2018**, *190* (6), 1–14.

(53) Sapota, G.; Wojtasik, B.; Burska, D.; Nowiński, K. Persistent Organic Pollutants (POPs) and Polycyclic Aromatic Hydrocarbons (PAHs) in Surface Sediments from Selected Fjords, Tidal Plains and Lakes of the North Spitsbergen. *Polish Polar Research* **2009**, 59–76.

(54) Wong, C. S.; Mabury, S. A.; Whittle, D. M.; Backus, S. M.; Teixeira, C.; DeVault, D. S.; Bronte, C. R.; Muir, D. C. Organochlorine Compounds in Lake Superior: Chiral Polychlorinated Biphenyls and Biotransformation in the Aquatic Food Web. *Environmental science & technology* **2004**, *38* (1), 84–92.

(55) Warner, N.; Wong, C. The Freshwater Invertebrate Mysis Relicta Can Eliminate Chiral Organochlorine Compounds Enantioselectively. *Environmental science & technology* **2006**, *40* (13), 4158–4164.

(56) Warner, N.; Norstrom, R.; Wong, C.; Fisk, A. Enantiomeric Fractions of Chiral Polychlorinated Biphenyls Provide Insights on Biotransformation Capacity of Arctic Biota. *Environmental Toxicology and Chemistry: An International Journal* **2005**, *24* (11), 2763–2767.

(57) Hung, H.; Blanchard, P.; Halsall, C.; Bidleman, T.; Stern, G.; Fellin, P.; Muir, D.; Barrie, L.; Jantunen, L.; Helm, P.; others. Temporal and Spatial Variabilities of Atmospheric Polychlorinated Biphenyls (PCBs), Organochlorine (OC) Pesticides and Polycyclic Aromatic Hydrocarbons (PAHs) in the Canadian Arctic: Results from a Decade of Monitoring. *Science of the Total Environment* **2005**, *342* (1-3), 119–144.

(58) Hung, H.; Katsoyiannis, A. A.; Brorström-Lundén, E.; Olafsdottir, K.; Aas, W.; Breivik, K.; Bohlin-Nizzetto, P.; Sigurdsson, A.; Hakola, H.; Bossi, R.; others. Temporal Trends of Persistent Organic Pollutants (POPs) in Arctic Air: 20 Years of Monitoring Under the Arctic Monitoring and Assessment Programme (AMAP). *Environmental Pollution* **2016**, *217*, 52–61.

(59) Hallanger, I. G.; Ruus, A.; Warner, N. A.; Herzke, D.; Evenset, A.; Schøyen, M.; Gabrielsen, G. W.; Borgå, K. Differences Between Arctic and Atlantic Fjord Systems on Bioaccumulation of Persistent Organic Pollutants in Zooplankton from Svalbard. *Science of the Total Environment* **2011**, *409* (14), 2783–2795.

(60) Sobek, A.; McLachlan, M. S.; Borgå, K.; Asplund, L.; Lundstedt-Enkel, K.; Polder, A.; Gustafsson, Ö. A Comparison of PCB Bioaccumulation Factors Between an Arctic and a Temperate Marine Food Web. *Science of the total environment* **2010**, *408* (13), 2753–2760.

(61) Hoekstra, P.; O'hara, T.; Fisk, A.; Borgå, K.; Solomon, K. R.; Muir, D. Trophic Transfer of Persistent Organochlorine Contaminants (OCs) Within an Arctic Marine Food Web from the Southern Beaufort–Chukchi Seas. *Environmental Pollution* **2003**, *124* (3), 509–522.

(62) Borgå, K.; Gabrielsen, G.; Skaare, J. Differences in Contamination Load Between Pelagic and Sympagic Invertebrates in the Arctic Marginal Ice Zone: Influence of Habitat, Diet and Geography. *Marine Ecology Progress Series* **2002**, *235*, 157–169.

(63) Fisk, A. T.; Stern, G. A.; Hobson, K. A.; Strachan, W. J.; Loewen, M. D.; Norstrom, R. J. Persistent Organic Pollutants (POPs) in a Small, Herbivorous, Arctic Marine Zooplankton (Calanus Hyperboreus): Trends from April to July and the Influence of Lipids and Trophic Transfer. *Marine Pollution Bulletin* **2001**, *43* (1-6), 93–101.

(64) Borgå, K.; Poltermann, M.; Polder, A.; Pavlova, O.; Gulliksen, B.; Gabrielsen, G.; Skaare, J. Influence of Diet and Sea Ice Drift on Organochlorine Bioaccumulation in Arctic Ice-Associated Amphipods. *Environmental pollution* **2002**, *117* (1), 47–60.

(65) Galbán-Malagón, C.; Berrojalbiz, N.; Ojeda, M.-J.; Dachs, J. The Oceanic Biological Pump Modulates the Atmospheric Transport of Persistent Organic Pollutants to the Arctic. *Nature communications* **2012**, *3* (1), 1–9.

(66) Sverdrup, H. On Conditions for the Vernal Blooming of Phytoplankton. *J. Cons. Int. Explor. Mer* **1953**, *18* (3), 287–295.

(67) Dachs, J.; Eisenreich, S. J.; Baker, J. E.; Ko, F.-C.; Jeremiason, J. D. Coupling of Phytoplankton Uptake and Air- Water Exchange of Persistent Organic Pollutants. *Environmental science & technology* **1999**, *33* (20), 3653–3660.

(68) Everaert, G.; De Laender, F.; Goethals, P. L.; Janssen, C. R. Multidecadal Field Data Support Intimate Links Between Phytoplankton Dynamics and PCB Concentrations in Marine Sediments and Biota. *Environmental science & technology* **2015**, *49* (14), 8704–8711.

(69) Skogsberg, E.; McGovern, M.; Poste, A. E.; Jonsson, S.; Arts, M.; Varpe, Ø.; Borgå, K. Seasonal Pollutant Levels in Littoral High-Arctic Amphipods in Relation to Food Sources and Terrestrial Run-Off. *Environmental Pollution* **in review**.

(70) Frantzen, S.; Måge, A.; Iversen, S. A.; Julshamn, K. Seasonal Variation in the Levels of Organohalogen Compounds in Herring (Clupea Harengus) from the Norwegian Sea. *Chemosphere* **2011**, *85* (2), 179–187.

(71) Nyberg, E.; Faxneld, S.; Danielsson, S.; Eriksson, U.; Miller, A.; Bignert, A. Temporal and Spatial Trends of PCBs, DDTs, HCHs, and HCB in Swedish Marine Biota 1969–2012. *Ambio* **2015**, *44* (3), 484–497.

(72) Moring, J. R. Appearance and Possible Homing of Two Species of Sculpins in Maine Tidepools. *Northeastern Naturalist* **2001**, *8* (2), 207–218.

(73) Vieweg, I.; Hop, H.; Brey, T.; Huber, S.; Ambrose Jr, W. G.; Gabrielsen, G. W.; others. Persistent Organic Pollutants in Four Bivalve Species from Svalbard Waters. *Environmental pollution* **2012**, *161*, 134–142.

(74) Evenset, A.; Hallanger, I.; Tessmann, M.; Warner, N.; Ruus, A.; Borgå, K.; Gabrielsen, G.; Christensen, G.; Renaud, P. Seasonal Variation in Accumulation of Persistent Organic Pollutants in an Arctic Marine Benthic Food Web. *Science of the Total Environment* **2016**, *542*, 108–120.

(75) Evenset, A.; Christensen, G.; Palerud, R. Miljøgifter i Marine Sedimenter i Isfjorden, Svalbard 2009. *Undersøkelser utenfor Longyearbyen, Barentsburg, Pyramiden og Colesbukta, Akvaplan-niva rapport. Akvaplan-niva, Tromsø* **2009**.

(76) Jartun, M.; Ottesen, R. T.; Volden, T.; Lundkvist, Q. Local Sources of Polychlorinated Biphenyls (PCB) in Russian and Norwegian Settlements on Spitsbergen Island, Norway. *Journal of Toxicology and Environmental Health, Part A* **2009**, *72* (3-4), 284–294.

(77) Evenset, A.; Christensen, G. Tilførsler Og Opptak Av PCB i Marine Naeringskjeder Utenfor Pyramiden, Svalbard. *Akvaplan-niva rapport:5227 -1, Akvaplan-niva, Tromsø* **2011**.

(78) Warner, N. A.; Sagerup, K.; Kristoffersen, S.; Herzke, D.; Gabrielsen, G. W.; Jenssen, B. M. Snow Buntings (Plectrophenax Nivealis) as Bio-Indicators for Exposure Differences to Legacy and Emerging Persistent Organic Pollutants from the Arctic Terrestrial Environment on Svalbard. *Science of The Total Environment* **2019**, *667*, 638–647.

(79) Marzeion, B.; Jarosch, A.; Hofer, M. Past and Future Sea-Level Change from the Surface Mass Balance of Glaciers. *The Cryosphere* **2012**, *6* (6), 1295–1322.

(80) Wania, F.; Mackay, D. Global Fractionation and Cold Condensation of Low Volatility Organochlorine Compounds in Polar Regions. *Ambio* **1993**, 10–18.

(81) McGovern, M.; Warner, N. A.; Poste, A. E. Replication Data for: Is glacial meltwater a secondary source of legacy contaminants to Arctic coastal food-webs?, 2022. https://doi.org/10.18710/KYIZOQ.

Figures and Tables

Table 1. Summary statistics of sample means and 95% CI for zooplankton.[1]

Feeding Group	Month	n	Lipid (%)	δ^{13}C (‰)	$\sum_8$PCB (ng g^{-1} lw)	HCB (ng g^{-1} lw)	$\sum$DDT (ng g^{-1} lw)	$\sum$Chlordanes (ng g^{-1} lw)	$\sum$HCH (ng g^{-1} lw)	EF-αHCH
Herbivores	May	8	1.63 (1.21–2.04)	-19.68 (-20.38 to -18.94)	4.43 (2.75–6.31)	14.9 (10.45–18.87)	4.77 (3.16–6.73)	3.54 (2.18–5.16)	1.3 (0.88–1.7)	0.39 (0.38–0.39)
	June	16	1.58 (1.25–1.98)	-21.77 (-22.48 to -21.18)	2.52 (2.07–3.01)	4.47 (3.86–5.1)	2.6 (2.17–3.11)	1.98 (1.74–2.24)	1.18 (1.06–1.29)	0.41 (0.39–0.42)
	August	8	3.19 (2.2–4.13)	-24.31 (-24.71 to -23.82)	1.6 (1.3–1.93)	1.62 (1.42–1.88)	2.1 (1.75–2.48)	1.54 (1.42–1.63)	1.57 (1.45–1.72)	0.41 (0.4–0.43)
Omnivores/ Predators	May	3	1.91 (0.67–3.72)	-21.29 (-22.45 to -20.08)	6.91 (5.04–9.78)	21.38 (15.76–31.7)	9.46 (6.27–14.72)	11.1 (8.69–15.85)	1.25 (0.56–1.74)	0.39 (0.39–0.39)
	August	11	1.36 (0.63–2.53)	-21.86 (-22.57 to -21.18)	4.8 (2.12–9.16)	6.72 (3.81–10.69)	2.61 (1.55–3.87)	2.7 (1.69–4.01)	1.08 (0.73–1.44)	0.41 (0.39–0.44)

[1] Zooplankton samples collected by fjord (and month) included n=6 in Adventfjorden (May: 2, June: 4, Aug: 0), n=8 in Billefjorden (May: 1, June: 3, Aug: 4), n=14 in Tempelfjorden (May: 3, June: 5, Aug: 6), and n=18 in outer Isfjorden (May: 5, June: 4, Aug: 9).

Table 2. Summary statistics of sample means and 95% CI for benthic invertebrates (filter/deposit feeders) and sculpin.

Zoobenthos	Fjord	n	% Lipid	$\delta^{13}C$ (‰)	$\delta^{15}N$ (‰)	$\sum_8$PCB (ng g^{-1} ww)	HCB (ng g^{-1} ww)
Filter/deposit-feeders	Billefjorden	3	0.54 (0.28–0.7)	-21.8 (-23.12 to -20.82)	6.96 (6.59–7.28)	0.1 (0.04–0.2)	0.08 (0.03–0.16)
	Adventfjorden	3	0.09 (0.02–0.15)	-21.17 (-22.57 to -20.15)	8.53 (6.67–10.24)	0.13 (0.04–0.3)	0.04 (0.04–0.05)
	Tempelfjorden	3	0.6 (0.29–1.07)	-20.9 (-21.7 to -20.36)	7.6 (6.16–10.19)	0.06 (0.04–0.09)	0.05 (0.02–0.09)
	Isfjorden	3	0.36 (0.3–0.44)	-20.23 (-20.5 to -19.95)	9.62 (7.55–10.74)	0.25 (0.16–0.37)	0.15 (0.11–0.19)
Sculpin	Billefjorden	9	0.5; (0.2–0.9)	-19.35 (-19.77–-18.95)	14.27 (14-14.57)	0.22 (0.13–0.33)	0.1 (0.08–0.12)
	Adventfjorden	3	0.02 (0.01–0.02)	-19.39 (-19.47–-19.3)	13.39 (13.11–13.59)	0.08 (0.06–0.1)	0.06 (0.05–0.07)
	Tempelfjorden	18	0.4; (0.1–0.8)	-19.15 (-19.52–-18.76)	13.41 (13.03–13.76)	0.09 (0.06–0.13)	0.06 (0.05–0.08)

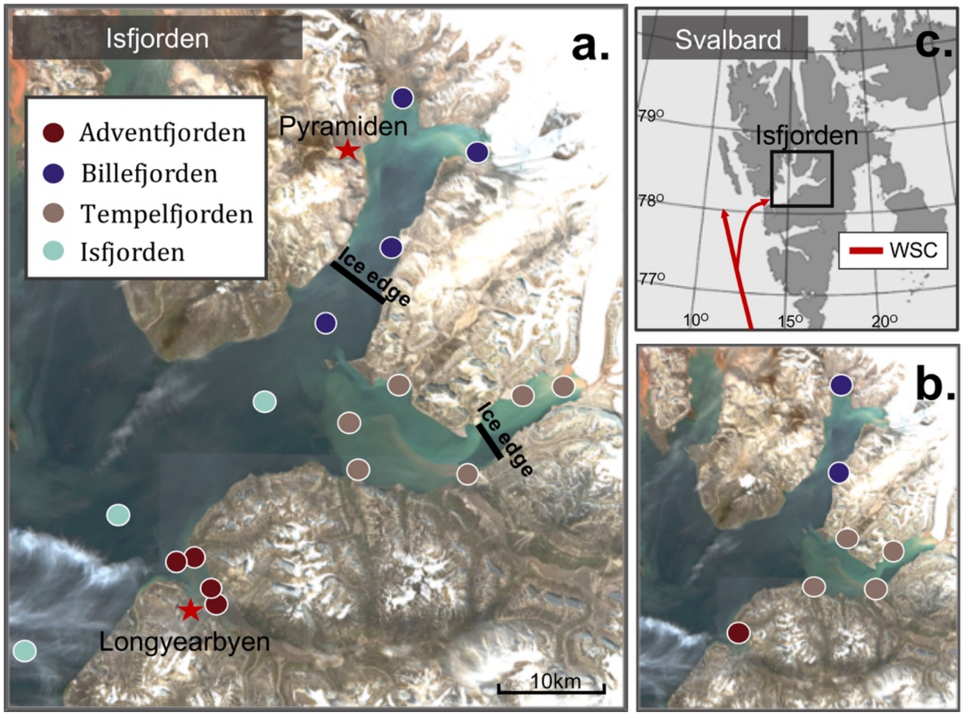

Figure 1. (a) Satellite image (taken August 20, 2018; Sentinel-2 (https://scihub.copernicus.eu/) of Isfjorden where zooplankton were sampled in May, June and August 2018 and benthic invertebrates in August 2018. The position of the ice edge in May 2018, when land-fast ice prevented sampling at the innermost stations, is indicated in black. Stars represent the city of Longyearbyen and the abandoned mining village of Pyramiden, which represent local sources of contamination. (b) Isfjorden station map showing stations where sculpin were sampled using gill nets in August 2018. (c) Map of Svalbard with the West Spitsbergen Current (WSC) depicted in red.

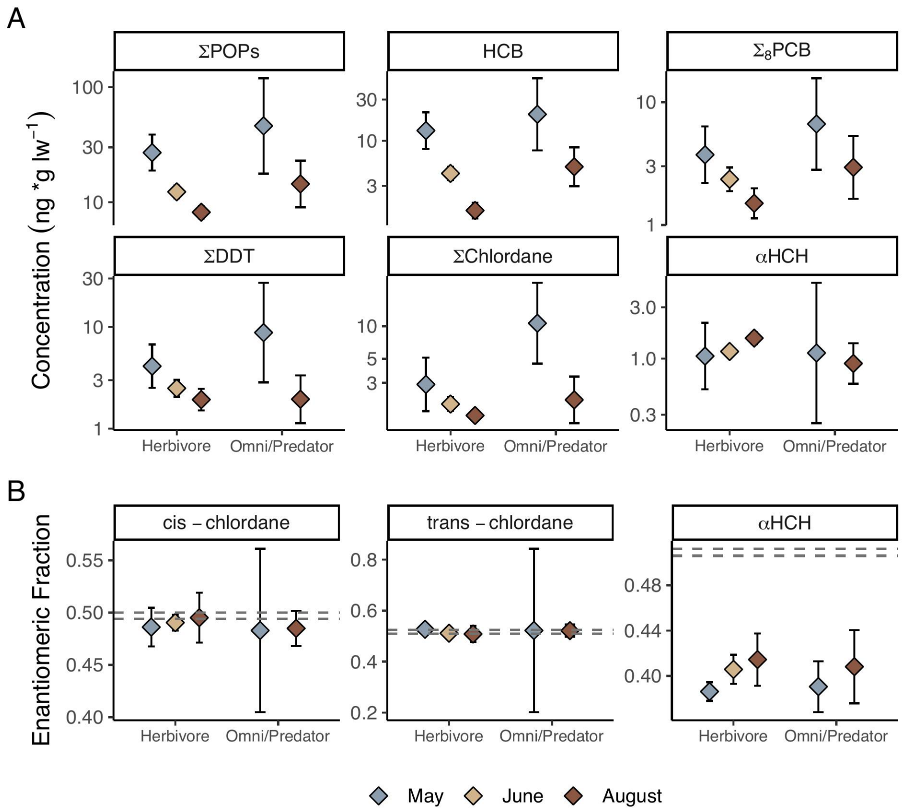

Figure 2. A) POP concentrations and (B) EFs in bulk zooplankton by month for each plankton type: Herbivorous zooplankton (*Calanus* spp., Meroplankton) and omnivorous and predator zooplankton (Macrozooplankton and Jellyplankton). Diamonds and error bars represent the bootstrapped mean and 95% confidence interval. $\sum_8$PCB is defined as the sum of CB-28, CB-31, CB-52, CB-101 and CB-153 (CB-118, CB-138 and CB-180 were < LOD in zooplankton). The racemic ranges (determined using laboratory standards) are indicated as dashed gray lines. POP concentrations on a wet weight basis can be found in Figure S8.

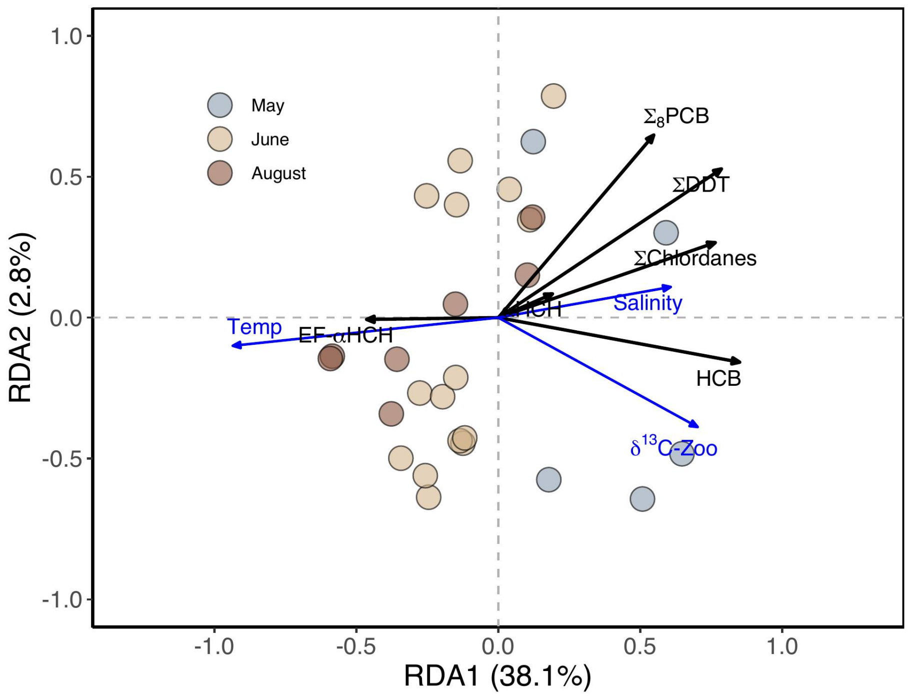

Figure 3. Partial RDA based on log transformed concentrations of sums of PCBs, chlordane pesticides, DDTs and α-HCH in herbivorous zooplankton with variance (20.6 %) due to lipid content removed. Constraining variables: δ^{13}C-Zoo, salinity, and temperature, which explain 41% of the residual variance, are shown in blue. EF of α-HCH (in black) is included as a passive vector. Each point represents one individual sample and color represents sampling month with blue = May, light brown = June and dark brown = August.

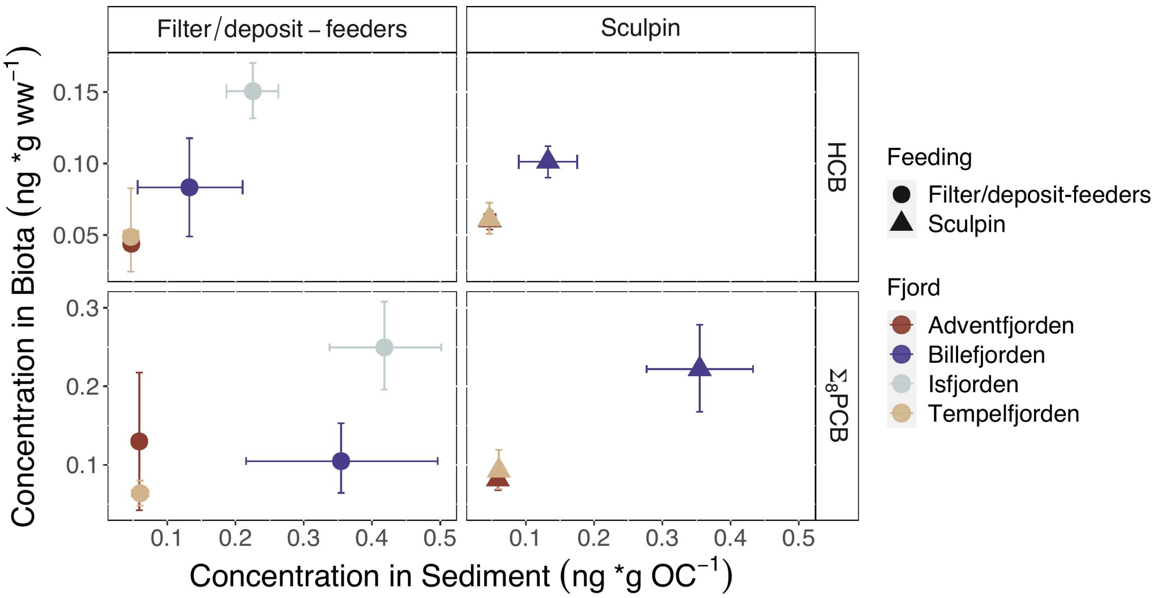

Figure 4. HCB and ∑PCB concentrations in filter and deposit feeding benthic invertebrates and sculpin vs. fjord sediment concentrations.[23] Points and error bars represent the bootstrapped mean and 95% confidence intervals based on all fjord replicates. $\sum_8$PCB is defined as the sum of CB28/31, CB-52, CB-101, CB-118, CB-138, CB-153 and CB-180 for zoobenthos and CB-52, CB-138, CB-153 and CB-180 for sculpin.

Supporting Information

Is glacial meltwater a secondary source of legacy contaminants to Arctic coastal food-webs?

Maeve McGovern[1,2,3]*, Nicholas A. Warner[4,5,6], Katrine Borgå[7,8], Anita Evenset[2,9], Pernilla Carlsson[1], Emelie Skogsberg[10,11], Janne E. Søreide[3], Anders Ruus[7,11], Guttorm Christensen[9], Amanda E. Poste[1,2]

[1]Norwegian Institute for Water Research, 9007 Tromsø, Norway, [2]Department of Arctic Marine Biology, UiT, The Arctic University of Norway, 9019 Tromsø, Norway, [3]University Centre on Svalbard, 9170 Longyearbyen, Norway, [4]NILU-Norwegian Institute for Air Research, The Fram Centre, 9007 Tromsø, Norway, [5]Department of Chemistry, UiT, The Arctic University of Norway, 9019 Tromsø, Norway, [6] Thermo Fischer Scientific, 28199 Bremen, Germany, [7]Department of Biosciences, University of Oslo, 0316 Oslo, Norway, [8]Centre for Biogeochemistry in the Anthropocene (CBA), University of Oslo, 0316 Oslo, Norway, [9]Akvaplan-niva, Fram Centre, 9007 Tromsø, Norway, [10]Norwegian University of Life Sciences, Faculty of Environmental Sciences and Natural Resource Management, 1430 Ås, Norway, [11]Norwegian Institute for Water Research, 0579 Oslo, Norway

*Corresponding author: maeve.mcgovern@niva.no

Content Summary:

20 pages

4 Tables

12 Figures

Table S1. Table presenting the target chemicals and add CAS numbers.

Compound name	**CAS#**
α-Hexachlorocyclohexane (HCH)	319-84-6
β-HCH	319-85-7
γ-HCH	58-89-9
trans (γ)-chlordane	5103-74-2
cis (α)-chlordane	5103-71-9
trans-nonachlor	39765-80-5
cis-nonachlor	5103-73-1
Hexachlorobenzene (HCB)	118-74-1
p,p'-dichlorodiphenyltrichloroethane(DDT)	50-29-3
o,p',-DDT	789-02-6
p,p'-dichlorodiphenyldichloroethane(DDD)	72-54-8
o,p',-DDD	53-19-0
p,p'-dichlorodiphenyltrichloroethylene (DDE)	72-55-9
o,p',-DDE	3424-2-6
Mirex	2385-85-5
Polychlorinated biphenyl (PCB) 28	7012-37-5
PCB 31	16606-02-3
PCB 52	35693-99-3
PCB 101	37680-73-2
PCB 118	31508-00-6
PCB 138	35065-28-2
PCB 153	35065-27-1
PCB 180	35065-29-3

Table S2. Summary of detection limits (LOD) and concentrations for each compound and each sample group. Mean concentrations are calculated using imputed values. Compounds which fell below 60% detection and were removed from analysis are indicated in the 'removed' column.

Group	Compound	Det-ected (%)	Re mo ved	n	LOD (ng/g) (range)	LOD (ng/g) (mean ± sd)	Concentration (ng/g ww) Range	Concentration (ng/g ww) (mean ± sd)
Zooplankton	HCB	100		46	0.001 - 0.016	0.005 ± 0.002	0.011 - 0.586	0.114 ± 0.124
Zooplankton	PCB_101	91.3		46	0.001 - 0.013	0.004 ± 0.002	<LOD - 0.054	0.013 ± 0.011
Zooplankton	PCB_118	30.4	Yes	46	0.002 - 0.038	0.011 ± 0.005	<LOD - 0.03	0.016 ± 0.008
Zooplankton	PCB_138	30.4	Yes	46	0.002 - 0.047	0.014 ± 0.006	<LOD - 0.044	0.021 ± 0.01
Zooplankton	PCB_153	65.2		46	0.001 - 0.031	0.009 ± 0.004	<LOD - 0.138	0.028 ± 0.027
Zooplankton	PCB_180	32.6	Yes	46	0 - 0.011	0.003 ± 0.001	<LOD - 0.022	0.007 ± 0.005
Zooplankton	PCB_28_31	91.3		46	0 - 0.005	0.001 ± 0.001	<LOD - 0.02	0.006 ± 0.004
Zooplankton	PCB_52	91.3		46	0 - 0.007	0.002 ± 0.001	<LOD - 0.065	0.014 ± 0.011
Zooplankton	aHCH	100		46	0.0001 - 0.0001	0.0001 ± 0	0.001 - 0.086	0.023 ± 0.021
Zooplankton	bHCH	82.6		46	0.0001 - 0.0001	0.0001 ± 0	<LOD - 0.04	0.011 ± 0.011
Zooplankton	cis-chlordane	100		46	0.0001 - 0.0001	0.0001 ± 0	0.001 - 0.187	0.027 ± 0.033
Zooplankton	cis-nonachlor	97.8		46	0.0001 - 0.0001	0.0001 ± 0	<LOD - 0.044	0.008 ± 0.009
Zooplankton	gHCH	73.9		46	0.0001 - 0.0001	0.0001 ± 0	<LOD - 0.022	0.007 ± 0.005
Zooplankton	mirex	6.5	Yes	46	0.0001 - 0.0001	0.0001 ± 0	<LOD - 0.001	0.001 ± 0.001
Zooplankton	opDDD	89.1		46	0.0001 - 0.0001	0.0001 ± 0	<LOD - 0.045	0.005 ± 0.008
Zooplankton	opDDT	56.5	Yes	46	0.0001 - 0.0001	0.0001 ± 0	<LOD - 0.015	0.004 ± 0.004
Zooplankton	ppDDD	95.7		46	0.0001 - 0.0001	0.0001 ± 0	<LOD - 0.06	0.008 ± 0.011
Zooplankton	ppDDE	84.8		46	0.002 - 0.017	0.006 ± 0.005	<LOD - 0.116	0.032 ± 0.03
Zooplankton	ppDDT	84.8		46	0.0001 - 0.0001	0.0001 ± 0	<LOD - 0.018	0.003 ± 0.004
Zooplankton	trans-chlordane	100		46	0.0001 - 0.0001	0.0001 ± 0	0 - 0.117	0.021 ± 0.022
Zooplankton	trans-nonachlor	100		46	0.0001 - 0.0001	0.0001 ± 0	0.002 - 0.136	0.022 ± 0.026
Benthos	HCB	100		26	0.002 - 0.009	0.005 ± 0.001	0.02 - 0.89	0.197 ± 0.185
Benthos	PCB_101	80.8		26	0.003 - 0.015	0.005 ± 0.002	<LOD - 0.066	0.031 ± 0.02
Benthos	PCB_118	61.5		26	0.008 - 0.02	0.013 ± 0.003	<LOD - 0.267	0.069 ± 0.073

Benthos	PCB_138	61.5		26	0.003 - 0.025	0.015 ± 0.004	<LOD - 0.268	0.059 ± 0.064
Benthos	PCB_153	76.9		26	0 - 0.016	0.01 ± 0.003	<LOD - 0.503	0.097 ± 0.128
Benthos	PCB_180	69.2		26	0.001 - 0.006	0.003 ± 0.001	<LOD - 0.179	0.031 ± 0.044
Benthos	PCB_28_31	76.9		26	0.001 - 0.003	0.002 ± 0	<LOD - 0.027	0.007 ± 0.006
Benthos	PCB_52	80.8		26	0.001 - 0.004	0.002 ± 0.001	<LOD - 0.027	0.011 ± 0.007
Benthos	aHCH	100		10	0.0001 - 0.0001	0.0001 ± 0.0001	0.001 - 0.178	0.05 ± 0.062
Benthos	bHCH	60		10	0.0001 - 0.0001	0.0001 ± 0.0001	<LOD - 0.043	0.018 ± 0.017
Benthos	cis-chlordane	90		10	0.0001 - 0.0001	0.0001 ± 0.0001	<LOD - 0.063	0.02 ± 0.02
Benthos	cis-nonachlor	80		10	0.0001 - 0.0001	0.0001 ± 0.0001	<LOD - 0.053	0.022 ± 0.021
Benthos	gHCH	40	Yes	10	0.0001 - 0.0001	0.0001 ± 0.0001	<LOD - 0.041	0.022 ± 0.018
Benthos	mirex	70	Yes	10	0.0001 - 0.0001	0.0001 ± 0.0001	<LOD - 0.011	0.003 ± 0.004
Benthos	opDDD	60		10	0.0001 - 0.0001	0.0001 ± 0.0001	<LOD - 0.005	0.002 ± 0.002
Benthos	opDDT	10	Yes	10	0.0001 - 0.0001	0.0001 ± 0.0001	<LOD - 0.003	0.003 ± NA
Benthos	ppDDD	40	Yes	10	0.0001 - 0.0001	0.0001 ± 0.0001	<LOD - 0.014	0.007 ± 0.007
Benthos	ppDDE	90		10	0.005 - 0.005	0.005 ± 0	<LOD - 0.405	0.1 ± 0.135
Benthos	ppDDT	60		10	0.0001 - 0.0001	0.0001 ± 0.0001	<LOD - 0.017	0.004 ± 0.006
Benthos	trans-chlordane	100		10	0.0001 - 0.0001	0.0001 ± 0.0001	0.001 - 0.041	0.018 ± 0.015
Benthos	trans-nonachlor	100		10	0.0001 - 0.0001	0.0001 ± 0.0001	0.001 - 0.148	0.056 ± 0.052
Sculpin	HCB	100		30	0.001 - 0.004	0.003 ± 0.001	0.022 - 0.145	0.073 ± 0.036
Sculpin	PCB_101	33.3	Yes	30	0.006 - 0.013	0.009 ± 0.003	<LOD - 0.093	0.052 ± 0.025
Sculpin	PCB_118	33.3	Yes	30	0.014 - 0.022	0.019 ± 0.002	<LOD - 0.257	0.14 ± 0.08
Sculpin	PCB_138	63.3		30	0.002 - 0.02	0.013 ± 0.008	<LOD - 0.192	0.06 ± 0.051
Sculpin	PCB_153	96.7		30	0 - 0.008	0.005 ± 0.003	<LOD - 0.228	0.066 ± 0.057
Sculpin	PCB_180	93.3		30	0.001 - 0.004	0.003 ± 0.002	<LOD - 0.058	0.018 ± 0.015
Sculpin	PCB_28_31	53.3	Yes	30	0.001 - 0.002	0.002 ± 0.001	<LOD - 0.004	0.003 ± 0.001
Sculpin	PCB_52	66.7		30	0 - 0.002	0.001 ± 0.001	<LOD - 0.019	0.008 ± 0.005

Table S3: Summary of recoveries for 13-C labelled internal standards in biota, lab blanks and standard reference materials (SRMs).

Group	Compound	n	Recovery (%) (mean ± SD)	Recovery (%) (range)
Zooplankton	13C_HCB	42	31.12 ± 8.77	10.94 - 45.77
Zooplankton	13C_PCB101	42	50.38 ± 14.17	15.77 - 79.14
Zooplankton	13C_PCB118	42	51.52 ± 13.86	15.94 - 77.75
Zooplankton	13C_PCB138	42	50.24 ± 12.56	16.04 - 74.04
Zooplankton	13C_PCB153	42	52.06 ± 13.61	16.85 - 76.93
Zooplankton	13C_PCB180	42	43.96 ± 11.15	14.36 - 62.73
Zooplankton	13C_PCB28	42	44.45 ± 12.37	13.96 - 67.95
Zooplankton	13C_PCB52	42	46.5 ± 14.16	14.24 - 73.54
Zooplankton	13C_aHCH	23	29.39 ± 8.49	10.38 - 40.82
Zooplankton	13C_bHCH	23	30.55 ± 9.79	9.56 - 47.71
Zooplankton	13C_cis-chlordane	23	42.29 ± 12.38	14.99 - 61.76
Zooplankton	13C_gHCH	23	29.75 ± 8.8	10.49 - 41.73
Zooplankton	13C_opDDD	23	48.36 ± 14	17.56 - 70.78
Zooplankton	13C_ppDDE	23	44.88 ± 13.95	14.77 - 67.32
Zooplankton	13C_ppDDT	23	73.48 ± 21.22	27.8 - 110.12
Zooplankton	13C_trans-chlordane	23	41.37 ± 13.47	14.7 - 60.55
Zooplankton	13C_trans-nonachlor	23	41.55 ± 12.4	13.2 - 60.94
Benthos	13C_HCB	34	32.21 ± 7.88	20.19 - 57.36
Benthos	13C_PCB101	34	49.33 ± 13.92	28.34 - 93.31
Benthos	13C_PCB118	34	51.55 ± 14.22	31.19 - 92.31
Benthos	13C_PCB138	34	53.94 ± 15.06	31.54 - 97.62
Benthos	13C_PCB153	34	54.75 ± 15	32.19 - 101.13
Benthos	13C_PCB180	34	49.55 ± 13.85	29.69 - 89.26
Benthos	13C_PCB28	34	42.61 ± 11.74	24.59 - 80.81
Benthos	13C_PCB52	34	44.25 ± 14.09	24.39 - 94.5
Benthos	13C_aHCH	10	32.04 ± 10.68	19.22 - 55.12
Benthos	13C_bHCH	10	35.05 ± 12.25	19.65 - 61.03
Benthos	13C_cis-chlordane	10	49.04 ± 15.13	27.92 - 82.28
Benthos	13C_gHCH	10	33.59 ± 10.77	19.78 - 56.5
Benthos	13C_opDDD	10	53.88 ± 16.11	29.73 - 86.83
Benthos	13C_ppDDE	10	47.21 ± 13.71	26.6 - 75.81
Benthos	13C_ppDDT	10	85.91 ± 22.89	49.13 - 123.12
Benthos	13C_trans-chlordane	10	49.29 ± 15	28.11 - 81.87

Benthos	13C_trans-nonachlor	10	45.6 ± 13.84	25.48 - 75.75
Sculpin	13C_HCB	30	37.62 ± 8.47	17.12 - 49.6
Sculpin	13C_PCB101	30	47.8 ± 10.91	25.33 - 63.57
Sculpin	13C_PCB118	30	49.7 ± 11.55	25.21 - 68.09
Sculpin	13C_PCB138	30	53.82 ± 12.99	26.92 - 73.81
Sculpin	13C_PCB153	30	54.52 ± 13.27	26.93 - 75.69
Sculpin	13C_PCB180	30	50.7 ± 12.75	24.32 - 70.62
Sculpin	13C_PCB28	30	46.08 ± 9.72	24.71 - 59.72
Sculpin	13C_PCB52	30	44.15 ± 9.66	23.87 - 56.97
Lab blank	13C_aHCH	10	36.67 ± 9.08	20.69 - 51.7
Lab blank	13C_bHCH	10	41.71 ± 8.99	31.07 - 56.18
Lab blank	13C_cis-chlordane	10	53.78 ± 10.82	38.11 - 69.35
Lab blank	13C_gHCH	10	39.76 ± 8.48	29.03 - 53.61
Lab blank	13C_opDDD	10	61.73 ± 13.4	45.46 - 82.87
Lab blank	13C_ppDDE	10	55.73 ± 11.63	38.72 - 72.27
Lab blank	13C_ppDDT	10	81.77 ± 25.2	40.79 - 119.57
Lab blank	13C_trans-chlordane	10	54.13 ± 10.69	37.98 - 70.03
Lab blank	13C_trans-nonachlor	10	50.26 ± 11.05	36.16 - 67.05
Lab blank	13C_HCB	17	31.28 ± 14.6	0.38 - 50.3
Lab blank	13C_PCB101	17	62.96 ± 14.46	39.9 - 90.03
Lab blank	13C_PCB118	17	61.38 ± 11.71	42.17 - 82.84
Lab blank	13C_PCB138	17	65.17 ± 10.94	45.31 - 81.91
Lab blank	13C_PCB153	17	66.62 ± 11.66	47.24 - 85.89
Lab blank	13C_PCB180	17	59.8 ± 9.34	42.87 - 74.01
Lab blank	13C_PCB28	17	52.27 ± 14.44	25.32 - 76.4
Lab blank	13C_PCB52	17	57.51 ± 15.73	37.01 - 86.67
SRM	13C_HCB	5	28.92 ± 13.5	11.88 - 41.14
SRM	13C_PCB101	5	41.08 ± 16.87	19.49 - 62.12
SRM	13C_PCB118	5	42.32 ± 17.87	20.4 - 64.65
SRM	13C_PCB138	5	45 ± 18.44	22.49 - 67.98
SRM	13C_PCB153	5	44.87 ± 18.88	22.27 - 68.25
SRM	13C_PCB180	5	41.28 ± 17.33	20.68 - 62.3
SRM	13C_PCB28	5	37.89 ± 15.55	20.95 - 53.57
SRM	13C_PCB52	5	36.55 ± 14.04	18.99 - 51.9
SRM	13C_aHCH	1	17.79 ± na	17.79 - 17.79
SRM	13C_bHCH	1	26.09 ± na	26.09 - 26.09

SRM	13C_cis-chlordane	1	28.81 ± na	28.81 - 28.81
SRM	13C_gHCH	1	21.06 ± na	21.06 - 21.06
SRM	13C_opDDD	1	35.34 ± na	35.34 - 35.34
SRM	13C_ppDDE	1	25.8 ± na	25.8 - 25.8
SRM	13C_ppDDT	1	50.73 ± na	50.73 - 50.73
SRM	13C_trans-chlordane	2	28.07 ± 0	28.07 - 28.07
SRM	13C_trans-nonachlor	1	26.3 ± na	26.3 - 26.3

Table S4. Chiral analysis description

Chiral analysis of α-HCH and *cis*- and *trans*-chlordane in zooplankton samples was performed using a chiralsil-dex column (12.5 m x 0.25 mm x 0.25 µm (Agilent (chrompack), USA) connected in tandem with a TG5-SILMS ((12.5 m x 0.25 mmx 0.25 µm (Thermo Scientific, UK). The chiral stationary phase is: β-cyclodextrin (chiral selector) that is directly bonded to the dimethylpolysiloxane stationary phase. PTV injection of 2 µL was perfomed using previously described conditions for achiral analysis. A carrier gas flow rate of 1.0 ml/min was used together with the following oven program for chromatographic separation: Initial oven temperature was held at 60°C for 1.5 min and increased at 20°C/min to 110°C, followed by a 1°C/min ramp to 210°C. Analytes were analyzed in electron impact mode using and advanced electron impact (AEI) ion source held at 340°C. Ion transitions and collision energies for α-HCH and chlordane isomers are described in the table below.

Table S4. Ion transitions and collision energies for α-HCH and chlordane isomers

Name	**Parent ion**	**Product ion**	**Collision energy (eV)**
α-HCH (quantification)	181	145	14
α-HCH (qualifier)	281	181	8
^{13}C-α-HCH (internal standard)	187	151	12
Chlordane (quantification)	373	266	20
Chlordane (qualifier)	375	266	20
^{13}C-Chlordane	383	276	14

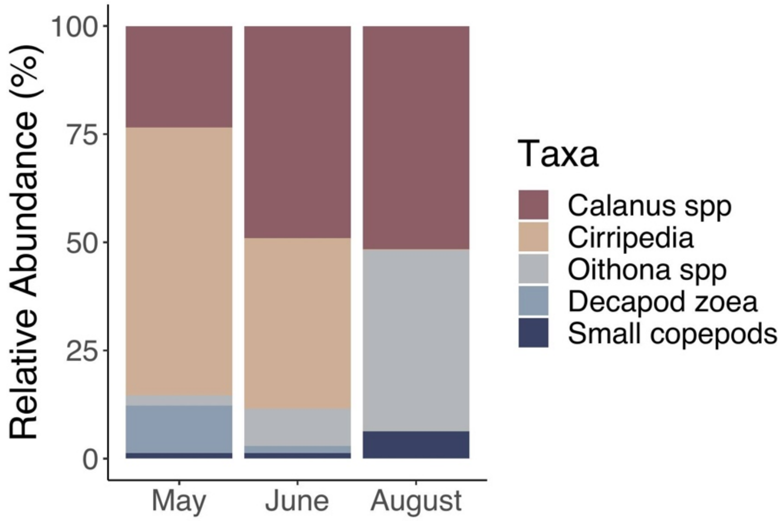

Figure S1. Relative abundance of main zooplankton taxa in size fractionated samples within each month.

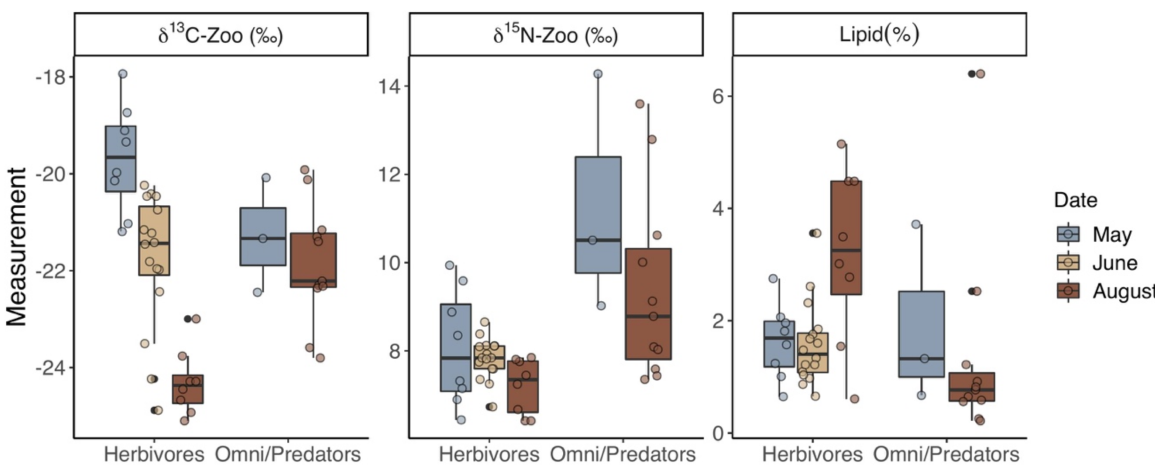

Figure S2. δ^{13}C, δ^{15}N and lipid content in zooplankton feeding groups within each month.

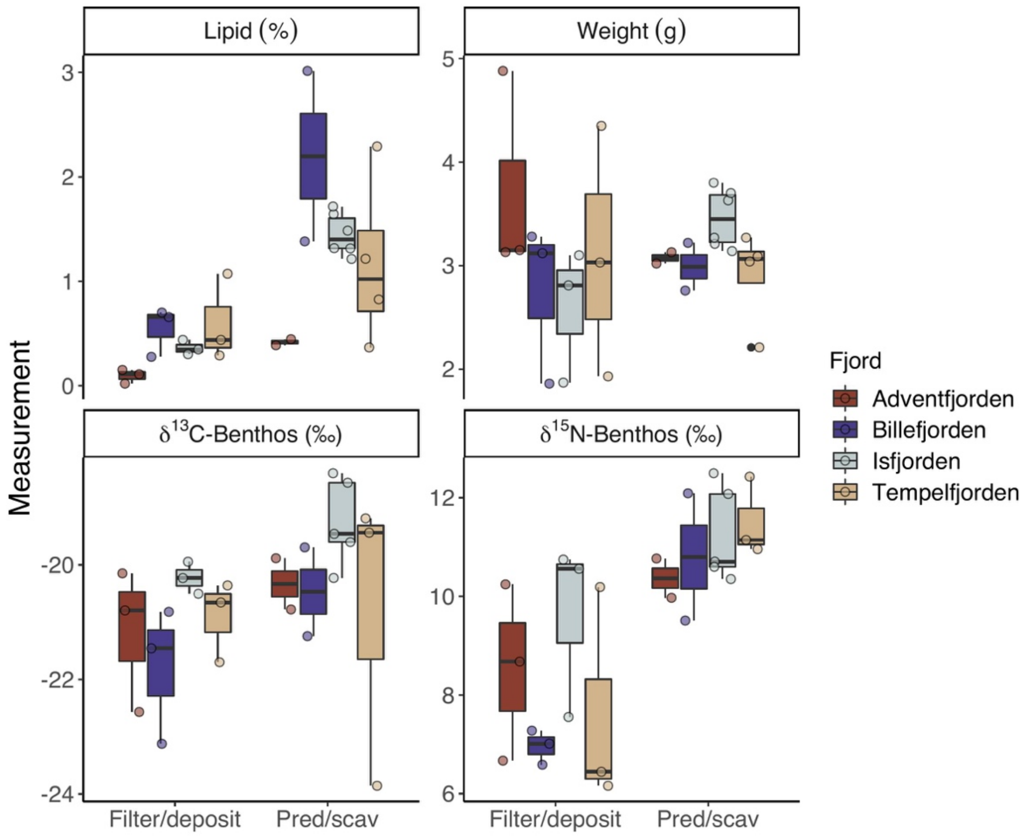

Figure S3. Lipid content, wet weight, $\delta^{13}C$ and $\delta^{15}N$ of benthic invertebrates (filter/deposit feeders and predator/scavengers) among sampled fjords.

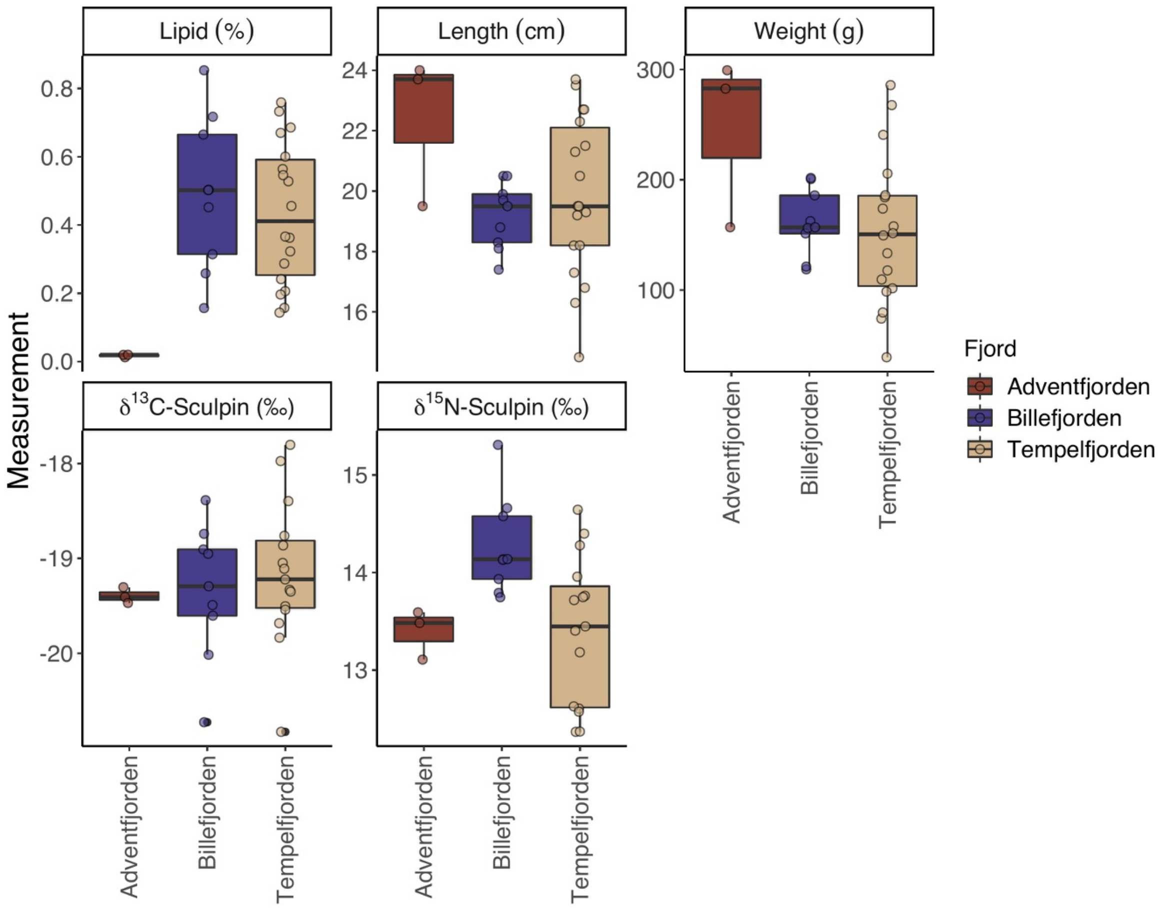

Figure S4. Lipid content, fish length, wet weight, $\delta^{13}C$ and $\delta^{15}N$ of sculpin among sampled fjords.

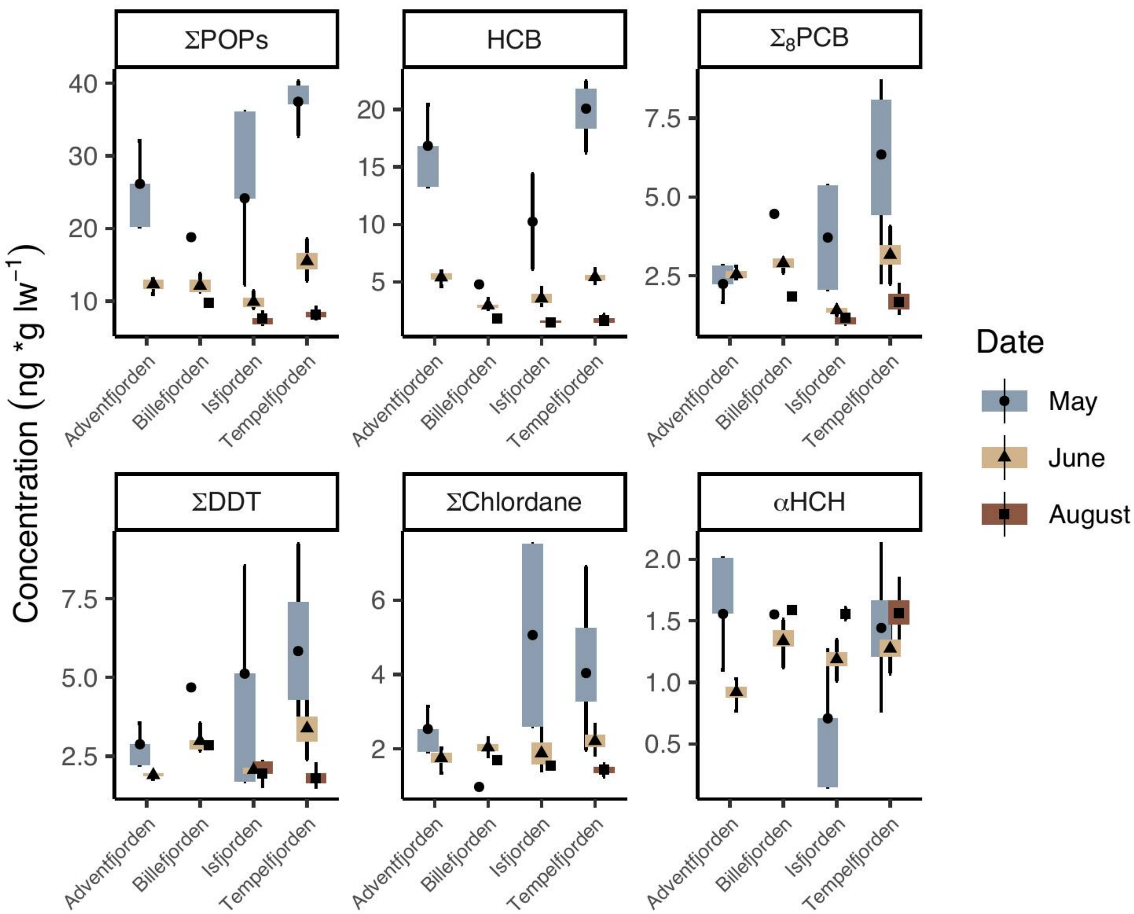

Figure S5. Spatial patterns in herbivorous zooplankton contaminant concentrations by fjord within each month.

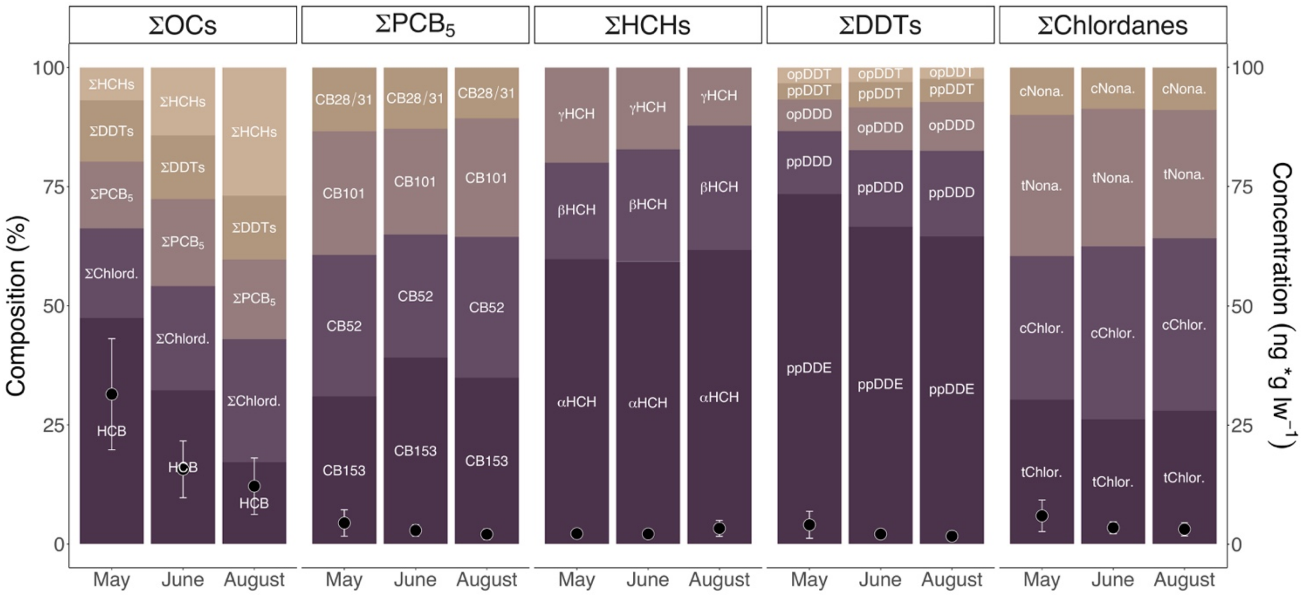

Figure S6. Compositional contaminant profiles for herbivorous zooplankton.

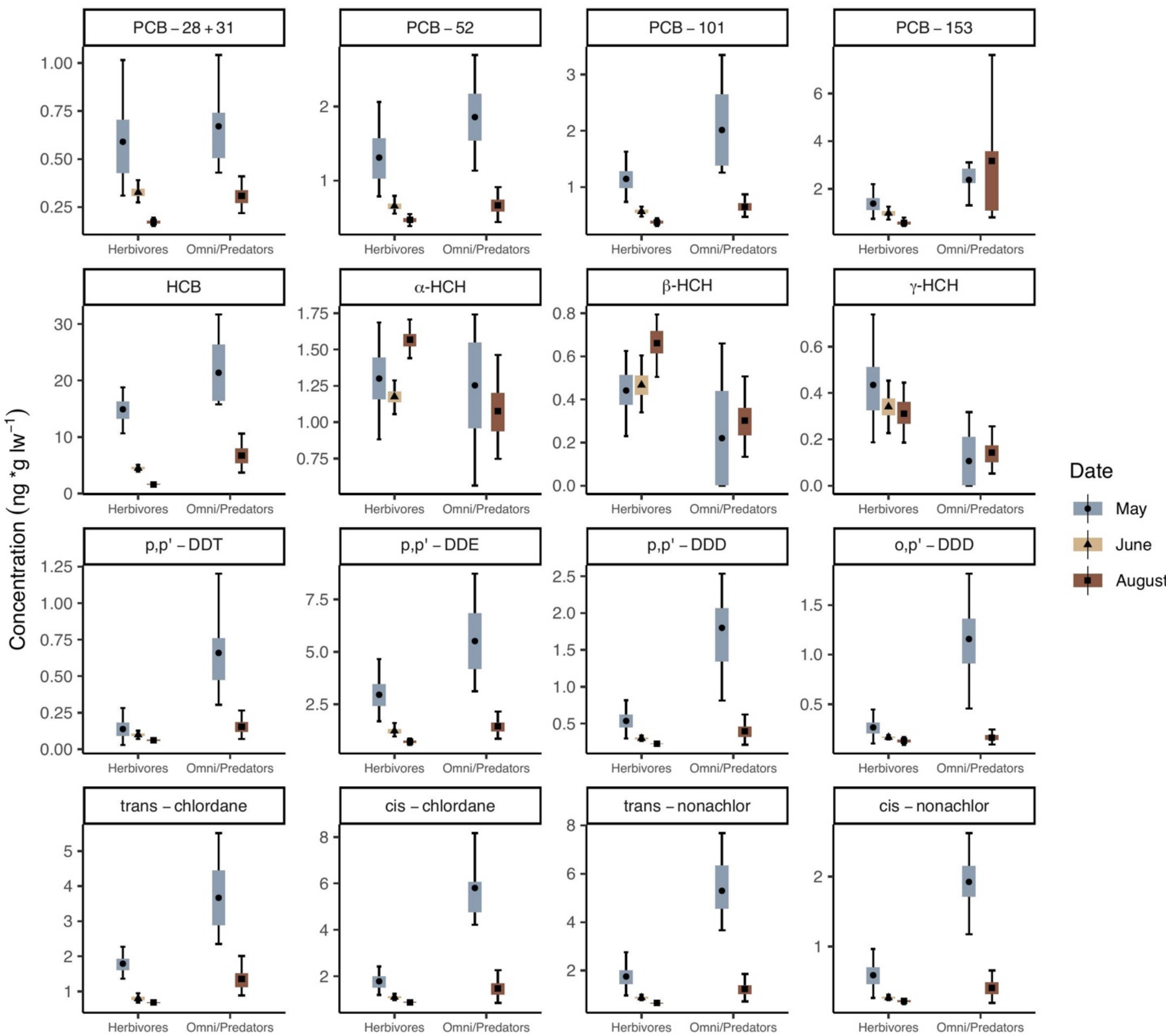

Figure S7. Congener- and isomer-specific contaminant concentrations in zooplankton on the lipid weight basis in each month.

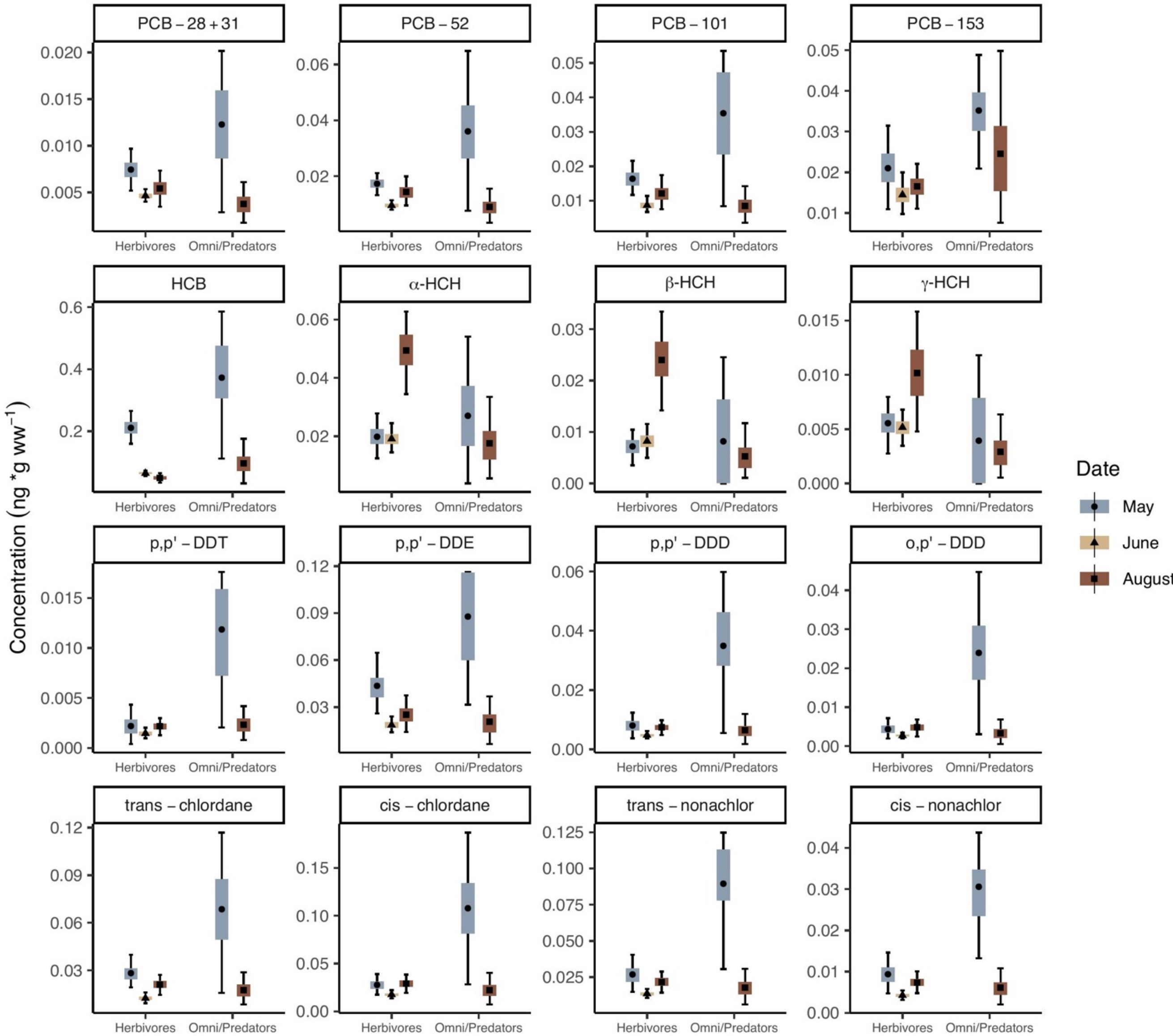

Figure S8. Congener- and isomer-specific contaminant concentrations in zooplankton on the wet-weight basis in each month.

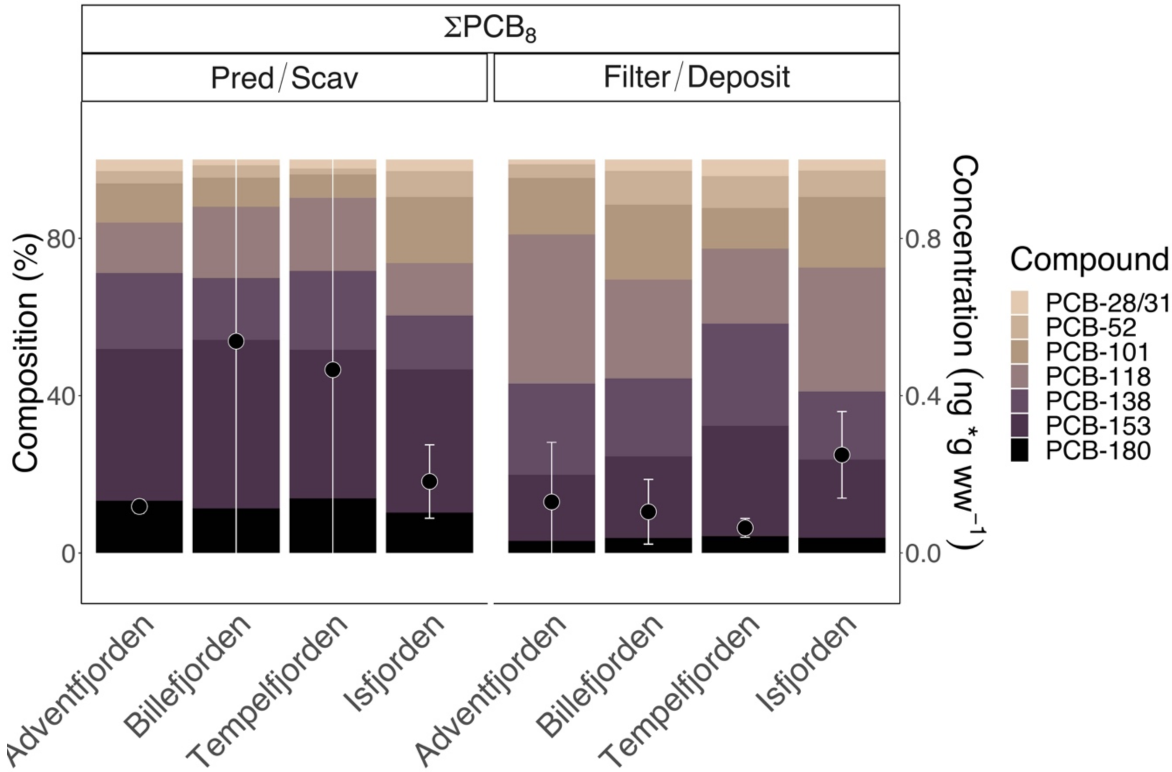

Figure S9. Composition of ∑PCB8 in benthos from each fjord grouped by feeding habit: predators and scavengers vs. filter- and deposit-feeders.

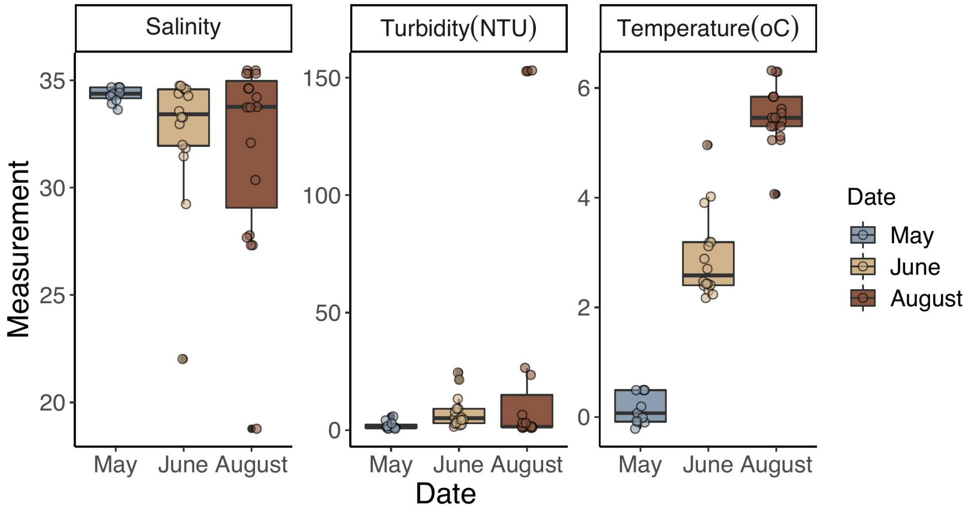

Figure S10. Overview of environmental variables used in RDA analysis and variance partitioning. For more information, see McGovern et al. (2020).

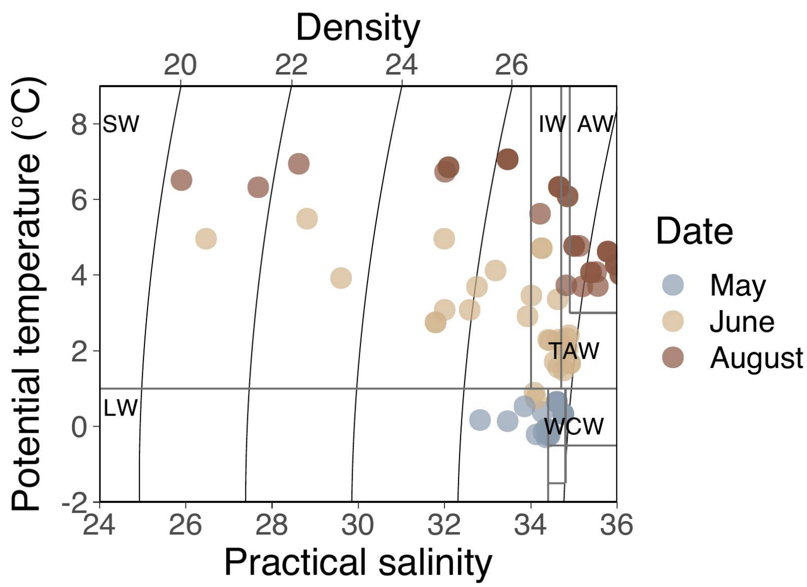

Figure S11. Temperature-Salinity diagram of water samples collected alongside zooplankton samples. Discrete water samples from surface and 15m are both included. This diagram was made using the PlotSvalbard R package (Vihtakari, 2019) using water mass determinations based on Nilsen et al. (2008). SW = surface water, IW= intermediate water, AW= Atlantic water, TAW = transformed Atlantic water, ArW = Arctic water, WCW = winter cooled water and LW = local water.

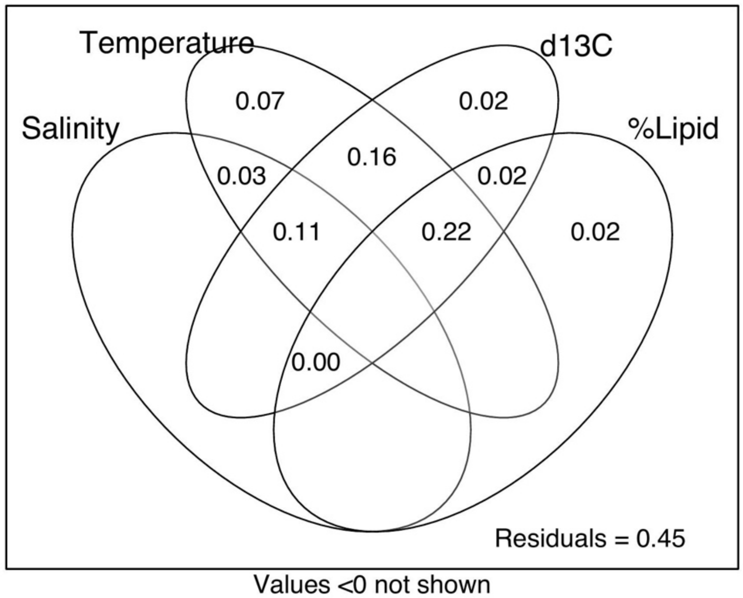

Figure S12. Results of variance partitioning based on log transformed contaminant concentrations in herbivorous zooplankton.

References

McGovern M, Pavlov A, Deininger A, Granskog M, Leu E, Søreide JE, Poste AE (2020). Terrestrial Inputs Drive Seasonality in Nutrient and Organic Matter Biogeochemistry in a High-Arctic Fjord System (Isfjorden, Svalbard). Frontiers Marine Science. doi: 10.3389/fmars.2020.542563

Nilsen, F., Cottier, F., Skogseth, R., and Mattsson, S. (2008). Fjord-shelf exchanges controlled by ice and brine production: the interannual variation of Atlantic Water in Isfjorden, Svalbard. Contin. Shelf Res. 28, 1838–1853. doi: 10.1016/j.csr.2008.04.015

Vihtakari, M. (2019). PlotSvalbard: PlotSvalbard – Plot Research Data From Svalbard on Maps. Rpackage version 0.8.5.